PL1-INV

10th Anniversary of High Tc Iron-based Superconductors: What we learned

*Hideo Hosono[1]

Tokyo Institute of Technology[1]

Iron had been believed to be the most harmful element for the emergence of superconductivity. However, the situation was totally changed since the discovery of an iron oxy-pnictide superconductor $LaFeAsO_{1-x}Fx$ with Tc=26 K in early 2008. This discovery sparked intense research activity on superconductivity in this system worldwide. As a consequence, more than 20,000 printed papers have been published to date along with comprehensive review articles.

What is the impact of iron-based superconductors (IBSC)? There will be two answers, i.e.

The first is the breaking of a widely accepted belief of "iron is antagonistic against superconductivity", which leads to the opening of a versatile material frontier for new superconductors. We have learned a fact through both extensive and intensive studies in the past decade that iron can be a good friend for high Tc superconductors under certain conditions. Almost 30 years ago, we examined whether or not superconductivity come out when carriers were doped to SrLaFeO4 (Physical Review B 49.15 (1994): 10194.). Of course, this attempt failed. The choice of partner anion is of primarily importance for explanation of superconductors.

The second is finding a rich variety in material candidate and in pairing interaction. It has turned out that there are many material varieties in iron-based superconductors such as 5-types of parent materials, 1111, 122, 111, 11, and thick-blocking layer materials, and each type has rather different superconducting properties. In particular, it turned out that 11 materials have rich materials as superconductors and physics. Alkali ion-intercalated FeSe compounds appear to contain a Mott-insulating compound with a high Neel temperature (~500 C). This finding is totally surprising, demonstrating that iron-based superconductors have a much larger spread than people felt at the initial stage. All the major actors are ready in this system associated with charge, spin, and orbitals. The research is now entering into a new phase in which materials are required to be tuned/designed so as to enable these actors to play their characteristic roles toward higher Tc,

Last is the advantageous grain boundary nature in IBSCs. This feature accelerates the wire fabrications for high field application.

Keywords: iron based superconductors

PL2-INV

Recent Topics and Future Prospects of Superconducting Joints Connecting HTS Materials

*Jun-ichi Shimoyama[1]

Aoyama Gakuin University[1]

In general, development of superconducting joint connecting cuprate superconducting materials had been considered to be intrinsically difficult because of their short coherence length, large electromagnetic anisotropy and chemical instability particularly at the surfaces of superconducting crystals, in other word, weak-link characteristics at grain boundaries. However, recent progresses in HTS conductors have triggered us to consider fabrication of superconducting joints between these tapes. Melt-solidification is one of the promising methods to fabricate superconducting joints without weak-link problems, this method was applied for connecting Gd123 tapes and Bi2212 wires, though former study suggested difficulty in oxygen annealing after crystal growth.

Establishment of more versatile technologies to produce superconducting between HTS tapes will open windows toward various types of HTS superconducting magnets equipped with the persistent current circuit and long length superconducting cables. Toward this target, several challenges have started in Japan since last year and most of them are supported by the JST Mirai-Program. Following points are considered as the generic concept for the development of superconducting joint using HTS materials.

1. Without significant degradation of superconducting properties of HTS tapes/wires after the heat-treatment for jointing
2. Moderate carrier doping state can be easily achieved at the joint region by post-annealing, if necessary.
3. Uniform and well-connected interface in terms of both mechanically and electrically between HTS tapes or HTS tape and intermediate layer
4. Robust against heat cycles

It should be noted that, high J_c performance is not important for the joint region. Therefore, strategies to fabricate superconducting joint is different from those for synthesis of high J_c HTS materials.

In this talk, recent topics on development of superconducting joints between RE123 coated conductors, Bi2223 tapes and other combinations of superconducting materials will be introduced including discussions on the determining factors of current carrying properties and future prospects of their applications up to 77 K.

Acknowledgements:
This work was partly supported by the JST Mirai-Program with a Grant Number JPMJMI17A2.

Keywords: superconducting joint, HTS materials

PL3-INV

Superconducting Technology for Future Aircraft Electric Propulsion

*Hiroyuki Ohsaki

Graduate School of Frontier Sciences, the University of Tokyo, Japan

In the 21st century, the importance of low carbon technologies is more strongly recognized. Under such circumstances, research and development for electric propulsion of aircraft has attracted much attention.

Manned flight of 1-2 seater small electric aircrafts, in which a reciprocating engine was replaced with a propulsion system equipped with a synchronous motor and battery, was carried out. Development of electric air taxis is also progressing. Airbus, Rolls-Royce and Siemens announced the E-Fan X project, which will demonstrate a hybrid electric aircraft with about 100 seats. In this aircraft, one of the turbo fan engines will be replaced by an electric motor. Research and development of all-electric passenger aircrafts is under way for their future realization. They requires high power density (kW/kg) in the electric propulsion system, and, therefore, the application of superconducting technology has been studied. It was reported that electric propulsion system based on superconducting technology could reduce energy consumption and CO_2 emission drastically.

Full electrification of passenger aircrafts is a challenging subject. A propulsion system of electric passenger aircrafts will have some distributed fans driven by electric motors, an energy management system, a gas turbine generator, or a hybrid power supply composed of a gas turbine generator and a fuel cell, etc. Superconducting technology can be applied to not only the motor but also the generator, the power cable for energy transmission, etc. Power converter systems for AC/DC electric power conversion and cryogenic systems for cooling the superconducting equipment are also key components for realization of high power density and high efficiency of a propulsion system.

Keywords: Electric propulsion, Aircraft, Electrical machine, Power cable

PL4-INV

High Temperature Superconductors for High Field Magnets

*David C Larbalestier[1]

Applied Superconductivity Center, Florida State University, National High Magnetic Field Laboratory, 2031 East Paul Dirac Drive, Tallahassee FL 32310, USA[1]

Although the major hopes for applications of HTS perhaps still lie with electric utility applications, there are growing numbers of magnets, including some real user magnets, being made with HTS that address the most classical and successful use of superconductors for magnets I want to address my thoughts about the challenges posed by today's HTS conductors based on work carried out over the last decade at the NHMFL. During the last decade Plan A for high field superconducting magnets at the NHMFL has been to use REBCO coated conductor. It was the first HTS conductor to have both high J_c and high strength in one conductor package and with it we have built the 32 T user magnet and multiple test magnets that (inside our 20 T and 31 T resistive magnets) have yielded fields ranging from 27 to 45.5 T. The initial technology of insulated REBCO is now being challenged by much higher current density, No Insulation (NI) designs that are potentially much more economical. But recent post mortems of not fully successful REBCO magnets suggest that important features of the single filament architecture of REBCO coated conductors need attention. In the last 5 years, Bi-2212 has been redeveloped, not just because it is round, multifilament, twisted, of high J_c and macroscopically isotropic, but because the challenges of using it in small magnets have mostly been overcome. Not to be outdone, Bi-2223 has also seen significant recent development by effective lamination of the conductor with strong superalloy sheaths that make it rather suitable for solenoid use. In my talk, I will describe my view of this recent progress and the various pluses and minuses of the three present high-temperature superconductor types.

**Work carried out with many collaborators at the MagLab, especially with programs led by Huub Weijers, Hongyu Bai, Denis Markiewicz (Insulated REBCO), Ulf Trociewitz, Youngjae Kim, Ernesto Bosque (Bi-2212 coils), Seungyong Hahn, Iain Dixon and Kwanglok Kim (NI REBCO), Scott Marshall (Bi-2223), Eric Hellstrom, Jianyi Jiang, and Fumitake Kametani (Bi-2212 conductors), and Dmytro Abraimov, Paul Hu, Jan Jaroszynski and Lance Cooley (REBCO conductors). Work supported by the National Science Foundation under Cooperative Agreement DMR-1644779, by the State of Florida and the US Department of Energy Office of High Energy Physics under DE-SC0010421.*

PL5-INV

A Snapshot of Superconductivity Activities in the United States

*Bruce P. Strauss[1]

U. S. Department of Energy[1]

This talk will cover a number of applications including High Energy Physics, Ultra High Magnetic Fields, Light Sources, MRI, Quantum Materials, etc. The superconducting materials requirements as well as other technology limitations will be examined. The talk will conclude with an examination of figures of merit for performance and cost and question if these are still relevant.

PL6-INV

Superconducting quantum-classical information processing systems

*Oleg Mukhanov[1,2]

Hypres[1]
SeeQC[2]

Superconducting Josephson-junction Single Flux Quantum (SFQ) circuits are now successfully used in practical high speed signal digitizing systems. More sophisticated superconducting digital processors and memories are being developed for energy efficient data processing for the next generation data centers. The digital technology for these applications is superconducting Rapid Single Flux Quantum (RSFQ) logic and its energy efficient successors such as energy-efficient SFQ logic (ERSFQ and eSFQ), ac-driven Reciprocal Quantum Logic (RQL) and Adiabatic Quantum Flux Parametron (AQFP) circuits. Recently, SFQ logic applications were extended to the realization of classical control infrastructure for scalable quantum processors including qubit control, measurement, and error correction functions. Traditionally, all classical control operations are performed at room temperature. Such system configuration is inherently noisy and difficult to scale. It also introduces a long latency in quantum operations. For scalable low-latency qubit control infrastructure, the first layer of control electronics should located as close to the quantum chips as possible. Superconducting SFQ circuits proximally located to the quantum circuits can be the technology of choice due to its low power (10^{-19} Joule to 10^{-21} Joule to per switching at 4K and 20-30 mK, respectively). They can be engineered to produce the minimal back action to qubits. The ability to operate at very high speed (tens of gigahertz clock) opens a way for digitizing and fast processing qubit output data for error correction and generation of qubit control signals. Furthermore, hybrid systems are envisioned which integrate together the quantum and classical processing units to enable various quantum application algorithms which typically combine quantum and classical modules. The implementation of scalable quantum-classical 3D integrated system spreading across multiple temperature stages will be discussed.

Keywords: RSFQ, qubit, cryogenic, hybrid

OR-1-INV

Development of metal exploration system using high-Tc SQUID

*Eiichi Arai[1], Satoshi Ueda[1], Masayuki Motoori[1], Kazuo Masuda[1], Akira Tsukamoto[2], Tsunehiro Hato[2], Hidehiro Ishikawa[3], Hidehisa Watanabe[3]

Japan Oil, Gas and Metals National Corporation[1], Superconducting Sensing Technology Research Association[2], Mitsui Mineral Development Engineering Co., Ltd[3]

Metal exploration is generally conducted in sequence from regional reconnaissance survey by remote sensing analysis and geological survey, to the target identification survey using geochemical survey, geophysical survey and drilling. Drilling is the direct method to check whether the metal deposits are placed and to investigate the size of mineralization. Time domain electromagnetic method (TEM) is in the vanguard of geophysical methods and a well-established place in metal exploration to find the locations of mineralization. Since the recent metal exploration targets become deepening which makes the conventional TEM tools incapable of detecting unknown mineralization, recent mining geophysics is aspiring for emergence of a new TEM equipment with larger penetration depth.

JOGMEC has been developing the data acquisition system of TEM using a high-temperature superconducting interference device (HTS-SQUID) since 2001, which innovated system is named as SQUITEM. Its third-generation system (SQUITEM III) had been completed in 2013, and its three-component system (3-component SQUITEM III) had been just fabricated to acquire three components of the magnetic field generated by diffused induction current in the ground originated from the abrupt current stop into the copper electric wire loop on the surface. This 3-component SQUITEM III has a wide dynamic range, a high slew rate (time rate of change of the magnetic field which SQUID magnetometer is capable of following), and superior handleability and transportability. The HTS-SQUID of the latest SQUITEM III is based on the Ramp-edge Josephson Junctions with $La_{0.1}Er_{0.95}Ba_{1.95}Cu_3O_y$ and $SmBa_2Cu_3O_y$ electrode layers, which are fabricated by using an HTS multi-layer fabrication technology. The system noise level of it is 30fT/√Hz at 10 kHz. The slew rate of SQUITEM III is 10.5 mT/sec, which is one of the highest figure among the existing SQUID-TEM data acquisition systems in the world.

Since 2005 when the first-generation SQUITEM (SQUITEM I) was completed, JOGMEC has been applying SQUITEM to its metal exploration in the world. The first trial using 3-component SQUITEM III was conducted over the Mallee Bull copper deposit, Australia in 2017. This trial proves that SQUITEM III can delineate the mineralization zone with higher accuracy than the conventional TEM tools.

Keywords: TEM, SQUID, metal exploration

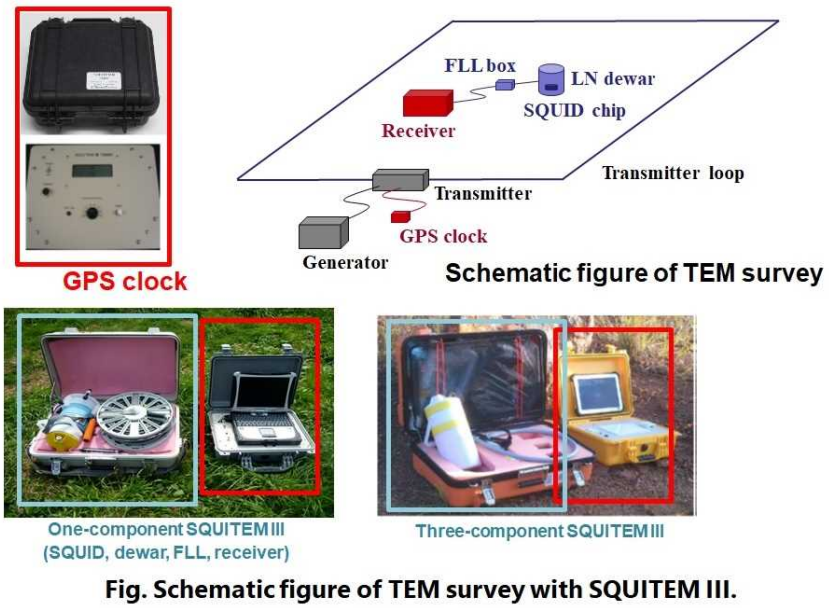

Fig. Schematic figure of TEM survey with SQUITEM III.

OR-2-INV

Economy of thermal energy storage power plant and usage of superconductivity

*Toru Okazaki[1]

The Institute of Applied Energy[1]

Generation cost of renewables are decreasing rapidly. Several projects already underrun 3 cent per kWh. Renewable energy installation is no longer an ethical obligation of OECD countries but prime energy source for emerging countries too. The most severe issue to be solved is intermittency of power generation in this situation. Thermal energy storage power plant (TESP) becomes the most economy solution when it comes to stabilization longer than several hours interval. Conversion efficiency of electricity from thermal energy storage is much lower than batteries but the storage cost is less than 1/20 or less than that of batteries. A heater is employed to convert surplus or fluctuated part of energy to thermal energy. TESP becomes economy when rotating heater is employed instead of simple resistive heater. The rotating heater utilizes induction heating. Static magnetic field is mechanically rotated by synchronous motor, which can supply inertia power to the power grid. Half of the power in power grid must be supplied or consumed by synchronous machine to keep stability of electricity. This issue is different from well-known power balancing of demand and supply. Amount of non-synchronous power source such as PV and battery is automatically limited if TESP is not installed. Superconductivity is employed in this system with two different ways. Firstly, it is employed in rotating heater to earn higher temperature than Curie temperature. The principle is the same as the superconducting furnace, which is already industrialized. This high temperature enables increase of thermal to electricity conversion efficiency up to 60%, and enables various chemical reactions such as artificial fuel production. Secondly, economical improvement of superconducting cable, which is employed to connect remote renewable energy farm and main grid, is realized.

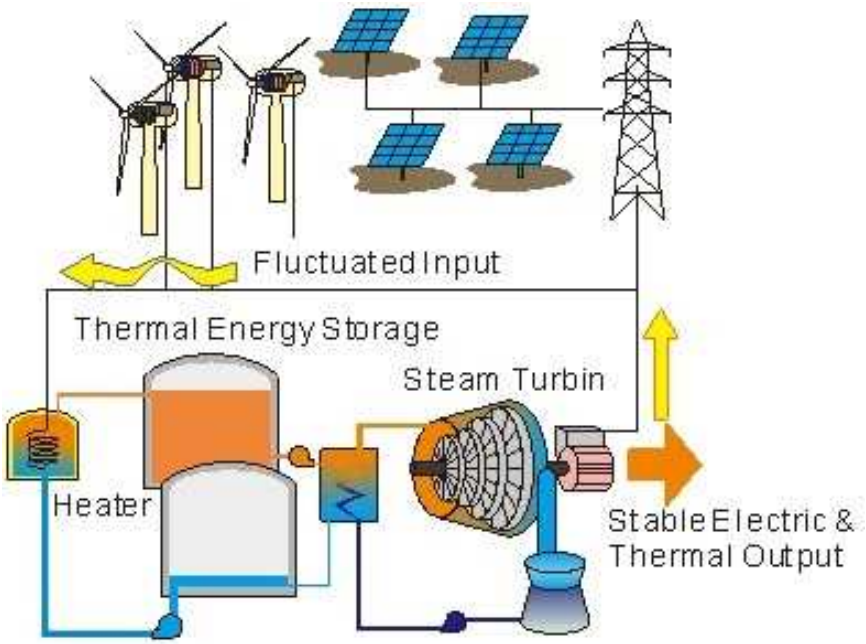

PC1-1-INV

Guiding Vortex Matter via Magnetic Patterned Structures

*Wai-Kwong Kwok[1], Vitalii K. Vlasko-Vlasov[1], Timothy Benseman[2], Daniel Rosenmann[3], Yong-Lei Wang[1,4], Xiaoyu Ma[5], Jing Xu[1,6], Yangyang Lyu[1,4], Zhi-Li Xiao[1,6], Alexey Snezhko[1], Boldizsar Janko[5], Fabiano Colauto[7], Ralu Divan[3], John E. Pearson[1]

Materials Science Division, Argonne National Laboratory, Argonne, Illinois 60439, USA[1]
City University of New York, CUNY Queens College, Queens, NY 11367, USA[2]
Center for Nanoscale Materials, Argonne National Laboratory, Argonne, Illinois 60439, USA[3]
Research Institute of Superconductor Electronics, School of Electronic Science and Engineering, Nanjing University, Nanjing 210093, China[4]
Department of Physics, University of Notre Dame, Notre Dame, Indiana 46556, USA[5]
Department of Physics, Northern Illinois University, DeKalb, Illinois 60115, USA[6]
Federal University of Sao Carlos, Physics Department, SP, Brazil[7]

The advent of nanofabrication has opened new venues for controlling vortex matter, which is responsible for the electro-magnetic response of all applied superconductors. For example, nano-hole structures with innovative patterns have emerged as a versatile platform for controlling and optimizing vortex pinning in superconductors for enhanced critical current. Magnetic field pinning of vortices with meso and nanoscale magnetic structures has also shown great potential for in-situ manipulation of vortex behavior. Here, I will present brief highlights of our work on tailoring vortex behavior with mesoscopic magnetic strips and arrays of nano-magnets. In particular, we demonstrate the use of mesoscopic ferromagnetic strips on a superconductor to mimic a vortex triode device and to guide thermomagnetic avalanches and the use of nano-magnetic patterned structures based on spin-ice rules to explore the effect of geometric frustration in a flux quanta system. Finally, I will present some recent progress in applying these nano-magnetic patterns to high temperature superconductors.

This work was supported by the U.S. Department of Energy, Office of Science, Materials Sciences and Engineering Division. Use of the Center for Nanoscale Materials, an Office of Science user facility, was supported by the U.S. Department of Energy, Office of Science, Office of Basic Energy Sciences, under Contract No. DE-ACO2-06CH11357.

Keywords: magnetism, superconductivity, vortices

PC1-2-INV

Theory of Forces on Quantum Vortex in Type II Superconductors

*Yusuke Kato[1], Shunki Sugai[1], Noriyuki Kurosawa[1]

Department of Basic Science, The University of Tokyo[1]

Dynamics of topological defects play crucial roles in many condensed matters such as, magnets, liquid crystals, superfluids (Helium and cold atoms) and superconductors. Among them, vortex motion in type II superconductors are particularly important in the sense that it is relevant to the magnetization curves, pinning effects, critical currents and stability of two-dimensional systems (Kosterlitz-Thouless transition). However, the character of force on vortices in type II superconductors has not been clearly identified for long terms; One called the driving force on the vortex “the Lorentz force” and another called it “Magnus force”. In this presentation, we show theoretically that[1][2]

・The driving force $J \times \varphi_0$ is neither purely magnetic nor purely hydrodynamic for SC with finite λ.

・Only the sum of the hydrodynamic force and magnetic force is physically meaningful as the driving force on vortex.

・The current density J_{tr} in the driving force $\mathbf{J}_{tr} \times \boldsymbol{\varphi}_0$ is not either the average of the current density nor local value of physical current density $\mathbf{J}(\mathbf{r})$ at the vortex core.

・Underlying physics are the path-independency of London’s fluxoid.

・Our results are valid for dirty SC where conventional and generalized TDGL can be used.

[1] Y. Kato and C-K Chung, J. Phys. Soc. Jpn. **85** 033703/1-5 (2016)

[2] S. Sugai, N. Kurosawa and Y. Kato, in preparation (2018)

Keywords: vortex, type II superconductors, Magnus Force, Lorentz force

PC1-3

Competition between dynamic ordering and disordering for vortices under asymmetric periodic drive

*Mihaly Dobroka[1], Koichiro Ienaga[1], Shin'ichi Kaneko[1], Satoshi Okuma[1]

Tokyo Institute of Technology[1]

When vortices (or particles) with random initial distribution are periodically driven over a random pinning potential, the particles gradually self-organize to avoid future collisions and transform into an ordered structure, which is known as dynamic ordering [1-3]. By contrast, when an initially organized vortex configuration is driven over random pinning potential by a small dc force, dynamic disordering occurs and the vortices finally reach disordered plastic flow [4]. It is interesting to investigate how the dynamic ordering and disordering compete with each other, and what configuration these vortices take.

Form measurements of the time-evolution of voltage $V(t)$, we find that the dynamic ordering is suppressed with increasing DC drive superimposed with AC drive and eventually vanishes when the DC voltage V_{DC} becomes equal to the amplitude of the AC voltage V_{∞}. This implies that for dynamic ordering to occur by an AC drive, the return motion of the vortices with respect to the random pinning centers is necessary. We also find that the steady-state vortex configuration created by superimposed DC and AC drives is not homogeneous but consists of disordered (DR) and ordered regions (OR). The area ratio of OR decreases monotonically with V_{DC} and disappears at $V_{DC} = V^{\infty}$ where the vortices move only in the forward direction. Here, the square AC drive with symmetric time duration is used, resulting in the slower return motion than forward motion for $0 < V_{DC} < V^{\infty}$. We also perform the same experiment using AC drive with asymmetric time duration without superimposing DC drive, where velocities of the forward and return motion are identical. We again find the competition between dynamic ordering and disordering, the coexistence of DR and OR in the steady state, and the suppression of OR with decreasing return motion. All these results show that the area ratio of OR is determined only by the ratio of the return path to the forward path and independent of the velocity.

[1] L. Corte et al., Nat. Phys. 4, 420 (2008).
[2] S. Okuma, Y. Tsugawa, and A. Motohashi, Phys. Rev. B 83, 012503 (2011).
[3] M. Dobroka *et al.*, New J. Phys. 19, 053023 (2017).
[4] S. Okuma and A. Motohashi, New J. Phys. 14, 123021 (2012).

Keywords: vortex, dynamic ordering, dynamic disordering

PC2-1-INV

Vortex dynamics in Noncentrosymmetric 2D Superconductors

Y. Itahashi[1], Y. Saito[1], T. Ideue[1], T. Nojima[2], *Y. Iwasa[1,3]

QPEC & Department of Applied Physics, University of Tokyo, Tokyo 113-8656, Japan[1]
Institute for Materials Research, Tohoku University, Sendai 980-8577, Japan[2]
RIEN Center for Emergent Matter Science, Wako 351-0198, Japan[3]

Recently developed highly crystalline 2D superconductors are shading new light on physics of 2D superconductivity, since their properties are strongly affected by the crystal structure, which is not possible in the conventional amorphous metallic superconductors [1]. Among them, ion-gated MoS_2 is known as the first noncentrosymmetric 2D superconductor with trigonal symmetry. A well-known manifestation of noncentrosymmetric nature is the enhanced Pauli limit for the in-plane magnetic field that arises in conjunction with the strong spin-orbit interaction [2]. Another unique properties in noncentrosymmetric superconductors is the nonreciprocal responses [3]. In this talk we report that the quantum and classical vortex dynamics are well identified in noncentrosymmetric systems *via* nonreciprocal resistance measurements.

One of the uniqueness of highly crystalline nature of 2D superconductos is the quantum metallic state, which is characterized by the temperature-independent resistance down to low temperatures, dominating the *B-T* phase diagram in between the zero-resistance superconducting and insulating states [4]. This feature is in sharp contrast with the conventional 2D superconductors, where a metallic state is observed only at a single quantum critical point. We measured the second harmonic resistance to probe the vortex ratchet motions in gated MoS_2. The second harmonic magnetoresistance was observed down to the lowest temperature, satisfying selection rules for trigonal crystal symmetry. This behavior implies that lower temperature transport is governed by the vortex ratchet effect, i.e., inequivalent motion of vortices originating from the asymmetric pinning forces of threefold symmetry. Furthermore, we succeeded in identifying the quantum and classical motions of vortex ratchet effects by the magnitude of the second harmonic generation [5]. The present result not only clarified the nature of quantum metallic state in the 2D superconductors, but also proves that the nonreciprocal transport is a powerful tool for noncentrosymmetric systems including superconductors.

References

[1] Y. Saito et al., *Nat. Rev. Mater.* **2,** 16094 (2016).
[2] Y. Saito et al., *Nat. Phys.* **2,** 16094 (2016).
[3] R. Wakatsuki et al., *Sci. Adv.* **3**, e1602390 (2017).
[4] Y. Saito et al., *Science* **350**, 409 (2015), Y. Saito et al., *Nat Comm.* **9**, 778 (2018).
[5] T. Itahashi et al., submitted.

Keywords: 2D superconductivity, noncentrosymmetric system, nonreciprocal response, vortex ratchet

PC2-2-INV

Unconventional gate-induced superconductivity in transition metal dichalcogenides

*Alberto Morpurgo[1]

University of Geneva, Switzerland[1]

The possibility to induce and control superconductivity at the surface of insulating materials by means of electrostatic gating is a breakthrough development that has taken place during the last decade. Probing the nature of the gate-induced superconducting state is however extremely difficult, because the superconducting surface –buried between the gate electrode and the insulating material itself– is difficult to access with most experimental probes. This is why, until now, the superconducting properties of these systems have been studied almost exclusively by means of transport measurements. Here, I will discuss our work on gate induced superconductivity on exfoliated MoS_2 crystals. I will first show that superconductivity survives down to the ultimate level of an individual monolayer. I will then discuss tunneling spectroscopy measurements in the gate-induced superconducting state that we succeeded in doing using suitably nano-fabricated devices. The measurements allow us to determine the density of states in the superconducting regime as a function of carrier density, and demonstrate that the superconducting state is not fully gapped. We find that throughout the carrier density range investigated, a finite sub-gap density of states vanishing linearly at low energy is present, indicative of unconventional superconductivity. I will point to different aspects of the measurements and discuss which indications they provide as to the nature of the superconducting state.

Keywords: gate induced superconductivity, tunneling spectroscopy, 2D materials

PC2-3-INV

Superconducting Atomic-layers on Silicon: Superconductivity Meets Surface Science

*Takashi Uchihashi[1]

National Institute for Materials Science, Japan[1]

The recent discovery of superconductivity in atomic-layer materials has attracted extensive attentions from the viewpoint of fundamental physics, materials science and device applications [1]. Among all, metal atomic layers on semiconductor surfaces prepared in ultrahigh vacuum (UHV) environment are particularly interesting because of their unique atomic and electronic structures, which can be directly probed with advanced surface-sensitive tools such as scanning tunneling microscopy (STM) and angle-resolved photoemission spectroscopy (ARPES) [2-4]. In this talk I will report on two recent developments in our group on this type of atomic-layer superconductors. First, we found that highly ordered layers of metal-phthalocyanine (MPc, M = Mn, Cu) molecules can modify the superconducting transition temperature (Tc) of In atomic layers on Si(111) surfaces in a controllable manner [5]. The strong influences of charge transfer and local magnetic moments were clarified, and this 2D system can be considered a molecule-based van der Waals heterostructures (Fig.1). Second, we performed magneto-transport measurements of atomic-layer superconductor consisting of In or TlPb alloy down to T = 900 mK and up to B = 5 T in the UHV condition. We found that the superconductivity is highly robust when a magnetic field was applied to the sample in an in-plane direction. The results are discussed based on spin-split Fermi surfaces of these atomic layer superconductor, which have been directly confirmed by ARPES measurement.

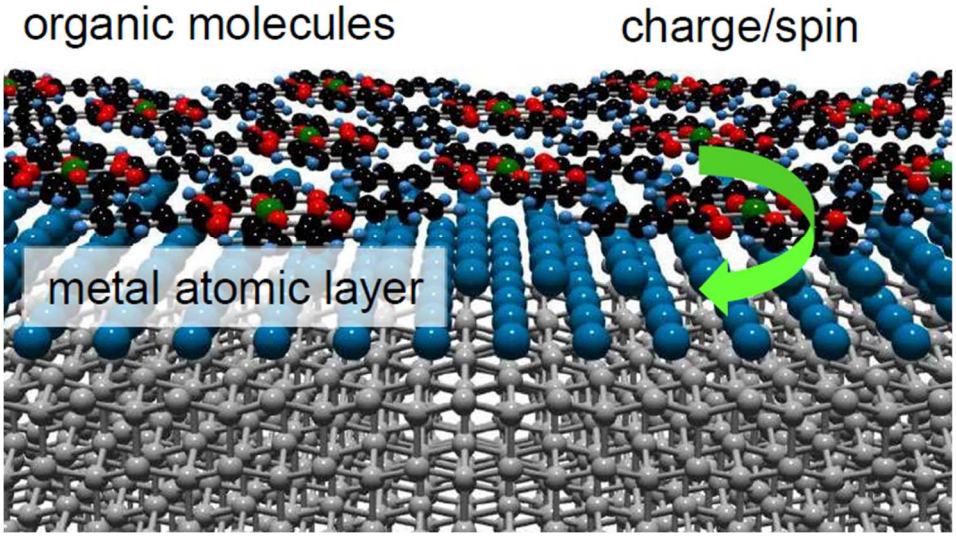

Fig.1: Schematic diagram of molecule-based superconducting van der Waals heterostructure

[1] T. Uchihashi, Supercond. Sci. Technol. **30**, 013002 (2017).
[2] T. Zhang et al., Nat. Phys. **6**, 104 (2010).
[3] T. Uchihashi et al., Phys. Rev. Lett. **107**, 207001 (2011).
[4] S. Yoshizawa, TU et al., Phys. Rev. Lett. **113**, 247004 (2014).
[5] S. Yoshizawa, TU et al., Nano Lett. **17**, 2287 (2017).

Keywords: surface atomic layers, van der Waals heterostructures, in-plane critical field , spin-split Fermi surface

PC2-4

Angular Dependence of Upper Critical Field Enhanced by Spin-Orbit Interaction in Ion-gated $SrTiO_3$

*Takumi Ouchi[1], Sunao Shimizu[2], Yoshihiro Iwasa[2,3], Tsutomu Nojima[1]

Institute for Materials Research, Tohoku University, Japan[1]
RIKEN Center for Emergent Matter Science, Japan[2]
QPEC and Department of Applied Physics, The University of Tokyo, Japan[3]

Recently, the ion gated electron systems in electric double layer transistor (EDLT) configuration have been intensively studied from the viewpoint of high crystallinity two-dimensional (2D) superconductivity with strong spin-orbit interaction (SOI) [1]. Among them, the ion-gated $SrTiO_3$ (001) surface, showing the superconducting transition temperature $T_c \sim 0.4$ K and the in-plane upper critical field H_{c2} higher than the Pauli limit value (1.86 T_c) by 2.5 times with a surface carrier density n_S of order of 1×10^{14} cm^{-2} [2], is a typical 2D system with Rashba type SOI. However, the relation between the enhancement of the in-plane H_{c2} and the characteristic SOI has not been clarified yet. In this work, to examine the effect of SOI on H_{c2} more clearly, we studied the resistive transition of $SrTiO_3$-EDLTs in a wide range of n_S as a function of temperature T, magnetic field H, and its direction θ.
We prepared the conducting surfaces with n_S and T_c, ranging from 0.5 to 6.2×10^{14} cm^{-2} and from 0.4 to 0.2 K, respectively. For all the samples, we observe the unusual in-plane $H_{c2}(T)$, which deviates from $(1-T/T_c)^{1/2}$ law upward and reaches 4 T_c in maximum at low temperature. Furthermore, $H_{c2}(\theta)$ does not show the simple cusp-like peak known as Tinkham's formula [3] around $\theta = 90°$ (parallel to the surface and the current). We will discuss that such anomalous results, which cannot be explained by the orbital-limit theory, are ascribed to the enhancement of the Pauli limit due to the Rashba SOI in combination with the multi-orbital effect of Ti-3d electrons in $SrTiO_3$-EDLTs.
[1] Y. Saito *et al.*, *Nat. Rev. Mater.* **2**, 16094 (2016).
[2] K. Ueno *et al.*, *Phys. Rev. B* **89**, 020508(R) (2014).
[3] F. E. Harper and M. Tinkham, *Phys. Rev.* **172**, 441 (1968)

Keywords: 2D superconductivity, Spin-orbit interaction, Upper critical field

PC2-5

Pressure-induced superconductivity and topological quantum phase transitions in topological materials

*Yanpeng Qi[1]

School of Physical Science and Technology, ShanghaiTech University[1]

Superconductivity and topological quantum states are two frontier fields of research in modern condensed matter physics. The realization of superconductivity in topological materials is highly desired; however, superconductivity in such materials is far from being thoroughly investigated. In this talk, we will discuss the electronic properties of some topological materials by applying high pressure. Pressure-induced topological quantum phase transitions and superconductivity is observed in $MoTe_2$ and BiTeI. The superconducting transition temperature T_c increases with applied pressure and a dome like phase diagrams were observed, which provides insights into the interplay between superconductivity and topological physics. Our theoretical calculations suggest the presence of pressure-induced topological quantum phase transitions as well as a structural–electronic instability.

Keywords: Superconductivity, High pressure, Topological materials

PC3-1-INV

Ultra-high-resolution laser-photoemission spectroscopy on Fe(Se,Te)

*Shik Shin[1]

Institute for Solid State Physics, University of Tokyo, Kashiwa, Chiba 277-8581, Japan [1]

Angle resolved photoemission spectroscopy (ARPES) is very powerful to know the solid-state properties, because one can know the solid state electrons directly. ARPES has been studied by synchrotron radiation or noble-gas-discharge lamp. Recently, ultra-violet(UV)- and soft-X-ray(SX)-lasers have been developed very rapidly, and it is found that they are very powerful for the photoemission spectroscopy as the new light source. Laser has excellent properties, such as coherence, monochromaticity, polarization, ultra-short pulse, very high intensity, and so on. Each excellent property of laser will give us the fruitful results to see the deep insights into the various nature of the materials. I would like to introduce laser-photoemission is very powerful for the materials science, such as high resolution ARPES, spin-resolved ARPES, time-resolved ARPES, and photoemission microscopy (PEEM). Based on these recent experimental results, I would like to introduce the present status and future prospects of various laser photoemission spectroscopy on Fe(Fe,Se).

I found the nematic domain structure of FeSe by PEEM and its time resolved ARPES. Futhermore topoligical superconductivity was found in the Fe(Se, Te) by Ultra-high resolution AREPES and spin-resolved ARPES .

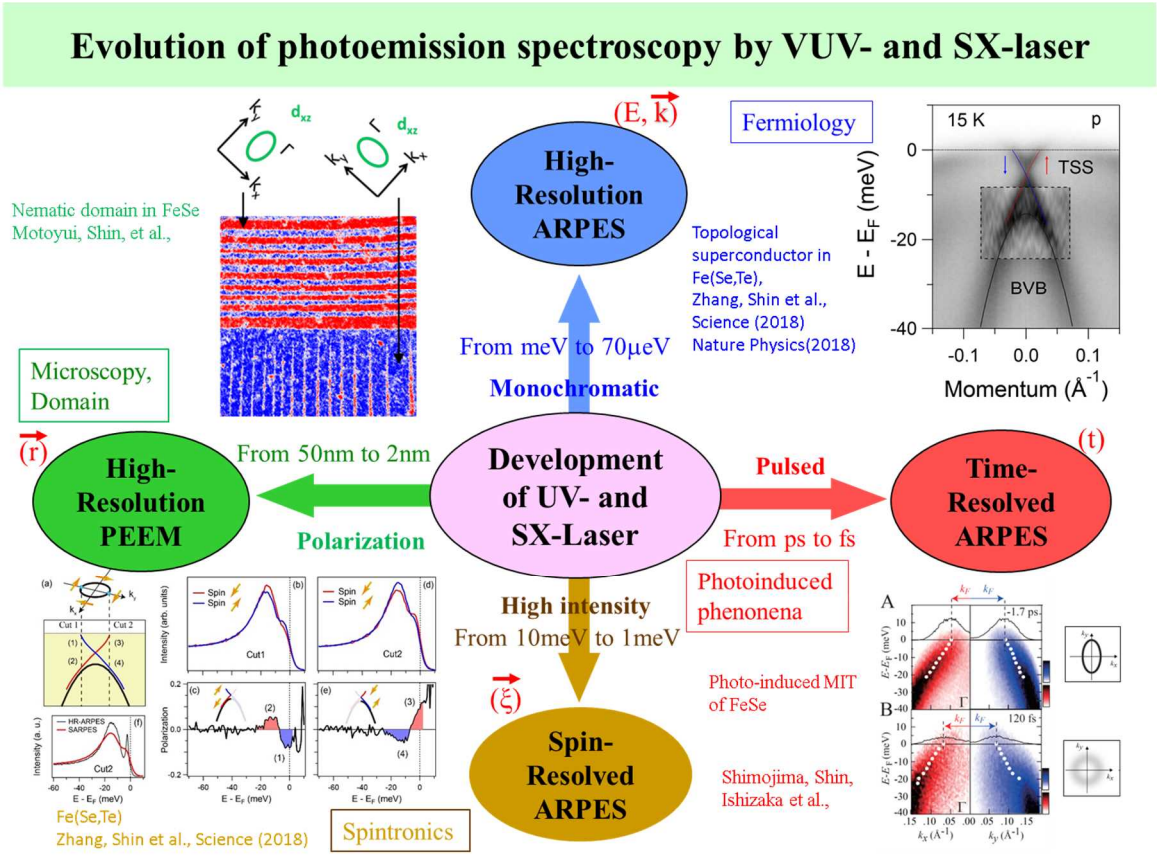

PC3-2-INV

Nematicity in heavily hole-doped iron-pnictides $Ba_{1-x}Rb_xFe_2As_2$

*Yuta Mizukami[1]

Department of Advanced Materials Science, University of Tokyo, Japan[1]

One of the key issues in the iron-based superconductivity is the relationship between the electronic nematicity and high-T_c superconductivity. It is well known that in iron pnictides and iron chalcogenides the superconductivity often emerges in the vicinity of the B1g (Fe-Fe direction) nematic states[1,2] with doping or applying pressure on their parent compound with $3d^6$ configuration of Fe atom. On the other hand, it has recently been pointed out that electron correlations are strongly enhanced with hole doping in $BaFe_2As_2$ system, leading to a proximity to a possible half-filled Mott insulting state with $3d^5$ configuration[3]. This fact impies that the other exotic electronic states may emerge in the heavily hole-doped regime of iron pnictides similar to the case of underdoped cuprates.
Here we report the results of elastoresistance and specific heat measurements on heavily hole-doped $Ba_{1-x}Rb_xFe_2As_2$. In the overdoped regime, it is found that B2g (Fe-As direction) nematic fluctuations develop and the specific heat exhibits two-fold oscillations in the superconducting states. These results provide evidence for the nematicity with B2g symmetry in iron-pnictide superconductors with $3d^{5.5}$ configuration.

In collaboration with K. Ishida, M. Tsujii, O. Tanaka, T. Shibauchi (Department of Advanced Materials Science, University of Tokyo), S. Ishida, A. Iyo, H. Eisaki (National Institute of Advanced Industrial Science and Technology, Japan) K. Grube, T. Wolf, Hilbert. v. Löhneysen (Karlsruhe Institute of Techonology, Germany), and R. M. Fernandes (University of Minnesota, Unites States of America).

[1] J. H. Chu et al., Science 337, 710 (2012).
[2] S. Hosoi *et al.*, Proc. Natl. Acad. Sci. USA **113**, 8139 (2016).
[3] L. de' Medici et al., Phys. Rev. Lett. 112, 177001 (2014).

Keywords: iron-pnictide, orbital-selective Mott phase, nematic fluctuations

PC3-3

Pulsed Laser Deposition of Iron Oxypnictide Thin Films

*Silvia Haindl[1], Erik Kampert[2], Kota Hanzawa[3], Masato Sasase[3,4], Hidenori Hiramatsu[3,4], Hideo Hosono[3,4]

World Research Hub Initiative (WRHI), Institute of Innovative Research, Tokyo Institute of Technology, 4259 Nagatsuta-cho, Midori-ku,Yokohama, Kanagawa 226-8503, Japan[1]
Dresden High Magnetic Field Laboratory (HLD-EMFL), Helmholtz-Zentrum Dresden-Rossendorf, 01328 Dresden, Germany[2]
Laboratory for Materials and Structures, Institute of Innovative Research, Tokyo Institute of Technology, Mailbox R3-3, 4259 Nagatsuta-cho, Midori-ku, Yokohama, Kanagawa 226-8503, Japan[3]
Materials Research Center for Element Strategy, Tokyo Institute of Technology, Mailbox SE-1, 4259 Nagatsuta-cho, Midori-ku, Yokohama, Kanagawa 226-8503, Japan[4]

Fluorine containing iron oxypnictides have the largest critical temperature among iron pnictide superconductors and exhibit promising high upper critical fields in the range of 100 T as well as high critical current densities (in the range of 0.1 – 1 MA/cm²) for superconducting applications. However, a major difficulty lies in their synthesis and in the fabrication of device structures [1,2]. For a long time it was believed that due to the volatility of fluorine epitaxial $SmFeAsO_{1-x}F_x$ films could not be grown by pulsed laser deposition. However, we demonstrated that fluorine containing substrates such as the alkaline earth fluorides act as a dopant source during film deposition [3,4]. In this talk we are going to review $SmFeAsO_{1-x}F_x$ thin film growth by pulsed laser deposition, present a microstructural analysis and discuss superconducting properties including measurements in high magnetic fields up to 65 T. We further evaluate the implications of alkaline earth fluoride substrates such as CaF_2, SrF_2 and BaF_2 that became attractive for the deposition of Fe-based superconductors and point out future directions in oxypnictide thin film growth.

[1] S. Haindl *et al.*, Rep. Prog. Phys. 77, 046502 (2014)
[2] S. Haindl *et al.*, Appl. Surf. Sci. 437, 418 (2018)
[3] S. Haindl *et al.*, Sci. Rep. 6, 35797 (2016)
[4] S. Haindl *et al.*, J. Phys. D: Appl. Phys. 49, 345301 (2016)

Keywords: iron pnictides, doping, pulsed laser deposition, thin films

PC3-4

Transport Properties of CaFeAsF Single Crystals Under High Magnetic Fields

*Gang Mu[1], Yonghui Ma[1], Xiaoming Xie[1]

Shanghai Institute of Microsystem and Information Technology, Chinese Academy of Sciences[1]

Here, we report high-field experiments up to 65 T on a single-crystalline CaFeAsF, which shows a metal-insulator quantum phase transition tuned by the out-of-plane magnetic field. The obtained critical exponent z through the finite-size scaling analysis is very close to 4/3. This transition is closely associated with the evolution of electronic states approaching the quantum limit. The resistivity behaviors as a function of field and temperature were evaluated based on Adams-Holstein theory (A-H theory). Moreover, the in-plane component of the field, which does not affect the transport behavior in the classical region, suppressed the magnetoresistance near the quantum limit.

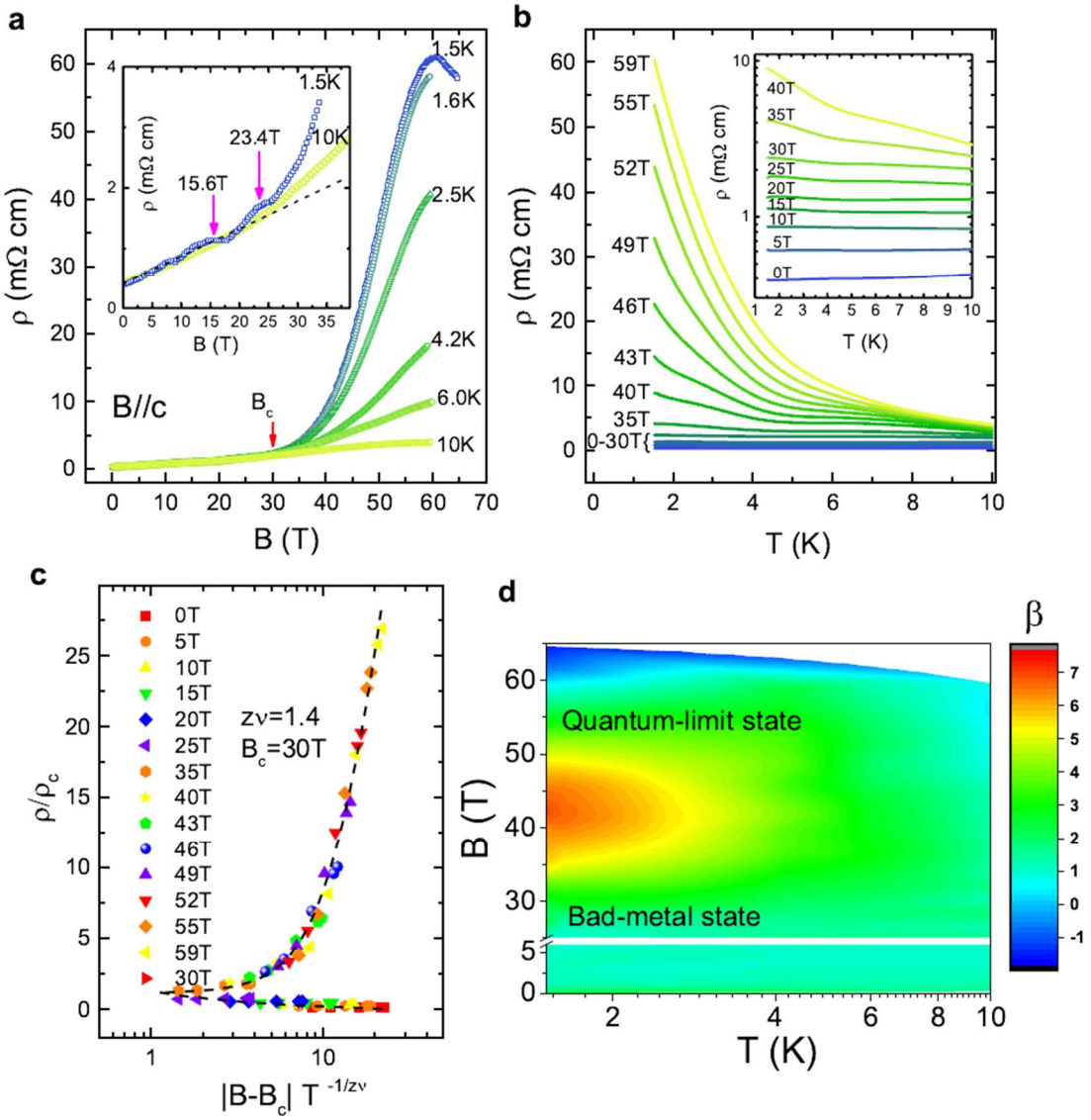

Keywords: CaFeAsF, High Magnetic Fields, Transport Properties

PC3-5

Effects of fast neutron irradiation on the doping dependence of the pinning efficiency in K-doped Ba-122 single crystals

*Daniel Kagerbauer[1], Shigeyuki Ishida[2], Ventsislav Mishev[1], Dongjoon Song[2], Hiraku Ogino[2], Hiroshi Eisaki[2], Masamichi Nakajima[3], Akira Iyo[2], Michael Eisterer[1]

Atominstitut, TU Wien, Stadionallee 2, 1020 Vienna, Austria[1]
Electronics and Photonics Research Institute, National Institute of Advanced Industrial Science and Technology (AIST), Tsukuba 305-8568, Japan[2]
Department of Physics, Osaka University, Toyonaka, Osaka 560-0043, Japan[3]

A sharp peak was observed in the doping dependence of the critical current density, J_c, in K-doped Ba-122 single crystals.[1, 2] This behavior is in contrast to the doping dependence of the transition temperature, T_c, which varies much smoother around its maximum. Furthermore, the maximum J_c is achieved in an underdoped crystal, which differs from the crystal that exhibits the highest T_c. To describe this discrepancy J_c was expressed as the product of the pinning efficiency and the depairing current density. While the first of these two parameters is extrinsic and given by the prevailing defect structure, the latter is a material parameter depending on the superfluid density and the coherence length. We performed fast neutron irradiation on the crystals in order to find out whether the J_c peak results from intrinsic parameters or the particular defect landscape. Fast neutrons are known to introduce defects up to a size of a few nanometers, which have proven to be more efficient for flux pinning than the crystallographic defects in the pristine crystals. Thus the pinning efficiency after irradiation is very similar for all our samples and the doping dependence of J_c is determined by the doping dependence of the depairing current density. We find that the peak in J_c shifts to higher doping levels after the irradiation, broadens, and roughly follows the shape of the T_c curve. Moreover, a power law between J_c and T_c is observed in the irradiated crystals, which is expected from relations between fundamental parameters and T_c observed previously in iron-based superconductors. Since the power law does not hold for the pristine crystals, the doping dependence of J_c results from an enhanced pinning efficiency in the underdoped area of the phase diagram.

References:
1) S. Ishida, D. Song, H. Ogino, A. Iyo, H. Eisaki, M. Nakajima, J. Shimoyama, M. Eisterer, *Phys. Rev. B*, **95**, 014517 (2017)
2) D. Song, S. Ishida, A. Iyo, M. Nakajima, J. Shimoyama, M. Eisterer, and H. Eisaki, *Sci. Rep.* **6**, 26671 (2016)

Keywords: Iron-based superconductors, critical current density, pinning efficiency, neutron irradiation

PC4-1-INV

BCS-BEC crossover in FeSe

*Yuji Matsuda[1]

Department of Physics, Kyoto University, Sakyo-ku, Kyoto 606-8502, Japan[1]

There is growing evidence that superconducting semimetal FeSe (T_c=8 K) is deep in the crossover regime between weak coupling Bardeen-Cooper-Schrieffer (BCS) and strongcoupling Bose-Einstein condensate (BEC) limits. Therefore FeSe offers a unique and fascinating platform to study the crossover physics. Here we discuss several unique features which may provide new insights into fundamental aspects of the crossover. First is the observation of giant superconducting fluctuations by far exceeding the standard Gaussian theory. Second is the electronic structure. FeSe is a compensated semimetal, and hence it is essentially multiband superconductor, which makes the crossover physics in FeSe distinguished from that in ultracold atomic gases. Third concerns the fate of the superfluid when the spin populations are strongly imbalanced. In FeSe in the crossover regime, the Zeeman effect is especially effective in shrinking the Fermi volume associated with the spin minority. We show the emergence of a distinct field induced superconducting phase, which has an unprecedentedly large spinimbalance. We also discuss the evolution of superconducting gap anisotropy in $Fe(Se_{1-x}S_x)$, in which nematicity decreases with x.

In collaboration with Y. Sato, S. Kasahara, T. Taniguchi, (Department of Physics, Kyoto University), Y. Mizukami, O. Tanaka, T. Shibauchi (Department of Advanced Materials Science, University of Tokyo) T. Hashimoto, K. Okazaki, S. Shin (ISSP, University of Tokyo), and T. Hanaguri (RIKEN).

Keywords, Iron-chalcogenide, BCS-BEC crossover, Superconducting fluctuation

PC4-2-INV

Chemical pressure effects in iron chalcogenide superconductor FeSe

*Fuyuki Nabeshima[1]

The University of Tokyo, Japan[1]

Iron chalcogenide superconductor, FeSe, is considered to be an ideal material for investigating the relation between the superconductivity and the electronic nematicity in iron based superconductors (FeSCs) because it shows no long-range magnetic order at ambient pressure, while most of other FeSCs exhibits an antiferromagnetic transition at a temperature very near the nematic transition. Previously, we succeeded in suppressing the miscibility gap by growing thin films, and obtaining single crystalline samples of $FeSe_{1-x}Te_x$ in the whole composition region.[1,2] We found that the Te substitution suppresses the nematicity, and the superconducting transition temperature, T_c, increases drastically when the structural transition disappears. Another isovalent S substitution also suppresses the nematicity. However, such enhancement in T_c in the tetragonal phase is not observed in $FeSe_{1-y}S_y$ bulk samples. To clarify whether this difference is due to the difference between S and Te substitution or between film and bulk, we grew S-substituted FeSe thin films and measured their transport properties. Figure 1 shows the schematic phase diagram of $FeSe_{1-y}S_y$ and $FeSe_{1-x}Te_x$ thin films. The $FeSe_{1-y}S_y$ films shows T_c monotonically decreases with increasing S content even when the structural transition disappears, similar to bulk samples. The two contrasting behaviors of T_c at the NEP in these materials demonstrate that the role of the nematicity in superconductivity in iron chalcogenides is not universal, suggesting that the nematicity does not have the primary role in superconductivity in FeSe. [3]

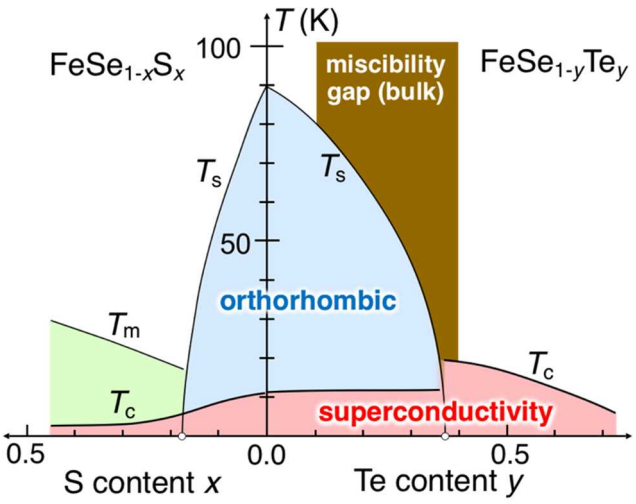

Fig. 1: Schematic phase diagram of FeSe1-xTex and FeSe1-ySy thin films.

[1] Y. Imai *et al.*, PNAS 112, 1937 (2015). [2] Y. Imai *et al.*, Sci. Rep. 7, 46653 (2017).
[3] F. Nabeshima *et al.*, JPSJ 87, 073704 (2018).

PC4-3

Vortex Dynamics in Isovalent Optimally Doped Pnictide Superconductor $BaFe_2(As_{0.68}P_{0.32})_2$ investigated by AC and DC magnetic measurements

*Adrian Crisan[1], Alina M Ionescu[1], Lucica Miu[1]

National Institute of Materials Physics Bucharest, 405A Atomistilor Street, 077125 Magurele, Romania[1]

We have investigated high-quality single crystals of isovalent optimally doped pnictide superconductor $BaFe_2(As_{0.68}P_{0.32})_2$ using DC magnetization, DC relaxation and frequency and amplitude dependent AC susceptibility measurements. Such single crystals have a very rich diagram of vortex matter with a pronounced second magnetization peak [1]. Our DC magnetization measurements up to 14 T revealed intersections between various isothermal magnetization curves, meaning that, for a fixed H, there is an increasing magnetization with increasing temperature, in a certain temperature range. In addition, AC susceptibility measurements show impressive anomalies, as seen in Fig. 1.
It can be seen that, in 1T, the diamagnetic response have a clear anomalous decrease with decreasing temperature between 25 and 22 K. Dissipation response has a complex feature, depending on the cooling/warming regime. Measurements done with a lower ac field amplitude revealed a Campbell regime, in which the movement of vortices is within the pinning potential well. Such measurements were performed also at 3, 5, and 7 T, the features being reproduced qualitatively (at 7 T the height of the anomalous peak decreasing), as well as on a different crystal from the same batch, with similar results. Magnetic relaxation measurements also showed anomalous behavior, suggesting various elastic/plastic creep regimes of vortex dynamics.

References
[1] S. Salem-Sugui Jr, J. Mosqueira, A. D. Alvarenga, D. Sóñora, A. Crisan, A. M. Ionescu, S. Sundar, D. Hu, S-L. Liand H-Q. Luo, Supercond. Sci. Technol. 30 (2017) 055003.

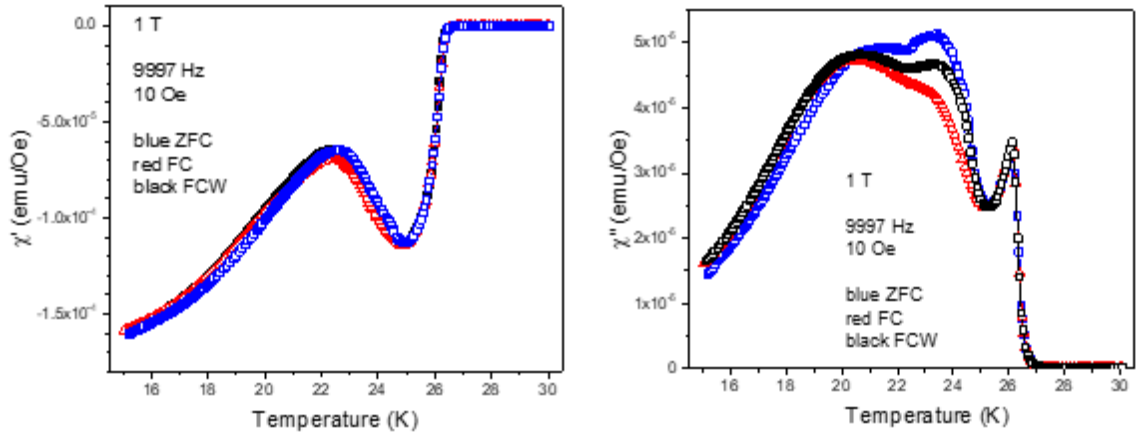

Figure Caption:
Fig. 1: *Temperature dependence of in-phase (left) and out-of-phase (right) susceptibility in 1 T.*

Keywords: vortex dynamics, pnictides, second mgnetisation peak, AC susceptibility

PC4-4

Effect of in-plane strain on charge dynamics in FeSe

*Masamichi Nakajima[1], Kazuya Yanase[1], Yuki Senoo[1], Masataka Kawai[2], Tomoya Ishikawa[2], Naoki Shikama[2], Fuyuki Nabeshima[2], Atsutaka Maeda[2], Setsuko Tajima[1]

Osaka University, Japan[1]
The University of Tokyo, Japan[2]

In iron-based superconductors, the electronic structure is strongly affected by in-plane strain. In particular, the band structure of FeSe thin films differs from that of bulk FeSe due to the epitaxial strain [1]. The correlation between a superconducting transition temperature (T_c) and the magnitude of strain indicates that the band-structure modification definitely altered physical properties [2], but how the electronic state changes with application of strain is still unclear.
To investigate the effect of in-plane strain on charge dynamics, we performed infrared spectroscopy on thin films of FeSe with different substrates. The spectral weight of the coherent Drude component, which is responsible for the coherent conduction channel, gradually decreases with decreasing temperature in the low-temperature orthorhombic phase [3]. With applying tensile strain, the coherent Drude weight decreases, which is likely related to the suppression of T_c. For the film on $LaAlO_3$ substrate with a tensile strain, we observed a transfer of the spectral weight below ~ 500 cm^{-1} to a higher energy region. This behavior, distinct from the charge dynamics of FeSe with compressive strain, will be discussed in light of the change in the band structure.

[1] G. N. Phan *et al.*, Phys. Rev. B **95**, 224507 (2017).
[2] F. Nabeshima *et al.*, arXiv:1806.05436.
[3] M. Nakajima *et al.*, Phys. Rev. B **95**, 184502 (2017).

Keywords: Iron-based superconductors, Optical spectroscopy, Thin films

PC5-1-INV

Genes of Unconventional High Temperature Superconductors

*Jiangping Hu[1, 2]

Beijing National Laboratory for Condensed Matter Physics, and Institute of Physics, Chinese Academy of Sciences, Beijing, 100190, People's Republic of China[1]
University of Chinese Academy of Science, Beijing, 100049, People's Republic of China[2]

In the past, both cuprates and iron-based high temperature superconductors (High Tc) were discovered accidentally. Lacking of successful predictions on new high Tc is one of major obstacles to reach a consensus on unconventional high Tc mechanism. In this talk, we address the key question related to these two special materials: Why are Cu and Fe special? We answer this question by suggesting a common electronic gene behind these two families of materials. The common electronic gene explains their rareness as unconventional high Tc superconductors and can guide us to search for new high Tc materials. We extend this idea to predict possible unconventional high Tc superconductors. Verifying the prediction can convincingly establish high Tc superconducting mechanism and pave a way to design new high Tc superconductors.

References

[1]. JP Hu et al, Phys. Rev. X 5, 041012 (2015).
[2]: JP Hu, Sci. Bull. 61, 561(2016)
[3]: JP Hu and CC Le, Sci. Bull. 62, 212 (2017)
[4]: CC Le, et al, arXiv:1712.05962 (2017)

PC5-2-INV

Superconductivity in $REO_{0.5}F_{0.5}BiS_2$ with high-entropy-alloy-type RE site

*Yoshikazu Mizuguchi[1], Ryota Sogabe[1], Yosuke Goto[1]

Tokyo Metropolitan University[1]

We have synthesized BiS_2-based superconductors with high-entropy-alloy-type (HEA-type) REO (RE: rare earth) blocking layers [1]. In the HEA-type samples, the RE site of $REO_{0.5}F_{0.5}BiS_2$ was occupied with five RE elements with a compositional range of 5–35%. The background concept of the study on HEA-type $REO_{0.5}F_{0.5}BiS_2$ is a normal HEA, which was proposed by Yeh et al. as an alloy containing at least 5 elements with concentrations between 5 and 35 atomic percent. In HEA-type $REO_{0.5}F_{0.5}BiS_2$, the HEA concept was extended to layered compounds. Notably, the superconducting properties seemed to be enhanced by making HEA-type REO blocking layer as compared to the BiS_2-based superconductors with a conventional REO blocking layer.
In this presentation, the superconducting properties and crystal structure evolution of the HEA-type REO0.5F0.5BiS_2 will be presented. In addition, the relationship between the mixing entropy and local structure is discussed on the basis of structural analysis with synchrotron X-ray diffraction data [2].

[1] R. Sogabe, Y. Goto, and Y. Mizuguchi, Appl. Phys. Express 11, 053102 (2018).
[2] R. Sogabe et al., arXiv:1808.04090.

PC5-3-INV

Exploration for novel superconductors in transition metal compounds

*Zhi An Ren[1]

Beijing National Laboratory for Condensed Matter Physics, and Institute of Physics, Chinese Academy of Sciences, Beijing, 100190,China[1]

The strongly correlated electrons in the transition metal compounds often exhibit various intriguing physical phenomena at low temperatures, and the most fascinating example is the coherent electron pairing for exotic superconductivity. Before the discovery of high-T_c superconductivity in cuprates, there were a large number of molybdenum chalcogenide superconductors $M_xMo_6X_8$ and $M_2Mo_6X_6$ (X = S, Se, or Te) discovered from the early 1970's, which also known as the Chevrel phases. And in 2015, a new family of chromium arsenide based quasi-one-dimensional superconductors $A_2Cr_3As_3$ (A = K, Rb or Cs) were reported with spin-triplet electron pairing suggested. Is there some common underlying origin for the occurrence of superconductivity in these group VIB transition metal compounds? Here we will report our recent discovery of superconductivity in several Cr/Mo related compounds that contain similar quasi-one-dimensional chain structures, which include the 133-type ACr_3As_3 (A = K, Rb) superconductors, the 233-type $Na_2Cr_3As_3$ superconductor with a T_c at 8.6 K, and the first MoAs-based $A_2Mo_3As_3$ (A = K, Rb, Cs) superconductors with higher T_c above 10 K. Besides, several novel superconductors in other transition metal compounds will also be reported.

Keywords: novel superconductors, K2Mo3As3, KCr3As3, Na2Cr3As3

PC5-4

Carrier doping effect on superconductivity of newly synthesized $La_2O_2M_4S_6$-(M=Bi, Ag) type compounds

*Rajveer Jha[1], Yosuke Goto[1], Yoshikazu Mizuguchi[1]

Tokyo Metropolitan University, 1-1 Minami-Osawa, Hachioji, Tokyo, Japan[1]

Recently, we have reported the superconductivity in the layered oxychalcogenide $La_2O_2Bi_3AgS_6$ compound [1]. Firstly, the $La_2O_2Bi_3AgS_6$ compound has been reported by our group for structural and other electronic properties [2]. This compound has the tetragonal structure with the space group $P4/nmm$. The estimated lattice parameters are a = 4.0568(1) Å and c = 19.348(1) Å. The crystal structure of $La_2O_2Bi_3AgS_6$ can be regarded as alternate stacks of the $LaOBiS_2$-type layer and rock-salt-type (Bi,Ag)S layer. We measured the electrical resistivity down to 0.1 K using an adiabatic demagnetization refrigerator (ADR) system. We observed superconductivity in $La_2O_2Bi_3AgS_6$ compound at T_c^{zero} = 0.5 K. Remarkably, we observed a broad hump in temperature dependence of electrical resistivity $\rho(T)$ curve below T^*~180 K, which is quite similar to the hump observed in the $\rho(T)$ curve below ~280 K for $EuFBiS_2$ compound, which shows superconductivity at 0.3 K [4].
The origin of the hump in the $\rho(T)$ curve was proposed as the charge density wave (CDW) transition in $EuFBiS_2$. From the analogy, we assume that the anomaly is caused by a CDW. In this ISS2018 abstract we are focusing on the carrier doping effect on the superconductivity of the $La_2O_2Bi_3AgS_6$ compound. We suppose that the CDW transition suppressed with carrier doping in resulting the enhancement of superconductivity of the $La_2O_2Bi_3AgS_6$ compound. We will present the main results in the ISS2018 proceeding.

References
1. R. Jha, Y. Goto, R. Higashinaka, T. D. Matsuda, Y. Aoki and Y. Mizuguchi, J. Phys. Soc. Jpn. **87**, 083704 (2018).
2. Y. Hijikata, T. Abe, C. Moriyoshi, Y. Kuroiwa, Y. Goto, A. Miura, K. Tadanaga, Y. Wang, O. Miura, and Y. Mizuguchi, J. Phys. Soc. Jpn. **86**, 124802 (2017).
3. H.-F. Zhai, Z.-T. Tang, H. Jiang, K. Xu, K. Zhang, P. Zhang, J.-K. Bao, Y.-L. Sun, W.-H. Jiao, I. Nowik, I. Felner, Y.-K.Li, X.-F. Xu, Q. Tao, C.-M. Feng, Z.-A. Xu, and G.-H. Cao, Phys. Rev. B **90**, 064518 (2014).
4. Y.-L. Sun, A. Ablimit, H.-F. Zhai, J.-K. Bao, Z.-T. Tang, X.-B. Wang, N.-L. Wang, C.-M. Feng, and G.-H. Cao, Inorg. Chem. **53**, 11125 (2014).

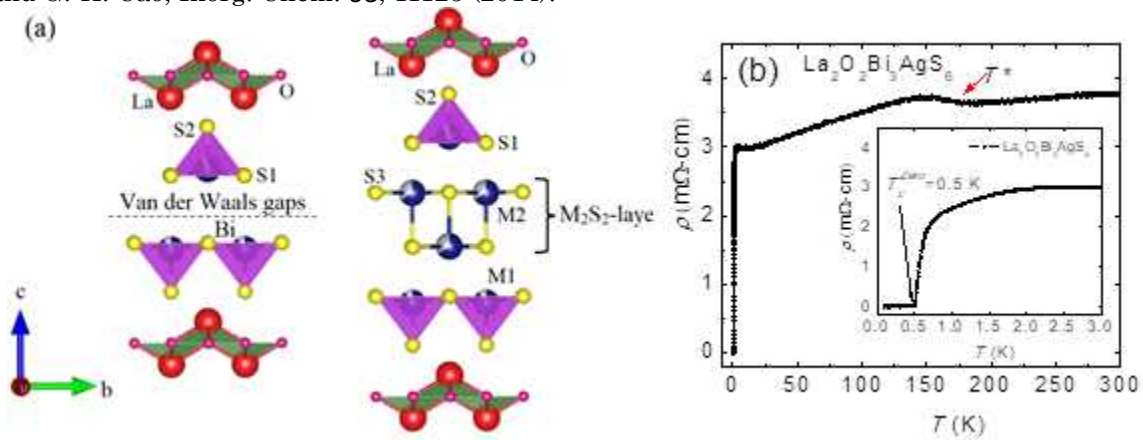

Fig. 1. (a) The schematic unit cell for $LaOBiS_2$ and $La_2O_2Bi_3AgS_6$. (b) The $\rho(T)$ from 300 to 0.1 K for the $La_2O_2Bi_3AgS_6$ compound, Inset is the $\rho(T)$ curve in the temperature range 3.0 to 0.1 K.

Keywords: BiS2 based superconductivity, Charge Density Wave, Electrical Resistivity

PC5-5

Quasi-particle evidence for the nematic state above superconductivity in $Sr_xBi_2Se_3$

*Yue Sun[1], Shunichiro Kittaka[2], Toshiro Sakakibara[2], Tsuyoshi Tamegai[3], Kazushige Machida[4], Jinghui Wang[5], Jinsheng Wen[5]

Department of Physics and Mathematics, Aoyama Gakuin University, Japan[1]
Institute for Solid State Physics, The University of Tokyo, Japan[2]
Department of Applied Physics, The University of Tokyo, Japan[3]
Department of Physics, Ritsumeikan University, Japan[4]
Department of Physics, Nanjing University, China[5]

Electronic nematic state characterized by a lowered symmetry of the electronic system compared to the underlying lattice has been observed in various unconventional superconductors such as the copper- and iron-based superconductors, the heavy fermion superconductors, and the topological superconductors. The relation between nematicity and superconductivity is a key issue in condensed matter physics, and still remains an open question. In this report, we show a bulk quasi-particle evidence for the nematicity in topological superconductor $Sr_xBi_2Se_3$ through the angle-resolved specific heat measurements. A clear two-fold symmetry in the specific heat was observed in spite of the six-fold symmetric lattice. More interesting, the two-fold symmetry is also observed in the normal state above the superconductivity, which is different from the similar compound $Cu_xBi_2Se_3$, where the nematicity exists only in the superconducting state. Such results highlight the interrelation of nematicity and unconventional superconductivity. The bulk quasi-particle evidence from specific heat also indicates the non-Fermi liquid behavior in the nematic state.

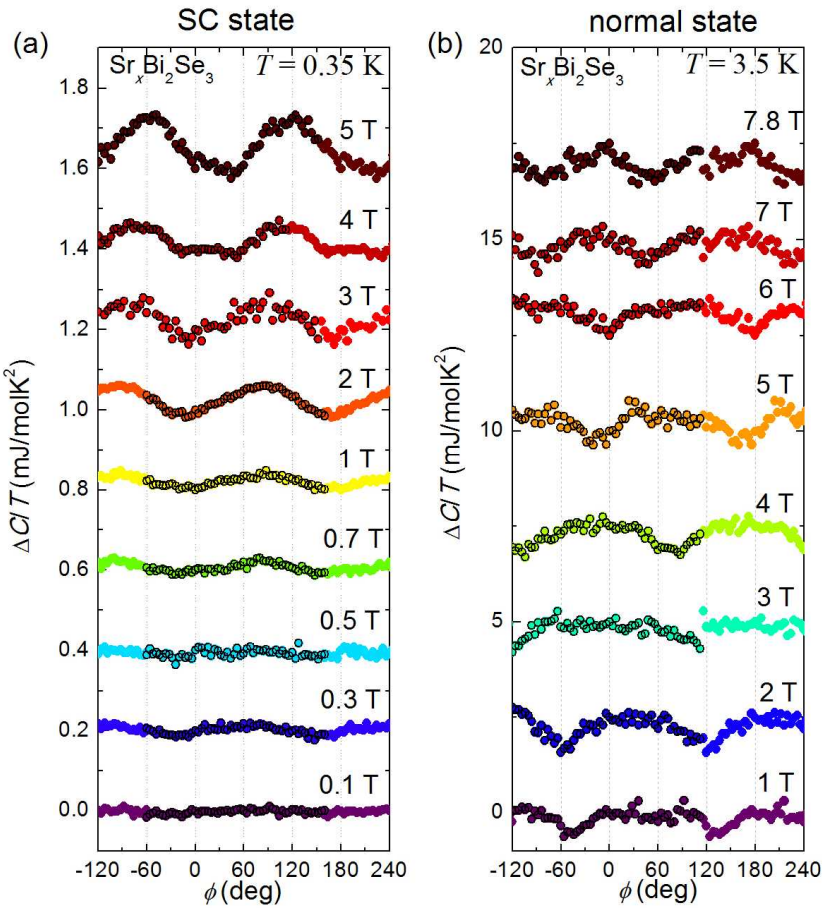

Figure caption: In-plane field-angle dependences of $\Delta C/T$ for $Sr_xBi_2Se_3$ in the (a) superconducting state at 0.35 K and (b) normal state at 3.5 K.

Keywords: nematicity, topological superconductor, SrxBi2Se3, angle-resolved specific heat

PC5-6

Determination of the Pairing State in a Superconducting Doped Topological Insulator $Sr_xBi_2Se_3$

*Takaaki Takenaka[1], Yijie Miao[1], Kota Ishihara[1], Yuta Mizukami[1], Marcin Konczykowski[2], Kazumune Tachibana[3], Takao Sasagawa[3], Takasada Shibauchi[1]

University of Tokyo, Japan[1]
Ecole Polytechnique, France[2]
Tokyo Institute of Technology, Japan[3]

Superconducting doped bismuth selenide (Bi_2Se_3) is a promising candidate of topological superconductors. For Cu, Nb, and Sr-doped Bi_2Se_3, many studies try to identify the pairing symmetry, which is a direct consequence of pairing mechanism, but no common understanding is established so far. Most remarkably, recent studies indicate that these materials have spontaneous rotational symmetry breaking (SRSB) in the gap function, which is called nematic superconductivity.

Among pairing symmetries proposed for superconducting doped Bi_2Se_3, only the odd-parity pairings with E_u representation generate SRBS in the superconducting gap. Eu pairing states allow two kinds of gap structures, $\Delta 4_x$ state with point nodes along k_y direction and $\Delta 4_y$ state with gap minima along kx direction. These two states can be distinguished from the measurements which are sensitive to low-energy quasiparticle excitations.

Here we report the magnetic penetration depth measurements in several samples of Sr-doped Bi_2Se_3 down to 40 mK measured by the tunnel-diode oscillator technique. All samples show a power-law behavior $(n=1\text{-}2)$ down to $0.05T_c$ indicating strong momentum dependence of the gap. However, the data give much higher exponent n>3 at the lowest temperature region below $0.05T_c$. Our data can be explained if tiny but finite gap minima exist on Fermi surface. Furthermore, we test the impurity effect in $Sr_xBi_2Se_3$, which is a sensitive probe of the sign change in the gap function. We observe the suppression of transition temperature by increasing the impurity concentration, but we find that low-energy quasiparticle excitation is robust against disorder. This result is consistent with the theoretical suggestion for $\Delta 4$ state. From the all experimental results, we conclude that the pairing state in $Sr_xBi_2Se_3$ is consistent with the odd-parity $\Delta 4y$ symmetry.

Keywords: Unconventional Superconductivity, Pairing Symmetry, Penetration Depth, Impurity Effect

PC5-7

Discovery of New Pressure-induced Superconductors Explored by Data-driven Approach

*Ryo Matsumoto[1,2], Zhufeng Hou[1], Hiroshi Hara[1,2], Masanori Nagao[3], Shintaro Adachi[1], Hiromi Tanaka[4], Tetsuo Irifune[5], Hiroyuki Takeya[1], Kiyoyuki Terakura[1], Yoshihiko Takano[1,2]

National Institute for Materials Science[1]
University of Tsukuba[2]
University of Yamanashi[3]
National Institute of Technology, Yonago College[4]
Geodynamics Research Center, Ehime University[5]

It has been recently started a use of a data-driven approach by a high-throughput computing for exploring new functional materials such as thermoelectric materials, superconductors, and so on, instead of a traditional carpet-bombing type experiment depending on experiences and inspirations of researcher. In this study, the candidates for new thermoelectric and superconducting materials, which have narrow band gaps and flat bands near band edges, were searched by high-throughput first-principles calculation from an inorganic materials database [1]. The synthesized $SnBi_2Se_4$ among the target compounds showed a narrow band gap of 200 meV and a thermal conductivity of ~1 $W \cdot K^{-1} \cdot m^{-1}$ at ambient pressure. As shown in Fig. 1, the $SnBi_2Se_4$ showed a metal–insulator transition at 11.1 GPa, as predicted by theoretical estimation. Furthermore, two pressure-induced superconducting transitions were discovered under 20.2 and 47.3 GPa. The data-driven search is a promising approach to discovering new functional materials. In the conference, a discovery of superconductivity in the other candidate $PbBi_2Te_4$ [2] will be also reported.

[1] R. Matsumoto et al., *Appl. Phys. Express* **11**, 093101 (2018).
[2] R. Matsumoto et al. arXiv:1808.07973.

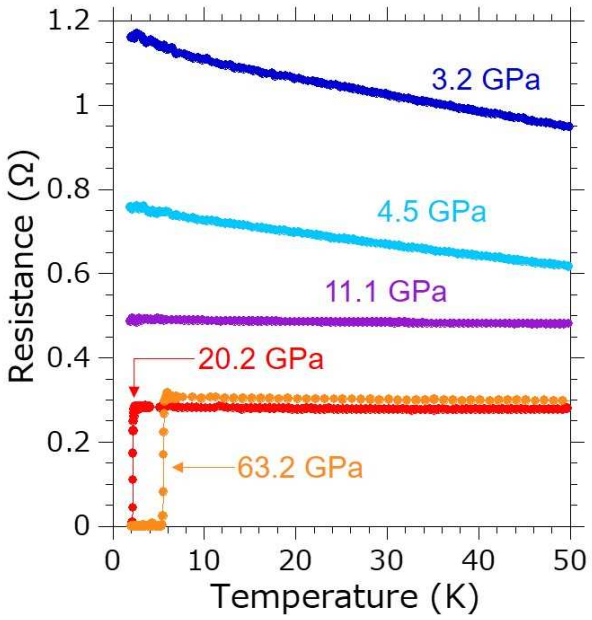

Fig. 1. R-T properties under high pressure of $SnBi_2Se_4$.

Keywords: Data-driven, Diamond Anvil Cell, High Pressure

PC5-8

Low-Energy Quasiparticle Excitations in Half-Heusler Superconductors with j=3/2 Fermions

*Kota Ishihara[1], Takaaki Takenaka[1], Yijie Miao[1], Yuta Mizukami[1], Orest Pavlosiuk[2], Piotr Wiśniewski[2], Dariusz Kaczorowski[2], Takasada Shibauchi[1]

Department of Advanced Materials Science, University of Tokyo[1]
Polish Academy of Sciences[2]

In noncentrosymmetric half-Heusler compounds, where the strong spin-orbit coupling causes a band inversion, fermions with total angular momentum j=3/2 contribute mainly the transport phenomena [1,2], including the superconductivity [3]. Interestingly, Cooper pairs formed by the j=3/2 fermions can form not only usual singlet and triplet states but also even-parity quintet (five-fold degenerate) and odd-parity septet (seven-fold degenerate) states [3]. Moreover, these unconventional pairings can lead to a topological nodal structure on the superconducting gap or the surface state [4].
Recently, it has been reported that the temperature dependence of magnetic penetration depth reflecting the low-energy quasiparticle excitations shows a power-law behavior in YPtBi, which suggests an unconventional gap structure [5]. Since mixed parity states are allowed by the lack of inversion symmetry, the mixed singlet-septet state with line nodes is proposed in YPtBi. On the other hand, a recent study indicates that time-reversal-symmetry breaking quintet pairings with Weyl points can also be consistent with the power-law behavior if nonmagnetic impurity scattering is sufficient [4]. Therefore, further studies on the superconducting gap structure in half-Heusler compounds are required.
Here, we will show the results of magnetic penetration depth measurements on YPtBi, LuPtBi, and LuPdBi. Our data suggest that the nodal structure of the gap function is not protected by symmetries. We would like to discuss universal gap structure of nonmagnetic half-Heusler superconductors.

[1] S. Chadov *et al.*, Nat. Mater. **9**, 541 (2010).
[2] H. Lin *et al.*, Nat. Mater. **9**, 546 (2010).
[3] P. M. R. Brydon *et al.*, Phys. Rev. Lett. **116**, 177001 (2016).
[4] B. Roy *et al.*, arXiv:1708.07825 (2017).
[5] H. Kim *et al.*, Sci. Adv. **4**, eaao4513 (2018).

Keywords: magnetic penetration depth, half-Heusler, j=3/2 fermions, spin-orbit coupling

PC6-1-INV

Superconductivity in light-driven materials

*Philipp Werner[1], Yuta Murakami[1], Hugo Strand[2], Shintaro Hoshino[3], Martin Eckstein[4]

Department of Physics, University of Fribourg, 1700 Fribourg, Switzerland[1]
Center for Computational Quantum Physics, Flatiron Institute, 162 Fifth Avenue, New York, NY 10010, USA[2]
Department of Physics, Saitama University, Saitama 338-8570, Japan[3]
Department of Physics, University Erlangen-Nuernberg, 91058 Erlangen, Germany[4]

The prospect of nonequilibrium control of material properties has caught the interest of the condensed matter community. In particular, recent experiments demonstrating a light-enhanced superconducting-like state in cuprates [1] and fulleride compounds [2] has triggered a number of theoretical studies on order parameter dynamics in lattice systems perturbed by periodic driving or strong quasi-static fields [3-7].

Here, we use the nonequilibrium dynamical mean field theory in a Kadanoff-Baym and Floquet implementation [8] to address some relevant issues, which have been ignored in previous studies. In particular, we will consider parametric phonon driving in the Holstein model, and show that the nonthermal energy distribution in the driven state generically leads to a weakening of the superconducting order [9].

As a second example, we will discuss the pairing susceptibility in a photo-doped Mott insulator [10]. In these systems, a large fraction of the injected energy is stored as potential energy and the charge fluctuations enabled by the photo-carriers indeed results in an enhanced pairing tendency, but the effect is not sufficient to trigger an actual symmetry breaking.

[1] S. Kaiser, C. R. Hunt, D. Nicoletti, W. Hu, I. Gierz, H. Y. Liu, M. Le Tacon, T. Loew, D. Haug, B. Keimer, and A. Cavalleri, Phys. Rev. B 89, 184516 (2014).
[2] M. Mitrano, A. Cantaluppi, D. Nicoletti, S. Kaiser, A. Perucchi, S. Lupi, P. Di Pietro, D. Pontiroli, M. Ricc, S. R. Clark, D. Jaksch, and A. Cavalleri, Nature 530, 461 (2016).
[3] M. Kim, Y. Nomura, M. Ferrero, P. Seth, O. Parcollet and A. Georges, Phys. Rev. B 94, 155152 (2016).
[4] A. Komnik and M. Thorwart, Eur. Phys. J. B 89, 244 (2016).
[5] J. Okamoto, A. Cavalleri and L. Mathey, Phys. Rev. Lett. 117, 227001 (2016).
[6] M. Babadi, M. Knap, I. Martin, G. Refael, and E. Demler, Phys. Rev. B 96, 014512 (2017).
[7] D. M. Kennes, E. Y. Wilner, D. R. Reichman and A. J. Millis, Nat Phys 13, 479 (2017).
[8] H. Aoki, N. Tsuji, M. Eckstein, M. Kollar, T. Oka, and P. Werner, Rev. Mod. Phys. 86, 779 (2014).
[9] Y. Murakami, N. Tsuji, M. Eckstein, and P. Werner, Phys. Rev. B 96, 045125 (2017)
[10] P. Werner, H. Strand, S. Hoshino, Y. Murakami, and M. Eckstein, Phys. Rev. B 97, 165119 (2018)

PC6-4-INV

Higgs Amplitude Mode in Superconductors Studied by Nonlinear Terahertz Spectroscopy

Ryusuke Matsunaga[1,2]

The Institute for Solid State Physics, The University of Tokyo, Japan[1]
PRESTO, Japan Science and Technology Agency, Japan[2]

We show our recent studies of ultrafast dynamics in superconductors by using intense terahertz pulse. Collective amplitude mode of superconducting order parameter, namely the Higgs mode, has been recently observed in *s*-wave superconductors $Nb_{1-x}Ti_xN$ [1,2]. The Higgs mode has evaded experimental detection for a long time because of the absence of interaction with electromagnetic wave in linear response regime, except for $NbSe_2$ where coexisting charge-density-wave order make the Higgs mode Raman-active [3]. But intense terahertz pulse recently realized on tabletop experiments can drive the system out of equilibrium, and the Higgs mode can be observed in nonequilibrium as an oscillation of response function in time in pump-probe spectroscopy [1], and third-harmonic generation with resonant enhancement when twice the incident terahertz frequency coincides with the Higgs mode frequency [2]. Although the resonant enhancement of third harmonic generation could occur even without the collective mode, our recent studies with polarization-resolved terahertz nonlinear transmission spectroscopy has revealed isotropic properties of third-harmonic generation [4], which indicates that the collective Higgs mode plays a dominant role on the terahertz nonlinear response of superconductors. The polarization-resolved nonlinear terahertz spectroscopy has also revealed the Higgs mode in a *d*-wave cuprate superconductor $Bi_2Sr_2CaCu_2O_{8+x}$ [5].

[1] R. Matsunaga *et al.* Phys. Rev. Lett. 111, 057002 (2013).
[2] R. Matsunaga *et al.* Science 345, 1145 (2014).
[3] R. Sooryakumar and M. V. Klein, Phys. Rev. Lett. 45, 660 (1980); P. B. Littlewood and C. M. Varma, Phys. Rev. Lett. 47, 811 (1981).
[4] R. Matsunaga *et al.*, Phys. Rev. B 96, 020505(R) (2017).
[5] K. Katsumi *et al.*, Phys. Rev. Lett. 120, 117001 (2018).

PC7-1-INV

The Renaissance of high-T_c superconductivity
— Discovery of undoped cuprate superconductors and revise of the electronic phase diagram

*Michio Naito[1], Yoshiharu Krockenberger[2], Ai Ikeda[2], Hideki Yamamoto[2]

Department of Applied Physics, Tokyo University of Agriculture and Technology[1]
NTT Basic Research Laboratories, NTT Corporation[2]

More than 30 years have passed since the discovery of high-T_c superconducting copper oxides. While the mechanism of the high-T_c superconductivity still remains elusive, the electronic phase diagram is a key ingredient to understand it. It has been believed that parent compounds of cuprates *were* universally antiferromagnetic Mott insulators and that superconductivity *would* develop upon doping either holes or electrons in the insulators ("doped Mott-insulator scenario"). However, our recent discovery of superconductivity in the parent and heavily-underdoped compounds with the Nd_2CuO_4 (T') structure urged a serious reassessment to the above scenario. We first overview our experimental results over a decade for the T' cuprates: one representative is illustrated in Figure that the T_c continues to increase down to the undoped state. Next we discuss their implications. The key material issue in square-planar cuprates is to remove excess oxygen ions residing in the interstitial apical sites without introducing oxygen vacancies in the CuO_2 planes (= the playground of high-T_c superconductivity) by elaborate synthesis procedures. During almost same period as our experimental works, there has been significant progress also in the electronic-structure calculation techniques. Unlike 30 years ago, it is now possible to predict the coordination-dependent different ground states between T- and T'-La_2CuO_4: Cu is octahedral and square-planar coordinated in the T and T' structures, respectively. High-T_c superconductivity remains confined, at least at present, only to copper oxides. Reassessment of the electronic state by the state-of-the-art calculation methods may unveil unique features of copper oxides not shared by other transition-metal oxides.

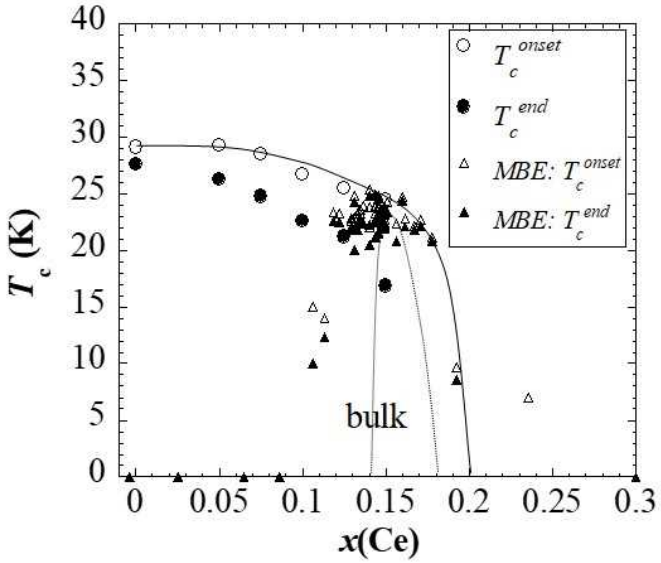

Figure caption:
T_c-versus-x of $Nd_{2-x}Ce_xCuO_4$ films prepared by MOD (metal-organic decomposition). For a comparison, the data of bulk samples (broken line) and MBE films (triangles) are also plotted. Open and filled symbols represent T_c^{onset} and T_c^{end}.

Keywords: Undoped cuprate superconductors, K2NiF4 vs Nd2CuO4 structure, Broken electron-hole symmetry , Doped Mott-insulator scenario

PC7-2-INV

Engineering the Mott State of Cuprates for High-Temperature Superconductivity

O. Ivashko[1], M. Horio[1], W. Wan[2], N. B. Christensen[2], D. E. McNally[3], E. Paris[3], Y. Tseng[3], N. E. Shaik[4], H. M. Rønnow[4], H. I. Wei[5], C. Adamo[6], C. Lichtensteiger[7], M. Gibert[1], M. R. Beasley[6], K. M. Shen[5], J. M. Tomczak[8], T. Schmitt[3], *J. Chang[1]

Physik-Institut, Universit¨at Zu¨rich, Winterthurerstrasse 190, CH-8057 Zurich, Switzerland[1]
Department of Physics, Technical University of Denmark, DK-2800 Kongens Lyngby, Denmark[2]
Swiss Light Source, Paul Scherrer Institut, CH-5232 Villigen PSI, Switzerland[3]
Institute of Physics, Ecole Polytechnique Federale de Lausanne (EPFL), CH-1015 Lausanne, Switzerland[4]
Department of Physics, Laboratory of Atomic and Solid State Physics, Cornell University, Ithaca, New York 14853, USA[5]
Department of Applied Physics, Stanford University, Stanford, CA 94305, USA[6]
Department of Quantum Matter Physics, University of Geneva, 24 Quai Ernest Ansermet, 1211 Geneva, Switzerland[7]
Institute of Solid State Physics, Vienna University of Technology, A-1040 Vienna, Austria[8]

Recent synchrotron (RIXS and ARPES) experiments on La-based cuprates will be presented [1-4]. The talk is taking basis on the recent identification of the dz2 band in overdoped $La_{2-x}Sr_xCuO_4$ (LSCO) [1]. Implications on superconductivity and pseudogap physics from of the resulting the Fermi surface structure (in- and out-of-plane) and orbital hybridization will be discussed. Topological aspects of the LSCO is being touch briefly [3]. Finally, the engineering of this electronic structure let us to find that the magnetic exchange interaction in La_2CuO_4 films can be tuned through strain [4]. We noticed that films with the largest exchange interaction also has the highest superconducting transition T_c upon doping – consistent with a magnetic pairing scenario.

References

[1] C.E. Matt et al., Nat. Comm. 9, 972 (2018)
[2] M. Horio et al., Nat. Comm. 9, 3252 (2018)
[3] M. Horio et al., PRL 121, 77004 (2018)
[4] O. Ivashko et al., arXiv:1805.07173 (2018)

PC7-3-INV

Exotic Z2 Symmetry Breaking Transitions: theory of pseudo-gap transitions

Sangjin Lee[1], Jun Jung[1], Ara Go[2], *Eun-Gook Moon[1]

Department of Physics, KAIST, Daejeon 34141, Korea[1]
Center for Theoretical Physics of Complex Systems, IBS, Daejeon 34051, Korea[2]

The Landau paradigm of phase transitions is one of the backbones in critical phenomena. With a Z_2 symmetry, it describes the Ising universality class whose central charge is one half (c = 1/2) in two spatial dimensions (2D). Recent experiments in strongly correlated systems, however, suggest intriguing possibilities beyond the Landau paradigm. We uncover an exotic universality class of a Z_2 symmetry breaking transition with c=1. It is shown that fractionalization of discrete symmetry order parameters may realize the exotic class. In addition to novel critical exponents, we find that the onset of an order parameter may be super-linear in contrast to the sub-linear onset of the Ising class. We argue that a super-linear onset of a Z_2 order parameter without breaking a bigger symmetry than Z_2 is evidence of exotic phenomena, and our results are applied to recent experiments in phase transitions at pseudo-gap temperatures.

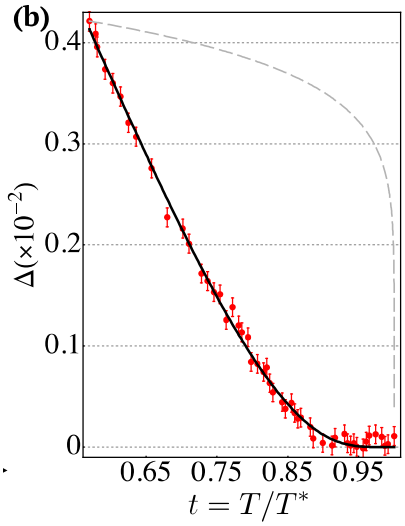

Fig. 1: *Order parameter onset of the proposed exotic Z2 transition. Data (red dots) fitting of the magneto-torque experiment [2] is presented. The dashed line is a typical onset of the Ising class.*

References

[1]. S. J. Lee, arXiv: 1803.00578 (2018).
[2]. Y. Sato et. al., Nature Physics 13, 1074 (2017).

PC7-4

Spin and Charge Excitations along the Direction Perpendicular to Charge Stripes in Cuprates

*Takami Tohyama[1]

Department of Applied Physics, Tokyo University of Science, Tokyo 125-8585, Japan[1]

The ground state of the *t*-*t*′-*J* ladder with four legs favors a striped charge distribution for the parameters corresponding to hole-doped cuprate superconductors. We investigate the dynamical spin and charge structure factors of a 24×4 *t*-*t*′-*J* ladder by using dynamical density-matrix renormalization group (DMRG) and clarify the influence of stripes on the structure factors [1]. The dynamical charge structure factor along the momentum direction from **q**=(0,0) to (π,0) perpendicular to the stripes clearly shows low-energy excitations corresponding to the stripe order in hole doping. On the other hand, the stripe order weakens in electron doping, resulting in less low-energy excitations in the charge channel. In spin channel, spin excitations are strongly influenced by the stripes in hole doping, resulting in two branches that form a discontinuous behaviour in the dispersion. In contrast, the electron-doped systems show a downward shift in energy toward (π,0). These behaviours along the (0,0)-(π,0) direction are qualitatively similar to momentum-dependent spin excitations recently observed by resonant inelastic x-ray scattering experiments in hole-doped [2] and electron-doped [3] cuprate superconductors.

[1] T. Tohyama, M. Mori, and S. Sota, Phys. Rev. B **97**, 235137 (2018).
[2] H. Miao *et al.*, PNAS **114**, 12430 (2017).
[3] K. Ishii *et al.*, Nat. Commun. **5**, 3714 (2014).

Keywords: Charge stripes, Cuprate superconductors, t-t'-J model, RIXS

PC7-5

Three-Dimensional Fermi Surface of Overdoped La-Based Cuprates

*Masafumi Horio[1], Kevin Hauser[1], Yasmine Sassa[2], Zarina Mingazheva[1], Denys Sutter[1], Kevin Kramer[1], Ashely M. Cook[1], Elisabetta Nocerino[3], Ola K. Forslund[3], Oscar Tjernberg[3], Masaki Kobayashi[4], Alla Chikina[4], Niels B. M. Schröter[4], Jonas A. Krieger[4], Thorsten Schmitt[4], Vladimir N. Strocov[4], Sunseng Pyon[5], Tomohiro Takayam[5], Hidenori Takagi[5], O. J. Lipscombe[6], Stephen M. Hayden[6], Motoyuki Ishikado[7], Hiroshi Eisaki[8], Titus Neupert[1], Martin Månsson[3], Christian E. Matt[1], Johan Chang[1]

Univ. of Zurich, Swizerland[1], Uppsala Univ., Sweden[2], KTH Royal Inst. of Technology, Sweden[3], Paul Scherrer Inst., Swizerland[4], Univ. of Tokyo, Japan[5], Univ. of Bristol, UK[6], Comprehensive Research Organization for Science and Society (CROSS), Japan[7], National Institute of Advanced Industrial Science and Technology, Japan[8]

The nature of the pseudogap in cuprates remains an outstanding issue. Recently, a connection between van-Hove singularity (VHS) and pseudogap collapse as a function of doping has been proposed both experimentally [1] and theoretically [2]. In this scenario, pseudogap exists only on a hole-like Fermi surface and vanishes when the Fermi surface turns electron-like with hole overdoping. In La-based cuprates, it is known that around this doping the electronic specific heat is dramatically enhanced [3]. This enhancement could be a signature of quantum criticality associated with the pseudogap collapse, but could also arise simply from VHS density-of-states (DOS) divergence. The latter scenario is expected to be significant in quasi-two-dimensional band structure where the VHS is well defined. It has thus become important to experimentally determine the band dispersion of La-based cuprates in a three-dimensional momentum space.

We have performed soft x-ray angle-resolved photoemission spectroscopy (ARPES) measurements on overdoped La-based cuprates $La_{2-x}Sr_xCuO_4$ and $Eu_{0.2}La_{1.8-x}Sr_xCuO_4$, and investigated the band structure over several Brillouin zones [4]. While nodal part of the Fermi surface was k_z independent, significant k_z-dispersion was observed in the antinodal portion (Fig. 1). To our knowledge, this is the first experimental observation of three-dimensional Fermi surface in La-based cuprates. From the band structure fitted to the tight-binding model, we have shown that the significant k_z dispersion suppresses the DOS enhancement, and hence VHS cannot account for the large enhancement of the electronic specific heat. Our results, therefore, support quantum criticality of the pseudogap collapse as a tangible explanation for the specific heat enhancement.

[1] N. Doiron-Leyraud *et al.*, Nat. Commun. 8, 2044 (2017). [2] W. Wu *et al.*, Phys. Rev. X 8, 021048 (2018). [3] N. Momono *et al.*, Physica C 233, 395 (1994). [4] M. Horio *et al.*, Phys. Rev. Lett. 121, 077004 (2018).

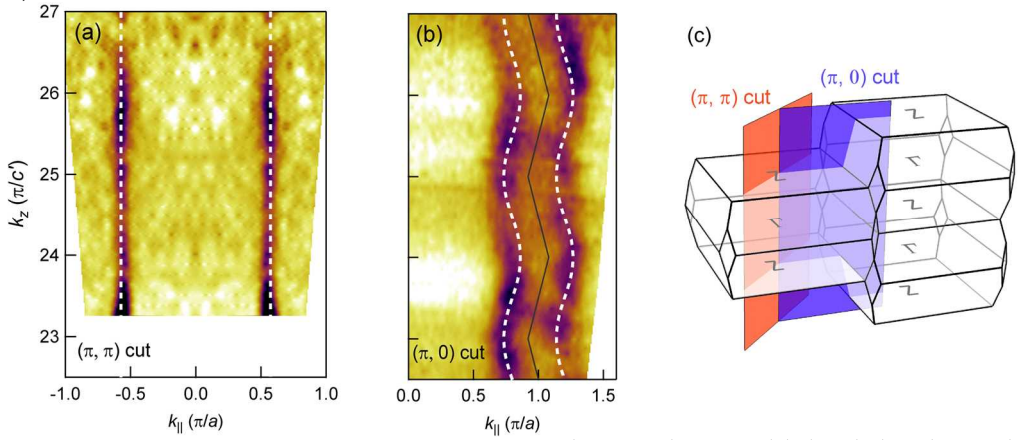

Fig.1: Out-of-plane Fermi surface of La2-xSrxCuO4 (x = 0.22) along (a) (0, 0)-(π, π) and (b) (0, 0)-(π, 0) directions. The cut positions in the momentum space are shown in (c).

Keywords: Cuprates, Soft x-ray ARPES, Fermi surface, Pseudogap quantum criticality

PC7-6

Pressure Effects on RT Measurements in the triple-layered cuprate Bi-2223

*Shintaro Adachi[1], Ryo Matsumoto[1,2], Yoshito Saito[1,2], Hiroshi Hara[1,2], Hiroyuki Takeya[1], Takao Watanabe[3], Yoshihiko Takano[1,2]

MANA, National Institute for Materials Science (NIMS), Tsukuba 305-0047, Japan[1]
Graduate School of Pure and Applied Sciences University of Tsukuba, Tsukuba 305-8577, Japan[2]
Graduate School of Science and Technology, Hirosaki University, Hirosaki 036-8561, Japan[3]

The superconducting transition temperature T_c of the cuprate superconductor increases on increasing the number of CuO_2 planes (n) per unit cell from 1 to 3. Here, we note that the number of charge-reservoir-layers (CRLs) does not change even when n increases. Generally, the carrier concentrations of CuO_2 planes changes by chemical controlling the amount or kind of the elements in CRLs. Therefore, chemical doping becomes more difficult as n increases. In this study, we performed *R-T* measurements using diamond anvil cell, because pressure-induced effective hole doping might be possible [1] even in situations are difficult to the chemical doping.

Figure 1a shows temperature dependence of resistance for Bi-2223 with small intergrowth of Bi-2212. As a result, we have succeeded in observing the T_c of Bi-2223 (T_c1) and Bi-2212 (T_c2) under high pressure. The up-turn at lower temperature suggests that there is a contribution of the out-of-plane resistance. Figure 1b shows pressure dependence of the T_c1 and the T_c2. Both T_c increased slightly by pressure *P*. After the T_c reaches maximum, the T_c decreased on increasing *P*. In order to show the maximum T_c, Bi-2223 was required higher pressure than Bi-2212. This trend reflects the difference in the number of CuO_2 plane n.

[1] M. Mito *et al.*, Phys. Rev. B **95**, 064503 (2017).

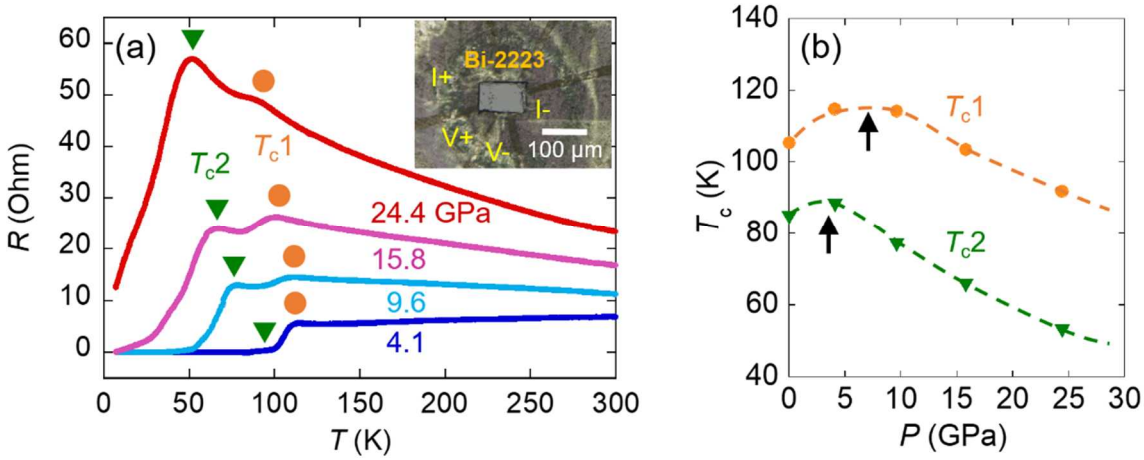

FIG. 1. (a) *R-T* curve for Bi-2223. Inset is an enlargement of the sample space with a Bi-2223 single-crystal. (b) Pressure dependence of the T_c. The arrows indicate the maximum T_c.

Keywords: Bi-2223, Bi-2212, high pressure, diamond anvil cell

WB1-1-INV

High Performance Coated Conductors for High Magnetic Field Applications

*Venkat Selvamanickam[1]

University of Houston[1]

The excellent properties of coated conductors over a wide temperature range in high magnetic fields make them attractive for a number of applications including accelerators for high energy physics, magnets for fusion reactors and industrial motors. In order for coated conductors to be cost effective, substantially high engineering current density is required in fields of 20T at 4.2K for use in accelerators and fusion magnets and in fields of 1.5-3 T at 65 K for industrial motors. This presentation will cover progress made at the University of Houston in these areas in two programs funded by the U.S. Department of Energy. Coated conductors with 4-5 μm thick REBCO films and 5-15% dopant addition made by an advanced metal organic chemical vapor deposition (MOCVD) process exhibit record-high engineering current density (J_e) of 5200A/mm^2 at 4.2K, 15T (corresponding critical current density (J_c) of 10MA/cm^2) which is more than a factor of five better than the J_e of the best Nb_3Sn wires and 10 times better than the J_e of commercial REBCO tapes. At 65K, 1.5T, critical currents exceeding 1750A/12mm have been achieved, meeting a key milestone of the program funded by the DOE-Advanced Manufacturing Office. We have also developed a Symmetric Tape Round (STAR) wire technique to fabricate 1.6 to 1.9mm diameter round REBCO wires with high J_e and excellent tolerance to bend strain. STAR REBCO wires can be bent to a radius of just 15mm while sustaining a J_e of 438A/mm^2 at 4.2K, 20T which meets key stringent requirements of accelerator magnets.

Keywords: superconductor, critical current, thin film, magnetic field

WB1-2-INV

Recent Activities on R&D of coated conductors in AIST

*Teruo IZUMI[1], Takato Machi[1], Akira IBI[1], Koichi NAKAOKA[1], Michio SATO[1], Takeharu KATO[2], Masataka IWAKUMA[3], Masashi MIURA[4], Takanobu KISS[3], Satoshi AWAJI[5]

Advanced Industrial Science and Technology, Japan[1]
Japan Fine Ceramics Center, Japan[2]
Kyushu University, Japan[3]
Seikei University, Japan[4]
Tohoku University, Japan[5]

R&D group for coated conductors (CCs) in AIST has activated for long time to achieve high performance long CCs for applications. We are mainly working in the two national projects at present, which are “Promotion Technology Development for Realization of HTS Applications” and “Feasibility Study of Innovative Electric Propulsion System for Aircraft”, both supported by NEDO. In the former project, we have taken charge of two topics for MRI application. One is the development of low ac-loss CCs with high in-field performance and the other is that of low resistant joint. On the other hand, we are going to supply the CCs to the motor and the cable developments for aircraft, and to develop CCs for magnetic shielding for the rotating machines in the latter project. In this presentation, the recent activities in AIST including the progress in the above projects are reviewed.

As low ac-loss CCs with high in-field performance, a plane-plume PLD was developed for improving a two-dimensional Ic(B) uniformity even in the APC doped CCs. The optimization of the process conditions in the plane-plume PLD made higher uniformity. The uniformity was evaluated as the distribution of filament-Ic values ((max.Ic-min.Ic)/(ave.Ic)) in the scribed tapes with the filament width of 450-500 μm. The distribution of CCs by the plane-plume PLD was improved as 4.3% , which is the equivalent to the pure REBCO (3.3%), from that of the conventional one (8.4%) in the CCs of EuBCO with BHO.

Concerning CCs for the aircraft, several issues have to be fixed such as wide CCs for effective magnetic shielding, stable process of scribed CCs for armature coils, and higher in-field performance even at the high temperature. For the last issue, the conceptual design consideration of rotating machine shows the tentative targets for the CCs performances. The Ic properties of 700 A/cmw under 2 T at ~70 K and 625 A/cmw under 1.5 T at ~65 K with 20-filamentations are required for the field coils and armature ones, respectively. From the in-field performance point of view, the UTOC-MOD films has a potential which satisfied the above targets, if the long tape with thick film processing is developed. Even in the PLD CCs, the improvement of Jc(B) properties at high temperature is much improved as competitive to UTOC-MOD films.

The part of the work was supported by METI, NEDO, AMED and AIST.

Keywords: coated conductor, REBCO, motor, MRI

WB1-3-INV

Preparation of YBCO Film on Conductive Nb-doped $SrTiO_3$ and Ni Buffered {100}<001> Cu/SS316 Lamination Tape

*Toshiya Doi[1], Kota Yamaguchi[1], Shigeru Horii[1], Ataru Ichinose[2]

Kyoto University, Japan[1]
Central Research Institute of Electric Power Industry, Japan[2]

YBCO films with high J_c have been grown on cube-textured metal tapes for the purpose of developing 2G superconducting wires for high temperature, high magnetic field applications. In the standard RABiTS approach, a biaxially aligned YBCO layer is deposited on Y_2O_3/YSZ/CeO_2 buffered Ni-W alloy tape. 2G superconducting wires become highly resistive when they are quenched, therefore, to manufacture reliable and safe HTS applications, it is necessary to use metal layers with low resistivity such as Cu and Ag to attach to the 2G wires to stabilize and protect the wires from damage due to quenches. Presently, insulative oxides, such as Y_2O_3, YSZ, CeO_2, are used for the buffer layers, thus thick Ag and Cu layers are required to be deposited as the stabilizer layers on the YBCO layer. However, the high material cost for the Ag layer is one of the major obstacles for achieving low-cost 2G wires. Because the resistivity of pure Cu is much lower than that of the Ni-W alloy, use of a conductive buffer layers instead of the insulative ones combining with textured Cu tape, enables the textured pure Cu tape to work as the electrical stabilizer layer as well as the template for biaxial crystal alignment. Thus our new configuration for CCs does not require the expensive Ag layer [1, 2].

YBCO and $Sr(Ti,Nb)O_3$ were epitaxially grown on the Ni-electroplated Cu/SUS316 lamination tape by a pulsed laser deposition method. Both YBCO and $Sr(Ti,Nb)O_3$ were confirmed to have excellent biaxial crystal orientation by X-ray pole figure measurements. From scanning transmission electron microscope observation of the cross-section of the YBCO/ $Sr(Ti,Nb)O_3$/Ni/Cu/SUS316 sample, no NiO was observed at the interface between the $Sr(Ti,Nb)O_3$ and the Ni layers. Excellent J_c of 2.5 x 10^6 A/cm^2 was achieved at 77 K under a magnetic self-field. By the comparison between the measured and simulated I-V curves, we confirmed that some of the current flowed in the Cu tape in $I > I_c$ region. The textured Cu tape in the YBCO/ $Sr(Ti,Nb)O_3$/Ni/Cu/SS316 tape worked as not only the biaxial crystal orientation template but also the electric stabilizer layer.

A part of this work was supported by JST ALCA Grant Number JPMJAL1109, Japan.

[1] A. Ichinose et al., Jpn. J. Appl. Phys. **56**(2017)103101.
[2] T. Doi et al., Materials Trans. **58**(2017)1493.

Keywords: REBCO, superconducting wire, coated conductor, conductive buffer layer

WB1-4-INV

Electromagnetic loss characterization of a flexible woven HTS Cable

Guy Dubuis[1,2], Zhenan Jiang[1], *Nicholas J Long[1]

Robinson Research Institute, Victoria University of Wellington, Lower Hutt, New Zealand[1]
The MacDiarmid Institute for Advanced Materials and Nanotechnology, Wellington, New Zealand[2]

We present electrical and mechanical measurements on a flexible sock-woven HTS cable made out of HTS coated conductor tapes in a manner that all strands are electromagnetically transposed. The cable assembly differs from existing HTS cables such as Roebel or Corc™ in a few key aspects. In particular, this construction does not need any complex cutout or punching to produce the strands, and thus the strands are not mechanically weakened. This also means that there is no wastage of material. The cable can also be designed so as to minimize the magnetic field at its core. Furthermore, this cable assembly offers a few advantages in terms of flexibility and is self-supporting. Possible applications would be flexible AC cryogenic current leads and low AC-loss superconducting electromagnets. It is an adaptation of a braiding concept developed for Nb_3Sn wire [1].

Here we present measurements of critical current, AC transport loss and magnetization loss characteristics of a set of samples with different weaving patterns. We show that the losses are significantly reduced compared to an equivalent single strand cable. We also investigate the cable flexibility, presenting results on the change in critical current with bend radius. We comment on possible real world applications of this novel cable. The properties suggest that a sock-woven cable may have a niche role to play for future industrial applications of HTS technologies.

[1] P Bruzzone, “Fully transposed braids for the cable-in-conduit superconductors”, IEEE Trans. Magn., **28**, 190-193, (1992)

Keywords: Coated conductor cable, AC losses, HTS, Braided cable

WB1-5

Asymmetric Critical Current in REBCO Films toward Novel Superconducting Diodes

*Yuji Tsuchiya[1], Keisuke Suzuki[1], Yusuke Ichino[1], Yutaka Yoshida[1]

Nagoya Univ.[1]

A superconducting diode with an asymmetric $I_c$has been proposed as a novel rectifying element operating at cryogenic conditions [1]. It has an opposite I-Vcharacteristic to the conventional semiconductor diode andis expected to be used for the application such as AC-DC conversion and superconducting electronics. However, little has been reported on rectifying properties in high-temperature superconducting REBCOfilms.In this study, we investigated the asymmetric $I_c$in $BaHfO_3$(BHO)-doped $SmBa_2Cu_3O_y$(SmBCO) films.
BHO-doped SmBCO films were fabricated on a $LaAlO_3$(LAO) and IBAD substrates with thicknesses of 150-1200 nm using a PLD method. The films were processed into micro bridges with a width of 100 μm. I-Vcharacteristics were measured at 0-9 T and 77 K by the four-probe method. An asymmetry a was defined as a ratio between a differential and an average amplitude of $I_c$for the different current direction.
Figure 1 shows I-Vcharacteristics in the BHO-doped film at an in-plane and an out-of-plane fields of 0.1 T at 77 K. In the in-plane field,$a$reached up to 41% where the vortex entered more easily from the interface between the film and the substrate than the other side. On the other hand, $a$was ~0% in the out-of-plane field. In the pure and BHO-doped film, $a$was ranged in 0-15% and 10-41%, respectively. Regardless of IBAD and LAO substrates, the maximum $a$was ~40%. The results indicate that introduction of BHO is effective to enhance the asymmetry.
On site, we will discuss origin of the asymmetricity toward superconducting diodes.

[1] X. Jiang *et al.*, Phys. Rev. B **49**, 9244 (1994).

Acknowledgement
This research was partly supported by JST-ALCA, KAKENHI (23226014, 15K14301, 15K14302, 15H04252, 16K20898, 16H04512). IBAD metal substrates were received from Dr. T. Izumi of AIST.

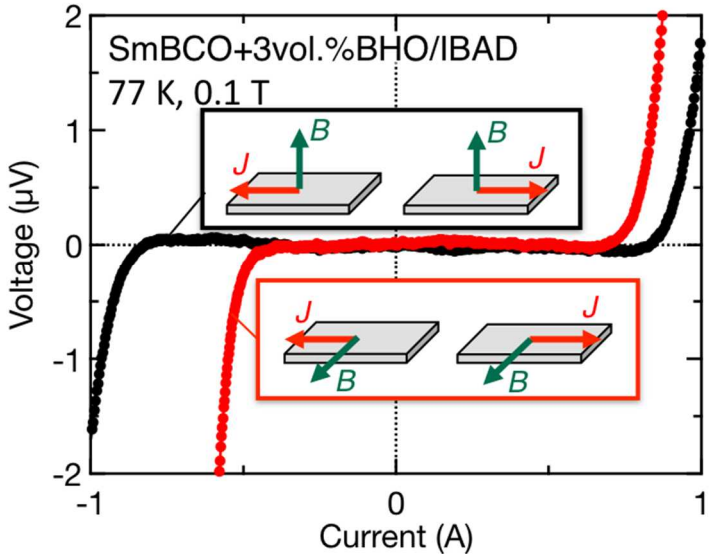

Fig. 1 I-Vcharacteristics in $SmBa_2Cu_3O_y$films with $BaHfO_3$nanorods grown on IBAD substrates at 77 K in in-plane and out-of-plane magnetic fields of 0.1 T.

Keywords: high temperature superconductors, coated conductors, superconducting diode, critical current

WB1-6-INV

Measurement and analysis of longitudinal Ic variation in long coated conductors fabricated by different processes: IBAD-PLD and ISD-coevaporation methods

*Takanobu Kiss[1], Takumi Suzuki[1], Shohei Noda[1], Yuki Yamauchi[1], Kohei Higashikawa[1], Wataru Hirata[2], Shinji Fujita[2], Yasuhiro Iijima[2], Markus Bauer[3]

Dept. of Electrical Engineering, Kyushu University, Fukuoka, Japan[1]
Fujikura Ltd. Sakura, Japan[2]
THEVA GmbH, Ismaning, Deutschland[3]

Spatial homogeneity of critical current, I_c, in a long coated conductor (CC) is one of the most important requirements for practical applications of CC based devices. However, not only fundamental issues such as the origin of the spatial I_c variation and the influence of fabrication processes, but also a measurement method for the longitudinal I_c variation in the long CCs is not yet established as a standard method. In this study, we have carried out spatially resolved I_c measurements of long CCs by use of reel-to-reel magnetization measurements at 77 K self-field and also at 65 K in subcooled LN_2 with applying external magnetic fields up to 2 T. Superconducting layers of the samples were deposited by 1) PLD method on an IBAD-MgO template, and 2) coevapolation method on an ISD-MgO template, respectively. In the former case, artificial pinning centers (APC) were also introduced using $BaHfO_3$. It has been shown that behavior of the spatial I_c variation under external magnetic fields are similar even though the microstructures of the CCs are quite different from each other. Namely, positional dependence of the I_c is collapsed on a single curve if it is normalize by the average value of I_c at each magnetic field condition. This indicates that the spatial variation is almost independent from that of magnetic field dependence. This behavior is similar even in the case of APC doped CC in the IBAD-PLD process. This strongly suggests that the spatial I_c variation comes from macroscopic defects and not from the fluctuation of flux pinning behavior controlled by nano-scale defects. This was also confirmed from very similar APC nano-structures obtained by site-specified TEM observations at high- and low- I_c positions, respectively. Lastly, we considered the influence of spatial resolution and electric-field criterion on the I_c measurements in long CCs by typical two methods, i.e., magnetization measurement and transport measurement from the view point of standardization. Relationship between these two measurements has been discussed quantitatively.

Acknowledgements: This work was supported by “JSPS KAKENHI (16H02334)”.

Keywords: critical current, coated conductor, spatial homogeneity, statistics, current transport

WB1-7

Characterization of Pinning Center in Zr-doped (Gd,Y)$Ba_2Cu_3O_x$Superconductor Tape by Anomalous Small-Angle X-ray Scattering

*Yojiro Oba[1], Hirokazu Sasaki[2], Satoshi Yamazaki[2], Ryusuke Nakazaki[2], Masato Ohnuma[3]

Japan Atomic Energy Agency[1]
Furukawa Electric Co., Ltd.[2]
Hokkaido University[3]

Pinning center in Zr-doped (Gd,Y)$Ba_2Cu_3O_x$ superconductor tape plays an important role to improve critical current. For further effective use of the pinning center, precise characterization and control of the nanostructures of the pinning centers are necessary. Small-angle X-ray scattering (SAXS) is a suitable technique to quantitatively characterize the nanostructures because of its large gauge volume compared to conventional electron microscopes. To extract the information of only the pinning center from the complex nanostructure of the tape, we performed anomalous SAXS (ASAXS) measurement in the energy range of the Zr*K* absorption edge. Since Zr is concentrated in only the pinning center, the scattering contrast of the pinning center has to be enhanced around the Zr *K* edge. The scattering profiles obtained by ASAXS show a shoulder and a broad peak. The intensities of these features increase when the energy of incident X-ray becomes close to the Zr *K* edge. These results indicate that the scattering of the pinning center containing Zr in the superconductor tape is successfully observed. The size of the pinning center can be evaluated from the shoulder. The broad peak results from an interparticle interference effect among the pinning centers and provides the information of the distance between the pinning centers. These parameters are useful to characterize the pinning center in the superconductor tapes.

Keywords: small-angle X-ray scattering, synchrotron radiation, pinning center

WB2-1-INV

Recent Progress in REBCO Coated Conductors and Their Superconducting Joints

*Tatsuoki Nagaishi[1], Kotaro Ohki[1], Takashi Yamaguchi[1], Tatsuhiko Yoshihara[1], Takeharu Kato[2], Daisaku Yokoe[2], Tsukasa Hirayama[2], Yuichi Ikuhara[3], Yoshinori Yanagisawa[4], Renzhong Piao[4], Hideaki Maeda[4]

Sumitomo Electric Industries, Ltd.[1]
Japan Fine Ceramics Center[2]
University of Tokyo[3]
RIKEN[4]

Among many prospective applications for high temperature superconducting coated conductors (CCs), high field magnets such as NMR and MRI are promising. For these applications superconducting joint technology capable of persistent current mode is desirable and indispensable from the perspectives of easy and stable operation, energy consumption and power failure. In the case of an extra high field NMR magnet such as one of more than 24 Tesla, a high strength tape of more than 500MPa is needed because of strong hoop stress induced by the magnetic field.

In the JST-Mirai Program the construction of a persistent current mode super-high field (1.3 GHz = 30.6 Tesla) NMR magnet is underway using REBCO CCs to progress in medical science in particular for the analysis of an amyloid protein which is thought to be the pathogenesis of Alzheimer's disease. A high strength clad type substrate REBCO CC and a high critical current superconducting joint were developed for a super-high field NMR magnet. A Hastelloy® based copper clad tape with a buffer layer and a superconducting layer deposited on it was fabricated for the first time. Superconducting characteristics and tensile/bending strengths were measured and will be presented. An intermediate grown superconducting (iGS) joint was previously developed [1]. An iGS joint is made by sandwiching a microcrystalline REBCO precursor between REBCO CCs at a temperature of 800 °C and a pressure of 40MPa in an oxygen atmosphere. The microcrystalline REBCO precursor was bi-axially grown and CCs were connected. Newly introduced equipment which enables constant high joint pressure at high temperature led to stable Ics of more than 150A at 77K. Furthermore, microscopic observations were carried out to understand the growth and glue mechanism of the precursor layer of iGS joints.

This work was supported by JST-Mirai Program Grant Number JPMJMI17A2, Japan.

[1] K. Ohki, et al., Supercond. Sci. Technol., 30, 115017, 2017.

Keywords: coated conductor, REBCO, superconducting joint, clad tape

WB2-2-INV

Superconducting Joint between BSCCO and NbTi using Bi-Pb-Sn Solder

*Yoshihiko Takano[1,2], Ryo Matsumoto[1,2], Gen Nishijima[1]

National Institute for Materials Science (NIMS), Tsukuba, Japan[1]
University of Tsukuba, Tsukuba, Japan[2]

Superconducting joints between NbTi and Bi2Sr2Ca2Cu3O10 superconducting wires were successfully fabricated using Bi-added PbSn solders with an in situ sheath-dissolution technique without a removal process for the sheath materials [1]. A backscattered electron image and an energy dispersive X-ray spectroscopy analysis of the cross-sectional plane of the joints using Bi-Pb-Sn solder revealed that the sheath had dissolved clearly and solder area had tiny non-superconducting islands which act as pining center. The superconducting joints exhibited high critical currents above 200A in self field and 50A under an applied magnetic field of 5 kOe as presented in Fig. 1. The evolution of this technology will make it possible to realize HTS/LTS hybrid high field magnets [2] with the persistent current operation.

[1] R. Matsumoto et al., Appl. Phys. Express 10, 093102 (2017).
[2] K. Hashi et al., J. Magn. Reson. 256, 30 (2015).

ACKNOWLEDGMENTS: This work is partly supported by JST-MIRAI.

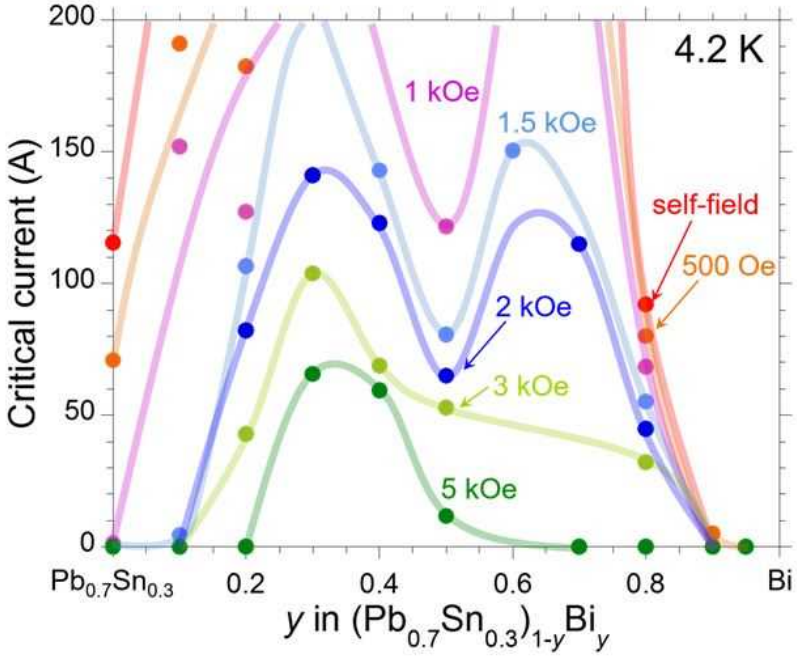

Keywords: Superconducting Joint, BSCCO, NbTi, Solder

WB3-1-INV

Development of BMO Doped REBCO Coated Conductors by Productive Hot-Wall PLD Process

*Yasuhiro Iijima[1], Kazuomi Kakimoto[1], Shinji Fujita[1], Shogo Muto[1], Wataru Hirata[1], Tomo Yoshida[1], Yutaka Adachi[1], Satoru Hanyu[1], Ryo Kikutake[1], Masanori Daibo[1], Satoshi Awaji[2], Takanobu Kiss[3]

Fujikura Ltd., Japan[1]
Tohoku University, Japan[2]
Kyushu University, Japan[3]

Though vapor phase grown $BaMO_3$(M : Zr or Hf etc.) doped REBCO film is a promising process to manufacture coated conductors with high in-field performance, multiplied deposition parameters come from BMO nano-rod structure should cause narrower deposition windows which could spoil longitudinal homogeneity, and productivity. To overcome the problem, we applied hot-wall type pulsed-laser-deposition (PLD) for BMP-doped REBCO process, which realized quite homogeneous crystalline growth conditions for REBCO by furnace-like, nearly equilibrium substrate heating. We surveyed growth condition dependence of BMO nano-rod structure, and J_c (B, θ, T) properties. Clear growth rate dependence were observed for nano-rod structure which should be affected by surface migration. Strongly c-axis correlated flux pinning were observed in those films with low growth rate of 5-7 nm/sec, where the minimum J_c (θ) increased at lower temperatures, up to four times bigger for low growth rate samples, and also two-times for high-growth rate of 20-40 nm/sec, than non-doped REBCO films at 4.2K, 15T. On the other hand, the minimum values of J_c (θ) were not so different among the samples with varied growth rate, at the temperature over 30 K.
We finally optimized the deposition parameters so that they contribute to both good productivity with high growth rate of 20-40nm/sec, and large in-field I_c performance, as 700A/cm at 30K, 7T, and also 1000A/cm at 4.2K, 15T. Production samples of 300-600m long were routinely fabricated and test samples of 1km long class also produced with good I_c uniformity comparable to non-doped REBCO wires. Additionally, we also studied mechanical reliability of those BMO-doped REBCO wires for magnet applications. The delamination strength were strengthened by total process refinement compared to past non-doped production wires. These results indicate good productivity, reliability, and controllability of deposition parameters, for vapor phase coated conductor process including high-rate APC introduction by using hot-wall PLD process.

Acknowledgements
A part of this work is based on results obtained from a project subsidized by the New Energy and Industrial Technology Development Organization (NEDO).

WB3-2-INV

Production and Development of REBCO (2G-HTS) Conductors

*Satoshi Yamano[1], Drew Hazelton[1], Paul Brownsey[1], Yifei Zhang[1], Aarthi Sundaram[1], Shinya Yasunaga[1], Gene Carota[1], Hiroshi Kuraseko[1], Toru Fukushima[1], Hisaki Sakamoto[2], Akinobu Nakai[2]

SuperPower Inc. at United states of America[1]
Furukawa Electric Co., Ltd. at Japan[2]

The potential applications of Rare-Earth Barium Cupper Oxide (REBCO), Second-Generation High-Temperature Superconductors (2G-HTS), have been demonstrated in many projects for the last several years. This would indicate the REBCO conductor is now being considered a robust and feasible solution to advanced devices and systems toward the future.

This paper describes recent approaches to produce accomplished REBCO conductors consistently. One of the key challenges is to find out the quality control scheme to keep wire performance as designed. In-field performance data of 30K-2T-Θ, 50K-2T-Θ and 4K-B//c for multiple production wires have been obtained repeatedly by utilizing In-house Ic-B-T-Θ measurement system at SuperPower Inc. and Ic-B measurement system at Furukawa Electric Co., Ltd. These measurement data help us understand what kind of quality and process control schemes are required.

WB3-3-INV

Recent Progress on Manufacturing of Coated Conductors

*Markus Bauer[1]

THEVA Dünnschichttechnik GmbH, Germany[1]

The pilot production line at THEVA is paving the way to high quality production of coated conductors. A general overview on the technology and latest achievements and properties of THEVA's Pro-Line tape will be presented in this talk. An all PVD approach is used with MgO buffer layers by Inclined Substrate Depostion (ISD).
The critical current of the wires was continuously increasing during the last year. Recently, 500 A/cm have been surpassed at high yield production conditions and already 650 A/cm have been demonstrated on production length.
Up to now, 100 µm thick Hastelloy C-276 substrates were used. First results on 50 µm thick substrates were achieved recently and will be shown. By switching from 100 µm thick substrates to 50 µm thick substrates the engineering current density will increase considerably so that the coated conductors are optimized for magnet applications.
In addition to the critical current, other requirements must also be considered. One other mayor demand especially for magnet applications is a well-defined mechanical shape. The copper stabilization layer, necessary in most applications, often has an inhomogeneous thickness at the edges (dog bone) which impedes the use of the conductor e.g. in coils. We will show our recent progress with copper coated conductors towards a smaller thickness variation of the copper using a new PVD approach. This technology allows to deposit different thicknesses of the coating on the HTS and Substrate side. Examples will be shown.
Finally, the resilience of the HTS properties against soldering temperatures is an important property for applications where tapes are stacked and soldered to achieve high current cables. The influence of the elevated temperature depending on the duration must be known and considered in order to avoid any degradation during this processing. We measured the critical current degradation at temperatures between 170°C and 300°C and durations up to several hours. The results give a good guideline for any soldering process.
Finally, a summary of the properties and performance will be given.

Keywords: coated conductors, copper stabilization, soldering

WB3-4-INV

Recent Progress on the Development of RE-123 CCs in SuNAM

*Seung-Hyun Moon[1]

SuNAM Co. Ltd., Anseong, Korea[1]

For the mass production of coated conductor, it is essential to choose raw materials with low prices and high-yield synthesis process for a superconducting layer. In this point of view, E-beam co-evaporation is one of the most promising method because simple elemental metal sources—Gd, Ba, Cu, are employed. However, we should answer the question of whether there is a thermodynamic reaction path from single element of Gd, Ba, Cu to a superconducting $GdBa_2Cu_3O_{7-\delta}$ (123) phase. In addition, growth kinetics are also greatly emphasized for the high-yield process. In the presentation, we will show the thermodynamic route for the RCE-DR process, which is essentially identical to the melt-textured growth, where a biaxially textured substrate plays a role of a seed for the growth of the superconducting layer. The route for the high-quality superconducting layer with the high growth rate will be discussed based on the phase diagram. And we'll show the results of $YBa_2Cu_3O_{7-\delta}$ (123) CC and discuss on a different temperature dependence of critical current and in field properties with different rare earth material including Y.

Usually scale-up of deposition system needs a variety of technical considerations, and we should consider the benefit of scale-up. Based on the potential application/market analysis, we'll discuss the suitable ways of CC production scale-up. We'll briefly show the schematic design of next generation deposition system based on production experiences. And also we'll show the some recent progress of SuNAM's CC and magnets.

Keywords: Coated Conductor, Scale-up, Industrialization, HTS magnet

WB3-5-INV

2G HTS Wire Production Status by the SuperOx Group of Companies

*Valery Petrykin[1], Sergey Lee[1], Alexander Molodyk[2], Sergey Samoilenkov[2]

SuperOx Japan LLC, Sagamihara, Kanagawa, Japan[1]
SuperOx, Moscow, Russia[2]

During the past two years, SuperOx group of companies have been increasing constantly the production capacity of the 2G HTS wires. Currently, both companies in Russia and in Japan operate in the continuous three shift pattern with the wires manufacturing volume exceeding 100 km/year. The typical yield of the commercial quality tape on the month-to-month timescale approaches 95%. The Ic values of the typical product exceed 500A. The lengths of the finished wires that come out of the manufacturing line are 300-400 m, while longer wires can be produced as well.

To meet the goal of the consistent manufacturing of the high-quality HTS tape with high yield and almost theoretically possible production volume for the current laser power, we had to solve numerous challenges in the scientific, engineering and personnel management dimensions.

This presentation will overview the similarities and differences in the SuperOx and SuperOx Japan operation; it will summarize the progress achieved in the past years and highlight the future plans and challenges. The manufacturing cost analysis data will be presented and the future prospects of the PLD method will be discussed.

Keywords: Coated conductors, GdBCO, PLD, SuperOx

WB3-6-INV

Present status of superconducting wire development in China: RE-123 CCs and related applications

*Yutaka Yamada[1,2], Yue Zhao[1,2], Zhiyong Hong[1,2], Zhijian Jin[2]

Shanghai Superconductor Technology Co. Ltd., 200240 Shanghai, P.R.C[1]
Shanghai Jiao Tong University, 200240 Shanghai, P.R.C[2]

Recently, China is much emphasizing high-tech R&D for further economic growth with maintaining sustainability. The total electric power consumption in China is rapidly increased by 70% in these 6 years as shown in Fig. 1. To reduce the effect of such large consumption on the environment and to use electric power efficiently, HTS technology is highly expected.

In this talk, I will introduce such background and HTS activities in China, especially RE-123 Coated Conductor. Fig. 2 is a CC fabrication process at SSTC by PLD-IBAD method. Normally we are producing constantly long CC as shown in Fig. 3. I_c (77K, 0T) around 400 to 500A/cm is supplied to the customer. In the Shanghai area, we have three CC companies using different methods.

Using these conductors, China is carrying out the HTS project or being ready for it, including HTS cable, current limiter, maglev train, high field magnet, accelerator and so on. Not only central government but also many cities or provincial governments and power grind companies have much interest in HTS applications, which will be introduced in this talk.

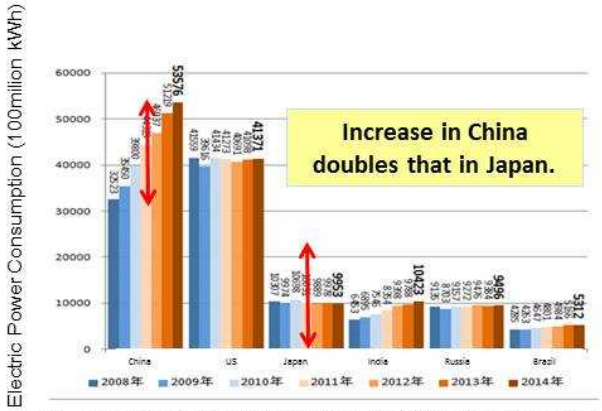

Fig. 1 Electric Power Consumption in 2008-2014 of each country
"Key World Energy Statistics 2016" in IEA publications

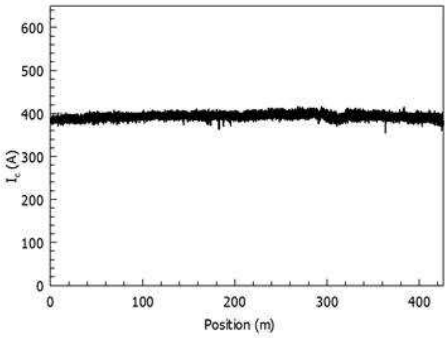

Fig. 3 Typical recent long CC . I_c (77K, 0T) ranging from 400 to 500 A/cm are being supplied.

Fig. 2 CC fabrication process of SSTC, Shanghai Superconductor Tech. by PLD-IBAD

Keywords: Superconducting Wire, Coated Conductor, China, R&D Activity

WB3-7-INV

Recent Developments of DI-BSCCO

*Soichiro Takeda[1], Shin-ichi Kobayashi[1], Goro Osabe[1], Masashi Kikuchi[1], Satoru Yamade[1], Takayoshi Nakashima[1], Tomoyuki Okada[1], Kenta Niki[1], Kazuhiko Hayashi[1], Takeshi Kato[1]

Sumitomo Electric Industries, Ltd., Osaka Japan[1]

Sumitomo Electric has been commercially producing the silver-sheathed Bi2223 multi-filamentary wires, especially under the name of DI-BSCCO (Dynamically-Innovative BSCCO). DI-BSCCO wire is practically used in various applications, for example, cable, magnet, motor, and so on.

In magnet application under high magnetic field, strong hoop stress is applied to HTS wire. Therefore, the wire needs to have high mechanical strength. For the purpose of using such applications, SEI has developed and commercialized a high-strength DI-BSCCO Type HT-NX wire reinforced with Ni alloy tapes. The wire obtained a critical tensile stress of 400 MPa at 77K. On the other hand, the resistivity of the Ni alloy is high, resulting in the generation of the high Joule heat at the joint. The newly developed spliced structure successfully reduced the splice resistance without sacrificing the mechanical properties. For MRI and other high field magnetic applications, the use of Type HT-NX wire is highly expected.

In this presentation, the recent developments of the currently available commercial wires and the updated R&D activities will be talked.

Keywords: Bi2223

WB3-8-INV

Recent progress on the development of MgB_2 wires in Hitachi

*Hideki Tanaka[1], Motomune Kodama[1], Takaaki Suzuki[1]

Hitachi, Ltd.[1]

MgB_2 wires and coils have great potentials for helium free superconducting magnet. We have been concentrated on improving the longitudinal homogeneity of MgB_2 wire, and it was confirmed by making some test coils made by Wind & React method. One of the issues of our MgB_2 wire is tuning it up for React & Wind method. Recently, we have measured the critical bending radius of our wires. In the symposium, we will talk about the homogeneity and bending radius of MgB_2 wires. A part of this work was supported by JST ALCA Grant Number JPMJAL1001, Japan.

Keywords: MgB2, homogeneity, bending radius

WB4-1-INV

Recent Progress of Iron Based Superconducting Round Wires

*Sunseng Pyon[1], Tsuyoshi Tamegai[1], Katsutoshi Takano[2], Hideki Kajitani[2], Norikiyo Koizumi[2], Satoshi Awaji[3]

Dept. of Appl. Phys., Univ. of Tokyo, Japan[1]
Naka Fusion Institute, National Institutes for Quantum and Radiological Science and Technology, Japan[2]
High Field Laboratory for Superconducting Materials, Institute for Materials Research, Tohoku University, Japan[3]

High critical current density, J_c, is realized in superconducting wires and tapes using 122-type iron-based superconductors (IBS). For fabrication of superconducting wires and tapes, application of pressure is the most effective method to eliminate weak links between superconducting wires. J_c in (Sr,K)Fe_2As_2 or (Ba,K)Fe_2As_2 tapes fabricated using uniaxial pressing achieved the practical level of 10^5 A/cm^2. In the case of round wires, hot isostatic pressing (HIP) technique is used for the fabrication. Although J_c in HIP round wires is still lower than that in pressed tapes, the HIP round wire is more promising for high-field applications because its round shape is much more advantageous and convenient than the textured tapes for a wide range of applications.
Here, recent progress of round wires using 122-type iron-based superconductors is reviewed. Both transport and magnetic J_c have been enhanced by several techniques such as purification of polycrystalline powders, high-pressure sintering (HIP), and control of drawing and sintering conditions. The present record of transport J_c of round wires is realized when the wire is processed at 175 MPa with a value at 4.2 K under 100 kOe being 38 kA/cm^2. We also fabricated HIP round wires of $CaKFe_4As_4$ for the first time, and modestly high J_c of 7 kA at 4.2 K under 100 kOe is achieved. Details of the optimization of round wires to achieve large J_c values will be reviewed.

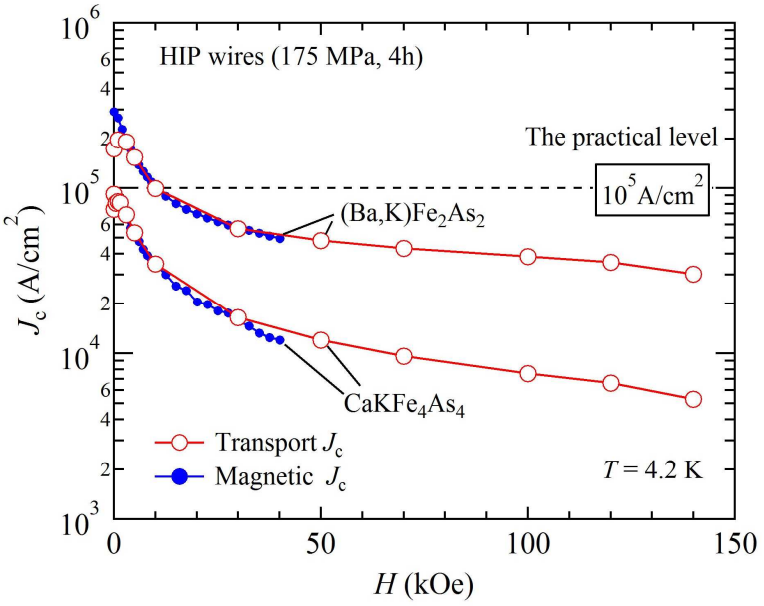

Figure. Temperature dependences of J_c of superconducting HIP wires of (Ba,K)Fe_2As_2 and $CaKFe_4As_4$.

Keywords: Iron-based superconductor, Critical current density, HIP wire, Ba1-xKxFe2As2 and CaKFe4As4

WB4-2-INV

How good are the grain boundaries in Iron-based superconductors to be practical?

*F. Kametani[1,2], Y. Collantes[1], Y. Su[1], T. Shelby[1], A. Oloye[1], C. Pak[1], G. Bovone[1], C. Tarantini[1], E. E. Hellstrom[1,2], D. C. Larbalestier[1,2]

National High Magnetic Field Laboratory, Florida State University[1]
Department of Mechanical Engineering, Florida State University[2]

A primary enabler for a future high-energy circular collider would be transformational high field magnet R&D with substantial performance increase and simultaneous cost reduction. Indeed, the US Magnet Development Program (MDP) accepted the ambitious challenge of 16 T accelerator dipoles with significant cost reduction. These are great challenges, because all present high field superconductors allowing such a performance increase (Nb_3Sn, $REBa_2Cu_3O_x$ (REBCO) or $Bi_2Sr_2CaCu_2O_x$ (Bi-2212)) are expensive. The recently discovered $K_x(Ba/Sr)_{1-x}Fe_2As_2$ (K-122) Fe-based superconductor (FBS) has the potential to enable a high field, round, twisted multifilament, Rutherford-cable-ready conductor at a price similar to Nb-Ti, well below the cost of Nb_3Sn. Technically, 122 uses inexpensive Ba, Fe, and As (and K as a dopant) constituents which can be processed in an inexpensive Cu matrix. It possesses very low anisotropy (γ ~1.2) and high single-crystal J_c, and, compared to Nb_3Sn, it has 2 times higher T_c (39 K) and 3 times larger H_{c2} (~90 T at 4.2 K). The only issue for Ba122 to become a competitive conductor is to increase its J_c by improving its grain-to-grain (intergrain) superconducting connectivity. Yet it is still largely unknown whether its poor connectivity is extrinsic or intrinsic as is the case for HTS cuprates. Recently we start to extensively utilize the atomic resolution analytical electron microscopes to correlate the GB nanostructures to the Ba122 polycrystalline bulks that are synthesized by the high pressure synthesis. The preliminary results suggested that even our highest quality Ba122 polycrystals had strong elemental segregation which appears to decouple most of the GBs. We found “pockets” of several nm in size at the triple junctions of Ba122 GBs where Ba preferentially segregates and compositional traces by Energy Dispersive Spectroscopy (EDS) revealed that these Ba-rich pockets contain carbon and oxygen, indicating the presence of $BaCO_3$. The EDS scan also indicates that carbon extends along the planar GB regions from the triple junctions, forming a network of insulating $BaCO_3$ at many GBs. The other GBs were found to have preferential K segregation that doesn’t always accompany with oxygen segregation. We believe the findings to be helpful in understanding how to make the distinction between intrinsic and extrinsic behavior as we will present in our presentation for details.

WB4-3

Slow Vortex Creep Induced by Grain Boundary Pinning in Advanced Ba122 Superconducting Tapes

*Chiheng Dong[1], He Huang[1,2], Yanwei Ma[1,2]

Institute of Electrical Engineering, Chinese Academy of Sciences, Beijing 100190, People's Republic of China[1]
University of Chinese Academy of Sciences, Beijing 100049, People's Republic of China[2]

Understanding the behavior of vortex matter is vitally important for practical application of superconducting wires and tapes. We investigate the temperature, magnetic field and time dependence of magnetization in advanced Ba122 superconducting tapes. The magnetization data indicates that the sample is of high quality with a 100% volume fraction of superconductivity and a high critical current density. In spite of the marginal flux jumps emerging at low temperature, the normalized magnetization relaxation rate $S=d\ln(-M)/d\ln(t)$ below 10 K shows a temperature insensitive plateau with a value comparable to that of the low temperature superconductors. The vortex creep behavior in the low and intermediate temperature regions can be well interpreted in the framework of the collective creep theory. Interestingly, the relaxation rate below 20 K tends to saturate with the increasing field. However, it changes to a power law dependence on field at higher temperature. Moreover, the Ba122 tape presents a lower relaxation rate than other high temperature superconductors at 20 K. We finally conclude a vortex phase diagram composed of the collective and plastic creep regions. Our results indicate that the advanced Ba122 tape has promising potential to be applied not only in liquid helium, but also in liquid hydrogen or at the temperature accessible with cryocoolers.

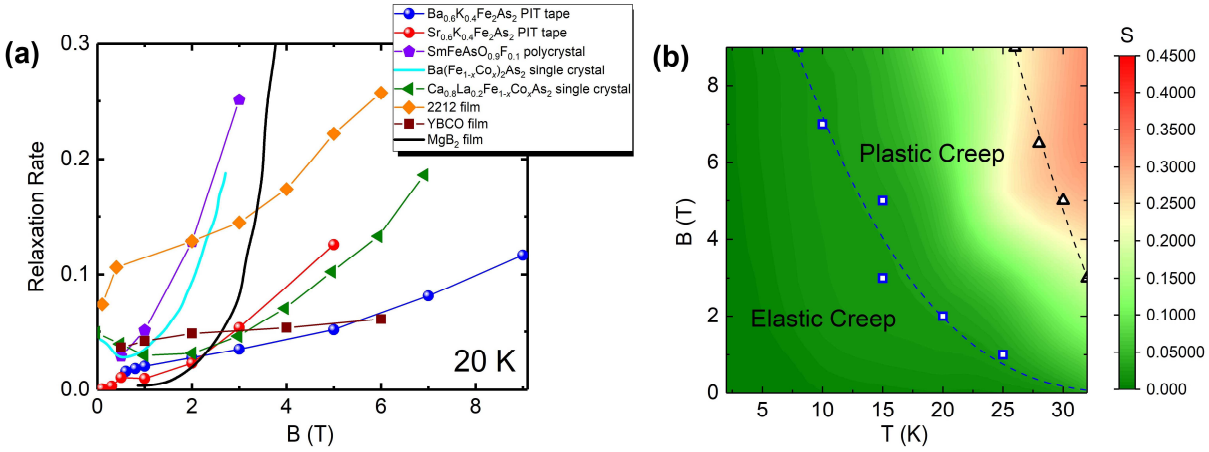

WB5-1-INV

Recent progress in a melt-growth processed YBCO superconductors with interior seeding

Chan-Joong Kim[1], Soon-Dong Park[1], *Byung-Hyuk Jun[1]

Korea Atomic Energy Research Institute[1]

YBCO bulk superconductors with a large magnetic levitation force are manufactured by a seeded melt growth (SMG) process. Among various SMG processes, a top-seeded melt growth (TSMG) process is most widely used to fabricate a large grain YBCO bulk superconductors. The large single grain YBCO bulk superconductors with a size of several cm can be fabricated by the TSMG process. The magnetic levitation force of the YBCO superconductors manufactured by the TSMG process is as large as several hundred N (the magnetic levitation force of the superconductor is a function of the magnetic force of the permanent magnet used and the distance between the superconductor and the permanent magnet). In the TSMG process, the YBCO crystal grows from the top seed to the lower part of the YBCO compact, and there is a property difference between the upper portion and the lower part of the final product. Recently, our research team has developed a process of growing YBCO crystals inside the sample. This method is called “interior seeding.” We made a proper space for seeding inside the YBCO compact, and the seed was placed there. A single YBCO grain grows simultaneously to the top and bottom of the specimen. Therefore, the property difference between the top and bottom became small. Also, due to simultaneous growth of the YBCO grain, the processing time for the fabrication of the single grain YBCO superconductor is shortened. Interior seeding can be used to adjust the ratio of the ab/ac growth sector on the upper surface of the YBCO superconductor. The TSMG process combined with interior seeding can improve the magnetic levitation force and the trapped magnetic field. In this research, we report how to create a space for seeding inside the powder compact during the internal seeding process, the control of magnetic levitation forces through the adjustment of the ratio of the ab/ac growth sectors of the single grain YBCO bulk superconductors.

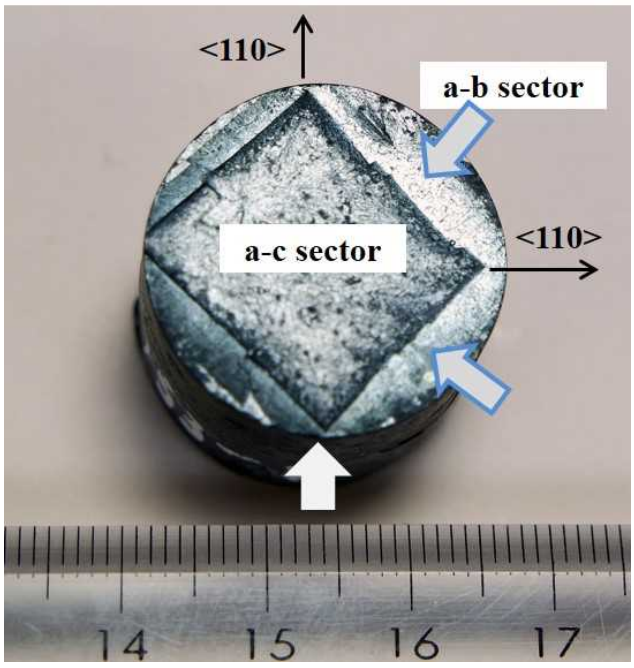

Keywords: seed growth, internal seeding, magnetic levitation force, control of ab/ac growth sectors

WB5-2-INV

Recent topics of iron-pnictide bulk superconductors

*Akiyasu Yamamoto[1,2], Shinnosuke Tokuta[1], Mark Ainslie[3], Jeremy Weiss[4], Anatolii Polyanskii[5], Eric Hellstrom[5], David Larbalestier[5]

Department of Applied Physics, Tokyo University of Agriculture and Technology, Japan[1]
Materials Research Center for Element Strategy, Tokyo Institute of Technology, Japan[2]
Department of Engineering, University of Cambridge, Cambridge CB2 1PZ, United Kingdom[3]
Department of Physics, University of Colorado, Boulder, 3082 Sterling Circle, Co 80301, USA[4]
Applied Superconductivity Center, National High Magnetic Field Laboratory, Florida State University, Tallahassee, FL 32310, USA[5]

Iron-based superconductors (IBSCs) with high T_c of ~60 K in 1111 and ~40 K in 122 are interesting for high field applications, owing to their high H_{c2} with small anisotropy nearly ~1 (in 122) [1,2]. The unique advantage which distinguishes IBSCs from cuprates is high critical misorientation angle of 9 degrees [3,4]. Thus high critical current over a sample is expected in randomly oriented, polycrystalline form, which leads to low-cost and scalable production. In the present study, we report (i) the enhancement of H_{c2} in Co doped 122 polycrystalline bulks and (ii) the field trapping properties of untextured polycrystalline K doped122 bulks. (i) The effects of lattice defects in $Ba(Fe_{0.92}Co_{0.08})_2As_2$ polycrystalline materials prepared by high energy ball-milling were investigated. Elemental metals (Ba, Fe, Co and As) were milled with planetary ball milling apparatus. The milling conditions were systematically changed and quantified using ball-milling energy (E_{BM}). Broadening of FWHM of XRD peaks, decreasing of residual resistivity ratio, shrinkage of *a*-axis, and expanding of *c*-axis were observed with increasing E_{BM}. T_c was slightly suppressed (−5.5%), however, the slope of $H_{c2}(T)$ near T_c was remarkably increased (+60%) [5]. (ii) Trapped fields of over 1 T at 5 K and 0.5 T at 20 K have been measured between a stack of magnetized cylinders of bulk polycrystalline $Ba_{0.6}K_{0.4}Fe_2As_2$ 10 mm in diameter [6]. Magneto-optical imaging revealed a trapped-field distribution corresponding to uniform macroscopic current loops circulating through the sample. A standard numerical modeling technique using the $J_c(B, T)$ characteristics measured from a small specimen performed well in reproducing the experimentally measured trapped fields, again indicating the homogeneous current loops [7]. Since field dependence of J_c is much better than that of MgB_2, larger IBSC bulks would be interesting for high field trapping magnet and other magnet applications to be operated by compact cryocoolers.

[1] Y. Kamihara, T. Watanabe, M. Hirano, and H. Hosono: "Iron-Based Layered Superconductor $La[O_{1-x}F_x]FeAs$ (x = 0.05−0.12) with T_c = 26 K," J. Am. Chem. Soc. **130** (2008) 3296–3297.
[2] H. Hosono, A. Yamamoto, H. Hiramatsu, and Y. Ma: "Recent advances in iron-based superconductors toward applications," Materials Today **21** (2018) 278–302.
[3] S. Lee, et al.: "Weak-link behavior of grain boundaries in superconducting $Ba(Fe_{1-x}Co_x)_2As_2$ bicrystals," Appl. Phys. Lett. **95** (2009) 212505.
[4] T. Katase, Y. Ishimaru, A. Tsukamoto, H. Hiramatsu, T. Kamiya, K. Tanabe, et al.: "Advantageous grain boundaries in iron pnictide superconductors," Nat. Commun. **2** (2011) 409.
[5] S. Tokuta, and A. Yamamoto: ASC2018, ISS2018.
[6] J. D. Weiss, A. Yamamoto, A. A. Polyanskii, R. B. Richardson, D. C. Larbalestier, and E. E. Hellstrom: "Demonstration of an iron-pnictide bulk superconducting magnet capable of trapping over 1T," Supercond. Sci. Technol. **28** (2015) 112001.
[7] M. D. Ainslie, A. Yamamoto, H. Fujishiro, J. D. Weiss, and E. E. Hellstrom: "Numerical modelling of iron-pnictide bulk superconductor magnetization," Supercond. Sci. Technol. **30** (2017) 105009.

Keywords: iron-based superconductors, polycrystalline bulk materials, trapped field magnets

WB5-3

Growth and Properties of RE123 Bulks for Practical Applications

*Xin Yao[1]

School of Physics and Astronomy, Shanghai Jiao Tong University[1]

In this presentation, our recent progress in high superconducting properties of RE123 bulks grown by top-seeded melt-growth (TSMG) will be presented. Regarding to the refinement of Y_2BaCuO_5 (Y211) particles in the matrix of Y123 bulks, two approaches were developed. Firstly, instead of Y123+Y211, modified precursor powders (MPP, Y_2O_3 and $Ba_2Cu_3O_x$) were employed. As a result, massive Y211 nanoparticles were derived from the homogeneous nucleation through peritectic solidification of Y_2O_3+Ba_x-Cu_y-O=Y211. Secondly, we found that the Fe-doping elevates the nucleation barrier in the peritectic melting of Y123 and causes a massive homogeneous nucleation, leading to nanosized and dispersive Y211 particles, which readily and almost fully dissolve in the subsequent peritectic solidification of Y123. Furthermore, we also report two novel seed/buffer-layer constructions for enlarging c-directional growth sector and enhancing the seed thermal stability in the growth of $REBa_2Cu_3O_x$/Ag superconductor bulks. Finally, melting driven approaches for recycling failed REBCO (RE= Nd, Sm, Gd, Y) bulks are demonstrated.

Keywords: superconductor bulk, Y211 refinement, seed/buffer-layer construction, recycling

WB5-4-INV

Mechanical reinforcement of REBaCuO bulk during magnetizing process to achieve higher trapped field without fracture

*Hiroyuki Fujishiro[1], Tomoyuki Naito[1], Yousuke Yanagi[2], Yoshitaka Itoh[2], Takashi Nakamura[3], Mark D. Ainslie[4]

Iwate University, Japan[1]
IMRA Material R&D Co., Ltd, Japan[2]
RIKEN, Japan[3]
University of Cambridge, United Kingdom[4]

The trapped-field ability in REBaCuO superconducting bulks estimated by critical current density, J_c, isextremely high at low temperatures. However, the mechanical fracture of the brittle ceramic bulk when trapping large magnetic fields restricts practical trapped field values. For this reason, the mechanical reinforcement of the superconducting bulk is an important issue to realize stronger trapped field magnets (TFMs). There have been several experimental challenges using field-cooled magnetization (FCM), and trapped fields of over 17 T have been achieved by mechanical reinforcement using resin impregnation and carbon-fibre wrapping and by using shrink-fit steel. Analytical results of the electromagnetic stress during FCM for superconducting ring and disk bulks with infinite height were presented in [1], but there were not analytical results for the electromagnetic and thermal stresses of the bulk with finite height and for the reinforcement effect by a metal ring. We have performed the numerical simulation of mechanical stresses and strains in REBaCuO ring bulks with a finite height reinforced by a metal ring during FCM [2, 3]. The thermal compressive stress due to the difference in the thermal contraction coefficient between the ring bulk and metal ring was reduced comparatively at the uppermost surface of the ring bulk because of the larger thermal contraction of the metal ring along the axial direction. As a result, the bulk is likely to break due to the electromagnetic tensile stress. We have proposed a new reinforcement structure of the metal ring to prevent such fracture [4]. In this study, we review and summarize previous studies and our recent research activities for the numerical simulation of the mechanical properties of REBaCuO bulks reinforced by a metal ring. We propose a new reinforcement structure for practical bulks to avoid any mechanical fracture, and discuss the possibility of achieving higher trapped fields over 20 T, based on these numerical simulations.

[1] T. M. Johansen, Supercond. Sci. Technol. **13** (2000) R121.
[2] H. Fujishiro *et al.*, Supercond. Sci. Technol. **30** (2017) 085008.
[3] K. Takahashi *et al.*, IEEE Trans. Appl. Supercond. **28** (2018) 6800705.
[4] H. Fujishiro *et al.*, Physica C **550** (2018) pp. 52-56.

Keywords: field cooled magnetization, numerical simulation, REBaCuO bulk, mechanical properties

WB5-5-INV

Pulse Field Magnetization to Bulk Superconductor for Applications

*Tetsuya Ida[1], Masahiro Watasaki[1,2], Koji Shigeuchi[3], Mitsuru Izumi[1]

Tokyo University of Marine Science and Technology, Japan[1]
National Institute of Technology, Hiroshima College, Japan[2]
Chiba University, Japan[3]

Over the past 15 years, we have been developing synchronous motors using high-temperature superconductor (HTS) materials for the field pole. Pulse field magnetization (PFM) technique is a relatively simple and inexpensive method to magnetize a plurality of high temperature superconducting bulk materials constituting the field pole inside the motor. However, as is well known, the HTS bulk is trapped unevenly distorted magnetic field distribution, low maximum trapped magnetic flux density and total magnetic flux as compared to field cooling (FC) by PFM. In order to enhance the performance of the synchronous motor incorporating the superconducting field, we worked on improving the trapped magnetic field characteristics by PFM.

Until now, it has been tried by several researchers that HTS bulk traps the magnetic flux optimally by combining multiple PFM and temperature control although as the HTS motor has many HTS bulks, it is preferable to complete magnetization immediately as possible. The pulsed magnetic field generated by the LCR transient response achieves a high penetration magnetic flux density rapidly and therefore activates the flux motion. Especially, the magnetic flux penetrated into the HTS bulk by PFM caused flux jump when the magnitude of the trapped magnetic flux density by the FC was exceeded. In order for the HTS bulk to obtain a high magnetic field and homogeneity, the PFM technique for suppressing the local heat generation accompanying this excessive magnetic flux motion is important. The waveform controlled pulse magnetization (WCPM) makes it possible to apply pulsed magnetic field waveforms independent of LCR transient response to the HTS bulk, it may improve the trapped magnetic field characteristics by PFM in order to obtain the excellent magnetic field properties. Since the state of flux jumps fluctuates, the behavior of the penetrating magnetic flux should be reflected immediately in the control of the pulse magnetic field waveform during PFM. By feeding back the magnetic flux density measured on the GdBCO bulk surface to the magnetizer, we obtained a trapped magnetic flux density comparable to FC from applying a single pulse magnetic field. In the near future WCPM technology will be useful as a practical magnetization method in HTS applications such as motors.

Keywords: Pulse Field Magnetization, GdBCO, Synchronous Motor, Generator

WB5-6

Generation of Uniform Magnetic Field between Face-to-Face HTS Bulk Magnets

*Tetsuo Oka[1], Kazuya Higa[2], Shunta Tsunoda[2], Jun Ogawa[2], Satoshi Fukui[2], Natsuki Inoue[1], Muralidhar Miryala[1], Masato Murakami[1], Kazuya Yokoyama[3], Takashi Nakamura[4]

Shibaura Institute of Technology[1]
Niigata University[2]
Ashikaga Institute of Technology, Japan[3]
RIKEN[4]

Aiming to develop the compact-scale nuclear magnetic resonance devices, the authors have been developing the uniform magnetic fields in the space between the face-to-face settled magnetic poles which contain HTS bulk magnets. In general, since the NMR magnets require highly uniform field, it was expected to be difficult to form such homogeneous magnetic-field distribution with use of HTS bulk magnets, which are originally exhibit the inhomogeneous magnetic field with steep field gradient. The authors curved the shape of the magnetic field distribution from convex to concave by attaching a ferromagnetic plate on the pole surface. When the magnet poles were settled face-to-face, the magnetic-field uniformity in the space of 4 x 4 mm2 reached under 500 ppm. The uniformity under 1,500 ppm is necessary to detect NMR signals, and the performance is regarded as available for detecting the signals.

Keywords: high Tc superconductor, bulk magnet, uniformity, field trapping

ED1-1-INV

Superconducting Detector Technologies for Single Photonics and Quantum Information

*Sae Woo Nam[1]

National Institute of Standards and Technology, Boulder, CO USA[1]

Single-photon detectors are increasingly becoming an essential tool for a wide range of applications in physics, chemistry, biology, communications, medicine, and remote sensing. Ideally, a single photon detector generates a measurable signal only when a single photon is absorbed. Furthermore, the ideal detector would have 100% detection efficiency, no false positive (dark counts), and transform-limited timing resolution. Recently, there has been tremendous progress in the development of superconducting devices with nearly ideal performance. There have been significant effort to package superconducting detectors into systems that could be used in real-world applications. I will review a few technological breakthroughs detector design / performance, will briefly review a few applications relevant to quantum information science.

ED1-2-INV

Study of Low Temperature Detectors in INFN

*Flavio Gatti[1,2]

Department of Physics, University of Genova, Section of Genova. Via Dodecaneso 33, 16146, Genova, Italy[1]
INFN, Section of Genova. Via Dodecaneso 33, 16146, Genova, Italy[2]

The first significant developments of Low Temperature Detectors (LTD) in INFN date back to the late sixties, with the development of first full superconducting bolometers for applications to the detection of molecular beams [1] and the first studies of STJs as particle detectors. Later, in the nineties, the quest for determining the neutrino mass scale and its nature has driven the investigations of new LTDs, such as small superconducting rhenium micro-calorimeters for the precise single beta spectroscopy of Re-187, as well as the very large tellurium oxide cryogenic calorimeters for double beta decay searches with Te-130. Thanks to rhenium superconducting detectors, it has been possible to discover the tiny influence of the surrounding crystal structure on the beta nuclear decay [2], that must be taken into account as additional term to the original Fermi formulation of the beta decay. The legacy of these pioneering neutrino LTD developments has led to the present projects HOLMES [3], CUORE [4] and PTOLEMY, that will be presented in more details. INFN is also collaborating with Universities and other National and International Institutions in the field of astroparticle physics, for hunting the elusive Dark Matter particles with massive LTDs in the Gran Sasso Underground Laboratory, as well as to investigate the origin of the Universe with sensitive measurements of the cosmic microwave background with TES bolometers on board of stratospheric balloons, or contribute with its own LTD expertise to the focal plane TES instrument of the future X-ray Space Telescope ATHENA. An overview of the present and future LTD developments will be done.

[1] M. Cavallini et al., A Superconducting Bolometer as a High Sensitivity Detector for Molecular Beams, *Z. Naturforsch.* 24 a, 1850—1851 (1969)
[2] F. Gatti et al., Detection of the Beta Environmental Fine Structure, *Nature*, 397, 137-139 (1999).
[3] B. Alpert et al, HOLMES: the electron capture decay of 163-Ho to measure the electron neutrino mass with sub-eV sensitivity, *EPJ C* (2015) 72:112.
[4] C. Alduino et al., First Results from CUORE: A Search for Lepton Number Violation via 0νββ Decay of Te-130. *Phys. Rev. Lett.* 120, 132501 (2018)

ED1-3-INV

X-ray Microcalorimeters for High Resolution X-ray Spectroscopy of Astrophysical Plasmas

*Yuichiro Ezoe[1]

Tokyo Metropolitan University[1]

A new era of high resolution X-ray spectroscopy of astrophysical plasmas is opened up with X-ray microcalorimeters. The X-ray microcalorimeter measures an energy deposition of an X-ray photon and precisely determines the X-ray energy. In comparison with gratings, it can be applied for diffuse X-ray plasmas in such as supernovae and clusters of galaxies and has a higher energy resolution around Fe K lines around 6 keV.

The Japanese Hitomi satellite launched in 2016 carried the X-ray microcalorimeter SXS. In spite of its short life due to an unexpected incident, the SXS achieved unprecedented energy resolution of ~5 eV in FWHM at 6 keV in space. We succeeded in conducting the first astronomical observation by an orbiting X-ray microcalorimeter. Now we plan to launch basically the same detector in the early 2020's.

Toward future space missions in the late 2020's and early 2030's, we are developing transition edge sensor (TES) microcalorimeters. While the SXS was based on semiconductor thermistors, it uses a sharp normal-to-super transition as a thermistor. A very high responsivity and low impedance of the TES allows higher energy resolution and higher density readout by SQUID amplifier. While the SXS was a 36 pixel array, we aim at a more than 100 pixel array with better energy resolution (<5 eV in FWHM at 6 keV). In this talk, we review the X-ray microcalorimeters and our development of the TES microcalorimeters for future missions [2-3].

[1] Hitomi Collaboration, "The Quiet Intracluster Medium in the Core of the Perseus Cluster", Nature Letters, 2016, 535, 117-121
[2] Y. Ezoe, et al., "Tapered Edge Readout Wiring for Transition Edge Sensor Calorimeter Arrays Using Ion Milling", IEEE Trans. Appl. Cond., 2015, 25, 2100805
[3] K. Kosaka, Y. Ezoe, et al., "Study of Surface Roughness Effect on Super-normal Transition of Ti/Au Transition Edge Sensor Calorimeters ", J. Low Temperature Detectors, in press

Keywords: X-ray microcalorimeter, transition edge sensor, space application

ED2-1-INV

Development of Low Tc DC SQUID and its Applications in China

*Xiaoming Xie[1, 2], Y. Zhang[1,2], Z. Wang[1,2], L.L. Rong[1,2], S.L. Zhang[1,2], H. Dong[1,2], L.Q. Qiu[1,2], X.Y. Kong[1,2], L. Chen[1,2]

Center for excellence in superconducting electronics, Chinese Academy of Sciences, China[1]
Shanghai Institute of Microsystem and Information Technology, Chinese Academy of Sciences, Shanghai, China[2]

SQUID offers extreme low noise detection of magnetic flux and other physical quantities which can be converted to magnetic flux. In this talk, I will summarize the development of low Tc dc SQUIDs and their applications at Shanghai Institute of Microsystem and Information Technology (SIMIT) over the last ten-years. With the advanced Superconducting Electronics Facility (SELF), and high quality Nb/AlOx/Nb and NbN/AlN/NbN junction fabrication technology, SIMIT has developed a series of dc SQUIDs including SQUID magnetometers, planar magnetic gradiometers and 3D Nano-SQUIDs. We have investigated systematically dc SQUID with slightly under-damped Josephson junctions. The increased flux-to-voltage transfer coefficient enabled the direct readout of SQUID signals with one operational amplifier. The greatly simplified SQUID sensor show acceptable noise and superior performances for outdoor applications. On system integration and applications: SIMIT has commercialized China's first 4-9 channel MCG systems for reliable operation in unshielded environment. We have developed a multichannel ultra-low field magnetic resonance imaging system with a pair of permanent magnets for pre-polarization and demonstrated the 3D imaging of fruit/vegetable samples with long relaxation time. The system is being upgraded with electromagnetic coil replacing the permanent magnetic imaging bio-tissues with larger sample size and shorter relaxation time. We have developed a ground based SQUID receiver for geophysical transit magnetic method (TEM). The low noise and high bandwidth allowed for accurate measurement for signals from shallow area down to depth over 1000 meters. The system was tested at many areas with different geological conditions and available drilled results show excellent agreement. We have also developed China's first air-borne full tensor magnetic gradient measurement system. The system has been optimized for several cycles and it is expected the system will soon be ready for services.

ED2-2-INV

Vortices in Mesoscopic Superconductors and SQUID microscopy for 3D Imaging

*Takekazu Ishida[1,2], The Dang Vu[3,4,5], Masaki Toji[5], Yoshitdugu Ninomiya[5], Shigeyuki Miyajima[5,6], Thanh Huy Ho[4], Hiroaki Shishido[2,5], Masaru Kato[2,5], Masaaki Maezawa[7], Mutsuo Hidaka[7], Masahiko Hayashi[8]

Division of Quantum and Radiation Engineering, Osaka Prefecture University, Sakai 599-8570, Japan[1]
NanoSquare Research Institute, Osaka Prefecture University, Sakai 599-8531, Japan[2]
Materials and Life Science Division, J-PARC Center, JAEA, Tokai, Ibaraki 319-1195, Japan[3]
University of Sciences, Vietnam National University HCMC, Ho Chi Minh, Viet Nam[4]
Department of Physics and Electronics, Osaka Prefecture University, Sakai 599-8531, Japan[5]
National Institute of Information and Communications Technology, Kobe, Hyogo, 651-2492, Japan[6]
National Institute of Advanced Industrial Science and Technology, Tsukuba 305-8568, Japan[7]
Faculty of Education and Human Studies, Akita University, Akita 010-8502, Japan[8]

The size requirements for satisfying the mesoscopic nature can be relaxed by thinning a superconducting film so that Pearl vortices are evident, exhibiting a long effective penetration depth [1,2,3,4]. We introduce a sectoral defect into a disk to investigate effect of the symmetry breaking of a perfect disk on vortex dynamics, where the sectoral defect acts as a preferential gateway for vortices to enter the disk [5]. A characteristic of the vortex configuration is the critical number of vortices (or 'magic number') at which the single-arc structure becomes a multiple-arc structure, which can be tuned by changing the opening angle of the sectoral defect.

Superconducting quantum interference device (SQUID) is a fundamental sensor in constructing an ultrasensitive magnetic measurement equipment [6]. However, a typical scanning SQUID microscope has a single pick-up coil and a single channel SQUID readout circuit to obtain the distribution of local magnetic field component only perpendicular to the sample surface along the Z direction. Recently, we started to develop a scanning SQUID vector microscope equipped with a vector pickup coil [7,8,9]. Scanning vector SQUID microscopy gives good vortex images by using a 3-channel SQUID readout circuit.

This work was partially supported by Grant-in-Aid from JSPS (No. 25600018, No. 26820130, No. 26800192, No. 23226019, No. 15K13979).

References

[1] J. Pearl, Appl. Phys. Lett. 5, 65 (1964).
[2] Ho T. Huy *et al.*, Supercon. Sci. Tech. 26, 065001 (2013).
[3] N. Kokubo *et al.*, Phys. Rev. B 82, 014501 (2010).
[4] Ho T. Huy *et al.*, P Physica C 484, 86 (2013).
[5] T.S. Alstrøm *et al.*, Acta Applicandae Mathematicae 115, 63 (2010).
[6] J. R. Kirtley *et al.*, Appl. Phys. Lett. 66, 1138 (1995).
[7] M. Hayashi *et al.*, Appl. Phys. Lett. 100, 182601 (2012).
[8] Vu T. Dang *et al.*,J. Phys. Conf. Ser. 871, 12075 (2017).
[9] S. Miyajima *et al.*, IEEE Trans. Appl. Supercond. 25, 3 (2015).

Keywords: SQUID microscopy, Vortex, Mesoscopic superconductor, 3D imaging

ED2-3-INV

Fabrication of MoN Superconducting Single Photon Detector

*Hiroyuki Shibata[1], Naoto Kirigane[1], Kento Sakai[1], Hiromichi Niii[1], Kentaro Fukao[1], Daisuke Sakai[1], Kou Ohnishi[2], Wakako Nakano[2], Yasutaka Matsuo[2]

Kitami Institute of Technology, Hokkaido, Japan[1]
Hokkaido University, Hokkaido, Japan[2]

For the fabrication of superconducting nanostrip photon detector (SSPD, SNSPD), NbN has been commonly used as a superconducting material. Although the performance of NbN-SSPD has been significantly improved in the last decade, there have been some reports using alternative materials for SSPD. It may be possible to increase the operating temperature, to increase system detection efficiency, or to increase detection speed of SSPD using alternative materials. Here, we study our fabrication of SSPD based on MoN.

MoN has a T_c of 12 K and long electron-phonon interaction time, which is favorable for SSPD. The 7 nm thick MoN film with T_c = 7 K is grown by magnetron sputtering on sapphire substrate. The meander pattern with a line and space width of 150 nm is fabricated by the standard electron beam process and SF_6 dry etching. As shown in the figure, the system detection efficiency reaches 15 % at 1560 nm and 32 % at 405 nm without cavity structure. These values are higher than those of NbN-SSPD with a same cross-section and indicates that the MoN is the attractive materials for SSPD with high detection efficiency.

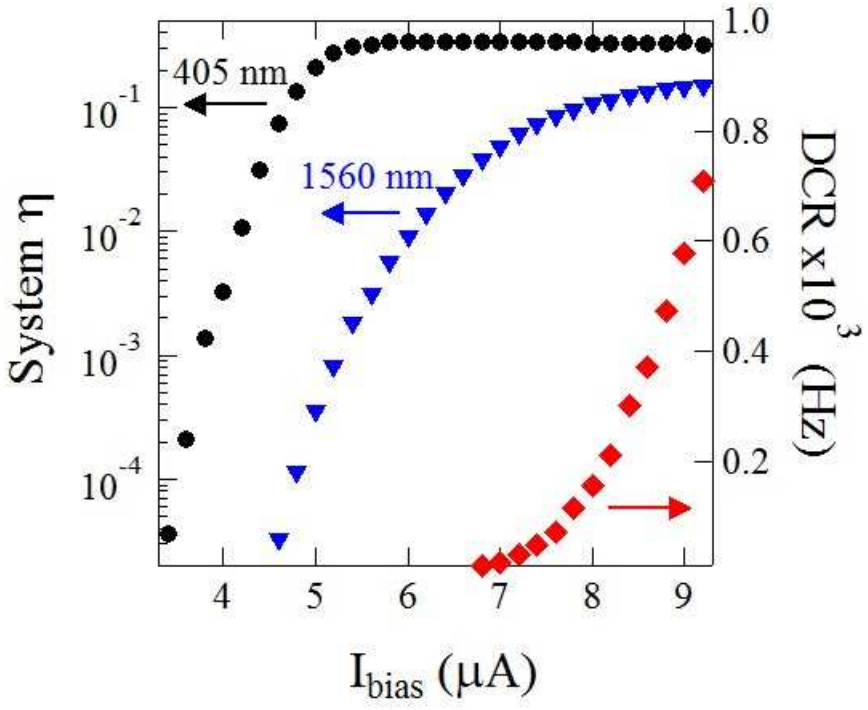

Keywords: SSPD, SNSPD, MoN

ED2-4

Research toward realization of large-scale superconducting nanowire single photon detector system

*Shigehito Miki[1,2], Masahiro Yabuno[1], Shigeyuki Miyajima[1], Fumihiro China[1], Naoki Takeuchi[3], Taro Yamashita[4], Hirotaka Terai[1]

National Institute of Information and Communications Technology[1]
Kobe University[2]
Yokohama National University[3]
Nagoya University[4]

Superconducting nanowire single-photon detector (SSPD or SNSPD) has high detection efficiency, low dark count rate, low timing jitter and wide spectral sensitivity, making it one of the most attractive detectors in a broad research fields ranging from life science to quantum information science. Therefore, two-dimensionally arranged multi-pixel SSPD array would be a novel single photon imaging system, which allow the detection of incident photons not only with position sensitivity but also with high temporal resolution. Due to this unique feature, the SSPD imaging array is expected to open new applications, such as a time-of-flight range imaging, a spatial correlation measurement of photons and a spectral correlation measurement combined with a spectrometer. A critical issue in a development of practical large-scale SSPD imaging array is to reduce an enormous number of readout lines which lead to a heat inflow from the room temperature. To overcome this problem, we have proposed and been developing multi pixel SSPD array system with cryogenic signal processor based on superconducting digital circuits, which can drastically reduce the number of readout cables to room temperature. In this work, we will present the current status of research and development toward realization of large scale SSPD array system

Keywords: superconducting nanowire, single photon detector, detector array

ED3-1-INV

RF Waveform Synthesizers with quantum-based accuracy for communications metrology

*Manuel A. Castellanos Beltran[1], Justus A. Brevik[1], Christine A. Donnelly[1], Anna E. Fox[1], David I. Olaya[1,2], Adam Sirois[1], Paul D. Dresselhaus[1], Peter Hopkins[1], Samuel P. Benz[1]

NIST[1]
University of Colorado Boulder[2]

The NIST Superconductive Electronics Group is developing cryogenic synthesizers to produce quantum-accurate, spectrally-pure waveforms in the microwave and millimeter-wave frequency bands. These superconducting RF references have immediate utility in the wireless communications industry as quantum-accurate sources. NIST research to extend quantum-based synthesis from audio frequencies to RF has followed two parallel approaches: first, a theoretical and experimental investigation to extend the existing JAWS (Josephson arbitrary waveform synthesizer) technology from 20 kHz to 1 GHz or higher (RF JAWS), and second, a fundamentally new approach based on single-flux-quantum (SFQ) superconducting digital circuits which has the potential to synthesize millimeter wave (> 30 GHz) signals (SFQ JAWS).

Limitations to amplitude accuracy and spectral purity for RF JAWS will be addressed, including those from timing jitter, impedance matching, and transmission-line delays. By carefully designing the RF JAWS circuits around those constraints, we have recently synthesized single and multiple tones at 1 GHz and X mV amplitude with an array of 1000 junction.

SFQ JAWS consists of an RSFQ driver used to generate SFQ pulses that are then multiplied with a parallel network of splitters and SQUIDs and recombined coherently to give larger amplitude, multi-flux quanta pulses. We have designed and tested a prototype SFQ JAWS circuit, which includes an 8X pulse-multiplier, to synthesize 4 GHz tones with 160 uV amplitude. Faster clocking of pulses and more splitter stages to increase the multiplication factor will be exploited to increase the synthesis amplitude and frequency.

Both the RF JAWS and SFQ JAWS circuits were fabricated in NIST's Boulder Microfabrication Facility using self-shunted Nb/NbxSi1-x/Nb Josephson junctions (JJs), with the barrier composition tuned differently for use in RF JAWS or SFQ JAWS.

For both approaches we are developing a 50 GHz broadband cryogenic calibration system to transfer the quantum accuracy from our 4 K superconducting integrated circuits to room temperature measurements. Preliminary results of this calibration technique will be presented as applied to a JAWS device.

Keywords: Josephson arrays, Signal synthesis, Standards, Digital-analog conversion

ED3-2-INV

High-Transition Temperature Josephson Junctions

*Shane Cybart[1]

Department of Mechanical Engineering, Materials Science and Engineering Program, University of California Riverside, U.S. A.[1]

The 1987 discovery of high-T_C superconductivity in ceramic materials at temperatures around 90K set off a frenzy of research in the development of high-T_C electronics, motivated by the prospects of electronics operating in liquid nitrogen at 77 K opposed to 4 K liquid helium. Unfortunately, researchers soon discovered that these new materials were much more difficult to process than conventional metal superconductors. High-T_C materials are very anisotropic and the superconducting properties vary along the different crystallographic directions which complicates manufacturing of the basic building blocks of superconducting electronics: Josephson junctions. Furthermore, the length scale of superconductivity in high-T_C ceramics is very short compared to low-T_C metals. Despite these challenges many high-T_C Josephson junction manufacturing techniques have emerged over the last three decades but none is able to generate large numbers of junctions with predictable characteristics necessary for large scale circuits.

Recently, my group has demonstrated a new scalable nanomanufacturing method of high-T_C electronics using the finely focused beam from a helium ion microscope, which has the potential to deliver large numbers of high-quality circuits while at the same time reducing their costs by orders of magnitude. The gas field ion source of the helium microscope produces a beam with a diameter less than 0.5nm that can disorder the oxygen lattice to tune transport properties on a local atomic scale. Increasing doses of irradiation reduces T_C and increases resistivity in a controllable way. At moderate levels of irradiation ~10^{15} ions/cm^2 the material is completely transformed into a non-superconducting insulator. I will discuss recent progress in this area and describe the device capabilities of single junctions, nanowires and super conducting quantum interference devices fabricated from this approach.

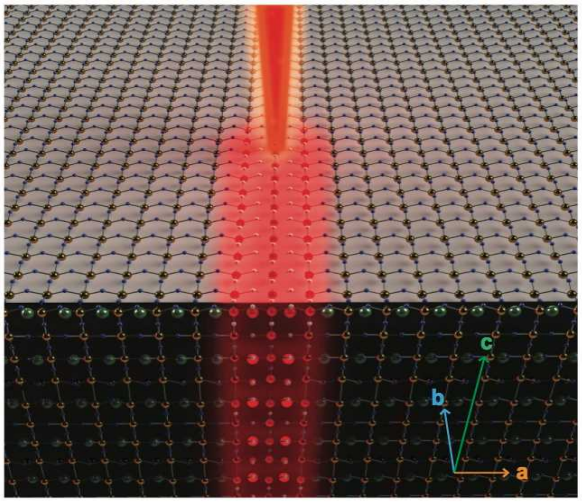

Representation of sub-10nm materials modification in a single crystal film of yttrium barium copper oxide to create a planar superconductor insulator superconductor Josephson junction.

ED3-3

Transport Properties and Pinning Analysis for Co-doped $BaFe_2As_2$ Thin Films on Metal Tapes and Single Crystal Substrates

*Zhongtang Xu[1], Yanwei Ma[1,2]

Key Laboratory of Applied Superconductivity, Institute of Electrical Engineering, Chinese Academy of Sciences, Beijing, 100190, People's Republic of China[1]
University of Chinese Academy of Science, Beijing, 100049, People's Republic of China[2]

Improving the critical current density in iron-based superconductors is an important strategy for applications. We investigate the transport properties and pinning analysis of $BaFe_{1.84}Co_{0.16}As_2$ (Ba122:Co) thin films on metal tapes with a large in-plane misorientation and on CaF_2 single crystal substrates by pulsed laser deposition. High transport J_c occurs in both thin films, with 2.6 MA/cm^2 and 0.98 MA/cm^2 in 9 T at 4.2 K for thin films on CaF_2 and metal tapes [1, 2], respectively, promising for high field applications. Microstructure investigations reveal a high density of *ab*-planar defects (stacking faults) and localized vertical defects present in the sample. The Dew–Hughes mode analyses prove that pinning centers by surface defects and by point defects are responsible for *H*//*ab* and *H*//*c*, respectively. In particular, Pinning force analysis indicates a significant enhancement compared with similar Ba122:Co coated conductors. Therefore, the high Jc in high magnetic field for both *H*//*ab* and *H*//*c* are related to surface and point defects which act as the pinning centers in Ba122:Co films.

References

[1]. Z. T. Xu, P. S. Yuan, F. Fan, Y. M. Chen and Y. W. Ma, Supercond. Sci. Technol. **31**, 055001 (2018).
[2]. P. S. Yuan, Z. T. Xu, D. L. Wang, M. Zhang, J. Q. Li and Y. W. Ma, Supercond. Sci. Technol. **30**, 025001 (2017).

Keywords: iron-based superconducting films, PLD, coated conductors

ED3-4

TiN coplanar waveguide resonators fabricated on Si (100) substrates

*Hirotaka Terai[1], Wei Qiu[1]

National Institute of Information and Communications Technology, Japan[1]

The low-loss microwave resonator is an important element for realizing a quantum computer based on circuit quantum electrodynamics. Nitride superconductors such as TiN, NbTiN have been studied as low-loss materials to realize microwave resonators with high quality factors [1,2]. We fabricated and measured coplanar waveguide (CPW) resonators made of TiN films on Si (100) substrates. The TiN films were deposited by a DC reactive sputtering method introducing a mixture of Ar and N_2 gases in an ultra-high-vacuum chamber with a background pressure below 10^{-7} Pa. The TiN films deposited at room temperature has polycrystalline structures, and a smaller grain size for the TiN film deposited at a higher pressure, resulting in a higher resistivity. The TiN films were patterned into half-wave CPW resonators to estimate internal quality factors, where London penetration depths of the TiN films were also estimated from the resonance frequency shift. The CPW resonators were measured below 20 mK in the dilution refrigerator (Oxford Inst. Triton400). The results were summarized in Table. 1. The estimated penetration depths of the TiN films were 680, 1060 and 1290 nm for the TiN films prepared at the total gas pressures of 4, 6 and 8 mTorr, respectively, which agree well with penetration depths of 660, 1070 and 1250 nm calculated from the relationship among l, r and T_C in the weak-coupled BCS limit. The TiN films deposited at a higher gas pressure tends to have a higher internal quality factor, which was 7.7 x 10^5 for the TiN film at 8 mTorr close to the single photon regime. The TiN film deposited at 850°C on hydrogen-terminated silicon (100) substrates grew with (100) orientation and showed the resistivity of 3.7 mWcm and T_C of 5.4 K (#4 in Table 1), giving the penetration depth of around 80 nm. However, the observed internal quality factor was not high as 1 x 10^5, which was lower than those in the CPW resonators made of polycrystalline TiN films.

Acknowledgement
This work is supported by JST ERATO (grant no. JPMJER1601) and CREST (grant no. JPMJCR1775).

Reference
[1] M. R. Vissers *et al.*, Appl. Phys. Lett. 97, 232509, 2010.
[2] J. M. Sage *et al.*, J. Appl. Phys. 109, 063915, 2011.

Table 1 Summery of properties of TiN CPW resonators fabricated under various sputtering conditions

Sample	N_2 (Ar=25)	Pressure (mTorr)	Deposition Temp. (°C)	T_C (K)	Resistivity (μΩ cm)	Thickness (um)	f_{obs} (GHz)	L_K (nH)	λ_{RES} (nm)	λ_{BCS} (nm)	Qi (n) x 10^5
#1	3	4	RT	4.7	221.9	0.158	6.0368	1.176	679	663	1.8 (4)
#2	3	6	RT	4.3	531.6	0.152	4.3832	2.995	1062	1073	3 (21)
#3	3	8	RT	4.7	785.6	0.121	3.4105	5.503	1285	1247	7.7 (11)
#4	4	1	850	5.4	3.7	0.198	9.2523	0.011	72	85	1.3 (1)

Keywords: Superconducting qubit, Nitride superconductor, Coplanar waveguide resonator, Kinetic inductance

ED4-1-INV

Quantum Engineering of Superconducting Qubits

*William D. Oliver[1,2]

Massachusetts Institute of Technology, USA[1]
MIT Lincoln Laboratory, USA[2]

Superconducting qubits are coherent artificial atoms assembled from electrical circuit elements. Their lithographic scalability, compatibility with microwave control, and operability at nanosecond time scales all converge to make the superconducting qubit a highly attractive candidate for the constituent logical elements of a quantum information processor. In this talk, we review this progress and the challenges ahead as we create the future of engineered quantum systems.

Keywords: Quantum Engineering, Superconducting Qubit

ED4-2-INV

Coherent quantum quantum phase slip effect in nano-wires from ultrathin niobium-nitride films

*O. V. Astafiev[1,2,3]

Royal Holloway, University of London, Egham, Surrey TW20 0EX, United Kingdom[1]
National Physical Laboratory, Teddington, TW11 0LW, United Kingdom[2]
Moscow Institute of Physics and Technology, Dolgoprudny, Russia[3]

Ultrathin superconducting films of highly disordered materials are very promising for several applications including devices based on the coherent quantum phase slip effect. We develop a process of growing ultrathin superconducting niobium nitride films fabricated with a plasma-enhanced atomic layer deposition (PEALD. By adjusting parameters, the chemical embedding of undesired oxygen into the films was minimised and a film structure consisting of mainly polycrystalline niobium nitride with a small fraction of amorphous niobium oxide and niobium oxo-nitrides were formed. The film thickness variation between 40 and 2 nm exhibits a pronounced change of the electrical conductivity at room temperature and reveals a superconductor–insulator-transition in the vicinity of 3 nm film thickness at low temperatures. The thicker films with resistances up to 5 kΩ per square in the normal state turn to the superconducting one at low temperatures. Using the films, we have developed phase-slip quantum bit with a nano-wire and demonstrated quantum interference of two phase slip amplitudes. This effect is dual to superconducting quantum interference with two Josephson junctions.

Keywords: Superconductivity, Coherent Quantum Phase Slip, Qubits

ED4-3-INV

Quantum hybrid system with a superconducting qubit and surface acoustic waves

*Atsushi Noguchi[1, 2]

Research Center for Advanced Science and Technology (RCAST), The University of Tokyo, Meguro-ku, Tokyo, 153-8904, Japan[1]
PRESTO, Japan Science and Technology Agency, Kawaguchi-shi, Saitama 332-0012, Japan[2]

Hybrid quantum systems have been widely studied in quantum information science [1]. Among the several quantum systems, surface acoustic waves (SAW) have recently attracted much interest as an alternative quantum mode localized on a surface of a material [2]. In piezoelectric materials, SAW can be strongly coupled to electric fields between surface electrodes and are widely applied in compact microwave components because of their short wavelength and small losses. SAW can also couple to other physical systems [3] such as superconducting qubit, quantum dots and NV centers through various form of elastic effects. Opto-elastic interaction of SAW opens the possibility to achieve a quantum transducer from microwave photons to optical photons in the telecommunication band.

Here, we report experiments on a hybrid quantum system consisting of a SAW resonator and a superconducting quantum circuit [4]. We demonstrate microwave-driven parametric couplings induced by the nonlinearity of the qubit, which serves as a transducer between the phonons in the SAW resonator and the photons in the superconducting MW resonator. The thermal phonons in the sub-GHz SAW resonator are up-converted to the MW frequency range where near-quantum-limited measurement of photons is available. We observe thermal fluctuations in the SAW resonator below the mean phonon number of unity with an unprecedented sensitivity.

We also report the opto-(electro-)mechanical system with SAW resonator using superconducting circuit [5]. A nonlinear element with multi Josephson junctions makes an artificial radiation pressure onto the electromagnetic waves. We achieve the optomechanical system in the single photon quantum regime with this nonlinear superconducting circuit.

[1] G. Kurizki, P. Bertet, Y. Kubo, K. Mølmer, D. Petrosyan, P. Rabl, and J. Schmiedmayer, Proc. Natl. Acad. Sci. U.S.A. 112, 3866 (2015).
[2] M. V. Gustafsson, P. V. Santos, G. Johansson, and P. Delsing, Nat. Phys. 8, 338 (2012).
[3] M. J. A. Schuetz, E. M. Kessler, G. Giedke, L. M. K. Vandersypen, M. D. Lukin, and J. I. Cirac, Phys. Rev. X 5, 031031 (2015).
[4] A. Noguchi, R. Yamazaki, Y. Tabuchi, and Y. Nakamura, Phys. Rev. Lett. 119, 180505 (2017)
[5] A. Noguchi, R. Yamazaki, Y. Tabuchi, and Y. Nakamura, arXiv:1808.03372 (2018)

ED4-4-INV

Scalable superconducting quantum annealer based on 2.5D packaging technology and application specific architecture

*Shiro Kawabata[1]

National Institute of Advanced Industrial Science and Technology (AIST)[1]

Quantum annealing is a promising technique which leverages quantum mechanics to solve hard combinatorial optimization problems. D-Wave Systems Inc. is the first company to commercialize superconducting quantum annealer in 2011 and ship a new machine with 2048 qubit in 2017. However, integration of larger number of qubit as well as improvement of qubit coherence are required for practical applications. In this talk we will overview our technological integration scheme for large-scale superconducting quantum annealer in AIST. The scalability is achieved by QUIP (QUbit, Interposer and Package substrate) structure, which is based on our multi-layer fabrication and multi-chip 2.5D packaging technology such as Through Silicon Via (TSV) and flip-chip bonding. We have also developed an Application Specific Annealing Computing (ASAC) architecture in order to increase the available hardware budget and reduces the cost and time for R&D. In addition, we will explain how to design special quantum anneaaler for prime factoring.

Keywords: Quantum annealing, Superconducting quantum circuit, Packaging technology, Superconducting electronics

ED4-5

Principle Verification of the Superconducting Flux Qubit Cell Toward the Quantum Sampling Approach for Training of Deep Neural Networks

*Daisuke Saida[1], Hayato Ariyoshi[2], Yuki Yamanashi[2]

MDR Inc.[1]
Yokohama National University[2]

An approach for training of Deep Neural Networks (DNNs) utilizing a quantum annealing machine for updates of weights and biases (named as a quantum sampling) has been proposed [1]. The quantum sampling potentially provides better accuracy with fewer iterations of training compared to a classical contrastive divergence training in typical DNNs. However, further investigations are needed to characterize what determines an accuracy and how the performance scales with the size of problems increases in the quantum sampling approach. By utilizing openly available fabrication process, we aimed for a construction of the system in the superconducting flux qubit on quantum sampling.

We started the development of the quantum sampling system based on the openly available AIST 2.5 kA/cm^2 Nb standard process 2. For its first step, principle verification of a superconducting flux qubit cell including the qubit and its readout circuit is indispensable. Figure 1 (a) shows the overview of the qubit cell composed of the tunable rf-SQUID quantum bit (qubit) and the read-out dc-SQUID. I_c of the Josephson junction in the qubit and β_L of the read-out dc-SQUID are tunable by adjusting magnetic flux applied to each loop. Figure 1(b) shows calculated energy potential of the qubit. According to Ref. [3], the quantum tunneling can be utilized when height of energy barrier exists in the range surrounded by red dotted lines in Fig. 1 (b). We chose the I_c of 50 μA and L of 15-20 pH of the qubit. Figure 1(c) indicates layout of the qubit cell. To achieve efficient detection in the read-out SQUID, threshold current characteristic having strong asymmetry for the flux was considered.

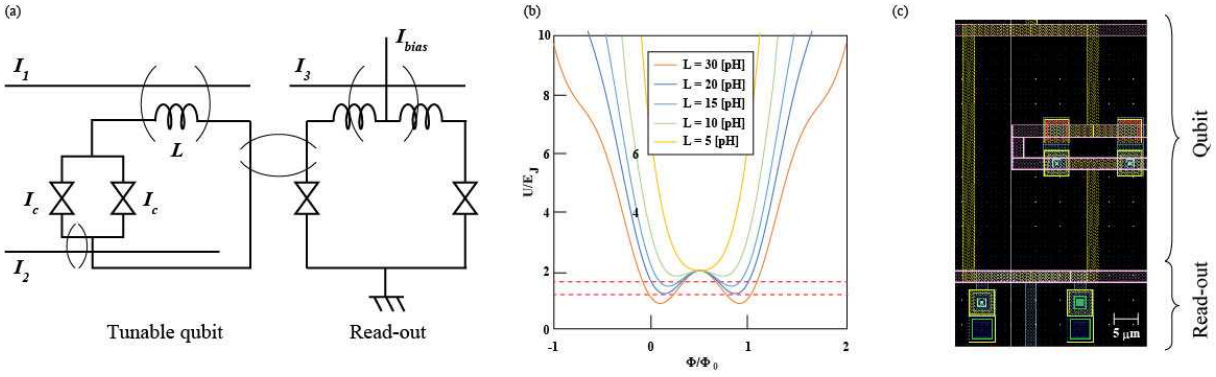

Figure captions

Fig. 1(a) The superconducting flux qubit cell having the qubit and its readout. (b) An analysis of potential energy in the qubits. The potential energy was calculated using inductances in the range of 5-30 pH. (c) A layout of the qubit cell.

References

[1] S. Adachi et al., *arXiv*:1510.06356 (2015).
[2] M. Hidaka et al., *Supercond. Sci. Technol. Supercond.*, **19** (2006) S138.
[3] R. Harris et al., *Phy. Rev. B*, **82** (2010) 024511.

Keywords: quantum sampling, Josephson junction (JJ), SQUID, flux qubit

ED5-1-INV

Implementation of a Synchronous Front-end and Addressing Circuit for Using in Superconducting Stripline Detector Arrays

Eren Can Aydogan[1], Kubra Usenmez[1], Sasan Razmkhah[1], *Ali Bozbey[1], Akira Fujimaki[2]

TOBB University of Economy and Technology, Department of Electrical and Electronics Engineering, 06560, Ankara, Turkey[1]
Department of Quantum Engineering, Nagoya University, Nagoya 464-8603, Japan[2]

Single Flux Quantum (SFQ) technology has already proven itself that it is a suitable alternative to CMOS technology to overcome some of the fundamental limits of speed, power consumption and sensitivity. SFQ logic offers about three orders of magnitude lower power consumption while maintaining a much higher switching speed. With the advancements in the SFQ technology, it becomes feasible to implement high density cryogenics read-out circuits for superconducing dedector arrays.

In this work, a synchronous addressing circuit is designed for reading the response of Superconducting Stripline Detector (SSLD) arrays. Each of these SSLDs is coupled to a comparator circuit. The addressing circuit triggers the comparator circuits coupled to the individual SSLDs in order and would send the address of that pixel to output together with the data of the triggered detector synchronously. Addressing circuit consists of a demultiplexer unit, counter circuit, array of D-Flip Flops (DFFs) and parallel to serial converter for decreasing the number of room temperature connections. After an SSLD pixel is irradiated, if the generated voltage value is more than the threshold level of the comparator, the comparator generates an SFQ pulse asynchronously. Generated SFQ pulses are transmitted to DFFs and when the addressing circuit triggers the clock of the DFFs, they release the SFQ pulse synchronously. At the end, address of the irradiated pixel and its own output are converted to serial pulse trains.

The designed architecture is a synchronous one that is activated by an external clock pulse. The clock period has a wide range of operation. So, it can be fed externally as well as with an on-chip clock generator to increase the frame rate of the array if desired. The circuit architecture is stackable and the number of bits can be increased without much effort. In this study, we report the results of a 2-bit and 4-bit addressing circuit to be used to read-out a 4x4 and 10x10 detector matrix respectively.

ED5-2-INV

Development of an extremely energy-efficient AQFP microprocessor

*Christopher L. Ayala[1], Olivia Chen[1], Ro Saito[2], Tomoyuki Tanaka[3], Naoki Takeuchi[1], Yuki Yamanashi[1,3], Nobuyuki Yoshikawa[1,3]

Institute of Advanced Sciences, Yokohama National University, Japan[1]
Department of Information Media and Environment Sciences, Yokohama National Univ., Japan[2]
Dept. of Electrical Engineering and Computer Engineering, Yokohama National Univ., Japan[3]

Adiabatic quantum-flux-parametron (AQFP) logic is an emerging technology in superconducting electronics that shows promise towards building extremely energy efficient computing systems with bit energies approaching $100k_BT$. In the effort of building an AQFP-based microprocessor, we have developed a prototype reduced instruction set computer (RISC)-based architecture called MANA (Monolithic Adiabatic iNtegration Architecture). A total of 19 core instructions have been defined for this architecture, enabling it to perform branching, load immediate data, perform various arithmetic and logic operations, and interface with external input/output such as off-chip memory.

In order to actually build and demonstrate the MANA chip, we are faced with the constraints of fitting the entire design on a 7 mm x 7mm chip using the AIST 10 kA/cm^2 high-speed standard process (HSTP). With this consideration, we have configured MANA with a 4-bit data word size and a 12-bit instruction word size. The main stages of MANA are the following:

1. **I**nstruction buffer, **d**ecode, and **i**ssue stage (IDI)
2. **R**egister **f**ile and e**X**ternal I/O stage (RFX)
3. **Ex**ecution stage (EX)
4. **W**rite **b**ack stage (WB)

Assuming the aforementioned configuration, we estimate 20,000 Josephson junctions (JJs) (5000 JJs for IDI, 8000 JJs for RFX, 2000 JJs for EX, and 5000 JJs for WB) are needed to implement this demonstrator chip.

Thus far, we have designed two key execution units using a 4-phase AQFP logic library: a 4-bit arithmetic logic unit (ALU), and a 4-bit data shifter. The ALU is based on the Kogge-Stone prefix-adder using a semi-custom approach and supports arithmetic addition and subtraction operations, as well as logical operations, namely: AND, OR, XOR and XNOR. The data shifter has been completely synthesized using our EDA toolchain based on the open-source 'yosys' logic synthesis tool with an AQFP cell mapping file. This combinational data shifter supports left/right logical shift, and arithmetic right shift operations. Full operation of these units with wide excitation margins was demonstrated.

Lastly, we look ahead and briefly discuss what other unique design approaches and architectures that can exploit the advantages of the AQFP logic, such as majority logic design and neuromorphic computing.

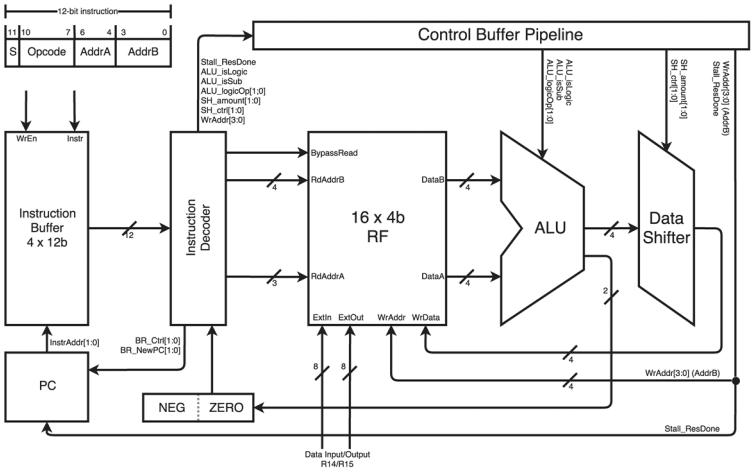

Figure 1: System-level architecture diagram of MANA.

Keywords: superconductor, aqfp, microprocessor, energy-efficiency

ED5-3

Numerical Analysis of Low-Power Half Single Flux Quantum Circuits Based on 0-π SQUIDs

*Masamitsu Tanaka[1], Yuta Yoshinomoto[1], Tomohiro Kamiya[1], Kyosuke Sano[1], Taro Yamashita[1,2], Akira Fujimaki[1]

Nagoya University, Japan[1]
JST-PRESTO, Japan[2]

We report numerical analysis on superconductor logic circuits based on "0-π SQUID" elements, which are composed of pairs of π-shifted Josephson junction (π-junction) such as ferromagnetic Josephson junction and conventional Josephson junction (0-junction). In such circuits, a π-leap in superconductor phase is observed at a single switching event of a 0-π SQUID, which correspond to a half magnetic flux quantum, and lower power consumption is expected compared to the conventional single flux quantum (SFQ) circuits.

Figure 1 (a) shows the schematic diagram of a 0-π SQUID. In the pendulum analogy, the direction of gravity is opposite for 0- and π-junctions. It suggests that if the loop inductance is very small, the 0-π SQUID can be switched by a smaller driving force like a pendulum in a gravity-free state. A 0-π SQUID has two stable states where the loop current flows in clockwise or counterclockwise. Our previous work [1] showed that a transmission line can be formed by connecting 0-π SQUIDs, where a flip of the state propagates. As shown in Fig. (b), π-leaps in the superconductor phase is observed, and we call this logic circuit family half single flux quantum (HSFQ) circuits.

We analyze more complex HSFQ wiring elements, including splitter, directional buffer, and merger using an analog circuit simulator [2]. These circuits are implemented based on conventional SFQ circuits, replacing Josephson junctions with 0-π SQUIDs. Our numerical results show the correct operations, and that the dc bias currents to 0-π SQUIDs can be controlled depending on loop inductance: for example, 20% of the sum of critical currents of junctions is sufficient when the product of loop inductance and critical current is reduced to $0.2\Phi_0$, while 70% of critical currents are typically used in conventional SFQ circuits.

[1] T. Kamiya et al. IEICE Trans. Electron. E101-C (2018) 385.
[2] Y. Yamanashi et al, Supercond. Sci. Technol. 31 (2018) 105003.

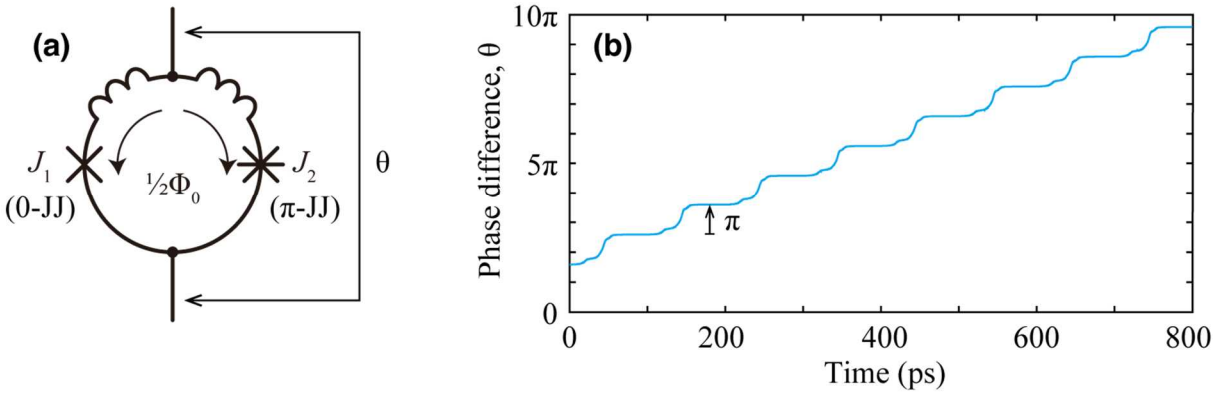

Fig. (a) schematic diagram and (b) phase difference transition of 0-π SQUID

Acknowledgment: This work was supported by JSPS KAKENHI Grant Numbers JP18H05211 and JP18H01498, and in part by VDEC, the University of Tokyo in collaboration with Cadence Design Systems, Inc. The authors would like to thank Yuki Yamanashi for help in the numerical simulation.

Keywords: π Josephson junctions, half single flux quantum, low-power consumption, energy-efficient logic circuits

ED6-1-INV

Recent progress of Chinese high-Tc superconductor filter to practical use

*Bin Wei[1]

State Key Laboratory of Low-Dimensional Quantum Physics, Department of Physics, Tsinghua University, Beijing 100084, China[1]

This paper reviews the recent progress of high temperature superconducting (HTS) filters in China and applications. With the development of high quality double-sided HTS films, HTS filters have been well studied and designed in the past few years. Novel designed methods, such as coupling matrix extracting method, dual-mode cascading method, and auxiliary line method are discussed in this paper. HTS filter devices, such as differential band-pass filters, absorptive filters, multiplexers, multi-band and multi-mode filters, wide-band filters, HTS linear phase filters, as well as tunable filters, are all studied recently. HTS filters have been used for mobile communication base stations and other wireless systems.

Reference

1. P. Ma, B. Wei, J. Hong, B. Cao, X. Guo and L. Jiang, "Design of Dual-Mode Dual-Band Superconducting Filters," in IEEE Transactions on Applied Superconductivity, vol. 27, no. 7, pp. 1-9, Oct. 2017, Art no. 1502809.
2. P. Ma et al., "A Design Method of Multimode Multiband Bandpass Filters," in IEEE Transactions on Microwave Theory and Techniques, vol. 66, no. 6, pp. 2791-2799, June 2018.
3. P. Ma, B. Wei, J. Hong, X. Guo, B. Cao and L. Jiang, "Coupling Matrix Compression Technique for High-Isolation Dual-Mode Dual-Band Filters," in IEEE Transactions on Microwave Theory and Techniques, vol. 66, no. 6, pp. 2814-2821, June 2018.
4. P. Ma et al., "Synthesis Design of Wideband High-Selectivity HTS Filter by Cascading Dual-Mode Resonators," in IEEE Transactions on Applied Superconductivity, vol. 28, no. 5, pp. 1-7, Aug. 2018, Art no. 1500807.
5. Y. He et al., "Novel Design of Band-Pass Waveguide Filter With HTS E-Plane Insert," in IEEE Transactions on Applied Superconductivity, vol. 27, no. 4, pp. 1-4, June 2017, Art no. 1501604.
6. L. Sun et al., "New Type of Microwave High-T_{c} Superconductor Microstrip Resonator and Its Application Prospects," in IEEE Transactions on Applied Superconductivity, vol. 27, no. 4, pp. 1-4, June 2017, Art no. 1501304.
7. H. Liu, S. Zhu, P. Wen, X. Zhang, L. Sun and H. Xu, "Design of Quad-Channel High-Temperature Superconducting Diplexer Using Spiral Stub-Loaded Resonators," in IEEE Transactions on Applied Superconductivity, vol. 27, no. 4, pp. 1-5, June 2017, Art no. 1502105.
8. X. Lu et al., "Superconducting Ultra-Wideband (UWB) Bandpass Filter Design Based on Quintuple/Quadruple/ Triple-Mode Resonator," in IEEE Transactions on Microwave Theory and Techniques, vol. 63, no. 4, pp. 1281-1293, April 2015.
9. P. Ma, B. Wei, Y. Heng, C. Luo, X. Guo and B. Cao, "Design of absorptive superconducting filter," in Electronics Letters, vol. 53, no. 11, pp. 728-730, 25 5 2017.

Keywords: Applications, HTS filters, dual-mode dual band filters, wide-band filters

ED6-2-INV

Wireless Power Transmission Technology using High-Tc Superconducting Wire

*Yoon Do Chung[1], Chang Young Lee[2], Eun Young Park[3]

Suwon Science College, Korea[1]
Korea Railroad Research Institute, Korea[2]
Korea Christian University, Korea[3]

The wireless power transfer (WPT) technology has received attention in recent years for industrial and high power applications; electric vehicles (EVs) and train. Eliminating the use of wiring can mitigate complicated charging operation and reduce the risk of accidents such as electric shock, cable disconnection, and so on. An effective power transmission and a stable supply of energy are important issues for implementing an actual WPT system. As WPT via magnetic resonance coupling provides a highly efficient mid-range transmission and robustness to misalignment, such a technology is suitable for dynamic charging of high-speed railways and EV system.

Generally, as the WPT system adopted normal conducting wire, the size of antenna is too large to be equipped to deliver the large power promptly due to the intrinsically property of the normal conducting wire. As well as, as the copper resonance keep low Q factor, the exchanges energy rate is limited. The high Q factor resonators exchange energy at a much higher rate than they lose energy due to low damping ratio for each resonance coil as well as they are possible to keep much stronger magnetic fields out in the peripheral regions.

From this reason, the WPT technology has been required for diffusion of various wires. As a reasonable approach, the superconducting wire is a noble option in order to improve transfer efficiency and extend the transfer distance. Fortunately, since the superconducting wires keep enough current density and higher Q value, it enables to exchange a massive electric power in spite of a small scale coil as well as to improve the efficiency.

This paper describe the performance and characteristics for WPT system combined with HTS resonance wires, compared with copper resonance wires.

Keywords: Wireless power transfer (WPT), High temperature superconducting wire, Electromagnetic resonance coupling

ED6-3-INV

Novel high-Tc superconducting wire for high quality factor at high-frequency and its applications

*Naoto Sekiya[1], Shinya Kobayashi[1]

University of Yamanashi[1]

We have developed a novel high temperature superconducting (HTS) wire structure that increases the coil quality factor at high-frequency and investigated the power transfer efficiency of a wireless power transfer (WPT) system using two coils with this structure. The proposed wire is shown in Fig. 1(a). The structure constructs of two conventional HTS wires and does not have a copper stabilizer and silver overlayer to reduce the conductor loss of the Hastelloy substrate and the skin effect of them. The quality factors of three spiral coils with three types of wires as shown in Fig. 1 were investigated by using three dimensional electromagnetic simulator. The structure of spiral coil is shown in Fig. 1(d). Figure 2 shows the simulated quality factors of the three spiral coils. In spite of using superconducting layer, the coil with conventional wire had a quality factor slightly larger than the one with copper wire. This is because the Hastelloy substrate greatly affected the conductor loss at high frequency. The coil with proposed wire achieved the highest quality factor (45289), which is a remarkable improvement. This shows that the proposed HTS wire suppressed the conductor loss of the Hastelloy substrate. We also investigated the quality factors of the three spiral coils with being embedded in styrene foam to maintain the coil configuration. We found that the dielectric loss of the foam limited the quality factor. We will show the measured quality factors of the three spiral coils with the foam. We also simulated the power transfer efficiency of a WPT system using two coils with different quality factors for different distances between the coils. Use of a high quality factor coil enabled the system to achieve a longer transfer range. The details will be shown in the conference.

Acknowledgments: This research and development work was supported by the JSPK KAKENHI Grant Number JP 18K04230 and the MIC/SCOPE #181603014.

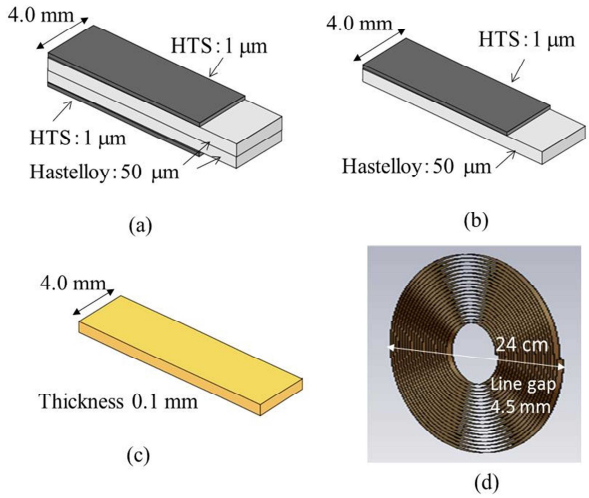

Fig. 1 (a) proposed wire, (b) conventional wire, (c) copper wire, and (d) designed coil.

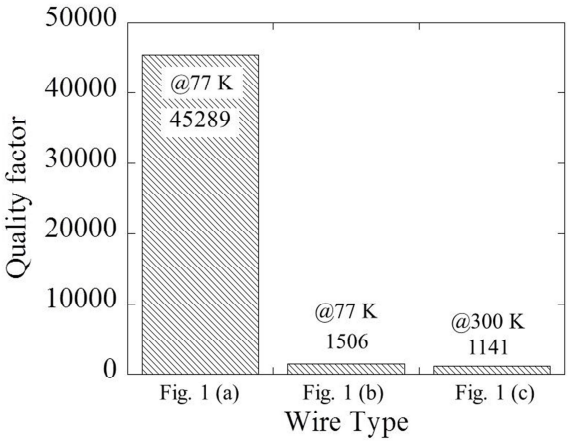

Fig. 2 Histogram of simulated quality factor.

Keywords: HTS wire, quality factor, wireless power transfer, spiral coil

ED6-4-INV

Superconducting submicron-CPW resonators for on-chip THz filterbank

*Masato Naruse[1], Ken'ichi Karatsu[2,3], Alejandro Pascual Laguna[2,3], Ozan Yurduseven[2], David J. Thoen[2,4], Vignesh Murugesan[3], Jochem J. A. Baselmans[2,3], Akira Endo[2,4]

Graduate School of Science and Technology, Saitama University, Japan[1]
Faculty of Electrical Engineering, Mathematics and Computer Science, Delft University of Technology, the Netherlands[2]
SRON-Netherlands Institute for Space Research, the Netherlands[3]
Kavli Institute of NanoScience, Faculty of Applied Sciences, Delft University of Technology, the Netherlands[4]

We demonstrate that superconducting resonators made of 300 nm-wide coplanar waveguides (CPW) are good candidates for the filters of on-chip spectrometers in the THz range. These filters will be useful for realizing filterbank spectrometers with medium frequency resolution (R~500) and a very wide bandwidth, such as the astronomical instrument DESHIMA that aims to cover the 240–720 GHz band in a single shot.

We need resonators with an internal quality factor (Q_i) that is significantly larger than R, for the filters to have a high transmission efficiency from a THz signal line to the detector. For R=500, we require a Qi of more than 5000, whilst reported Q_i's range from 1500 in the 250 GHz band [Hailey-Dunsheath+ 2016] to 500 in the 600 GHz band [Endo+2013]. These filters were made of microstrip lines, which can suffer from the losses in deposited dielectrics. Compared to microstrips, CPWs have an advantage that they require no deposited dielectric layer, but CPWs also have a disadvantage that it is difficult to suppress radiation loss.

Very narrow CPW lines could potentially have low radiation losses, while keeping the advantage of having no deposited dielectrics. Our simulations using Sonnet and CST have indicated that 300 nm-wide superconducting CPW lines should have low enough radiation loss. Using electron-beam lithography, we prepared on-chip filterbanks with 300 nm-wide CPW resonators patterned in a 100 nm-thick layer of NbTiN. We prepared two samples, one of which covers the 350 GHz band and the other for the 650 GHz band. For both samples, we obtained a R=500 as shown in the Figures. We measured Q_i=5000 at 300 GHz, and Q_i=1000 at 600 GHz. Whilst the Qi was comparable with the simulations in the 300 GHz band, the excess losses in the 600 GHz band requires additional investigations.

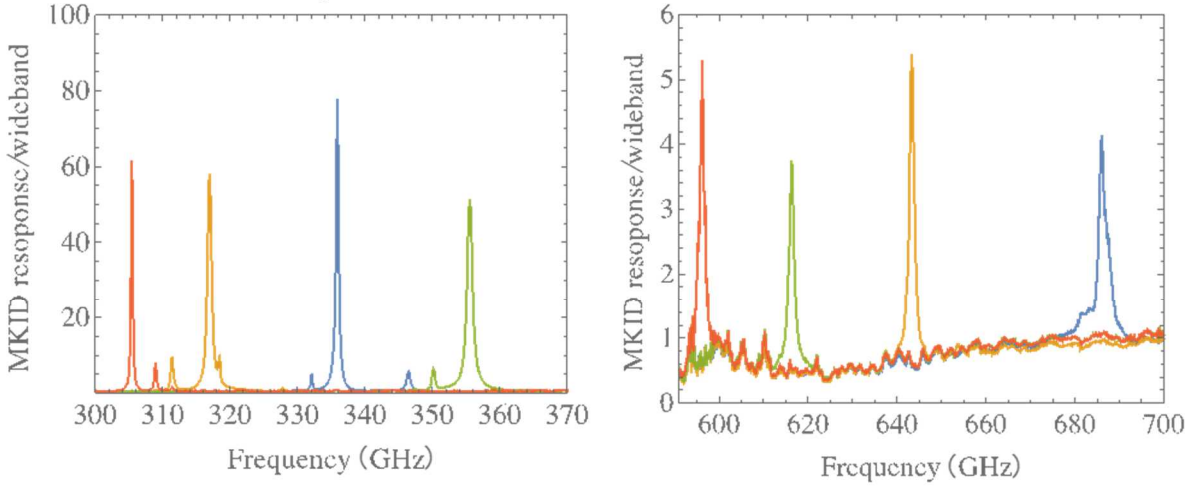

Fig: The filter responses in the 350 GHz band and the 650 GHz band. The frequency resolutions are around 500 in both bands.

Keywords: superconducting resonator, filter bank, kinetic inductance detector

AP1-1-INV

Development of fully-turbo electric propulsion systems for future aircrafts

*Masataka Iwakuma[1], Masataka Komiya[1], Takuya Aikawa[1], Kouichi Yoshida[1], Shun Miura[1], Takashi Yoshida[1], Teruyoshi Sasayama[1], Akira Tomioka[2], Masayuki Konno[2], Yuhji Aoki[3], Kazuhisa Adachi[3], Teruo Izumi[4]

Kyushu University[1]
Fuji Electric Co., Ltd.[2]
SWCC Showa Cable Systems Co., Ltd.[3]
AIST[4]

Low emission, low noise and low fuel consumption are strongly requested for future aircrafts. The most desirable solution is “electric aircrafts”. The power source should be the combination of a gas turbine and a generator from the viewpoint of total amount of energy and weight in relation to the flight distance and loading capacity. By using the generated electric power, motors drive the fans. However the conventional rotating machines which are composed of iron cores and copper windings are too heavy to apply to aircrafts. Therefore the development of fully superconducting rotating machines seems to be indispensable to realize the electric aircrafts. Our research group is developing fully superconducting rotating machines with REBCO superconducting tapes under the support of JST. In addition, we have started to study the fully-turbo electric propulsion systems for future aircrafts. In this symposium, the present status of the development of fully superconducting rotating machines will be mainly presented.

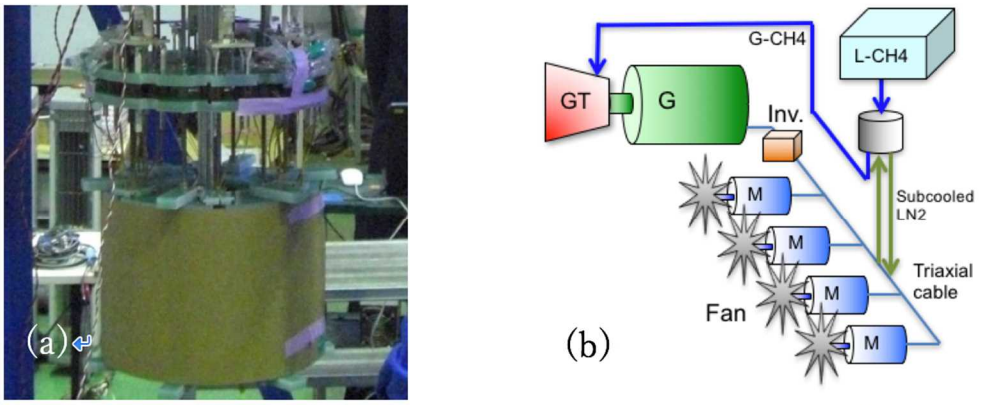

Fig. 1 (a) REBCO fully superconducting motor, (b) fully-turbo propulsion system

AP1-2-INV

Towards Superconducting Hybrid Electric Aircraft: KIT Research Activities within TELOS and ASuMED

*B. Holzapfel[1], T. Benkel[1], F. Grilli[1], J. Hänisch[1], A. Kudymow[1], M. Lao[1], Y. Liu[1], S. Schlachter[1], S. Strauss[1]

Institute for Technical Physics, Karlsruhe Institute of Technology, Karlsruhe, Germany[1]

Short Range Hybrid Electric Aircraft of the Airbus A320 class with strongly enhanced energy efficiency and noise reduction will not be possible without the use of high power density and light weight superconducting components. Within the German national research project “TELOS” and the European consortium “ASuMED”, the Institute for Technical Physics at Karlsruhe Institute of Technology is working together with different partners (among others Airbus, Siemens, Oswald, Rolls Royce, the Slovak Academy of Sciences and the University of Cambridge) on key technologies towards this goal. This talk will give an overview of the concept of Hybrid Electric Aircraft using superconducting technologies and the ongoing KIT activities within the projects TELOS and ASuMED. For TELOS, KIT is investigating the superconducting power distribution network with focus on cryogenic aspects and the realization of a >10 MW cable demonstrator, whereas within ASUMED, the research activities are concentrated on modelling the AC-losses of a fully superconducting synchronous motor consisting of permanent magnets based on stacked Coated Conductors and superconducting stator windings.

The project TELOS is funded by the German Federal Ministry for Economic Affairs and Energy under the LUFO-V funding program grant agreement No. 20Y1516C.
The project ASuMED has received funding from the European Union´s Horizon 2020 Programme for research, technological development and demonstration under grant agreement No. 723119.

AP1-3

Conceptual Study on Lighter and More Compact Transmission Cable Systems for More Electric Aircrafts

*Shigeki Isojima[1], Yoshiyuki Yoshida[2], Naoyuki Amemiya[3], Nobuyuki Sadakata[4], Michiya Okada[2], Hiroyuki Ohsaki[5]

Sumitomo Electric Industries,Ltd. Japan[1]
National Institute of Advanced Industrial Science and Technology Japan[2]
Kyoto University Japan[3]
Fujikura Ltd. Japan[4]
University of Tokyo Japan[5]

More electrically driven aircrafts with electric propulsion systems are supposed to require +1～+40MW. In order to realize such heavily electrical aircrafts, in addition to the development of higher voltage electrical systems with motors and generators with much higher power densities than those at present, compatible with low atmospheric pressure at a high altitude, the development of lighter and more compact transmission cable systems is also indispensable. As the initial step of this conceptual study, we performed feasibility study to compare metal cables and high temperature superconducting cables. We chose operational conditions, as close as current operations, such as voltage:230V ac, transmission capacity:4MW. cct,frequency:400Hz, current:10kA, cable length:50m,operation:100% output for 1hr,33% for 23hr, and cooling: no on-board refrigerator. As for metal cable design, we estimated the cable weight by following AS50881 with Cu wire (AWG3/0),with the result that the cable weight is 15000kg/50m. If we could use Aluminum cable with the same standard, the weight is reduced to 10000kg/50m, which is still too heavy.

As for superconducting cable, three types of cooling systems were studied. Type 1 is cooled by solid nitrogen. Type2 is cooled by circulating liquid nitrogen. Type3 is cooled by thermal conduction to preserved liquid nitrogen. The lightest system turned out to be Type3 whose weight is 3000kg/50m, including terminations. This is much lighter than metal cables, however it is still too heavy.

This is why increasing transmission voltage is now under extensive discussions. Deploying DC for transmission is also under wide studies to exclude AC loss, regardless of the heavy weight of convertors or invertors at present.
As the second step, we chose the higher voltage up to ±1500V DC and 1060V AC. As for the superconducting cables, the power lead from a hot outside termination to the superconducting cable at nitrogen temperature plays a key role to determine the cable system weight. This part was also studied. We compared several cases, and discussed merits and demerits of each case.

Keywords: superconducting cable, aircraft

AP1-4-INV

Challenging Several Hundred kW class Transportation Equipment Using High Temperature Superconducting Induction/Synchronous Motor

*Taketsune Nakamura[1], Liangliang Wei[1], Fuat Kucuk[1], Kentaro Kuroda[1], Masaaki Yoshikawa[2], Yoshitaka Itoh[2], Toshihisa Terazawa[2]

Kyoto University, Japan[1]
IMRA MATERIAL R&D Co., Ltd, Japan[2]

Our group has been developing High Temperature Superconducting Induction/Synchronous Motor (HTS-ISM) for transportation equipment. Based on our research experience for 20 kW class prototype and 50 kW class fully superconducting model, we are aiming to practical 100 kW class motor system.

In this paper, current status of designing several hundred class HTS-ISM system is reviewed and discussed.

This work has been supported by Japan Science and Technology Agency under the program of Advanced Low Carbon Technology Research and Development Program (JST-ALCA) in Japan.

Keywords: High Temperature Superconductor, HTS-ISM, Transportation equipment, Several hundred kW system

AP1-5

Experimental and Theoretical Discussion on Step Out Characteristics of High Temperature Superconducting Induction/Synchronous Motor

*Taketsune Nakamura[1]

Kyoto University[1]

This paper presents experimental and theoretical results of step out characteristics of a 20 kW class High Temperature Superconducting Induction/Synchronous Motor (HTS-ISM). A fabricated motor (3-phase, 8-pole, rotor windings: HTS, stator windings: Cu) is investigated, and its maximum quasi-synchronous output is 20 kW at line voltage of 400 V. The step out condition and its behavior is tested for different ratios of the input voltage and the drive frequency at 77 K (atmospheric liquid nitrogen), and then found that such characteristics are dominated by reactive power. Furthermore, the threshold power factor angle for the step out occurrence is quantitatively as well as reproducibly identified based on the experiment. Finally, such threshold value is theoretically explained by means of nonlinear electrical equivalent circuit. These results are really important for the consideration of stable rotation condition of the HTS-ISM.

This work has been supported by Japan Science and Technology Agency under the program of Advanced Low Carbon Technology Research and Development Program (JST-ALCA) in Japan. Fabrication of the 20 kW class motor was supported by the New Energy and Industrial Technology Development Organization (NEDO), Japan.

Keywords: High Temperature Superconductor, HTS-ISM, Step out, Equivalent circuit

AP1-6

Motor Structure and Output Density of IPM Motor Using Bulk Superconductors as Magnetic Field

*Wataru Akada[1], Yutaka Terao[1], Hiroyuki Ohsaki[1]

University of Tokyo[1]

Recently, electric transport equipment such as electric vehicles and electric ships are rapidly increasing. Various attempts were done to reduce the size of the motor, for freedom of the transport equipment system layout, and energy efficiency of the transport.
Interior permanent magnet synchronous motors (IPMSM) can realize higher torque than surface permanent magnet synchronous motors (SPMSM) by using reluctance torque occurred by magnetic saliency in addition to magnet torque. In comparison with SPMSM, IPMSM have broad operation range by applying control method such as maximum output control and field weakening control. Therefore, IPMSM are expected to be used for variety of application such as electric vehicles, heavy equipment and ships.
By replacing permanent magnets with bulk superconductors in the rotor of IPMSM, the magnet torque increases due to stronger magnetic field of magnetized bulk superconductors. And then, the reluctance torque also increases thanks to magnetic shielding effect of bulk superconductors. This leads to increase of total torque density of the motors, and result in contribution for motor size reduction.
Here, analysis based on finite element method is carried out for several types of motor which assume large transports, up to 1000 kW. In the analysis, magnet torque and reluctance torque are derived separately, in order to find out the reluctance torque considering the magnetic shielding effect of the bulk superconductors. In each motor output, IPMSM using permanent magnets or bulk superconductors as magnetic field are compared, and we verify the utility of bulk superconductors by showing the reduction of motor size and increase of torque density.
To use bulk superconductors as the magnetic field, cooling to maintain the superconducting state is necessary. Therefore we discuss the feasibility of the IPMSM considering cooling temperature, cooling method and motor structure.
Furthermore, we designed the optimal rotor structure which realizes the highest torque in the both cases, using permanent magnets or bulk superconductors. By doing so, the optimal condition to fully utilize the characteristics of bulk superconductors is discussed.

Keywords: Bulk Superconductor, IPMSM, Motor Structure, Output Density

AP2-1-INV

Conceptual design of Japan's fusion DEMO reactor JA DEMO with emphasis on superconducting magnet issues

*Kenji Tobita[1], Hiroyasu Utoh[1], Ryoji Hiwatari[1], Yuya Miyoshi[1], Shinsuke Tokunaga[1], Yoshiteru Sakamoto[1], Youji Someya[1], Nobuyuki Asakura[1], Yuki Homma[1], Noriyoshi Nakajima[2]

National Institutes for Quantum and Radiological Science and Technology (QST)[1]
National Institutes for Fusion Science (NIFS)[2]

Requirements for Japan's fusion DEMO reactor are to demonstrate (1) steady and stable electric power generation in a power plant scale, (2) reasonable availability using a remote maintenance scheme anticipated in a commercial plant, and (3) tritium breeding to fulfill self-sufficiency of fuel. For the purpose, Japan has been developing a steady state DEMO concept based on water-cooled solid breeder, as the next stage of ITER which is the international core project being under construction. The main design parameters of JA DEMO are a plasma major radius of 8.5 m, fusion output of 1.5-2 GW, magnetic field on the axis of 5.94 T.This paper presents the overview of Japan's fusion DEMO reactor development with emphasis on superconducting magnet issues.

The superconducting coil system of the reactor consists of a central solenoid (CS), 7 equilibrium field (EF) coils and 16 toroidal field (TF) coils. The CS is based on Nb_3Sn and vertically separated into 5 sectors or more. The EF coils are made of NbTi conductors except one or two coils (made of Nb_3Sn) on the high field side. Regarding CS and EF coils, SC technology on DEMO will be the same as that in ITER. On the other hand, as for TF coils, there is a technology gap between ITER and DEMO due to their size and magnetic energy, especially regarding design stress of cryogenic steel. The TF coils are designed using Nb_3Sn conductor, producing the maximum field of 13.05 T with 16 TF coils, 256 turns/coil and magnetic energy of 166 GJ. The design stress of 800 MPa, equivalent to the yield stress of cryogenic steel of 1,200 MPa, is required to withstand the anticipated electromagnetic forces. The prime option of TF coil fabrication is based on the ITER scheme with cable in conduit, radial plates and double pancakes. Alesson learned from ITER is that tolerances required for the fabrication of toroidal field (TF) coils are demanding, which poses considerable difficulties in coil fabrication. In order to resolve the problem, the target error field of DEMO is mitigated to $B_{err}/B_T \leq 10^{-4}$, being larger than that of ITER ($B_{err}/B_T \leq 5\times10^{-5}$). Instead, in preparation for a lower error field requirement for plasma operation, correction coils are installed to correct the error field to lower than 5×10^{-5}.

Keywords: fusion, DEMO reactor, superconducting magnet

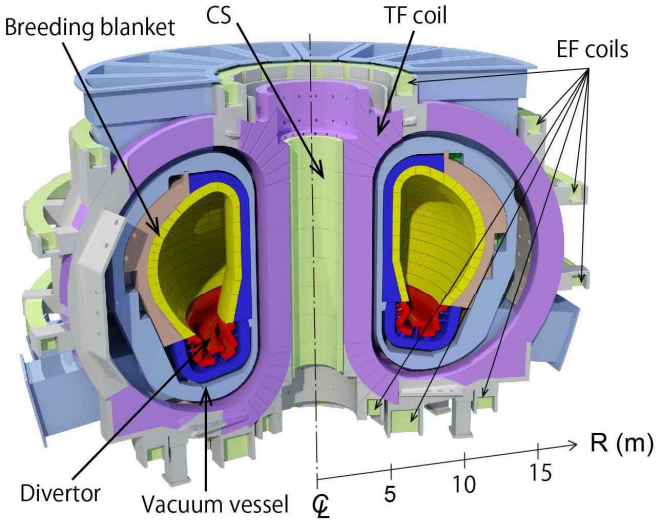

Fig.1 Conceptual view of fusion DEMO reactor (JA DEMO)

AP2-2-INV

SPARC: An Accelerated Pathway to Fusion Energy Based on High-Field REBCO Superconducting Magnets

*Zachary S. Hartwig[1], Joseph V. Minervini[1], the SPARC team[1,2]

Massachusetts Institute of Technology, USA.[1]
Commonwealth Fusion Systems[2]

The recent commercial availability of high-temperature superconductors (HTS), specifically second generation HTS REBCO coated conductors, at the volume and performance required to build highfield, large-bore magnets represents a breakthrough opportunity to accelerate fusion energy. This is because the key fusion energy performance metrics in a tokamak, the leading fusion energy concept, scale as the strength of the magnetic field confining the plasma to the third or fourth power. One of the most important consequences of these scalings is that increasing the magnetic field in a tokamak enables a dramatically smaller device to demonstrate net-energy production. A reduction in size allows important reductions in cost, timeline, and organization complexity required to construct and operate the device. These qualities enable a net-energy fusion device to be constructed at university or private company scale through innovative private funding models. In March of 2018, two entities announced an innovative, privately funded partnership to pursue this breakthrough path towards fusion commercialization. The MIT Plasma Science and Fusion Center has been a world leader in high-field fusion science and magnet engineering for over 40 years; Commonwealth Fusion Systems is a new startup company focused on the rapid commercialization of fusion. Their joint approach relies on starting at the scale and speed required to rapidly demonstrate a new generation of high-field, largebore, REBCO-based superconducting magnets. These magnets will be incorporated into SPARC, a compact net-energy tokamak that is being designed to produce 100 MW of fusion power. This talk will present the advantages of high magnetic field fusion physics and engineering and the approach to its technological foundation built on the design and demonstration of large-bore, REBCO-based superconducting magnets.

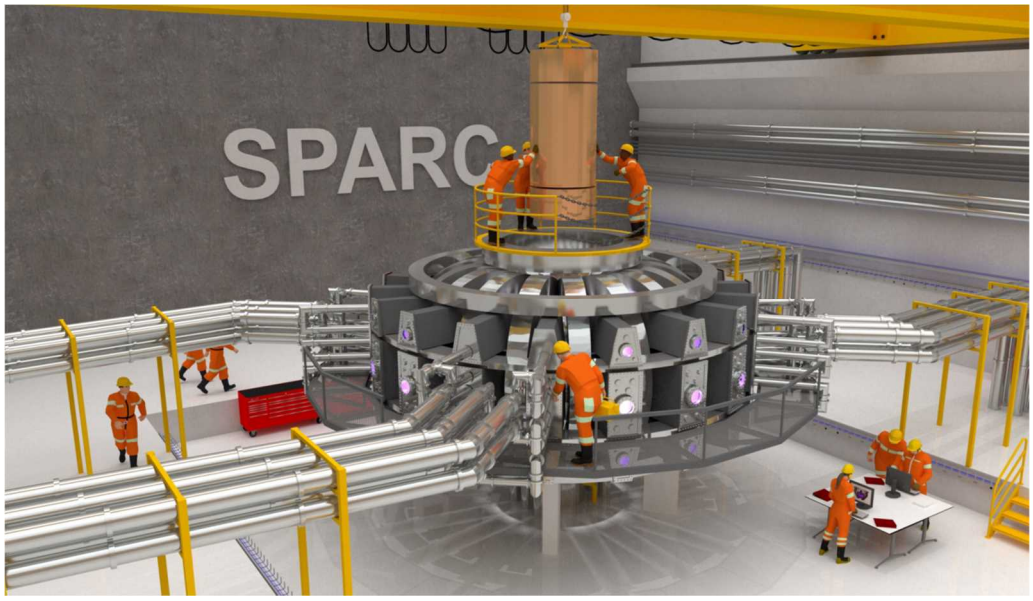

Figure: A visualization of the compact, high-field SPARC tokamak, which will use REBCO magnets to achieve 100 MW of net fusion power at small size.

AP2-3-INV

Development of the HTS Magnet System for the Next Stage of LHD Based on the Reliable 20 Years' Operation

*Toshiyuki Mito[1,2], Yuta Onodera[1,2], Kazuya Takahata[1,2], Nagato Yanagi[1,2], Shinji Hamaguchi[1], Suguru Takada[1]

National Institute for Fusion Science, National Institute of Natural Sciences, Toki, Gifu, Japan[1]
SOKENDAI (The Graduate University for Advanced Studies), Toki, Gifu, Japan[2]

The Large Helical Device (LHD) is a heliotron-type fusion plasma experimental device with the world's first fully superconducting magnetic confinement system. The LHD have been providing stable fusion plasma confinement experimental environment. The NbTi superconducting system of LHD executed a long-term stable operation for 20 years, and had been proving a high availability that passed 99 %. Deuterium plasma experiments started in March 2017, and the LHD experiment entered for final stage of the collected studies. Therefore, we started development research of the REBCO conductor aiming at the application to a next experimental device of LHD. The candidate conductor assumes rated current 12.5 kA in operating temperature 20 K, magnetic field up to 12 T. The stacked REBCO tapes are put in the groove of the aluminum alloy jacket with the circular cross section. After having welded a lid to the jacket by Friction Stir Welding (FSW), the conductor is twisted to equalize of the current distribution between the stacked REBCO tapes. The conductor has no cooling channel, so a cooling panel, which is inserted in the coil windings, cools it indirectly. Friction stair welding, an Aluminum alloy jacket, Indirect cooling, stacked REBCO tapes; we name it "FAIR conductor". The reliable operation history of LHD, the trial manufacturing of the FAIR conductor, the coil design configuration with the indirect cooling, and the quench protection scenario using the secondary normal conductor windings to induce rapid quench transformation are reported.

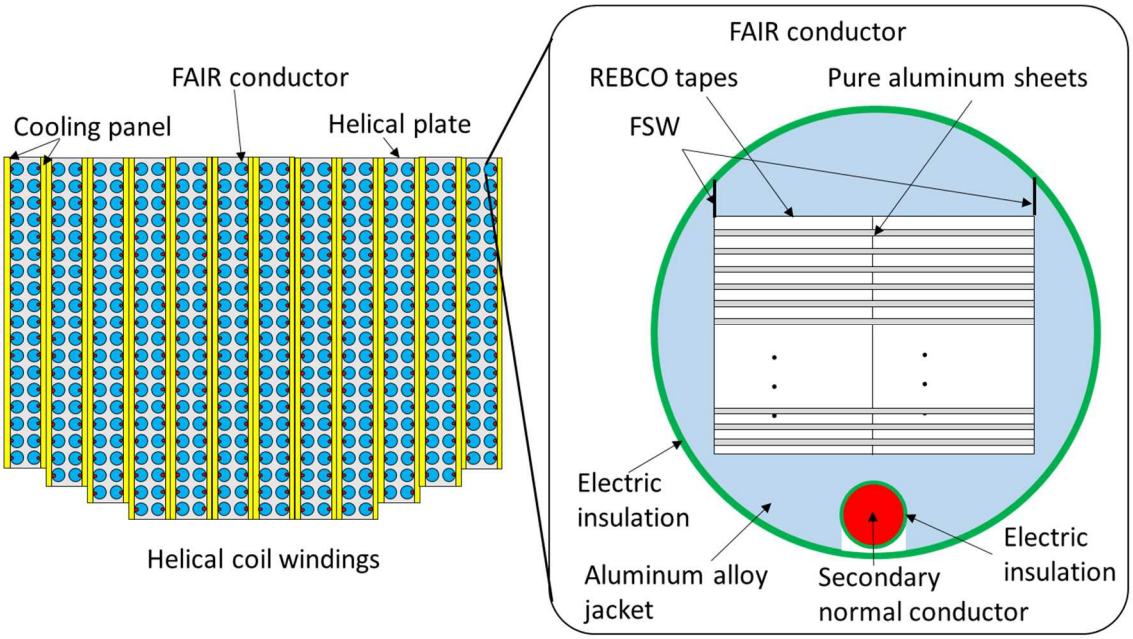

Keywords: HTS, REBCO, LHD, Fusion

AP3-1-INV

Ultra-High Field NMR Magnet Development at Bruker BioSpin

*Patrick Wikus[1]

Bruker BioSpin[1]

Due to the properties of LTS materials, superconducting magnets for high resolution NMR are currently limited to a proton resonance frequency of 1.0 GHz.

Bruker BioSpin is currently developing commercial NMR spectrometers which exceed this frequency – most notably systems with a proton resonance frequency of 1.2 GHz. One of the most significant technological hurdles in this endeavor is the development of HTS-based magnets which meet the requirements of high resolution NMR.

In addition to providing a status update on Bruker BioSpin's R&D progress, we will discuss the special magnet requirements that arise from high resolution NMR, and will highlight the main challenges that need to be overcome to successfully build NMR magnets for ultra-high field applications above 1.0 GHz.

Keywords: Magnet, NMR, HTS

AP3-2-INV

Development of HTS high stable magnetic field magnet system for MRI

*Shoichi YOKOYAMA[1], Tetsuya MATSUDA[1], Hideaki MIURA[1], Yusuke MORITA[1], Syunsuke OTAKE[1], Ryo EGUCHI[1], Tatsuya INOUE[1], Shinji SATO[1], Takanobu KISS[2], Makoto TSUDA[3], Taketsune NAKAMURA[4], Yasuyuki SHIRAI[4]

Mitsubishi Electric Corporation, JAPAN[1]
Kyusyu University, JAPAN[2]
Tohoku University, JAPAN[3]
Kyoto University, JAPAN[4]

Research and development for practical application of liquid helium free medical MRI superconducting magnet has been in progress as a NEDO project since FY2016. In this project, we developed a superconducting magnet system for practical application to MRI system and are investigating issues, etc. In this fiscal year (2018), we will prototype a half size active shield type 3T magnet, Verify the application.

There are two targets for this research and development. One is to develop an MRI magnet that does not use liquid helium, which is used in large quantities as a measure against depletion of helium gas. The other one is easily available by providing 3T aircraft with shape, weight and leakage magnetic field equivalent to 1.5T aircraft when 1.5T-MRI magnet currently used in many hospitals is replaced with 3T-MRI magnet in the future. It is the development of a magnet that can be replaced. For this purpose, we have developed a high temperature superconducting magnet that can be used at higher temperature and higher magnetic field than conventional metal superconducting, and are developing technologies to apply it to MRI.

Specifications of half-size 3 T coil.

Item	Specification
Inner Diameter	560 mm
Outer Diameter	1200 mm
Axial Length	980 mm
Inductance	145 H
Rated Current	148 A
Rated Current Density	120 A/mm^2
Stored Energy	1.58 MJ
Central Magnetic Field	2.9 T
Maximum Magnetic Field	4.2 T
Magnetic Field Homogeneity	1.7 ppm (250 mmDSV)

Keywords: Superconducting magnet, MRI, REBCO coil, field stability

AP3-3-INV

Progress of Superconductors and Medical Applications in the US

*Mike Sumption[1]

CSMM, Materials Science Department, The Ohio State University, U. S. A.[1]

In this presentation, progress in medical applications in the US using HTS, MgB2, and LTS superconducting materials is discussed. Efforts in MRI, Proton therapy, and NRM are reviewed, with a particular focus on MRI. Drivers including reduced or eliminated liquid cryogen, siting requirements, and weight and size reductions are discussed. The prospects and potential for various materials for various applications are reviewed, while recent development and demonstrations for development efforts at various levels of maturity are described.

AP3-4-INV

Transient Heat Transfer Through the LHC Polyimide Cable Insulation

*Naoyuki Amemiya[1], Shigeki Takahama[2], Tsutomu Kurusu[2], Toru Ogitsu[3], Yoshiyuki Iwata[4], Koji Noda[4], Masahiro Yoshimoto[5]

Kyoto University[1]
Toshiba Energy Systems & Solutions Corporation[2]
High Energy Accelerator Research Organization[3]
National Institute of Radiological Sciences[4]
Japan Atomic Energy Agency[5]

We have been carrying out an R&D project of fundamental technologies for cryocooler-cooled accelerator magnets wound with RE-123 coated conductors funded by the Japan Science and Technology Agency under its S-Innovation Program. At the last stage of this project, we carried out the beam line test of a cryocooler-cooled HTS magnet made with RE-123 coated conductors. The magnet consists of six racetrack coils and generated 2.5 T of magnetic field in a room temperature bore, where carbon ion beam can pass, 4 T of magnetic field (maximum) in the coils by 200 A of its rated current. We demonstrated the guiding of 430 MeV/u carbon ion beam accelerated by the synchrotron for heavy ion cancer therapy. Next, we injected the carbon ion beam intentionally to the HTS coils through aluminum window of the vacuum chamber, simulating a serious incident of the injection of an uncontrolled high energy particle beam. Because of a high operating temperature, the temperature increase of the coil was small, and no normal transition was observed, at least, when the magnet was excited with a small current of 50 A. The results with a larger current will be reported in the presentation.

This work was supported by Japan Science and Technology Agency under Strategic Promotion of Innovative Research and Development Program (S-Innovation Program).

Keywords: coated conductor, magnet, accelerator

AP4-1-INV

Research of HTS for DC Power Transmission

*Liye Xiao[1,2]

Institute of Electrical Engineering, Chinese Academy of Sciences, China[1]
University of Chinese Academy of Sciences, China[2]

Due to the quick increasing of electricity from renewable energy, it is expected that the DC power transmission (especially the VSC-HVDC) would be widely used for power grid. For the VSC-HVDC power transmission, it is valuable to limit the short-circuit fault current so that the DC breaker can easily cut the fault line, and HTS DC fault current limiter (DC-FCL) would be a promising solution for this issue. On the other hand, HTS DC power transmission is also a possible technology for the large-scale electricity transmission over long distance. While the HTS DC power transmission is combined with liquid natural gas transmission, resulting in a energy pipeline mode, it would be more economic for energy transmission in the future.

In this presentation, we would like to report our recent research activities on the HTS application for DC-FCL and the DC energy pipeline. The structures of the DC-FCL and energy pipeline would be presented, and the technology issues and the research progresses would be reviewed, the designs and tests of the prototypes, where the DC-FCL is 40kV/2kA and the energy pipeline is 10kV/1kA, would be also presented.

AP4-2-INV

Current Status and Future Expectation of Korean Large Scale HTS Power Applications

*Minwon Park[1], Seokju Lee[1]

Changwon National University, school of mechatronics, the dept. of EE, Republic of Korea[1]

Since 2000, Korean researchers related with HTS power applications have been researching according to government and private company support. According to the earnest effort for around 2 decades, a HTS wire company was established and the 23kV class commercialization of HTS power cable was successfully commercialized. And also, the 154kV class SFCL was developed and ready to be commercial. Recently a new project for the development of 10MW class HTS wind generator was launched and the 23kV class tri-axial HTS power cable is under developing with several research institutes. In this paper, the current status of large scale HTS power applications in Korea will be kindly described considering the results of comparatively big R&D program. Furthermore, the future expectation including the planning program of HTS power application will be also touched. Even though the tremendously a lot of advantages of the high temperature superconductivity phenomena, the commercialization of HTS power devices is not easy as much as being expected in 1987. However, I believe that the dead end of HTS power application will not be happened.

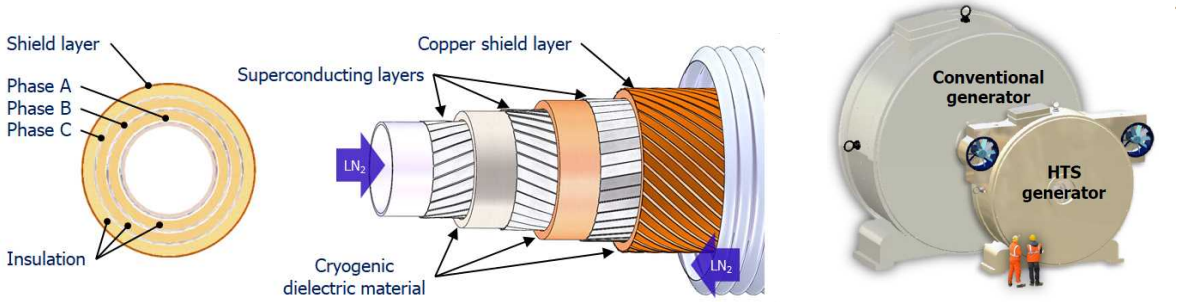

(a) (b)

Fig. (a) the cross section and structure of 23kV tri-axial cable in Korea,
(b) comparison of conventional wind generator and HTS wind generator

Keywords: HTS power application, grid study, HTS power cable, HTS wind generator

AP4-3-INV

Recent status of 220kV SFCL project

Mikhail Moyzykh[1], Sergei Samoilenkov[1], *Sergey Lee[2]

SuperOx[1]
SuperOx Japan[2]

SuperOx group is a producer of 2nd generation high temperature superconducting wire. Recently, SuperOx has developed superconducting fault current limiter (SFCLs) for high voltage grid. The device is perspective for application in densely populated urban areas with developed electric infrastructure. The reported project covers design, production and installation of first 220 kV-class SFCL in Moscow. This device includes such features as a compact dead-tank cryostat, proprietary superconducting element design, redundant cryocooler-based cooling system and integration with existing grid relay protection. SFCL test program is based on recently composed IEEE guidelines and was approved by the utility. The results of the device tests as well as prospects of an in-grid operation will be presented in the talk.

Keywords: superconducting fault current limiter, 2G HTS wires

AP4-4-INV

Cost effective FCL using advanced superconducting tapes for future HVDC grids – overview of European project FASTGRID

Michal Vojenciak[1], Pascal Tixador[2], Guillaume Escamez[3], Cornelia Pop[4], Albert Calleja[5], Markus Bauer[6], Giuliano Angeli[7], Christian Lacroix[8], Amir Saraf[9], Jens Hänisch[10], Bertrand Dutoit[8], Marcela Pekarcikova[1]

Institute of Electrical Engineering SAS, Dubravska cesta 9, Bratislava, Slovakia[1]
University of Grenoble Alpes, CNRS Grenoble-INP, G2Elab, Institut Neel, Grenoble, 38000, France[2]
Supergrid Institute, Villeurbanne, 69100, France[3]
Institut de Ciència de Materials de Barcelona, ICMAB - CSIC, Campus UA Barcelona, Bellaterra, Catalonia, E-08193, Spain[4]
Oxolutia SL, Barbera del Valles, 08210, Spain[5]
THEVA Dünnschichttechnik GmbH, Ismaning, 85737, Germany[6]
Ricerca sul Sistema Energetico, Milano, 20134, Italy[7]
Department of Electrical Engineering, Polytechnique Montréal, Montréal, QC H3C 3A7, Canada[8]
School of Physics and Astronomy, Tel Aviv University, Ramat Aviv, Tel Aviv, 69978, Israel[9]
Karlsruher Institut für Technologie (KIT), Institut für Technische Physik (ITEP), Hermann-von-Helmholtz-Platz 1, Eggenstein-Leopoldshafen, Germany[10]

High Voltage Direct Current (HVDC) links are worldwide used to transmit large amount of energy between two distant converter stations. This architecture is typical in case of a single power source (large power plant), but cannot be easily adopted for distributed power productions with small renewable energy sources. Connecting multiple converter stations raises challenges in control of power flow and handling of faults. The complexity of the later problem can be reduced by using a Fault Current Limiter (FCL). Since most of the FCL applications are in medium voltage grids and AC conditions, the technology of high voltage DC FCL is not ready for applications. The European project FASTGRID aims to covering this technological gap. The objective of the project is the enhancement of the technical and economical attractiveness of a superconducting FCL for hundred kV range HVDC grids. To reach this goal the project has to address several challenges including reduction of the conductor length required for the device, improvement of the conductor robustness against hot-spots and their detection.

Reduction of the conductor length means higher electric field sustain by the *RE*BCO superconducting tape during fault and thus higher dissipated energy. Pushing electric fields to higher levels requires to exceed frontiers of conventional technology and develop new conductor architecture. Three approaches are applied in the conductor architecture development: current-flow diverter concept, high heat capacity concept and conductor on flexible sapphire substrate concept. Furthermore, new functionalities are under development such as hot-spots detection utilizing an optical fiber.

The new design is going to be tested in a sub-size 50 kV demonstrator consisting of several superconducting modules. This FCL will be tested together with a circuit-breaker and control unit. The overall design including the cryostat is compatible with high-voltage technology.

In this contribution we summarize the main achievements during the first two years of the project run and we outline prospects for the next period.

Keywords: FCL, HVDC

AP4-5

Development of 220kV/1.5kA resistive type superconducting fault current limiter

*Shaotao Dai[1], Lianqi Zhao[2], Yong Huang[2], Tao Ma[1], Lei Hu[1], Xiaofei Xu[2], Linlin Cai[2]

School of Electrical Engineering, Beijing Jiaotong University, Beijing, P. R. China[1]
Jiangsu Zhongtian Technology Co., Ltd, Nantong, P. R. China[2]

To prevent damage to the electric equipment caused by fault current, many schemes and devices are proposed to alleviate the situation. However, the ever-increasing levels of fault current will soon exceed the breaking capabilities of existing devices. Superconducting fault current limiter (SFCL) technology utilizes superconductors, which possesses a highly non-linear resistivity, to reduce the current directly. In normal operation, current flows through the superconductor with negligible impedance. When fault current ignites the quench process, the superconductor's resistance sharply increases. Based on the phenomenon, the existing thousands of patents and papers show theoretical ways to build an rSFCL while few prototypes, not to say commercial product, have culminated. Beijing Jiao Tong University (BJTU) endeavors to make rSFCL a reality and have fabricated several rSFCL prototypes.

Within a collaboration of Jiangsu Zhongtian and Beijing Jiaotong University, one phase of resistive type superconducting fault current limiter (FCL) for the 220kV transmission voltage level has been designed and manufactured. The active part of the FCL consists of 128 bifilar coils made of 12mm wide steel-stabilized YBCO conductor supplied by Shanghai Superconductor, and is housed in a cryostat operated at normal state liquid nitrogen. The device was completely assembled and successfully subjected to steady-state tests, fault current limiting tests and high voltage tests, and the basic design of the system and the test results are reported. In total the FCL passed 20 power switching tests at voltages between 10 and 20 kV, at various prospective fault currents between 10 and 63 kA for a fault duration of 100 ms. The power frequency test at 360 kVrms for 1min and lightning impulse test at 850 kV(1.2 μs/50 μs) were carried out according to the Chinese national standard GB 1094.3.

Now, together with Guangdong Power Grid and other 8 institutions, we are undertaking a National Key Research and Development Program to develop a DC 160 kA/1 kA rSFCL, which will be installed in Nan'ao Island, Guangzhou Province in 2020. Basic information of AC 220kV rSFCL and progress of DC 160 kV rSFCL will be presented in detail.

Keywords: Superconducting fault current limiter, Resistive type, Current Limiting Tests, Insulation Tests

AP4-6

Thermo-Hydrodynamic Cable Designs for 10km to 100km Superconducting DC Power Transmission Line Using Experimental Data of Ishikari Project

Takao Yamada[1], Takashi Iitsuka[1], Akio Sato[2], Toru Sawamura[3], *Sataro Yamaguchi[4]

JGC Corporation[1]
JFE Steel[2]
Sakura Internet[3]
Chubu University[4]

Main merit of the DC superconducting power transmission line is low loss even in low voltage power transmission. It should be realized when the transmission length is long. Since it is a small system, its system cost will be lower than the copper cable system finally. Since the loss of the DC superconducting power transmission line depends on the heat leak from the cryogenic pipe, the main subject is to realize low heat leak from the cryogenic pipe and high COP of the refrigerator is required. At the same time, low circulation power of liquid nitrogen is also necessary. After these subjects are solved at the same time, we will be able to construct an ultra-long transmission line to connect all over the world. The heat leak is a sum of the round trip of cryogen in the pipes. The COP of refrigerator has the upper limit because of Carnot cycle efficiency. The heat leak of cryogenic pipe lower than 1 W/m for round trip was realized in Ishikari project in 2016 in very low pressure drop of the cryogen circulation. We also pay attention on the temperature rise of the cable for a longer transmission because if it is high, we should install the cooling stations along the transmission line for a short distance. In order to keep the operational current for a longer cable, the inlet and outlet temperatures of cryogenic pipe should be minimized for a long transmission line. The temperature rise of the cable depends on the heat leak and the flow rate of the cryogen, and the output pressure of the cryogenic pump should be proportional to the cubic of the length, and its rise is only 0.03 – 0.04 K/km in Ishikari project. This means that we could construct 10km ~ 100km transmission line basically. We analyze the experimental data, especially for the temperature rise and the pressure drop of cryogenic pipe from the heat leak and the flow rate of cryogen, and show some designs of 10 km ~ 100 km transmission line.

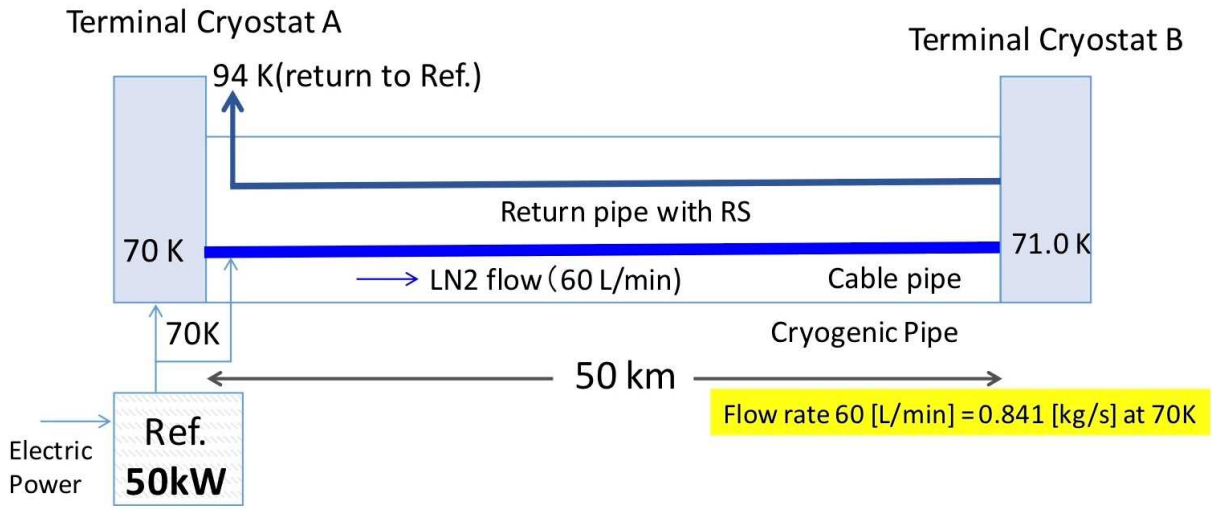

Keywords: long power transmission, thermal analysis, hydrodynamic analysis, Ishikari project

AP4-7-INV

Superconducting feeder cables for railway systems

*Masaru Tomita[1]

Research & Development Promotion Division, Applied Superconductivity Laboratory, Materials Technology Division, Railway Technical Research Institute, 2-8-38 Hikari-cho, Kokubunji-shi, Tokyo 185-8540, Japan[1]

Electric railway systems are widely used in the world as well as in Japan and DC systems have been employed in a number of metropolitan areas. However, they have some problems, such as cancelled regeneration and energy loss. From the viewpoint of saving energy, we have proposed Next Generation DC Railway System using superconducting feeder cables. Introducing superconducting feeder cables into railway feeding systems offers a lot of benefits: fewer substations, equalization of load between substations, reduction of cancelled regeneration and power transmission loss, and reduction of electrolytic corrosion.

In JST (S-innova) project since 2009, we started with fabricating and evaluating superconducting wire materials, and based upon various inquests and examination results, superconducting feeder cables system have been introduced to the test track. After checked from the aspect of cooling and current, the train running test succeeded. Next, we have aimed to introducing the superconducting feeder cable system to a commercial line. As a first step, superconducting feeder cables with cooling by immersion has been installed in a commercial line, and tested outside office hours with a test train. As future's schedule, the superconducting feeder cable is introduced into commercial lines of Tokyo metropolitan. Then, a cooling system for a long length superconducting feeder cable will be introduced in NEDO project. And, a jointing technology for a long length superconducting feeder cable will be developed in JST(Mirai) project.

Keywords: superconducting feeder cable, cooling system, current test, train running test

AP4-8-INV

Recent Progress of High Temperature Superconducting Cable Project in Japan

*Tomoo Mimura[1], Takato Masuda[2], Hiroharu Yaguchi[3], Hiroyuki Fukushima[4]

Tokyo Electric Power Company Holdings, Inc[1]
Sumitomo Electric Industries, Ltd.[2]
Mayekawa Mfg.[3]
Furukawa Electric Co., Ltd.[4]

We have studied high temperature superconducting (HTS) cable for a long time. In Japan, the national project of the HTS cable system in real grid operation funded by NEDO started 10 years before. As a result, we were able to carry out real system operation for one year several years ago.

After that, we have studied two issues on a new national project. One is to improve the performance of the cooling system. The other is safety verification against events that can occur in a system such as a ground fault or a short circuit. I will report on the outline.

Keywords: HTS cable, grid operation, safety verification

AP4-9-INV

Development of Hybrid Energy Storage System Using a SMES Coil Cooled by Thermo-Siphon Circulation of Liquid Hydrogen to Compensate for Output Fluctuation of Renewable Energy

*Daisuke Miyagi[1]

Tohoku University[1]

It is necessary to use some electric power storage systems to compensate for the output fluctuation. These electric power storage systems must have a large capacity and quick response. An advanced superconducting power conditioning system (ASPCS) which manages to convert the renewable energy into stable electricity has been proposed [1-3]. The configuration of ASPCS is shown in Fig. 1. The ASPCS is composed of renewable energy resources and a hybrid electric power storage system which is consist of a hydrogen electric power storage system (H_2 system) and a superconducting magnetic energy storage (SMES) system. The H_2 system is composed of a fuel cell (FC), a hydrogen storage container, and an electrolyzer (EL). The output fluctuation of renewable energy is resolved into long and short period component by a Kalman filter algorithm. The long period component is compensated by the H_2 system. The short period component is compensated by the SMES system. The SMES system has the high potential of quick response of large input-output power and the disadvantage of small storage capacity. The H_2 system has the potential of large storage and the disadvantage of slow response.
In the ASPCS, the SMES coil is cooled by thermos-siphon circulation of liquid hydrogen [4, 5]. This is a kind of indirect cooling system with limited performance, thus the temperature rise of SMES coil due to frequent input/output power control makes long time running impossible. Therefore, a suitable control method of SMES coil operation for suppressing temperature rise of SMES coil and securing sufficient precision of fluctuation compensation should be investigated. A control method of threshold voltage range was introduced into the SMES coil system. It has been applied in a long time continuous operation in a 1kW class ASPCS model system having a small Bi2223 SMES coil with 10kJ stored energy. The fluctuation output of solar power generator was compensated by the electrolyzer and SMES system individually. The threshold voltage control method was effective for AC loss reduction. Furthermore, our group is trying to develop MgB_2 cable and SMES coil with 30kJ stored energy cooled by thermos-siphon circulation of liquid hydrogen to compensate for output fluctuation of renewable energy. The progress of the development status of MgB_2 SMES coil will be presented.

This work was supported by JST ALCA Grant Number JPMJAL1002.

[1]M. Sander et al., IEEE Trans. Appl. Supercond. 21, pp. 1362-1366, 2011.
[2]T. Hamajima, et al., IEEE Trans. Appl. Supercond., 22, 3, 2012, Art. ID. 5701704.
[3]H. Louie et al., IEEE Trans. Appl. Supercond. 17, pp. 2361-2364, 2007.
[4]T. Shintomi, et al., IEEE Trans. Appl. Supercond., 22, 3, 2012, Art. ID. 5701604.
[5]Y. Makida, et al., IEEE Trans. Appl. Supercond., 17, pp. 2006-2009, 2007.

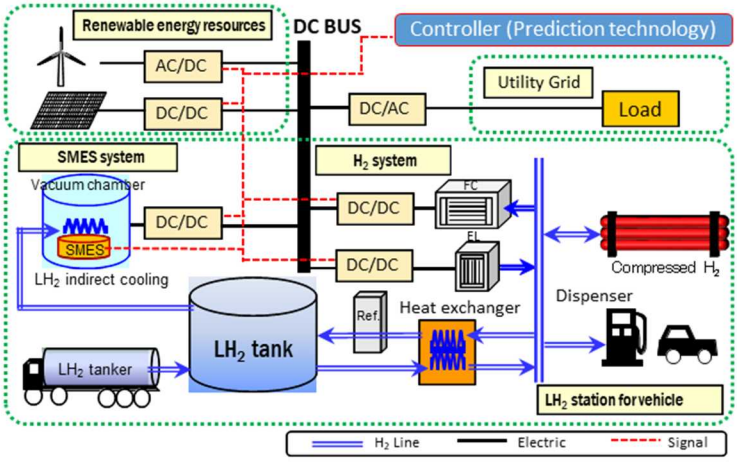

Fig. 1 ASPCS is composed of H_2 system and SMES system and is used to compensate both long and short period output fluctuations of renewable energy.

AP4-10-INV

Recent Progress on Applications Using MgB_2 and Nb_3Sn Superconductors at Hyper Tech

*Michael Tomsic[1], Matthew Rindfleisch[1], David Doll[1], Xuan Peng[1], Michael Sumption[2], Michael Martens[3]

Hyper Tech Research Inc., USA.[1]
Ohio State University, USA.[2]
Case Western Reserve University, USA.[3]

This presentation will discuss Hyper Tech's latest progress on applications using MgB_2 and Nb_3Sn wires, cables, and coils. It will include latest improvements with regard to low AC loss MgB_2 wires and coils. The primary applications being pursued are MRI, NMR, SMES, FCL, rotors and stators for wind turbine generators, and high speed motors and generators for all electric aircraft.

Keywords: Nb_3Sn, MgB_2, superconductor, wire, coils, MRI, NMR, fault current limiters, SMES, generators, and motors

AP5-1

Strain control of HTS superconductors to prevent degradation of superconducting magnets during a quench

*Tengming Shen[1], Xiaorong Wang[1], Shijian Yin[1]

Lawrence Berkeley National Laboratory, Berkeley, CA 94720, USA[1]

In this talk we will probe characteristics and failure mechanisms of composite superconductors during a quench, arriving at the conclusion that strain control of composite superconductors is the key to prevent degradation of superconductors within a superconducting magnet during a quench. Experimental data and analysis will be given to support the arguments that for Nb3Sn wire, Bi-2212 wire, MgB2 tape and wire, and Bi-2223 tape, degradation during a quench is driven by axial strain, and that for ReBCO coated conductors, degradation is mostly driven by the tendency of REBCO coated conductor to delaminate, caused by the thin film multilayered structure developing peeling stress when experiencing localized temperature rises. We will introduce a simple experimental technique for evaluating strain effects under various bending strain (flatwise bending, edgewise bending, or a combination), high Lorentz forces in high magnetic fields, and high current and with presence of a quench. We will also discuss a technique for minimizing dangers of delamination of REBCO coated conductors due to epoxy impregnation while retaining high superconducting coil current density.

This work is supported by the U.S. Department of Energy, Office of Science, Office of High Energy Physics.

AP5-2

Unbalanced Torque Simulation on NI REBCO Pancake Coils during Quench

*So NOGUCHI[1], Seungyong HAHN[2], Yukikazu IWASA[3]

Hokkaido University, Japan[1]
Seoul National University, Republic of Korea[2]
Massachusetts Institute of Technology, USA[3]

Recently, a stack of no-insulation (NI) REBCO pancake coils is applied to generate a magnetic field higher than 20 T. The no-insulation winding technique provides a high thermal stability to REBCO pancake coils. When a normal local zone appears in one pancake, a current is induced in other pancake coils. It causes other quenches in the stack of REBCO pancake coils. The quenches have not resulted in the burning-out of the NI REBCO pancake coils due to the high thermal stability of NI winding technique.

However, some unbalanced forces work to NI REBCO pancake coils during quench. As a result, these large forces give an irreversible damage to REBCO tapes or a mechanical damage to REBCO magnets.

Therefore, we have developed a method to simulate the forces, especially for unbalanced torques, for NI REBCO pancake coils during quench.

AP5-3-INV

A Hybrid Trapped Field Magnet Lens (HTFML): concept and realisation

*Mark D Ainslie[1], Hiroyuki Fujishiro[2], Devendra K Namburi[1], Sora Namba[2], Yunhua Shi[1], Anthony R Dennis[1], John H Durrell[1]

Department of Engineering, University of Cambridge, UK[1]
Department of Physical Science and Materials Engineering, Iwate University, Japan[2]

In this presentation, the concept of a Hybrid Trapped Field Magnet Lens (HTFML) is described, which exploits two different characteristics of type II superconductors: the "vortex pinning effect" of an outer superconducting bulk cylinder, which acts as a trapped field magnet (TFM) using field-cooled magnetization (FCM), combined with the "diamagnetic shielding effect" of an inner bulk magnetic lens. The HTFML can reliably generate a concentrated magnetic field in the centre of the lens that is higher than the trapped field from the cylindrical bulk TFM and the external magnetizing field, even after the externally applied field decreases to zero. This requires that, during the FCM process, the outer cylinder is in the normal state ($T >$ superconducting transition temperature, T_c) and the inner lens is in the superconducting state ($T < T_c$) when the external magnetizing field is applied, followed by cooling to an appropriate operating temperature, then removing the external field. The concentrated magnetic field in the HTFML changes depending on the superconducting characteristics of the materials used, their shape and size, as well as the magnetizing conditions. This is explored for two potential cases: 1) exploiting the difference in T_c of two different bulk materials ("case-1"), e.g., MgB_2 (T_c = 39 K) and Gd-Ba-Cu-O (T_c = 92 K) or 2) using the same material for the whole HTFML, e.g., Gd-Ba-Cu-O or (RE)-Ba-Cu-O (where RE is rare-earth element), but utilizing individually-controlled cryostats, the same cryostat with different cooling loops or coolants, or heaters that keep the outer bulk cylinder at a temperature above T_c to achieve the same desired effect. We will also report sample fabrication and preliminary experimental results towards realising such HTFML practically.

Keywords: bulk superconductors, trapped field magnet, magnetic lens, hybrid trapped field magnet lens

AP5-4

Removal of Scale from Feed-water in Thermal Power Plant by Magnetic Separation -Composition Analysis of Oxygenated Treatment Scale-

*Mami Hiramatsu[1], Junya Yamamoto[1], Yoko Akiyama[1], Fumihito Mishima[2], Shigehiro Nishijima[2], Hidehiko Okada[3], Noriyuki Hirota[3], Tsuyoshi Yamaji[4], Hideki Matsuura[4], Seitoku Namba[4], Tomokazu Sekine[5]

Osaka Univ., Japan[1], Fukui Univ. of Technology, Japan[2], National Inst. for Materials Science, Japan[3], Shikoku Research Institute Inc., Japan[4], Ebara Industrial Cleaning Co., Ltd., Japan[5]

The technology to prevent generation efficiency of thermal power plant from deterioration is needed in order to reduce CO_2 emissions. One of the reasons for the deterioration is adhesion of the scale generated by corrosion on the piping inner wall in the feed-water system which causes a drop in heat exchange efficiency. Chemical feed-water treatment such as total volatile treatment (AVT) and oxygenated treatment (OT) is performed in order to suppress the scale generation. However, these methods cannot prevent the scale generation completely. Focusing on the magnetic property of scale, we studied on removal of scales in feed-water system by high gradient magnetic separation (HGMS) using the superconducting magnet.

We targeted the thermal power plants adopting OT which was increasing in recent years. To clarify the magnetic property of the actual scale, the composition of the scale collected at 6 sampling points in the feed-water system were analyzed by physical property measurement system and Mössbauer spectrometry to examine the magnetization and the composition of the scale.

Figure 1 shows the sampling points in the feed-water system of the thermal power plant, and Figure 2 shows the magnetization curves of the scale at each point. It was found that the composition of the scale differed depending on the sampling points, and that the ferromagnetic magnetite and maghemite were contained more in the scale collected at low pressure feed-water heater drain (LPD) than any other sampling points, showing the highest magnetization. It is considered that ferromagnetic magnetite changes into paramagnetic hematite by oxidation at higher temperature.

Based on the results, lab-scale magnetic separation experiments by superconducting magnet were conducted, assuming the introduction of HGMS into LPD. The experiments were conducted both for the actual scale collected at LPD and the simulated sample of mixed iron oxide and hydroxide, in order to examine the effect of aggregation in the actual scale.

Acknowledgment: This work is partly supported by Advanced Low Carbon Technology Research and Development Program (ALCA) of JST Strategic Basic Research Programs.

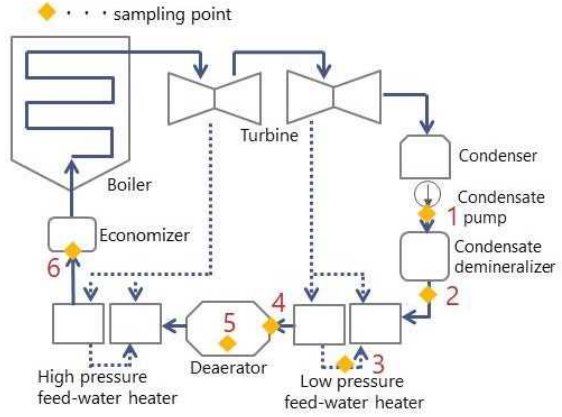

Fig.1 The sampling points in the feed-water system of the thermal power.

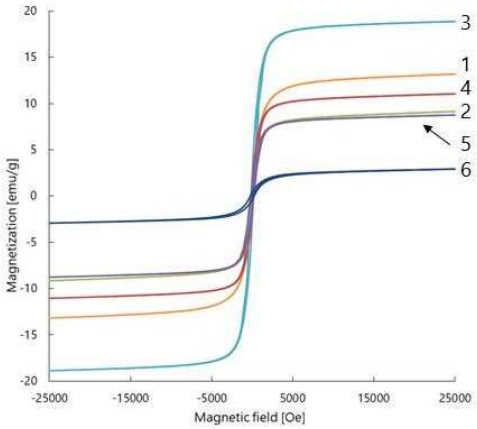

Fig.2 The magnetization curves of the actual scales at 6 sampling points.

Keywords: Thermal power plant, Scale, Iron oxide, High Gradient Magnetic Separation (HGMS)

AP5-5

Remediation of Groundwater Contaminated by Heavy Metals Using Magnetic Separation Technique

*Albino Jose Amosse[1], Yoko Akiyama[1]

Osaka University, Japan[1]

Studies on environmental pollution in Africa indicates that water pollution by heavy metals ions has reached unprecedented levels over the past decade. Mining activities are significant source of heavy metals contamination of both surface and groundwater. Environmentalists worldwide are researching for low cost, efficient and environment-friendly techniques for heavy metals removal. Remediation of contaminated water by heavy metals is of great importance to improve life quality of citizens and prevent them from their adverse effects.

Among the techniques used to remove heavy metals from contaminated water, Magnetic separation technique is a low cost and environment-friendly method, beside that is the only method effective to remove both pollutants, ionic and particle state and is effective to remove pollutants in a successive and large scale treatment.

In this study, Magnetic Activated Carbon (MAC) coated with colloidal silica (MAC-Si) were prepared as a new adsorbent and used to adsorb heavy metals from artificial contaminated water with coexistence of copper, manganese and zinc ions as example of common heavy metals ions dominant in water across mining area. Colloidal silica is an industrial waste of polishing agent out of date with no economic value that can significantly enhance the adsorption capacity of heavy metals ions. Once these ions adsorbed onto surface of MAC-Si can easily be removed by magnetic separation technique.

Figure 1 shows the schematic view of MAC surface modification to MAC-Si adsorbent. MAC modification will offer more active sites for ions adsorption. Silica surface is negatively charged at pH>2 (isoelectric point of silica), what make it effective to adsorb cations. This study intend to examine the adequate system to separate the MAC-Si adsorbent from water in large processing speed by applying superconducting magnet. Figure 2 represents ions adsorption using MAC and MAC-Si adsorbents for water containing 10 ppm of Cu^{2+}, Mn^{2+} and Zn^{2+} ions respectively, and it suggest that MAC-Si is more effective to adsorb large amount of ions than MAC.

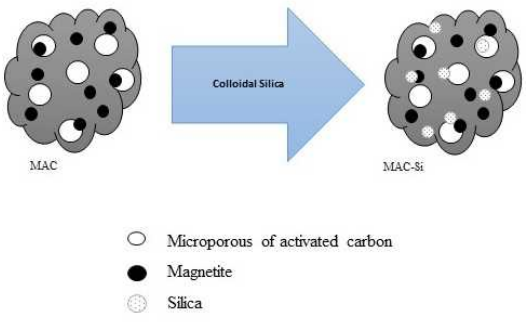

Fig. 1 Schematic diagram of MAC modification to MAC-Si

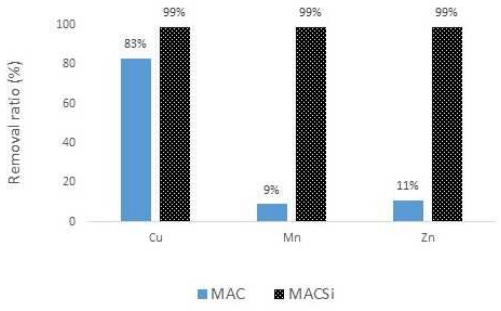

Fig. 2 Ions removal ratio using MAC and MACSi

Keywords: Colloidal silica, Groundwater, Heavy metals, Magnetic separation system

AP5-6

Development of a contactless cryogenic rotation mechanism employed for a polarization modulator unit in cosmic microwave background polarization experiments

*Yuki Sakurai[1], Tomotake Matsumura[1], Teruhito Iida[2], Kunimoto Komatsu[3], Nobuhiko Katayama[1,2], Hajime Sugai[1], Hiroyuki Ohsaki[4], Yutaka Terao[4], Yukimasa Hirota[4], Hisashi Enokida[4]

Kavli IPMU, The University of Tokyo[1]
ispace, inc.[2]
Okayama University[3]
Department of Advanced Energy, Graduate School of Frontier Sciences, The University of Tokyo[4]

We present the design and the performance of a contactless cryogenic rotation mechanism used in cosmic microwave background (CMB) experiments. A precise measurement of the CMB polarization is possible to verify the cosmic inflation theory that describes the very beginning (10^{-38} seconds) of the early universe. The polarization modulator, that rotates a half wave plate continuously at the aperture of the telescope, is one of the key instruments in the experiments. In order to reduce noise and systematic uncertainties, the polarization modulator is required a stable rotation with minimal heat dissipation in a cryogenic environment less than 10 K. Thus, we adopted the rotation mechanism that combines completely contactless bearing and motor, a superconducting magnetic bearing, and a hollow bore synchronous motor. The heat dissipation and the load torque due to the friction can be minimized by avoiding physical contacts. We constructed the prototype of the rotation mechanism with the inner diameter of 380 mm and carried out the performance test. In this presentation, we discuss the rotation stability and the thermal characteristics of the developed rotation mechanism.

Keywords: Cosmic inflation, Cosmic microwave background, Cryogenic rotation mechanism, Superconducting magnetic bearing

BN-1-INV

Superconductivity above 280 K in superhydrides at megabar pressures

Russell J. Hemley[1], Maddury Somayazulu[1], Muhtar Ahart[1], Ajay K Mishra[2], Zachary M. Geballe[2], Maria Baldini[2], Yue Meng[3], Viktor V. Struzhkin[2]

School of Engineering and Applied Science, The George Washington University, Washington DC 20052, USA[1]
Geophysical Laboratory, Carnegie Institution of Washington, Washington DC 20015, USA[2]
HPCAT, X-ray Science Division, Argonne National Laboratory, Argonne IL 60439, USA[3]

Recent predictions and experimental observations of high T_c superconductivity in hydrogen-rich materials at very high pressures are driving the search for superconductivity in the vicinity of room temperature. We confirmed the existence of a new class of such materials – so-called superhydride phases (MH_x, $x > 6$), and have developed preparation techniques for their syntheses and characterization, including measurements of structural and transport properties, at megabar pressures. Four-probe electrical transport measurements of lanthanum superhydride samples display signatures of superconductivity at temperatures ranging from 210 K to above 280 K near 200 GPa. The experiments are supported by pseudo-four probe conductivity measurements, critical current determinations, low-temperature x-ray diffraction, and magnetic susceptibility measurements. These near room temperature measurements of superconductivity are in good agreement with density functional and BCS theory-based calculations.

LN-1-INV

Controlling Hysteresis in Superconducting Weak Links and Nano-Superconducting Quantum Interference Devices

*Nikhil Kumar[1], C.B. Winkelmann[3], H. Courtois[3], Anjan K. Gupta[2]

Department of Physics, DDU Gorakhpur University, Gorakhpur, Uttar Pradesh, India -273009[1]
Department of Physics, Indian Institute of Technology Kanpur, Uttar Pradesh, India -208016[2]
Institute Neel, CNRS and University Joseph Fourier, 25 Avenue des Martyrs, BP 166, 38042, Grenoble, France[3]

We have fabricated and studied the current-voltage characteristics of a number of niobium thin film based weak-link devices and nano-SQUIDs, showing a critical current and two re-trapping currents. We have proposed a new understanding for the re-trapping currents in terms of thermal instabilities in different portions of the device. We also find that the superconducting proximity effect and the phase-slip processes play an important role in dictating the temperature dependence of the critical current in the non-hysteretic regime. The proximity effect helps in widening the temperature range of hysteresis-free characteristics. Finally we demonstrate control on temperature-range with hysteresis-free characteristics in two ways: 1) By using a parallel shunt resistor in close vicinity of the device, and 2) by reducing the weak-link width. Thus we get non-hysteretic behavior down to 1.3 K temperature in some of the studied devices.

1. Nikhil Kumar, T. Fournier, H. Courtois, C. B. Winkelmann, Anjan K. Gupta, Phys. Rev. Lett., 114, 157003, (2015).
2. Nikhil Kumar, C. B. Winkelmann, Sourav Biswas, H. Courtois, Anjan K. Gupta, Supercond. Scien. And Technol. as Fast Track Communication, 28, (2015), 072003.

LN-2

Fabrication of 4-Superconducting Layers Coated Conductors

*Hongsoo Ha[1], Jaehun Lee[2], Seung-Hyun Moon[2], Sangsoo Oh[1]

Korea Electrotechnology Research Institute, Changwon, Gyeongnam, 51543 Korea[1]
SuNAM Co., Anseong, Gyeonggi, 17554 Korea[2]

ReBCO coated conductors have been developed and commercialized for various applications such as, cables, fault current limiters, motors, generators and so on. On the other hand, huge applications such as NMR, accelerator and fusion reactor demand high performance coated conductors that has high operating current over thousands ampere at high magnetic field.

A number of studies have been carried out to make high temperature superconducting(HTS) conductor with higher critical current over thousands ampere by using stacking methods. Several types of conductors using coated conductors such as CORC(Conductor on Round Core) cable, Roebel conductor, TSTC(Twisted Stacked-Tape Conductor) and round wire have been developed. In this study, 4-superconducting layers coated conductor has been suggested that transport higher current and has high engineering critical current density. Coated conductor has usually low c-axis strength and is easily delaminated between superconducting layer and ceramic buffer layer. In order to make 4-superconducting layers coated conductor, delaminated silver coated superconducting layers were stacked on a coated conductor. The transport current of 4-superconducting layers coated conductor can be increased with the number of superconducting layers. Finally, 4-superconducting layers coated conductor shows critical current of 2,000A/cmw. at 77K, self-field. And also engineering critical current density becomes almost four times because of four superconducting layers on a substrate.

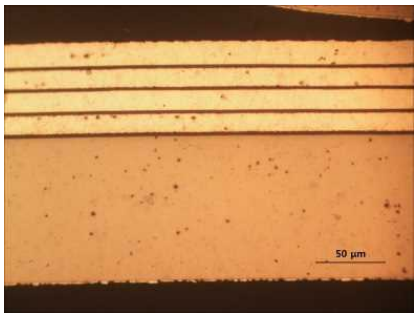

Fig. Longitudinal cross-section of 4-superconducting layers coated conductor

This research was supported by Korea Electrotechnology Research Institute(KERI) Primary research program through the National Research Council of Science & Technology(NST) funded by the Ministry of Science and ICT (MSIT) (No. 18-12-N0101-08), Republic of Korea

Keywords: Coated conductor, Multi superconducting layers, Engineering critical current density

LN-3

None s-wave triplet pairing in Superconducting boron doped diamond; a platform for all diamond based quantum information technology

*Somnath Bhattacharyya[1]

University of the Witwatersrand[1]

Having only been discovered around 15 years ago, superconducting boron doped diamond has thus far not been thoroughly investigated as a suitable platform for the development of novel quantum technology. Considering that diamond presents well-established quantum states such as the diamond nitrogen-vacancy centres (NV-centres) as well as superconductivity, diamond thus demonstrates a potential platform for the realization of all diamond based quantum circuitry. Thus far STM measurements have indicated some unusual features including a mixed phase of BCS and non-BCS paring, zero bias conductance as well as resonance states within the vortex core. Following our investigation on the unconventional quantum transport in heavily boron doped diamond films, a few key features such as re-entrant effects, magnetoresistance oscillations as well as anisotropic magnetoresistance have been identified as signatures of non s-wave order parameter and may be of interest for developing novel qubits. We have also identified a number of features related to low dimensional superconductivity including the BKT effect and bound states such as those observed in High Tc materials. Transport studies are complimented by high resolution transmission electron microscopy studies focused on the grain boundary region. We show that some of the unconventional features, particularly a pronounced zero bias conductance peak, can be related to the formation of a bound state generated at the boundaries of the crystallites. This ZBCP shows a robust nature with respect to applied field and bares a number of characteristics related to a possible triplet state. We advance the understanding of superconducting diamond as a potential new type of qubit system, we present various aspects of fabricating and measuring diamond based quantum information device elements including nanowires and SQUID loops. Firstly, the fabrication of monolithic circuit elements is investigated using a focused ion beam patterning technique. Although deeper investigations are required, there are already reports on a possible topological phase in the nanocrystalline boron doped diamond system. This includes the realization of a two-dimensional phase and most notably the possibility of spontaneous time reversal symmetry breaking through the accumulation of the Berry phase.

Keywords: triplet superconductivity, BKT transition, Qubit, unconventional superconductivity

PCP1-1

Negative magnetoresistance due to the depression of Quantum phase slip in NbN nanowires

*Bunju Shinozaki[1], Kazumasa Makise[2], Takayuki Asano[3]

Department of Physics, Kyushu University, 744 Motooka Fukuoka 819-0395, Japan[1]
National Institute of Advanced Industrial Science and Technology, Tsukuba 305-8560, Japan[2]
Department of Applied Physics, University of Fukui, Fukui 910-8507, Japan[3]

The temperature and magnetic field dependences of the resistance R were investigated for quasi-one dimensional superconducting NbN nanowires with length L=600 and 900nm, and the width w=20nm and thickness d=20nm prepared on 3C-SiC substrate. It has been found that 1) both $R(T)$ characteristics with broad superconducting transition at temperatures below T_c~13.5K in the absence of magnetic field H can be well explained by the sum of the thermal activated phase slip(TAPS) model near T_c and the quantum phase slip(QPS) model below T_c. 2) In the magnetic field H, $R(T)$ shows the characteristic expressed by only the TAPS model in H=0, that is, the magnetic field enhances the superconductivity. The $R(T)$ of specimen with L=600nm shows nearly zero resistance in the restricted temperature region which depends on the magnitude of H, that is, the huge negative magneto-resistance is observed. With decreasing temperature, $R(T)$ finally recovers the QPS resistive state observed in H=0. 3) At low temperatures where the $R(T)$ takes the recovered QPS resistive state, the $R(H)$ for the specimen with L=900nm shows the oscillation behavior. 4) The upper critical magnetic field $H_{c2}(T)$ can fit to the theoretical expression $H_{c2,theo.}(T)=\Phi_0/[2\xi_{GL}(T)\times w] \propto (1-T/T_c)^{1/2}$, where$\Phi_0$ and $\xi_{GL}(T)$ are the flux quantum and the Gintzburg-Landau superconducting coherence length, respectively. Although the relation $H_{c2,exp}(T)\propto(1-T/T_c)^{1/2}$ is satisfied, the magnitude of $H_{c2,exp}(T)$ is about 5 times larger than that of the theoretical one.

Keywords: Negative magnetoresistance, Quantum phase slip, NbN nanowires

PCP1-2

Detecting Vortex Penetration and Expulsion in Mesoscopic Thin Layered Superconductor $NbSe_2$ Using Small Tunnel Junctions

Naoki Hoshi[1], Dai Inoue[1], Hikari Tomori[1], *Akinobu Kanda[1]

University of Tsukuba, Japan[1]

In a mesoscopic superconductor, which has a lateral size comparable to the magnetic penetration depth and/or the coherence length, not only the vortex-vortex interaction but the vortex-boundary interaction affects the vortex configuration, and so there appear novel vortex states such as a giant vortex state, opening possibility that one can manipulate the quantum vortex states for the application to quantum devices such as sensors.

So far, we have investigated the mesoscopic vortex states in thin aluminum (Al) superconductors formed with e-beam lithography followed by vacuum deposition, and succeeded in observing novel vortex states such as a giant vortex [1] and one-dimensional vortex [2], and controlling the vortex states using applied currents.[3] Vortices were detected using small tunnel junctions attached to the superconductor. In spite of the successful observation of the novel vortex states, their control was extremely difficult, presumably due to the inevitable surface roughness in the deposited superconducting films, which tends to trap the vortices.

Here, we are trying to apply our technique to layered superconductors obtained with mechanical exfoliation. Layered superconductors have ideally no surface roughness, so that we expect that the control of the vortex states is much easier. Here, as the first step toward the goal, we report the observation of vortex penetration/expulsion in a flake of layered superconductor $NbSe_2$ using tunnel junctions. The behavior is quite different from that for Al samples, indicating the penetration/expulsion of multiple vortices at the same time.

[1] A. Kanda *et al.*, Phys. Rev. Lett. 93 (2004) 257002.
[2] A. Kanda *et al.*, Phys. Rev. B 76 (2007) 094519.
[3] M.V. Milosevic *et al.*, Phys. Rev. Lett. 103 (2009) 217003.

Keywords: vortex, layered superconductor, NbSe2, mesoscopic superconductor

PCP1-3

Evaluation of Layer Thickness Dependence of Critical Current Density Characteristics using Longitudinal Magnetic Field Effect in Superconducting Coated Conductors

*Tomohiro Yonenaka[1], Edmund Soji Otabe[1], Vladimir Vyatkin[2], Sergey Lee[2], Tadahiro Akune[3], Terukazu Nishizaki[3]

Kyushu Institute of Technology Japan[1], SuperOx Japan[2], Kyushu Sangyo University Japan[3]

The critical current I_c of the superconductor depends on the thickness of the superconducting layer. That is, as thickness increases, I_c increases. However, in the case of the superconducting coated conductor, when the superconducting layer exceeds about 1 μm, the I_c does not increase. This is because the critical current density J_c decreases due to deterioration of crystal orientation. The layer thickness dependence of J_c has already been investigated by transverse magnetic field. In this study, the dependence of the critical current density on the layer thickness was investigated using the longitudinal magnetic field effect. It is known that when the current and the magnetic field are parallel (longitudinal magnetic field), the current density increases as increasing the magnetic field. This is because the crystal orientation is fine.

The sample used in present measurement is a Gd-based coated conductor obtained by forming an intermediate layer on the HASTELLOY substrate by IBAD method and forming a superconducting layer by PLD method. Table 1 shows the sample name and the thickness of the superconducting layer. The $J_c - B$ characteristics of this sample were measured by applying the magnetic field B up to 0.5 T under the temperature conditions of 65.0 K, 70.0 K and 77.3 K by four-terminal method.

Figure 1 shows the measurement results of $J_c - B$ characteristics at 65.0 K. It is considered that Jc of sample A is smaller than others because the layer thickness is too thin and crystal growth is insufficient. In the transverse magnetic field, Jc of samples B, C and D decreases similarly. In the longitudinal magnetic field, Jc of sample D decreases as compared with B and C as the magnetic field increasing. This is considered to be due to deterioration of the crystal orientation described as aforementioned. Thus, by using the longitudinal magnetic field effect, the difference in the critical current density characteristics due to the layer thickness is more clearly appeared. From these results, it is considered that the optimum thickness of this sample is 0.9 — 1.2 μm under the longitudinal magnetic field.

Sample	Thickness [μm]
A	0.6
B	0.9
C	1.2
D	1.5

Table 1 Superconducting layer thickness in each sample

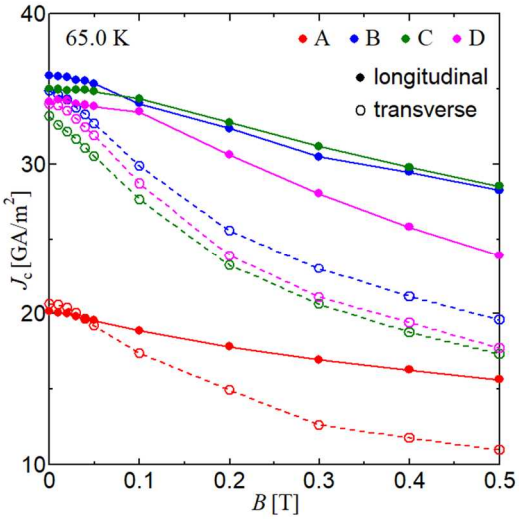

Figure 1 $Jc - B$ characteristics of each sample in longitudinal and transverse magnetic fields at 65.0 K

Keywords: Coated conductor, Critical current density, Longitudinal magnetic field effect

PCP1-4

TDGL Simulation on the Angular Dependence of the Critical Current Density in Superconductors with Columnar Defects

*Rina Yonezuka[1], Yusei Hamada[1], Kazunori Kamiji[1], Kenta Tanimura[1], Takaki Yoshihara[1], Edmund Soji Otabe[1], Yasunori Mawatari[2], Tetsuya Matsuno[3]

Kyushu Institute of Technology, Japan[1]
National Institute of Advanced Industrial Science and Technology, Japan[2]
National Institute of Technology Ariake College, Japan[3]

We numerically investigate the angular dependence of pin of critical current density in a small superconducting cube exposed to a transport current and a transverse magnetic field. By using the Euler method, we numerically solve the time-dependent Ginzburg-Landau (TDGL) equations for the superconducting cube, of which dimensions are smaller than the London penetration depth.
In this study, The parameters using in the original TDGL equations is normalized using the coherence length ξ and the upper critical field B_{c2} and soon for reducing the number of the constants in TDGL equations.
We consider a superconducting cube of which side length is 10ξ in the vacuum. In addition, 4 columnar pins of diameter ξ were introduced as shown in Fig. 1. In the region of the pins, we define the order parameter Ψ as 0.
We give the boundary condition corresponding to the normal component of the electric current density $\boldsymbol{J}$ is zero at the surfaces of the cube. $\boldsymbol{J}$ and $\boldsymbol{B}$ are applied to the y axis and the z axis, respectively. Hence, the vector potential can be given by $(A_x,A_y,A_z)=(0,B_x,0)$ for the transverse magnetic field. The electric current density and the magnetic field at each time were kept constant at a normalized value.
Fig. 2 shows the superconducting cube with different angle of columnar pins. It is assumed that $\theta=0°$ represents for the case when the pin and the magnetic field are parallel. Therefore, Figs. 2(b), (c), and (d) show $\theta=0°$, $\theta=45°$, and $\theta=90°$,respectively. Although rotation of the magnetic field is possible, the pin is rotated to suppress the surface effects. Calculations were made with external magnetic field B=0.4, current density J=0.01,0.02,⋯,0.30, and angle $\theta=0,10,\cdots,90°$.Fig. 3 shows the simulation results of the angular dependence of J_c at B=0.4. J_c decreases as increasing the angle, and J_c abruptly decreases when θ is between 20° and 30°. Although magnetic flux lines could be trapped by columnar pins for $\theta=0$-20°, magnetic flux lines could not be trapped and slip through at high magnetic fields. In this way, angular dependence of J_c was confirmed in the present simulation.

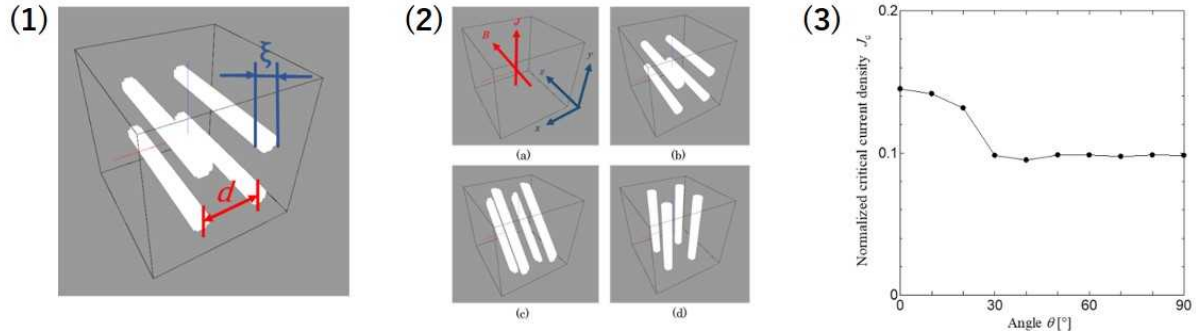

Fig. 1: Geometry of the superconducting cube
Fig. 2: The superconducting cube with different angle of columnar pins
Fig. 3: The simulation results of the angular dependence of J_c at B=0.4

Keywords: Critical current density, time-dependent Ginzburg-Landau equation

PCP1-5

Dynamics of a vortex system in a layered high-temperature superconductor under a pulsed current impact

*Igor Rudnev[1], Anastasiia Maksimova[1], Anna Moroz[1], Vladimir Kashurnikov[1]

National Research Nuclear University MEPHI (Moscow Engineering Physics Institute)[1]

Numerical modeling of the vortex system in a layered high-temperature superconductor under the influence of a short-time rectangular impulses of the transport current was carried out. The calculations were performed by the Monte Carlo method in the framework of a two-dimensional model of a layered high-temperature superconductor. It is assumed that the vortices enter the superconductor under the influence of the intrinsic field of the transport current at the sample boundary. The algorithm is realized taking into account the processes of creation, annihilation, motion of vortices and annihilation of a pair of vortices of the opposite sign in the center of the sample. The electric field strength in the superconductor was calculated from the energy released during annihilation at the center of the vortices of the opposite sign, the value of which is proportional to the number of pairs annihilated during the calculation. For the critical current is accepted, at which the field strength is 1 mkV/cm. The results of calculations show that in a pulsed regime, a superconductor can withstand a current several times higher than the critical current, determined from the current-voltage characteristic. The dependences of the threshold pulse duration on its amplitude are calculated, as well as the maximum values of the current flowing through the superconductor without the release of energy. The influence of various parameters of artificial pinning centers on the threshold duration and pulse amplitude is analyzed. The cases of a regular (rectangular and triangular lattice with different periods) and a chaotic arrangement of defects are considered. It is shown that a regular lattice of defects can lead to a decrease in the threshold amplitude and pulse duration. Vortex configurations that arise when a current pulse is applied to a superconductor are obtained.
The work is supported by the Russian Foundation for Basic Research under the grant 17-29-10024.

Keywords: HTSC, Monte-Carlo simulations, dynamic of vortex system, pulsed transport current

PCP1-6

Observation of vortex trapping and expulsion in superconducting rings of amorphous MoGe thin films

*Nobuhito Kokubo[1], Satoru Okayasu[2], Tsutomu Nojima[3], Takahiko Sasaki[3]

University of Electro-Communications[1]
Japan Atomic Energy Research Institute[2]
Tohoku University[3]

Investigations of fluxoid states of field cooled superconducting rings of amorphous MoGe thin films have been made with a scanning superconducting quantum interference device microscope. The magnetic flux integrated over the centered hole of the ring exhibits non monotonous behavior with applied magnetic field, indicating the field evolution of the vorticity of the closed ring. Further increase of the magnetic field traps a vortex (vortices) in annular region. The characteristic field of complete vortex expulsion depends on the sample size and is scaled inversely with squared ring width.

Keywords: Superconducting rings, Fluxoid States, Scanning SQUID microscope

PCP1-7

Observation of Fractional Vortices in a Superconducting Double Layer

*Taichiro Nishio[1], Shunichi Arisawa[2], Hirotake Yamamori[3], Takashi Yanagisawa[3], Yasumoto Tanaka[3]

Tokyo University of Science, Japan[1]
National Institute for Materials Science, Japan[2]
National Institute of Advanced Industrial Science and Technology, Japan[3]

Two-band superconductors have internal degrees of freedom in a quantum phase. It has been shown in theory [1] that a soliton-shaped phase difference wave can be excited and it emerges accompanied by fractional quantum vortices in two-band superconductors. However, experimental evidence of a fractional vortex as well as a soliton has not been reported yet as far as we know. Thus, we attempt to create a fractional vortex and observe it as a token of a soliton, using double-layered superconducting films as two-band superconductors. We designed and fabricated artificial two-band superconductors based on ultra-thin films of a Nb/AlO/Nb layered structure, where a Nb layer corresponds to a one-band superconductor and the upper Nb layer has holes, as shown in Fig. 1a. Magnetic images of vortices were obtained by scanning superconducting-quantum interference device microscopy after samples were cooled down to 4 K under magnetic fields of a few microtesla. Figure 1b shows magnetic images of vortices in the B field [2]. Clearly, one vortex in the middle part has the higher magnetic flux density in comparison with others. The others have only half of the magnetic flux density that it has. Integrals of the magnetic flux density approximate to Φ_0 in the former and to $0.5\Phi_0$ in the latter. It indicates that the latter vortices are fractional vortices created in an artificial two-band superconductor. Its implications of a soliton will be discussed in the presentation. This work was partially supported by JSPS KAKENHI Grant Number JP 16K06275 and the TIA collaborative research program KAKEHASHI.

[1] Y. Tanaka, Phys. Rev. Lett. 88 (2002) 017002.
[2] Y. Tanaka et al., Physica C 548 (2018) 44.

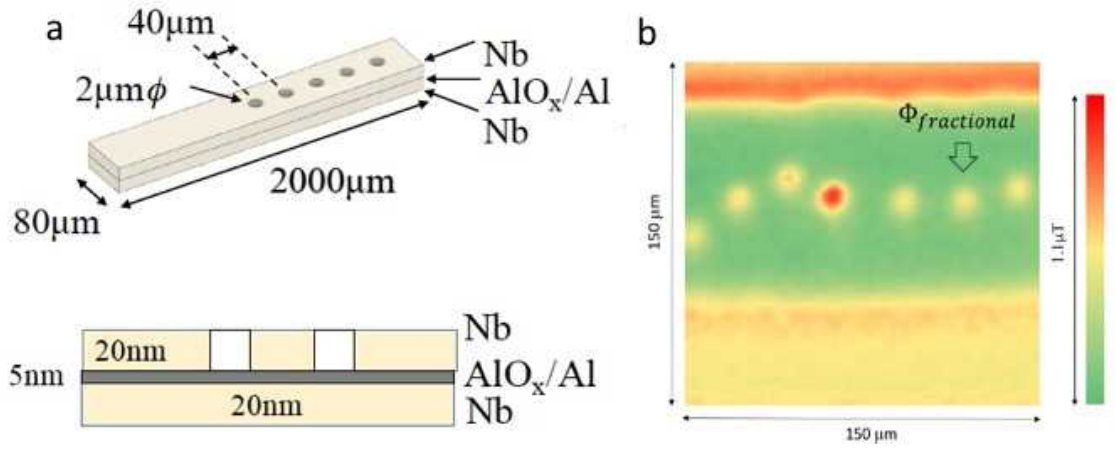

Fig.1a Schematic illustrations of a sample. 1b Magnetic image of the sample.

Keywords: Two-band superconductor, Fractional vortex, Soliton, Scanning SQUID microscopy

PCP1-8

Critical states in superconducting plates: Shape dependence

Shinsuke Ooi[1], Masaru Kato[1]

Osaka Pref. Univ. Japan[1]

When an external perpendicular magnetic field applied to a superconducting strip is increased, magnetic flux penetrates into the superconductor from its edge. Depending on ramping rate of increased applied field, there are two types of flux penetration. If ramping rate is small, a critical state appears. On the other hand, the ramping rate is large, a vortex avalanche occurs. The critical state is a metastable equilibrium state in which Lorentz force from a local current, and pinning force are balanced. The vortex avalanche is a thermo-magnetic instability phenomenon, in which heat generation due to vortex motion, heat transfer and vortex jump between pinning centers play important roles.

We have investigated the critical state and the vortex avalanche in a layer structure. We found the critical state and the vortex avalanche depend on the three-dimensional structure of superconducting plate as well as local magnetic field divergence and thermal conductivity. In this study, we investigate the critical states in various structures composed of several superconducting plates. Using three-dimensional finite element methods, we solve the heat transport equation and the Maxwell equations with current-voltage relation for the superconductors. In this model, the heat transport equation has a heat generation term added to the usual form, the Maxwell equations are expressed by the vector potential and in the current-voltage relation the electric resistivity of the superconducting state depends on the temperature and the current. We will report the magnetic flux density, the current density and the electric field in three-dimensional structural superconducting plates.

Keywords: theory, vortex, mesoscopic, simulation

PCP2-1

Simulation of vortex lattice melting in a dirty superconductor

Takashi Kusafuka[1], Masaru Kato[1], Osamu Sato[2]

Osaka Pre. Uni.[1]
Osaka Pre. Uni. Collage of Technology[2]

IT IS KNOWN THAT VORTICES IN A MESOSCOPIC SUPERCONDUCTOR SHOW CHARACTERISTIC STATES WHICH DEPEND ON THE SHAPE OF THE SUPERCONDUCTOR. OOI ET AL [1] FOUND THAT MELTING TRANSITION TEMPERATURES OF VORTEX LATTICES IN A SQUARE SUPERCONDUCTING PLATE BECOME MAXIMUM WHEN THE VORTEX NUMBER IS SQUARE NUMBER. SOLVING THE GINZBURG-LANDAU EQUATIONS, THEY SHOWED THAT THE LATTICE OF SQUARE NUMBER VORTICES BECOMES STABLE. THEN USING THE MOLECULAR DYNAMICS METHOD (MD), KATO AND KITAGO INVESTIGATED THE VORTEX LATTICE MELTING TRANSITION IN A PURE SUPERCONDUCTOR. THEY SHOWED STANDARD DEVIATION OF VORTEX POSITION INCREASES RAPIDLY WITH INCREASING TEMPERATURE.
WE INVESTIGATE THIS MELTING OF VORTEX LATTICE IN A DIRTY SUPERCONDUCTOR, USING MD. IN THE MD SIMULATION, WE SOLVE EQUATIONS OF MOTION OF INDIVIDUAL VORTICES, INCLUDING PINNING FORCE FROM IMPURITIES, REPULSION BETWEEN VORTICES AND A FLUCTUATION FORCE. WE SHOW HOW IMPURITIES EFFECT THE MELTING TRANSITION.

[1] S.OOI, T. MOCHIKU, M. TACHIKI, AND K. HIRATA PRL 114, 087001 (2015)
[2] M. KATO, H. KITAGO, J. PHYS. CONF. SER. 871,012028 (2017)

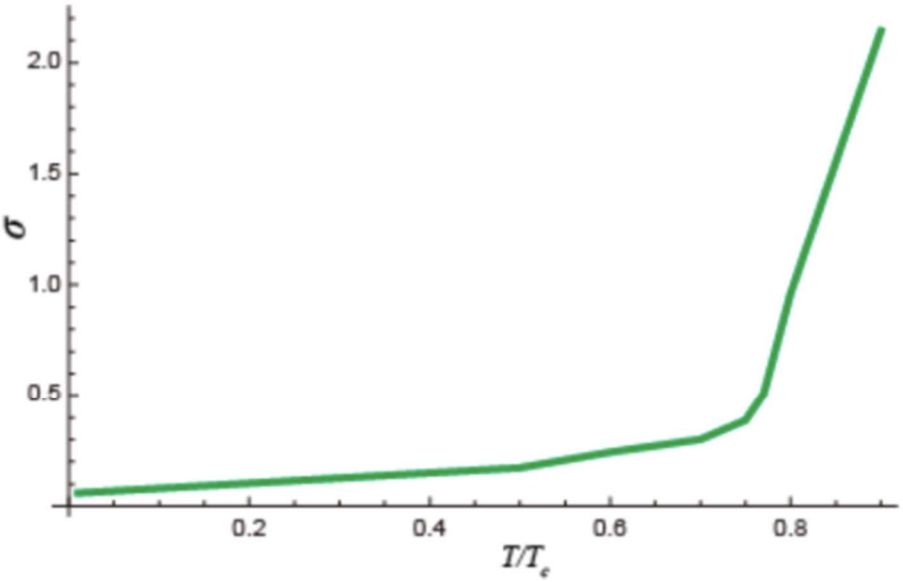

Fig. In $3\lambda_0 \times 3\lambda_0$ square superconductor, the relation of standard deviation of the temperature and position of vortices.

PCP2-2

Molecular Dynamics Simulation for Random Organization of Vortex Matter

*Masaru Kato[1], Takashi Kusafuka[1], Osamu Sato[2]

Department of Physics and Electronics, Osaka Prefecture University[1]
Osaka Prefecture University College of Technology[2]

Physics of vortex matter has been studied widely since discovery of high-Tc cuprate superconductors. Recently, Dobroka et al. studied the random organization in vortex matter[1]. Applying AC or DC driving force to vortex matter in Mo_xG_{1-x} amorphous superconducting films, they found that DC driving force makes vortex matter in disordered state and AC driving force makes vortex matter in random organized state.
Experimentally, they measured the voltage due to vortex motion. Therefore, in order to find how vortices organize under the AC driving force, we investigate vortex motions using the molecular dynamics (MD) method. In the MD method, we solve the equations of motion of individual vortices. In the equation of motions, we include pinning forces from disorders, vortex-vortex repulsive forces, and a thermal fluctuation force. As the pinning force from disorders, we consider a random potential, because the amorphous MoxG1-x film is uniformly weekly disordered. We will show motions of vortices as well as time development of voltage due to the vortex motions.

[1] M. Dobroka et al. New J. Phys. 19 (2017) 053023.

Keywords: Vortex, Molecular dynamics method, Random Organization, Simulation

PCP2-3

Geometrical matching of vortex clusters in micron-sized superconducting regular polygons

*Shuuichi Ooi[1], Minoru Tachiki[1], Takashi Mochiku[1], Kazuto Hirata[1], Kazunori Komori[1], Shunichi Arisawa[1]

National Institute for Materials Science[1]

In a tiny superconductor with the lateral dimensions comparable to the penetration depth, vortices are confined inside by a screening current flowing around the sample edge and form unique configurations, i.e., vortex clusters, instead of the Abrikosov triangular lattice. The vortex configurations depend on the number of vortices, and the shape and size of the superconducting sample in the ground state. In higher temperatures, these vortex clusters melt into a liquid; the configurations would influence the melting temperatures. This has actually been observed in our experiments in a micron-sized square $Bi_2Sr_2CaCu_2O_{8+y}$ (Bi2212) [1]. It is possible to detect the penetration of individual vortices and the melting transition simultaneously by the *c*-axis resistance measurements using a stack of intrinsic Josephson junctions which are naturally contained in the crystal structure of Bi2212 [1,2]. We observed oscillatory behavior of the melting temperature with increasing the number of vortices. Although the main origin of this phenomenon is expected to be a two-dimensional geometrical matching between the vortex clusters and the sample shape [1,2], the configurations in the matching states are unsettled only from the *c*-axis resistance measurements. In this presentation, we show results of simulated vortex configurations based on the Ginzburg-Landau theory using a finite element method in various regular polygonal shapes of samples. Several experimental results for the case of a pentagon and hexagon will also be presented.

Keywords: vortex, melting transition, Bi2212, geometrical matching

PCP2-4

Detection of the vortex liquid phase in thick superconducting films by Nernst effect

*Koichiro Ienaga[1], Taiko Hayashi[1], Shin-ichi Kaneko[1], Satoshi Okuma[1]

Department of Physics, Tokyo Institute of Technology, Japan[1]

The field-induced superconductor-insulator transition (SIT) in a disordered two- dimensional superconductor is a typical example of a quantum phase transition [1]. According to the theory [2], the amplitude of the superconducting order parameter remains finite even on an insulating side of the SIT. In this insulating phase called a Bose-glass phase, Cooper pairs are localized and vortices Bose condense [2]. The presence of the mobile vortices in the Bose-glass phase has not yet been verified experimentally although some electrical transport measurements suggest the presence of the localized pairs [3,4]. To obtain clear evidence of the vortices in the Bose-glass phase, here we focus on a Nernst-effect measurement. Employing this measurement, we can clearly detect vortex motion driven by a thermal gradient without applying a current. We measure a voltage generated transverse to the vortex motion, which is called a vortex Nernst signal. Actually, large vortex Nernst signals have been observed in the vortex-liquid phase of bulk samples. For thin films, however, very limited measurements have been performed so far. This is because for thin films the contribution of the substrate to heat flow is so large, which makes the Nernst measurement difficult [5].

In this work, we constructed an experimental system for measuring the vortex Nernst signal in thin films. We started with amorphous Mo_xGe_{1-x} films with moderate thickness of 300 nm and with measurements at relatively high temperatures. As the field is increased in the vortex solid phase, the Nernst signal rises from zero at the boundary between the vortex solid and liquid phases, showing a peak in the middle of the vortex-liquid phase, and finally falls to zero at around the upper critical field. Thus, we have succeeded in detecting the vortex-liquid state of the superconducting films using the Nernst effect.

[1]A. M. Goldman and N. Marcovi´c, Physics Today **51**, 39 (1998).
[2] M. P. A. Fisher, G. Grinstein, and S. M. Girvin, Phys. Rev. Lett. **64**, 587 (1990), M. P. A. Fisher, Phys. Rev. Lett. **65**, 923 (1990).
[3] M. A. Paalanen, A. I. Hebard, and R. R. Ruel, Phys. Rev. Lett. **69**, 1604 (1992).
[4] S. Okuma, S. Shinozaki, and M. Morita, Phys. Rev. B, **63**, 054523 (2001).
[5] K. Behnia and H. Aubin, Rep. Prog. Phys. **79,** 046502 (2016).

Keywords: Nernst effect, vortex liquid, superconducting thin film

PCP2-5

Time evolution of the vortex configuration associated with dynamic ordering by dc drive

*Shun Maegochi[1], Mihaly Dobroka[1], Koichiro Ienaga[1], Shinichi Kaneko[1], Satoshi Okuma[1]

Tokyo Inst. Tech. Japan[1]

When a periodic shear with small shear amplitude d_{inp} is applied to many particle assemblies with a random distribution, the particles gradually self-organize to avoid future collisions and change into an ordered configuration. This is called random organization or ac dynamic ordering [1]. In contrast, when the particles with an ordered initial configuration are driven in a random pinning potential by a small dc drive, they gradually transform into a disordered configuration. This is called dc dynamic disordering. In our previous work, we used the vortex system in amorphous MoxGe1-x films and performed measurements of the time-evolution of voltage $V(t)$ (average velocity) associated with ac dynamic ordering. We found unexpectedly that the transient vortex configuration formed during the ac dynamic ordering is not microscopically homogeneous but consists of disordered and ordered regions [2]. In contrast, the transient vortex configuration formed during the dc dynamic disordering was found to be homogeneous. This leads to an interesting question: what is the origin of the coexistence regions? Previous results mentioned above [2] suggest that the ac drive and/or dynamic ordering process would be the necessary condition for the emergence of the coexistence regions.

To clarify the origin of the coexistence regions, in this work we study the transient vortex configuration formed during the dc dynamic ordering. We use the same vortex system and method as used in our previous work [2]. To realize the dynamic ordering by dc drive, we need a highly disordered initial vortex configuration, which was attained by using a field-cooling technique. Our results show that the transient vortex configuration formed during the dc dynamic ordering is not homogeneous but consists of disordered and ordered regions. Therefore, the origin of the coexistence regions is attributed to dynamic ordering instead of the ac drive.

[1] L. Corté *et al.*, Nat. Phys. **4**, 420 (2008).
[2] M. Dobroka *et al.*, New J. Phys. **19**, 053023 (2017).

Keywords: vortex, random organization

PCP2-6

Clogging in a dc driven vortex system

*Takahide Minemura[1], Koichiro Ienaga[1], Shun Maegochi[1], Shin-ichi Kaneko[1], Satoshi Okuma[1]

Department of Physics, Tokyo Institute of Technology, Japan[1]

The ceasing of flow of particles through a bottleneck is described by clogging. The clogging was reproduced in a recent simulation where a many-particle system was dc-driven in random pinning [1,2]. When the pinning density is increased, the free particles are clogged by pinned particles, resulting in clogging in which the system cannot move [1]. Furthermore, it has been shown that a change from the moving to clogging state is a non-equilibrium phase transition [2]. However, as far as we know, there is no experimental study demonstrating this prediction.

In this work we investigate the clogging phenomenon using a vortex system of an amorphous Mo_xGe_{1-x} film. First, we prepared steady state plastic flow by applying a small dc current I_{inp}, and froze its vortex configuration by switching off I_{inp}. Next, we applied a dc current I of the same amplitude as I_{inp} at time zero ($t = 0$) but the direction was either the same or opposite to the direction of I_{inp}, and measured the t-dependent voltage $V(t)$. When I is applied in the same direction as I_{inp}, $V(t)$ is t-independent. However, when I is applied in the opposite direction to I_{inp}, $V(t)$ shows a sharp rise at $t = 0$, followed by a fast and subsequent slow decay toward a steady-state voltage with characteristic times τ_f and τ_s, respectively. The result indicates that more vortices are mobile at $t = 0$ when I is applied in the opposite direction to I_{inp} than in the same direction. We attribute its origin to the clogging of free vortices by pinned vortices. When the direction of the current I is reversed, the clogged vortices move abruptly, yielding a sharp additional voltage at $t = 0$. The fast decrease in $V(t)$ represents a process that some moving vortices are clogged again. The slow relaxation toward the steady state represents a dynamic-disordering (pinning) process [3]. We also find that τ_f plotted against I shows a power-law divergence at the depinning current similarly to $\tau_s(I)$, which shows a critical behavior of a non-equilibrium depinning transition [3]. We suggest that the result of $\tau_f(I)$ is discussed in terms of a non-equilibrium clogging transition [2].

[1] C. J. Olson Reichhardt *et al.*, Phys. Rev. E **86**, 061301 (2012).
[2] H. Péter *et al.*, Sci. Rep. **8**, 10252 (2018).
[3] S. Okuma, Y. Tsugawa, and A. Motohashi, Phys. Rev. B **83**, 012503 (2011): S. Okuma and A. Motohashi, New J. Phys. **14** , 123021 (2012).

Keywords: Vortex pinning, Nonequilibrium phenomenon, Plastic flow, Amorphous film

PCP2-7

Observation of vortex configurations under dc drives using scanning tunneling spectroscopy

*Takashi Ogawa[1], Koshiro Kato[1], Kazuki Tsuchiya[1], Shin-ichi Kaneko[1], Koichiro Ienaga[1], Hideaki Sakata[2], Satoshi Okuma[1]

Department of Physics, Tokyo Institute of Technology,Japan[1]
Department of Physics, Tokyo University of Science,Japan[2]

We have constructed a scanning tunneling microscope/scanning tunneling spectroscopy (STM/STS) system which allows us to conduct transport and STM measurements at low temperatures and high fields for the same sample. Using this system, we examine the configuration of vortices driven by dc currents I over the wide I region, including plastic flow and flux flow regions. We study a vortex system in amorphous Mo_xGe_{1-x} films with weak random pinning. The vortices are driven by dc current I for a long time until the steady state is reached. After freezing the configuration of vortices by switching off I, we perform the STS measurement. We observed a triangular vortex lattice within the range of 240 × 240 nm^2 for all I studied, even in a non-linear current-voltage (I-V) region at low I where the configuration of vortices is expected to be disordered [1]. We find that in this region, so-called a plastic flow region, the orientation of the lattice with respect to I is different when we change the scanning area. These results suggest that the flow state in the nonlinear I-V region corresponds to the flow of vortex bundles whose sizes are larger than 240 × 240 nm^2. By contrast, in the linear I-V region at high I, we observe the vortex lattice with the same orientation over a wide area of the sample. This is consistent with the results of neutron scattering [2] and mode-locking measurements [3] performed in the large I region.

[1] C. J. Olson, C. Reichhardt, and F. Nori, Phys.Rev.Lett. 81, 3757(1998)
[2] E.M. Forgan *et al.,* Physica B 326, 342-345(2003)
[3] S. Okuma, D. Shimamoto, and N. Kokubo, Phys. Rev. B 85, 064508 (2012)

Keywords: STM, vortex, amorphous film

PCP2-8

STM and vortex images for Au/*a*-Mo_xGe_{1-x} films

*Kazuki Tsuchiya[1], Takashi Ogawa[1], Koshiro Kato[1], Shinichi Kaneko[1], Koichiro Ienaga[1], Hideaki Sakata[2], Satoshi Okuma[1]

Department of Physics, Tokyo Institute of Technology,Japan[1]
Department of Physics, Tokyo University of Science,Japan[2]

Investigation of vortex dynamics is important for the practical applications of superconductivity. It is also of fundamental importance, because a vortex system is a suitable system to study novel nonequilibrium phenomena and phase transitions. We have studied the dynamics of vortices driven by applied currents using various transport measurements, where we probe the mean velocity of vortices moving over the whole sample. However, it is not possible to observe a real space vortex configuration from the transport measurements. In this work, we construct a scanning tunneling microscope / spectroscopy (STM/S) system in which we can perform transport and STM/STS measurements for the same sample.

We have prepared amorphous Mo_xGe_{1-x} films with weak pinning by RF sputtering. After the deposition, the film must be exposed to the air to attach electrical wires to it for transport measurements. This results in slight surface oxidation and surface adsorption, and usually it becomes difficult to observe the superconducting gap. It has been reported previously [1] that the deposition of a thin Au film on the surface of the Mo_xGe_{1-x} film can prevent surface degradation and this enables us to observe the superconducting gap through penetration of the wave function on the Au surface. Here, we prepared amorphous Mo_xGe_{1-x} films with thickness of 280nm covered by a 4 nm thick gold film. Our STM images show the grain-like surface morphology with about 10 nm diameter and a few nm height. From STS measurements, we succeeded in observing vortices at 2.2 K and 1.0 T. It is found that the shape of the individual vortex is not uniform but correlated with the shape of grains. However, we are able to determine the position of the vortex center with an accuracy of one grain size.

[1] N. Kokubo, T. Nishizaki, B. Shinozaki, P.H. Kes, Physica C **470**, 43 (2010)

Keywords: STM

PCP3-1

Domain Structures and Spontaneous Abrikosov Vortex-Antivortex Generation in the Ferromagnetic Superconductor $EuFe_2(As_{1-x}P_x)_2$ with x ~ 0.2

*Ivan Veshchunov[1,2], Lev Vinnikov[3], Vasiliy Stolyarov[2,3], Nan Zhou[4], Zhixiang Shi[4], Xiaofeng Xu[5], Sunseng Pyon[1], Wenhe Jiao[6], Guang-Han Cao[6], Dimitri Roditchev[7], Alexander Buzdin[8], Tsuyoshi Tamegai[1]

Department of Applied Physics, The University of Tokyo, 7-3-1 Hongo, Bunkyo-ku, Tokyo 113-8656, Japan[1]
Moscow Institute of Physics and Technology (State University), Dolgoprudny, Moscow 141700, Russia[2]
Institute of Solid State Physics, Russian Academy of Sciences, Chernogolovka, Moscow 142432, Russia[3]
School of Physics and Key Laboratory of MEMS of the Ministry of Education, Southeast University, Nanjing 211189, China[4]
Department of Physics, Changshu Institute of Technology, Changshu 215500, China[5]
Department of Physics, Zhejiang University, Hangzhou 310027, China[6]
Laboratoire de Physique et d'Etude des Materiaux LPEM-UMR8213 ESPCI-Paris, PSL Research University, INSP - Sorbonne Universite, 10 rue Vauquelin, 75005 Paris, France[7]
University Bordeaux, LOMA, F-33405 Talence, France[8]

Magnetic flux structures on the surface of $EuFe_2(As_{1-x}P_x)_2$ single crystals with nearly optimal phosphorus doping levels x = 0.20, and x = 0.21 are studied by low-temperature Magnetic Force Microscopy and decoration with ferromagnetic nanoparticles. The studies are performed in a broad temperature range. It is shown that the single crystal with x = 0.21 in the temperature range between the critical temperatures T_{SC} ~ 24 K and T_{FM} ~ 18 K of the superconducting and ferromagnetic phase transitions, respectively has the vortex structure of a frozen magnetic flux, typical for type-II superconductors. The magnetic domain structure is observed in the superconducting state below T_{FM}. The nature of this structure is discussed. Spontaneous vortex-antivortex (V-AV) pairs are imaged in the vicinity of T_{FM} upon heating in zero external magnetic field [1-2].

[1] I. S. Veshchunov, L. Ya. Vinnikov, V. S. Stolyarov, N. Zhou, Z. X. Shi, X. F. Xu, S. Yu. Grebenchuk, D. S. Baranov, I. A. Golovchanskiy, S. Pyon, Yue Sun, Wenhe Jiao, Guanghan Cao, T. Tamegai, A. A. Golubov, JETP Lett. **105**, 98 (2017). (Preprints at arXiv: 1703.02235 and 1709.09802v1).
[2] V.S. Stolyarov, I.S. Veshchunov, S.Yu. Grebenchuk et al., Science Adv. **4**, 1 (2018).

Keywords: Magnetic Force Microscopy, Spontaneous Vortex Phase, Domain Structure, Iron-Based Ferromagnetic Superconductor

PCP3-2

Effects of Lattice Defects on the Superconducting Properties of Ba122 Polycrystalline Materials Prepared by High Energy Ball-Milling

*Shinnosuke Tokuta[1], Akiyasu Yamamoto[1,2]

Department of Applied Physics, Tokyo University of Agriculture and Technology, Tokyo, Japan[1]
Materials Research Center for Element Strategy, Tokyo Institute of Technology, Kanagawa, Japan[2]

The iron-based superconductors with high critical temperature (T_c < 60 K) and upper critical field (H_{c2} < 200 T) are promising candidates for high field magnet applications [1, 2]. In this study, we introduced lattice defects into grains of $Ba(Fe_{0.92}Co_{0.08})_2As_2$ [Ba122] polycrystalline materials by high energy ball-milling and evaluated their effects on superconducting properties (T_c, H_{c2}, and J_c). All the powder processing was performed under high purity Ar glove box. Elemental metals (Ba, Fe, Co and As) were milled with planetary ball milling apparatus. The milling conditions were systematically changed and quantified using ball-milling energy (E_{BM}) [3]. The milled powder was pelletized by uniaxial pressing, vacuum sealed into a quartz tube, and finally heat treated at 600ºC for 48 h. The phases and microstructure were evaluated by XRD, SEM, and EDS before and after heating. The inter- and intra-granular superconducting properties were evaluated by PPMS and SQUID VSM. The XRD and electrical resistivity measurements suggested that lattice defects were introduced into Ba122 grains as intended. Broadening of FWHM of XRD peaks, decreasing of residual resistivity ratio, shrinkage of *a*-axis, and expanding of *c*-axis were observed with increasing E_{BM}. As a result, T_c was slightly suppressed (-5.5%), however, the slope of $H_{c2}(T)$ was remarkably increased (+60%). In addition, the maximum J_c was obtained for the sample of E_{BM} = 80 MJ/kg and reached 1.7×10^4 A/cm² under self-field at 5 K, which is the highest of Co doped Ba122 polycrystalline materials synthesized under ambient pressure. Since remarkable improvement of the slope of $H_{c2}(T)$ has not been observed in irradiated Ba122 samples so far [4], it is considered that the defects introduced by high energy ball-milling are different from those introduced by irradiations.

[1] Y. Kamihara *et al.*, *J. Am. Chem. Soc.* **130(11)**, 3296-3297 (2008).
[2] H. Hosono *et al.*, *Mater. Today* **21**, 278-302 (2018).
[3] W. Häßler *et al.*, *Supercond. Sci. Technol.* **26**, 025005 (2013).
[4] M. Eisterer, *Supercond. Sci. Technol.* **31**, 013001 (2018).

Keywords: iron-based superconductor, polycrystalline bulk materials, high energy ball-milling

PCP3-3

Unusual Evolution of Nematic fluctuations in $Ba_{1-x}Rb_xFe_2As_2$

*Masaya Tsujii[1], Kousuke Ishida[1], Suguru Hosoi[2], Yuta Mizukami[1], Shigeyuki Ishida[3], Akira Iyo[3], Hiroshi Eisaki[3], Kai Grube[4], Thomas Wolf[4], Hilbert. v. Löhneysen[4], Rafael. M. Fernandes[5], Takasada Shibauchi[1]

University of Tokyo, Japan[1]
Osaka University, Japan[2]
National Institute of Advanced Industrial Science and Technology, Japan[3]
Karlsruhe Institute of Techonology, Germany[4]
University of Minnesota, Unites States of America[5]

Electronic nematicity, a correlated state that spontaneously breaks rotational symmetry, is a ubiquitous feature in unconventional superconductors. As for underdoped $BaFe_2As_2$-based superconductors, it is well established that tetragonal-to-orthorhombic structural transition is driven by electronic nematic instability. Several experiments have provided evidence for the nematic fluctuations along Fe-Fe bond direction in the tetragonal phase [1,2].

On the other hand, in the heavily hole-doped $BaFe_2As_2$, the effective mass of the carriers has been found to divergently increase with doping [3]. Theoretically, it has been proposed that AFe_2As_2 (A = K, Rb, Cs) with $3d^{5.5}$ configuration can be seen as the proximity to Mott insulator [4]. In the context of similarity to underdoped high-T_c cuprates, the electronic nematicity could emerge in AFe_2As_2 due to the quantum melting of the localized Mott insulating state [5]. In fact, it has been suggested that electronic nematicity reemerge in $RbFe_2As_2$ and $CsFe_2As_2$, whose director is rotated 45 degree from that of $BaFe_2As_2$ [6,7].

To investigate the crossover region of the two different nematic channels, we carried out the systematic elastoresistance measurements in $Ba_{1-x}Rb_xFe_2As_2$. Remarkably, for intermediate doping, we found that the nematic fluctuations of the two symmetry-irreducible nematic channels display comparable Curie-Weiss behaviors. Such nematic fluctuations are different from the Ising-type nematicity found in other iron-based superconductors, and implies the emergence of novel XY-type nematicity.

[1] J. H. Chu *et al.*, Science **337**, 710 (2012).
[2] A. E. Böhmer *et al.*, Phys. Rev. Lett. **112**, 047001 (2014).
[3] F. Hardy *et al.*, Phys. Rev. B **94**, 205113 (2016).
[4] L. de' Medici *et al.*, Phys. Rev. Lett. **112**, 177001 (2014).
[5] S. A. Kivelson *et al.*, Nature **393**, 550 (1998).
[6] J. Li et al., arXiv:1611.04694 (2016).
[7] X. Liu et al., arXiv:1803.07304 (2018).

Keywords: iron-based superconductor, hole-doped iron pnictide, nematicity, XY nematics

PCP3-4

Global Phase Diagram of Different Superconducting States in 1111-type Iron Pnictides *R*Fe(As,P/Sb)(O,F/H) Systems (*R*=La and Nd)

*T. Kawashima[1], H. Tsuji[1], M. Uekubo[1], M. Nakajima[1], S. Miyasaka[1], S. Tajima[1]

Department of Physics, Osaka University, Osaka 560-0043, Japan[1]

In LaFeAsO system, the electron doping level and the local crystal structure can be controlled by the F/H substitution for O and P for As. As a result, Fermi surface (FS) topology has been changed by these substitution effects, and three different superconducting (SC) phases appears in $LaFeAs_{1-x}P_xO_{1-y}(F/H)_y$ system. [1] In these SC states, the FS nesting in LaFeAsO-/ LaFePO-type FS, and the next nearest neighbor (NNN) magnetic interaction in the *xy* direction in real space play an important role for stabilizing superconductivity.

In the present work, we have investigated the transport properties and structural parameters of $NdFeAs_{1-x}P_xO_{1-y}(F/H)_y$ and $LaFeAs_{1-x}Sb_xO_{1-y}(F/H)_y$ (y=0~0.3) to clarify the correlation between the stability of superconductivity and the change of the FS accompanied by the P/Sb and F/H substitutions. In the Nd system with P substitution, the result of structural analysis revealed that the pnictogen height from the Fe plane h_{Pn} is larger than that in the La system. The Sb substitution in the La system also increases h_{Pn}. Resultantly, the nesting has been improved by the enlarging the *xy* FS near *R*FeAsO in the phase diagram, and the NNN interaction is also enhanced in heavy H doping region. These effects has stabilized the SC state and merges these SC phases near RFeAsO and in the highly H doping region in the phase diagram. The phase diagram for the present systems can be explained by the scenario for FS nesting and NNN interaction. [1]

[1] S. Miyasaka *et al.*, Phys. Rev. B 95, 214515 (2017).

Keywords: iron pnictide superconductor, P/Sb and F/H substitutions, transport properties, structural analysis

PCP3-5

Effect of Cr substitution for V in $Sr_2VFeAsO_3$

*Taihei Wakimura[1], Hiroaki Yokota[1], Masamichi Nakajima[1], Shigeki Miyasaka[1], Setsuko Tajima[1]

Department of Physics, Osaka University[1]

$Sr_2VFeAsO_3$, a member of iron-based superconductors, is characterized by a perovskite-type thick blocking layer and a relatively high superconducting temperature of T_c ~ 37 K without any chemical substitution [1]. In addition to superconductivity, this compound shows another phase transition at T_0 ~ 150 K, which is considered to occur at Fe sites with no magnetic ordering [2][3]. The underlying electronic state is still unclear and is an issue to be addressed.

In this study, we synthesized polycrystalline $Sr_2V_{1-x}Cr_xFeAsO_3$ and investigated the effect of Cr substitution. Cr is substituted in the blocking layer, and the Fe layer is kept clean. From X-ray absorption spectroscopy, we revealed that the valence of introduced Cr atoms is 4+, corresponding to electron doping. As Cr content is increased, T_c systematically decreases but survives at least up to $x = 0.3$. This indicates that the parent compound is already optimally doped or overdoped and that superconductivity is not very sensitive to the electron filling. On the other hand, the transition at T_0 disappeared quickly with Cr substitution. This is in contrast with the case for Sc substitution, in which despite a larger change in the local crystal structure, T_0 is discernible for a larger Sc content. Thus, the disappearance of this phase transition can be dominantly attributed to electron doping.

Keywords: Iron-based superconductor, chemical substitution

PCP3-6

Structural and magnetic transitions in 1111-type iron arsenide CaFeAsH

*Yoshinori Muraba[1], Soshi Iimura[2], Satoru Matsuishi[1], Hidenori Hiramatsu[1,2], Takashi Honda[3,4], Kazutaka Ikeda[3,4], Toshiya Otomo[3,4], Hideo Hosono[3,4]

Materials Research Center for Element Strategy, Tokyo Institute of Technology[1]
Laboratory for Materials and Structures , Tokyo Institute of Technology[2]
Institute of Materials Structure Science, High Energy Accelerator Research Organization (KEK)[3]
J-PARC Center, KEK[4]

The current interest in iron-based superconductors lies in understanding not only the mechanism of superconductivity, but also the relationship between structural and magnetic transitions (ST and MT, respectively) of the non-doped and non-superconducting (so-called parent) compounds.[1-2] From the view point of temperature-induced phase transitions, there exist two types of parent compounds, respectively exhibiting first order transitions such as 122- and 11-type compounds and second-order transitions such as 1111-type. Here we investigated the structural and magnetic transitions of 1111-type CaFeAsH by specific heat (Cp), x-ray diffraction (XRD), neutron powder diffraction (NPD), and electrical resistivity (r) measurements. The Cp measurement revealed that the second order phase transition accompanying an apparent single peak was observed at 96 K. However, a clear ST from tetragonal to orthorhombic and MT from paramagnetic to antiferromagnetic transition were observed, and the structural and Néel temperatures (T_s and T_N) are respectively determined to be 95(2) and 96K by combining XRD, NPD and r-T measurements. The small temperature difference, $T_s - T_N$, was attributed to the strong magnetic coupling along inter-layer direction derived from the shortest lattice constant c of CaFeAsH among the known 1111-type iron arsenides. Given a fact that a first-order transition takes place in 11- and 122-type compounds with a shorter inter-layer distance, we conclude that the nature of ST and MT for CaFeAsH is positioned in between second-order for 1111-type and first-order for other 11- and 122-type compounds.

1 R.M. Fernandes, *et al.*, Nat. Phys. 10, 97 (2014).
2 R.M. Fernandes, *et al.*, Phys. Rev. B **85**, 024534 (2012).

PCP3-7

Single Crystal Growth, Phase Diagram and Vortex Properties of 4*d* Transition Metal Pd Doped 112-Type Iron Pnictide Superconductors

Xiangzhuo Xing[1], Zhanfeng Li[1], Chunqiang Xu[1], Ivan Veshchunov[2], Tsuyoshi Tamegai[2], *Zhixiang Shi[1]

School of Physics, Southeast University, Nanjing 211189, People's Republic of China[1]
Department of Applied Physics, The University of Tokyo, 7-3-1 Hongo, Bunkyo-ku, Tokyo 113-8656, Japan[2]

4*d* transition metal Pd doped single crystals of $Ca_{0.755}La_{0.245}Fe_{1-x}Pd_xAs_2$ ($0 \leq x \leq 0.08$), recently discovered 112-type iron pnictide superconductors, were grown using the self-flux method and characterized by x-ray diffraction, resistivity, magnetic susceptibility and Hall effect measurements, mapping out the T-x phase diagram. Bulk superconductivity up to T_c~28.5 K was reemerged by only a small amount of Pd doping (x~0.013) in over-doped non-superconducting $Ca_{0.755}La_{0.245}FeAs_2$. The magnetization measurement reveals a fish-tail effect and relatively high critical current density J_c exceeding 10^5 A/cm^2 at low temperatures. The magneto-optical images reveal a homogenous current flow within the crystal. Moreover, according to the analyses of the vortex pinning force density vs magnetic field, we found that the normal point defects are the dominant pinning sources, which probably originate from the variations of Pd dopant. Lastly, the vortex diagram of $Ca_{0.755}La_{0.245}Fe_{1-x}Pd_xAs_2$ (x~0.013) was also established by combination of the magnetization and magneto-transport measurement.

Keywords: 112-Type Iron Pnictide Superconductors, Phase diagram, Vortex pinning

PCP3-8

Effects of Swift-Particle Irradiations on Critical Current Density in $CaKFe_4As_4$

*Ayumu Takahashi[1], Sunseng Pyon[1], Satoru Okayasu[2], Shigeyuki Ishida[3], Akira Iyo[3], Hiroshi Eisaki[3], Motoharu Imai[4], Hideki Abe[4], Taichi Terashima[4], Tsuyoshi Tamegai[1]

Dept. of Applied Physics, The Univ. of Tokyo, 7-3-1 Hongo, Bunkyo-ku, Tokyo 113-8656, Japan[1]
Advanced Science Research Center, Japan Atomic Energy Agency, Tokai, Ibaraki 319-1195, Japan[2]
National Institute of Advanced Industrial Science and Technology, 1-1-1 Umezono, Tsukuba, Ibaraki 305-8568, Japan[3]
National Institute for Materials Science, Tsukuba, Ibaraki 305-0047, Japan[4]

Introduction of columnar defects to superconductors through particle irradiation enhances their critical current density (J_c) [1,2]. It has been demonstrated that the maximum value of J_c and the corresponding dose depend on ion species and its energy [3]. The difference in the optimum dose among ion species may originate from the different diameters and lengths of created defects.

Iron-based superconductors (IBS) have been investigated as promising materials for practical applications because of their large J_c at high magnetic fields and temperatures. In the previous studies, remarkable effects have been demonstrated in IBS by irradiating heavy-ions and protons into Co or K doped Ba-122 single crystals [2,3]. Recently, another promising IBS $CaKFe_4As_4$ (1144-type IBS) was found [4], and attracts much interest due to its high J_c in the pristine sample [5].

Here, we compare effects of 800 MeV Xe, 3 MeV proton, and 320 MeV Au irradiations on the critical temperature (T_c) and J_c of $CaKFe_4As_4$ single crystals, and compare them with irradiation effects in $Ba_{0.6}K_{0.4}Fe_2As_2$. In the case of 800 MeV Xe, B_Φ dependences of J_c in both samples are similar, as shown in Fig. 1. We also demonstrate that introduction of splayed columnar defects and coexistence of columnar and point defects enhance J_c more than the case of only parallel columnar defects.

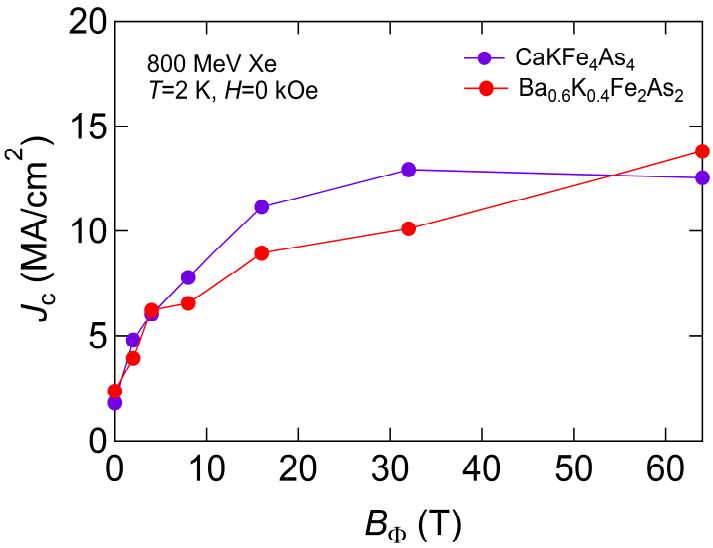

Fig. 1: B_Φ dependences of J_c of 800 MeV Xe irradiated $CaKFe_4As_4$ and $Ba_{0.6K0.4}Fe_2As_2$ at 2 K under zero field.

[1] Y. Nakajima *et al.*, Phys. Rev. B **80**, 012510 (2009).
[2] T. Tamegai *et al.*, Supercond. Sci. Technol. **25**, 084008 (2012).
[3] F. Ohtake *et al.*, Physica C **518**, 47 (2015).
[4] A. Iyo *et al.*, J. Am. Chem. Soc. **138**, 3410 (2016).
[5] T. Tamegai *et al.*, APS March meeting, H14.00013, 2018.

Keywords: CaKFe4As4, Particle irradiation, Critical current density, columnar defect

PCP3-9

Evaluation of Anisotropic Critical Current Density in $CaKFe_4As_4$

*Tsuyoshi Tamegai[1], Ayumu Takahashi[1], Sunseng Pyon[1], Ivan Veshchunov[1], Shigeyuki Ishida[2], Akira Iyo[2], Hiroshi Eisaki[2], Motoharu Imai[3], Hideki Abe[3], Taichi Terashima[3], Shuuichi Ooi[3], Ataru Ichinose[4]

The University of Tokyo, Japan[1]
National Institute of Advanced Industrial Science and Technology, Japan[2]
National Institute for Materials Science, Japan[3]
Central Research Institute of Electric Power Industry, Japan[4]

$CaKFe_4As_4$ is a member of newly found 1144-type iron-based superconductor (IBSs) with T_c~36 K [1]. 1144-type IBSs has a unique crystal structure similar to $BaFe_2As_2$ with ordered alternate occupation of Ba site by Ca and K. Hence, physical properties of $CaKFe_4As_4$ including critical current density (J_c) behavior is expected to be similar to related compounds $(Ba,K)Fe_2As_2$ and $(Ca,Na)Fe_2As_2$. We have grown high-quality single crystals of $CaKFe_4As_4$ using FeAs flux method, and made extensive studies on its J_c behavior including anisotropic properties. Figure 1(a) shows J_c as a function of magnetic field for $H//c$-axis. J_c at 2 K under self-field is ~1.7 MA/cm^2, which is slightly smaller than the value for optimally doped $(Ba,K)Fe_2As_2$ [2]. For $H//ab$-plane, there are two components of J_c one parallel to the ab-plane (J_{c2}) and another parallel to the c-axis (J_{c3}). In order to evaluate J_{c2} and J_{c3} properly, we need to make two independent M-H hysteresis measurements for $H//ab$-plane. To our surprise, such a decomposition of J_c into two components for fields parallel to the superconducting plane have not been undertaken by now. We clarify that there are three cases for rectangular samples depending on the in-plane aspect ratio and the anisotropy of J_{c2} and J_{c3}. Figure 1(b) shows an example of J_{c2} - H for $H//ab$-plane. It is remarkable that J_{c2} is weakly temperature dependent and is much larger than the in-plane J_c for $H//c$-axis. In addition, J_{c2} shows maxima at around H = 10 kOe. Extensive TEM observations on $CaKFe_4As_4$ clarified the presence of novel planar defects nearly parallel to the ab-plane. We discuss the origin of very large J_{c2} and its peak at H ~ 10 kOe.

[1] A. Iyo *et al.*, J. Am. Chem. Soc. **138**, 3410 (2016).
[2] T. Taen *et al.*, Supercond. Sci. Technol. **28**, 085003 (2015).

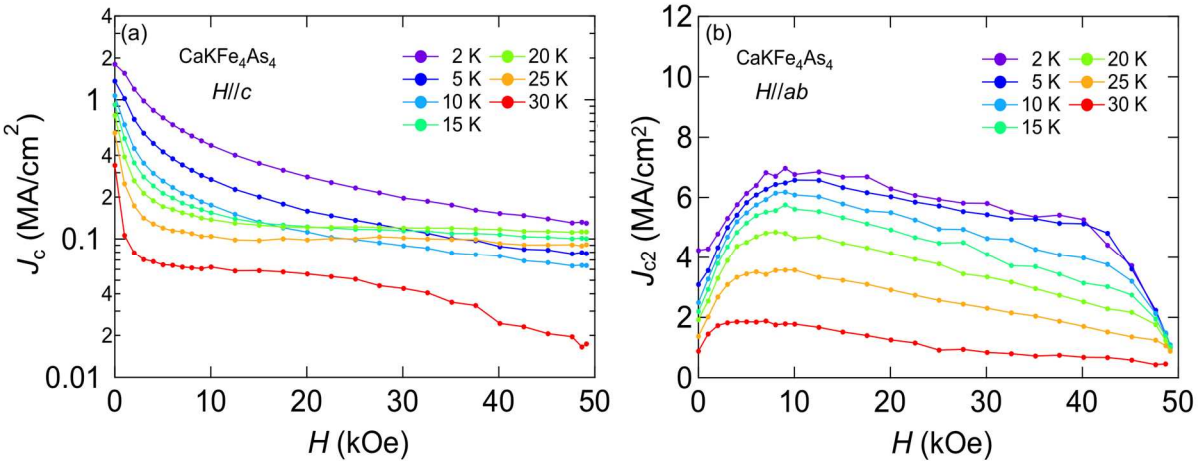

Fig. 1 (a) J_c as a function of magnetic field applied parallel to (a) c-axis (log scale) and (b) ab-plane (linear scale).

Keywords: CaKFe4As4, Anisotropic critical current density, Iron-based superconductor, Planar defect

PCP4-1

On The Growth of Co- and Ni-doped $BaFe_2As_2$ Thin Films on Fluoride Type Substrates

*Marco Langer[1], Sven Meyer[1], Saicharan Aswartham[2], Sabine Wurmehl[2], Jens Hänisch[1], Bernhard Holzapfel[1]

Karlsruhe Institute of Technology, Institute for Technical Physics, 76344 Eggenstein-Leopoldshafen, Germany[1]
Leibniz Institute for Solid State and Materials Research Dresden, Institute for Solid State Research, 01171 Dresden, Germany[2]

Among the different substrates commonly used for thin film deposition of iron-based superconductors, substrates with a fluoride structure have received a broad interest due to the typically enhanced transition temperature of the deposited thin films, e.g. [1-3]. The reason for the T_c enhancement is not completely understood. Here we analyze the growth conditions of Co- and Ni-doped $BaFe_2As_2$ thin films grown by pulsed laser deposition on these substrates and investigate the influence of the deposition parameters, such as temperature, growth rate, laser fluence on growth mode and defect formation. Furthermore, we discuss the influence of thermal stress during deposition and whether it is an appropriate explanation for the enhanced transition temperatures.

[1] F. Kurth et al., Applied Physics Letters 102, 142601 (2013)
[2] S. Yoon et al., Supercond. Sci. and Technol. 30, 035001 (2017)
[3] I. Tsukada et al., Applied Physics Express 4, 053101 (2011)

Keywords: Magnetic Force Microscopy, Spontaneous Vortex Phase, Domain Structure, Iron-Based Ferromagnetic Superconductor

PCP4-2

Electronic Anisotropy of NdFeAs(O,F) Epitaxial Thin Films Grown on Vicinal-Cut MgO Substrates

*Takuya Matsumoto[1], Keisuke Kondo[1], Takafumi Hatano[1], Takahiro Urata[1], Kazumasa Iida[1], Hiroshi Ikuta[1]

Department of Materials Physics, Nagoya University, Japan[1]

Since the iron-based superconductors have a layered structure, the electronic conduction is expected to be anisotropic. Measuring the resistivity anisotropy is therefore important for the basic understanding of the physical properties. However, the size of available *Ln*FeAs(O,F) (*Ln*: lanthanide elements) single crystals is still limited, which makes transport measurements very difficult. We have reported a simple method to measure both ρ^{ab} and ρ_c using NdFeAs(O,F) epitaxial thin films grown on vicinal-cut MgO substrates, where ρ_{ab} and ρ_c are the resistivity along the *ab*-plane and *c*-axis, respectively[1]. In the present study, NdFeAs(O,F) thin films were prepared with varying fluorine doping and the transport properties were investigated in detail.

NdFeAsO epitaxial thin films having a thickness of 90 nm were grown on vicinal-cut MgO (001) single crystalline substrates, followed by the deposition of NdOF, which served as fluorine reservoir to fluorinate the NdFeAsO layer. The vicinal angle was 5° measured from [001] towards the [100] direction. After confirming by X-ray diffraction that the NdFeAs(O,F) thin film is epitaxially aligned to the vicinal-cut MgO substrate, the NdOF layer was removed by Ar-ion beam etching and narrow wire structures were fabricated by photolithography and Ar-ion beam etching. (005) rocking curve measurements confirmed the same full width at half maximum values for the NdFeAs(O,F) film with and without the NdOF overlayer. Thereafter, we obtained ρ_{ab} and ρ_c by measuring the resistivity along the tilt direction of the substrate and the direction perpendicular to it. Fig. 1 shows the results of a sample whose superconducting transition temperature (T_c) was 49 K. It was found that ρ_c was larger than ρ_{ab}, and the anisotropy ratio $\gamma=\rho_c/\rho_{ab}$ was about 250 at T_c. ρ_c showed a metallic behavior similarly to other iron-based superconductors, but unlike the previous reports on *Ln*FeAsO systems [2-4].

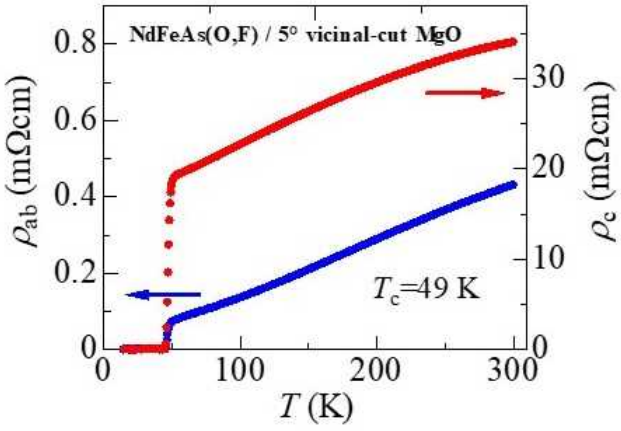

Fig.1. The temperature dependence of ρ_{ab} and ρ_c of a NdFeAs(O,F) thin film grown on a 5° vicinal-cut MgO substrate.

This work was partially supported by the JSPS Grant-in-Aid for Scientific Research (B) Grant Number 16H04646.

[1] T. Matsumoto *et al.*, 30th International Symposium on Superconductivity PCP4-3 (2017).
[2] P. J. W. Moll *et al.*, *Nat. Mater.* **9**, 628 (2010).
[3] H. Kashiwaya *et al., Appl. Phys. Lett.* **96**, 202504 (2010).
[4] S. Iimura *et al.*, *Asian Ceram. Soc.* **5**, 357 (2017).

Keywords: Iron-based superconductor, Oxypnictide, Vicinal growth, Anisotropy

PCP4-3

Transport properties of $FeSe_{1-x}S_x$ and $FeSe_{1-y}Te_y$ epitaxial thin films under magnetic fields

*Naoki Shikama[1], Tomoya Ishikawa[1], Fuyuki Nabeshima[1], Atsutaka Maeda[1]

Department of Basic Science, University of Tokyo, Japan[1]

FeSe, which has the simplest crystal structure in iron based superconductors (FeSCs), is a suitable material for understanding the superconductivity of FeSCs. It shows the structural phase transition without an antiferromagnetic (AFM) transition unlike other FeSCs. Since the structural phase transition has a possible electronic origin, it is often called the electronic nematic transition.

We previously fabricated $FeSe_{1-x}S_x$ and $FeSe_{1-y}Te_y$ films by the pulse laser deposition method (PLD) with a KrF laser [1][2][3]. Substituting S or Te for Se suppresses the structural phase transition of FeSe. We found that T_c of $FeSe_{1-x}S_x$ films monotonically decreases when the structural phase transition disappears, while that of $FeSe_{1-y}Te_y$ films jumps just after the structural phase transition disappears (Fig. 1). It indicates that the structural phase transition does not play a universal role for T_c. Intriguingly, the superconducting transition width of $FeSe_{1-y}Te_y$ films broadens under magnetic fields after the structural phase transition disappears (resistive broadening), while it is almost constant in the orthorhombic phase [4]. It is of great interest how the resistive transition of $FeSe_{1-x}S_x$ films looks like as a function of magnetic fields.

We measured the transport properties of the $FeSe_{1-x}S_x$ films under magnetic fields. Figure 2 shows the change of the superconducting transition width of an $FeSe_{0.74}S_{0.26}$ film under magnetic fields, which does not show the structural phase transition. Unlike $FeSe_{1-y}Te_y$ films, the superconducting transition width of the $FeSe_{1-x}S_x$ films hardly broadens after the structural phase transition disappears. We also measured the temperature dependence of the Hall coefficient of the $FeSe_{1-x}S_x$ films. We will discuss the meaning of the difference/similarity of these properties on superconductivity.

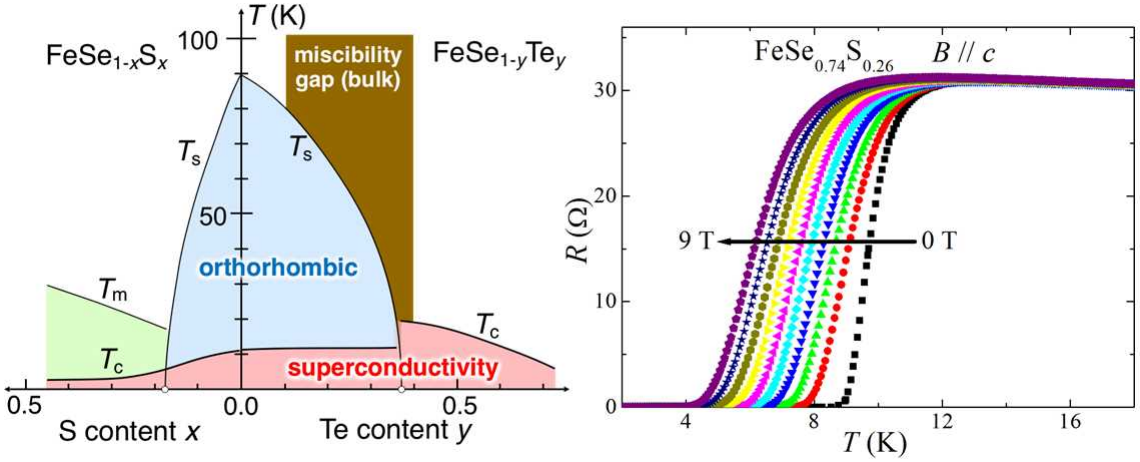

caption:

Fig. 1 Phase diagrams of $FeSe_{1-x}S_x$ films and $FeSe_{1-y}Te_y$ films. [3]

Fig. 2 Temperature dependence of the superconducting transition width of an $FeSe_{0.74}S_{0.26}$ film

[1] Y. Imai *et al.*, PNAS **112**, 1937 (2015).
[2] Y. Imai *et al.*, Sci. Rep. **7**, 46653 (2017).
[3] F. Nabeshima *et al.*, J. Phys. Soc. Jpn. **87**, 073704 (2018).
[4] Y. Sawada *et al.*, J. Phys. Soc. Jpn. **85**, 073703 (2016).

Keywords: iron chalcogenide, thin films, transport properties

PCP4-4

Electrical Transport Properties of Iron-Chalcogenide Epitaxial Thin Films Grown via Non-Equilibrium Process under Electric Field

*Kota Hanzawa[1], Masato Sasase[2], Hidenori Hiramatsu[1,2], Toshio Kamiya[1,2], Hideo Hosono[1,2]

Laboratory for Materials and Structures, Inst. of Innovative Research, Tokyo Inst. of Tech., Japan[1]
Materials Research Center for Element Strategy, Tokyo Institute of Technology, Japan[2]

Although T_c of tetragonal iron-chalcogenides (Fe*Ch*s) are relatively low (4 K for FeS [1] and 8 K for FeSe [2]), they have unique features such as dramatic enhancement of T_c via e.g., external pressures [3]. The most drastic case is one-unit-cell FeSe with T_c of ~100 K [4]. Because one of the origin for this extreme enhancement would be a charge transfer [5], one of promising ways for realizing high T_c is to dope carriers into Fe*Ch*s. In particular, we consider that insulating parents are better based on an expectation from a high-T_c cuprates' scenario. In this study, we grew Fe*Ch* (*Ch* = S and Se) epitaxial thin films and performed high-density carrier doping to them by using an electric double-layer transistor (EDLT) structure.

Since tetragonal FeS single-crystal is synthesized only by de-intercalation of K from $K_{0.8}Fe_{1.6}S_2$ [1], the tetragonal phase seems to be thermodynamically metastable. Thus, we employed one of non-equilibrium growth processes, pulsed laser deposition (PLD). By optimizing PLD conditions, tetragonal FeS was successfully stabilized on CaF_2 at 300 °C. The cross-sectional scanning-TEM image of the FeS film [Fig. 1(a)] indicated epitaxial growth of tetragonal FeS on 45°-rotated CaF_2. This is the first demonstration of single phase FeS epitaxial film, although Fe(S,Se) solid-solution films were previously grown by PLD [6]. Also in FeSe case, epitaxial films were grown by molecular beam epitaxy [7, 8].

Then, we fabricated EDLTs using the FeS and FeSe films as channel layers. The current modulation of both EDLT channels was observed at 220 K. Although the initial state in FeSe-EDLT is of insulator-like, superconductivity with the maximum T_c of 35 K was successfully induced at gate bias of +5.5 V [7]. By preparing three channels grown at different growth rates between 1.1 and 1.4 Å/min, different maximum T_c was obtained for each EDLT, and the T_c of 35 K was detected only in the channel grown at the intermediate rate (Fig. 1(b)) [8]. Finally, we concluded that this high-T_c transition is attributed to optimum doping density of ~1.5×10^{15} cm^{-2}.

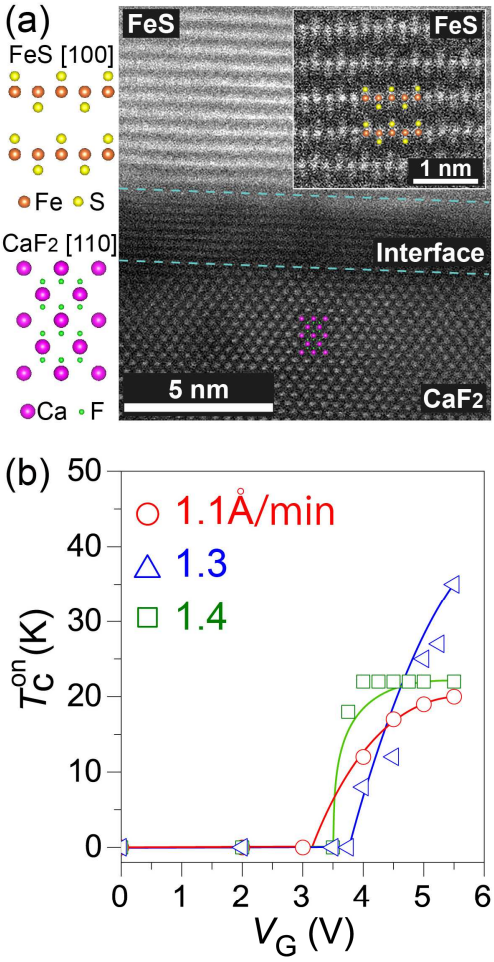

Fig. 1. (a) Cross-sectional scanning-TEM image of the FeS film viewed along with FeS [100] and CaF_2 [110]. Inset represents the high resolution image in a region of FeS. (b) Relationship between onset T_c and V_G of three FeSe-EDLTs grown at different growth rates.

[1] Borg *et al.*, *PRB* (2016). [2] Hsu *et al.*, *PNAS* (2008). [3] Mizuguchi *et al.*, *APL* (2008). [4] Ge *et al.*, *Nat. Mater.* (2015). [5] Wang *et al.*, *J. Phys.: Condens. Matter* (2017). [6] Fujiwara *et al.*, *Jpn. J. Appl. Phys.* (2017). [7] Hanzawa *et al.*, *PNAS* (2016). [8] Hanzawa *et al.*, *IEEE TAS* (2017).

Keywords: iron-based superconductors, electric double-layer transistors, MBE, PLD

PCP4-5

Complex Conductivity of a NbN Film Measured by Dielectric Resonator Technique

*Hodaka Kurokawa[1], Fuyuki Nabeshima[1], Atsutaka Maeda[1]

University of Tokyo[1]

Superconducting properties of thin films have attracted a lot of attention for a long time because of their controllable thickness, exotic phenomena originated from two-dimentionality, applications to various devices from superconducting magnets to quantum bits. A complex conductivity, σ, is a fundamental quantity which is important for explorations of the origin of superconductivity and for high-frequency applications. Several methods, including mutual inductance method and cavity resonance method, are proposed for the characterization of thin films. However, the mutual inductance method usually measures only the imaginary part of σ [1]. Cavity resonance method can measure real and imaginary part of σ. It needs a relatively large film (10 ×10 mm^2) [2,3], so that there is a huge limitation in the size of films. Depositing homogeneous film on a large substrate is sometimes a challenging task itself. Therefore, we designed a more adaptable 18 GHz dielectric resonator (Figure 1 (a)) with a few millimeter hole at its end plate, which enables the measurements of real part of σ of relatively small (< 3×3 mm^2) films. Figure 1(b) shows a temperature dependence of an inverse of the quality factor, Q^{-1}, and a center frequency, f_0, of the cavity with a NbN film. We observed sharp changes in both Q^{-1} and f_0 at the superconducting transition temperature. We will present the real part of σ and investigating how the size of the hole influences the measurements.

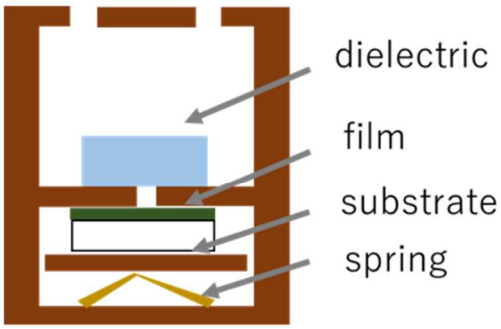

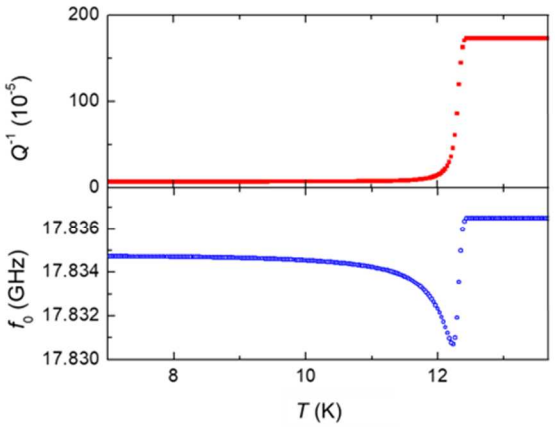

Keywords: complex conductivity, thin film, microwave

PCP4-6

Nernst effect measurements in disordered two-dimensional superconductors at very low temperatures

*Taiko Hayashi[1], Koichiro Ienaga[1], Shin-ichi Kaneko[1], Satoshi Okuma[1]

Tokyo Institute of Technology, Japan[1]

In disordered thin superconducting films the superconductor-insulator transition (SIT) takes place by increasing a magnetic field applied perpendicular to the film surface. The nature of the insulating phase close to the SIT has been debated for decades [1]. In one scenario, the amplitude of the superconducting order parameter decreases by increasing the field and completely vanishes at the SIT point. In this case, the insulating phase corresponds to a usual Fermi insulator of localized electrons. In another scenario, the amplitude of the order parameter remains nonzero even in an insulating phase close to the SIT, which corresponds to a Bose-glass insulator of localized pairs [2,3]. The Bose insulator has attracted much interest because the vortices are predicted to delocalize due to the duality between Cooper pairs and vortices. However, the presence of mobile vortices in the Bose insulator has not been demonstrated experimentally.

In this study, we perform a Nernst measurement to find the vortices that may be present in the insulating phase close to the SIT. In this measurement, the vortices are driven in the direction of a temperature gradient and a voltage is generated transverse to the vortex motion. We studied an amorphous Mo_xGe_{1-x} thin film with a thickness of 6 nm prepared by rf sputtering. We used a glass substrate with a low thermal conductivity to ensure a temperature gradient for the Nernst measurement. By using an amorphous sample whose mean free path of electrons is extremely short, the contribution of quasiparticles can be ignored and the Nernst signal serves as a sensitive probe to vortices [4]. In this presentation, we will show the phase diagram of the SIT obtained from the electric resistance and discuss the results of the Nernst measurement.

[1]A. M. Goldman and N. Marcovi´c, Physics Today **51**, 39 (1998).
[2] M. P. A. Fisher, G. Grinstein, and S. M. Girvin, Phys. Rev. Lett. **64**, 587 (1990), M. P. A. Fisher, Phys. Rev. Lett. **65**, 923 (1990).
[3] S. Okuma, S. Shinozaki, and M. Morita, Phys. Rev. B, **63**, 054523 (2001).
[4] K. Behnia and H. Aubin, Rep. Prog. Phys. **79,** 046502 (2016).

Keywords: Nernst effect, superconductor-insulator transition, superconducting thinfilm

PCP4-7

Superconductor-insulator transitions and T_c dependence of disorder in superconducting Mo alloy thin films

*Fusao Ichikawa[1], Kazumasa Makise[2], Genki Sawada[3], Yuya Mizokami[3], Sho Maeda[3], Bunju Shinozaki[4]

Department of Physics, FAST, Kumamoto University, 2-39-1 Kurokami Chuo-ku, Kumamoto 860-8555, Japan[1]
National Institute of Advanced Industrial Science and Technology (AIST), Tsukuba, Ibaraki, 305-8568, Japan[2]
Physics, GSST, Kumamoto University, 2-39-1 Kurokami Chuo-ku, Kumamoto 860-8555, Japan[3]
Department of Physics Kyushu University, 744, Motooka, Nishi-ku, Fukuoka, 819-0395, Japan[4]

To develop the low-dimensional superconducting devices optimum for its, it is necessary to provide a ultra-thin films which can be optimaized without deteriorating supercondcuting properties. For example, NbN films are widely used for superconducting devices like as superconducting nanowire single photon detectors because maintain superconducting properties even for ultra-thin films. However, the properties of NbN films are strongly dependent on the quality of crystallinity. It is necessary to find other materials whose superconducting properties are less sensitive with the quality of films. One possibility is amorphous film with relatively high T_c material.
We have studied that the superconducting properties in three type's molybdenum alloy thin films; MoN, MoRu and MoRe thin films [1-3]. All three kinds of materials show the thickness and the magnetic field driven superconductor-insulator transition (SIT). From thickness driven SIT results, the T_c depression with increasing the normal state sheet resistance were explained by the Finkel'stein formula [4]. From this analysis it is found that the critical sheet resistance R_c of MoN and MoRu thin films are about 2 kΩ, while one of MoRe is about 1.5 kΩ. These values are smaller than the quantum sheet resistance $R_Q = 6.45$ kΩ, expected from bosonic picture of SIT.
We also discuss dependence of disorder strength for Mo alloy thin films, that is the products of Fermi wave number k_F and mean free path l for MoN, MoRe and NbN thin films, k_Fl, were calculated as a function of T_c depression. The values of k_Fl for all films approach about 1 (Ioffe-Regel criterion) as T_c decreases to 0, while the values of k_Fl for thick films ($T_c \sim T_{c0}$) are different. The slopes of the T_c/T_{c0} vs k_Fl for MoN and MoRe thin films are larger than one for NbN thin films. It is possible that the difference of the sloop in the figure is related to the material and structure of thin films. In this symposium, we will also report on a one chip design made to measure other characteristics, such as vortex motion using corbino disk method and tunnel conductance.

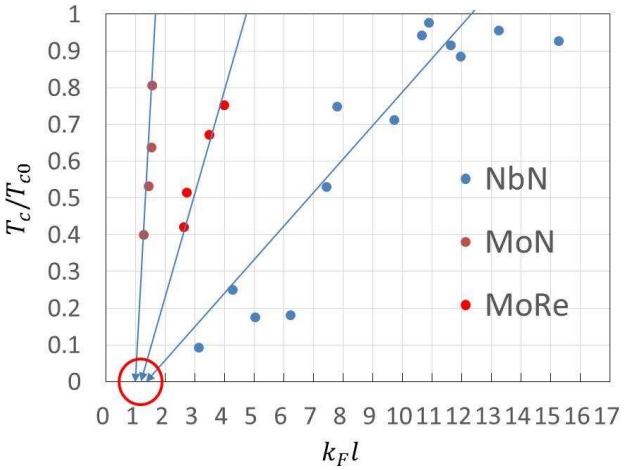

References
[1] T. Tsuneoka *et al.*, J. Phys.: Condens. Matter, **29** 015701 (2017).
[2] K. Makise *et al.*, J. Phys.: Condens. Matter, **30** 065402 (2018).
[3] K. Makise *et al.*, Mater. Res. Express., **5** 096406 (2018).
[4] A. M. Finkel'stein, JETP Lett., **45** 46 (1987).

Keywords: molybdenum alloy thin films, superconductor-insulator transition, disorder

PCP5-1

Superconductivity in Weyl Semimetal NbP: Bulk vs. Surface

M. Baenitz[1], M. Schmidt[1], V. Suess[1], C. Felser[1], *K. Lueders[1,2]

Max-Planck-Institut für Chemische Physik fester Stoffe, Nöthnitzer Str. 40, 01187 Dresden, Germany[1]
Fachbereich Physik, Freie Universität Berlin, Arnimallee 14, 14195 Berlin, Germany[2]

Transition metal monopnictides belong to the new class of semi metals where the bulk properties are determined by the presence of pairs of nodes with different chirality formed by linear dispersive states in the k-space. Beside the anomaly in the bulk magnetotransport superconductivity is frequently found in some Weyl semimetals. We found signatures of superconductivity in ac and dc magnetization of highly pure and stoichiometric NbP powder. We determined the lower and upper critical field and the Ginzburg Landau parameter. The relative small superconducting volume fraction is related to either effect of finite grain size and/or surface superconductivity. The last mentioned may originate from either off stoichiometric (Nb-rich) surface layers or a strained surface with different electronic properties. Furthermore the intrinsic normal state susceptibility is determined taking into account a paramagnetic contribution of a few ppm of magnetic impurities.

Keywords: Type-II superconductivity, Nb pnictides, Weyl semimetals

PCP5-2

Effect of non-magnetic rare earth substitution for Zr on mixed anion $Zr(P,Se)_2$ superconductors Ⅱ

*Kosuke Iwakiri[1,2], Taichiro Nishio[2], Kenji Kawashima[3], Shigeyuki Ishida[1], Kunihiko Oka[1], Hiroshi Fujihisa[1], Yoshito Gotoh[1], Yoshiyuki Yoshida[1], Akira Iyo[1], Hiraku Ogino[1], Hiroshi Eisaki[1], Hijiri Kito[1]

AIST[1]
Tokyo Univ. of Science[2]
IMRA Material R&D Co., Ltd[3]

In Zr-P-Se based superconductors(the superconducting transition temperature (T_c) ~ 6.3 K) [1] having a PbFCl type crystal structure(Space group $P4/nmm$)(Fig. (a)), we have reported various physical properties including T_c improvement by partial substitution of Zr atoms with nonmagnetic rare earth atoms(Y, La, Lu) [2,3,4].

This material has a layered crystal structure seen in copper oxide high temperature superconductors and iron based superconductors, further dependence on carrier doping amount, thus T_c improvement can be expected.

In this study, partial substitution of Zr atom with Sc atom increased the T_c to 7.55 K(Fig. (b)). T_c dependence on the substitution amount y ($0 \leqq y \leqq 1$), and change in crystal structure were investigated. In this presentation, we report the details and implications of these results.

[1] H. Kitô *et al.* : J. Phys. Soc. Jpn. 83 (2014) 074713.
[2] K,Iwakiri *et al.* : The Physical Society of Japan(Fall 2017 meeting) 23aPS-82.
[3] K.Iwakiri *et al.* : J. Phys. Conf. Ser. 1054 (2018) 012002.
[4] K.Iwakiri *et al.* : ISS2017(The 30st International Symposium on Superconductivity) PCP2-3.

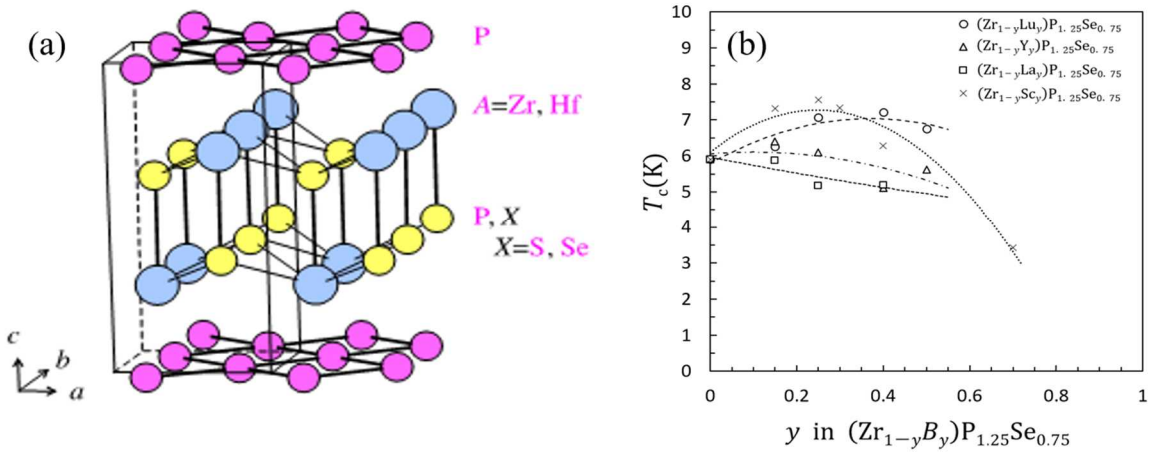

Fig.(a) The crystal structure of $AP_{2-x}X_x$(A = Zr, Hf; X = S, Se).

Fig.(b) T_c dependence on substitution amount y.

Keywords: Mixed anion superconductor, APX (A = Zr, Hf; X = S, Se), Hall effect

PCP5-3

Enhancement of the superconducting transition temperature and single crystal growth for PbFCl-type mixed anion *APX* superconductor

*Hijiri Kito[1], Kousuke Iwakiri[1,2], Taichiro Nishio[1,2], Kenji Kawashima[1,3], Shigeyuki Ishida[1], Kunihiko Oka[1], Hiroshi Fujihisa[1], Yoshito Gotoh[1], Akira Iyo[1], Hiraku Ogino[1], Hiroshi Eisaki[1], Yoshiyuki Yoshida[1]

National Institute of Advanced Industrial Science and Technology (AIST)[1]
Tokyo University of Science[2]
IMRA Material R&D Co., Ltd[3]

Physical properties for PbFCl-type mixed anion $AP_{2-x}X_x$ (*A*=Zr, Hf, *X*=S, Se) superconductor [1] have been reported. Single crystals were grain grown from nominal composition melts under a pressure and superconducting transition temperature (T_c) is 6.31 K for $ZrP_{1.25}Se_{0.75}$ single crystal [2]. Using the polycrystalline sample, the partial substitution of non-magnetic rare earth ions for *A* (*A*=Zr) site were the nominal composition $(Zr_{0.60}Lu_{0.40})P_{1.25}Se_{0.75}$ also successful and T_c was reached at 7.2 K [3]. In addition, the optimization of P and Se ions for *X* site in the nominal composition $(Zr_{0.60}Lu_{0.40})P_{2-x}Se_x$ were also successful and T_c was reached at 7.8 K for $(Zr_{0.60}Lu_{0.40})PSe$ [4]. By the partial substitution Sc atom for *A* (*A*=Zr) site, $(Zr_{0.50}Sc_{0.50})PSe$ single crystals was obtained and T_c was reached at 8.36 K. In this presentation, we discuss the physical properties for these obtained crystals.

[1] H. Kitô *et al.* J. Phys. Soc. Jpn. 83 (2014) 074713. [2] H. Kitô *et al.* J. Phys. Conf. Ser. 1054 (2018) 012003. [3] K. Iwakiri *et al.*, J. Phys. Conf. Ser. 1054 (2018) 012002. [4] H. Kitô *et al.*, private communication.

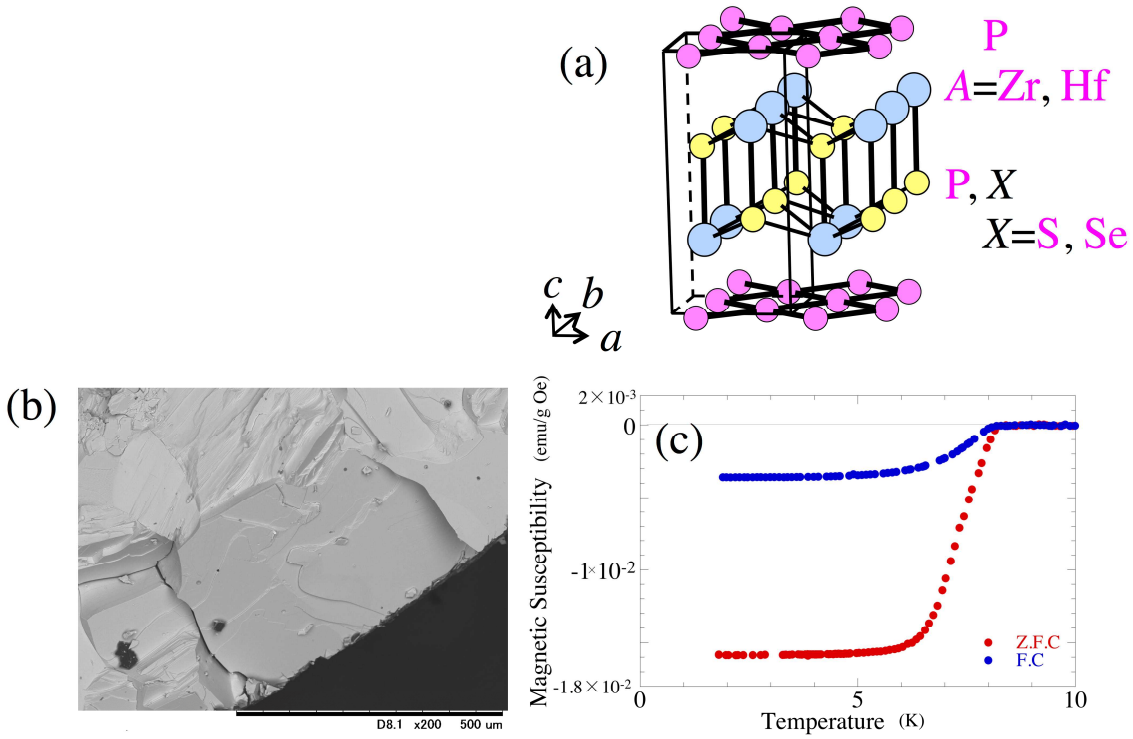

Fig.(a) The crystal structure for PbFCl-type $AP_{2-x}X_x$ (*A*=Zr, Hf; *X*=S, Se).
Fig.(b) SEM image of the obtained typical $(Zr_{0.5}Sc_{0.5})P_{2-x}X_x$ (*X*=Se) crystal.
Fig.(c) The temperature dependence of the magnetic susceptibility under H=20 Oe for the obtained $(Zr_{0.5}Sc_{0.5})P_{2-x}X_x$ (*X*=Se) crystal.

Keywords: Single crystal Growth, Mixed anion superconductor, AP2-xXx (A=Zr, Hf; X=S, Se)

PCP5-4

Synthesis of a non-centrosymmetric superconductor Mg_2Rh_3P

*Akira Iyo[1], Hiroshi Fujihisa[1], Yoshito Gotoh[1], Shigeyuki Ishida[1], Yoshiyuki Yoshida[1], Hiroshi Eisaki[1], Kenji Kawashima[1,2]

National Institute of Advanced Industrial Science and Technology (AIST)[1]
IMRA Material R&D Co., Ltd.[2]

Non-centrosymmetric superconductors recently attract much attention due to their potential to realize unconventional superconductivity [1]. We have succeeded in crystallizing a new Mg_2Rh_3P compound [2] which is isostructural (Mo_3Al_2C-type, $P4_132$) with Li_2M_3B (M= Pd, Pt) superconductors [3]. A polycrystalline Mg_2Rh_3P sample was synthesized by exposing a pellet mixed with Rh and P to Mg vapor in a sealed quartz tube as follows. Rh and P powders were mixed with a composition of Rh_3P with 5 at.% excess P. The mixed powder was pressed into a pellet and sealed in the quartz tube with Mg chips. The sample was heated at 925°C for 12 h. We found that superconductivity of Mg_2Rh_3P can be controlled by the amount of Mg chips. Mg_2Rh_3P did not show superconductivity when the amount of Mg chips was too large (e.g. Rh_3P+10Mg). On the other hand, Mg_2Rh_3P exhibited superconductivity at ~ 3.6 K when the amount of Mg chips was optimized (e.g. Rh_3P+5Mg). Composition analysis indicated that superconducting Mg_2Rh_3P had about 5 at. % Mg deficiency.

[1] M. Smidman *et al.*, Rep. Prog. Phys. **80**(2017) 036501.
[2] A. Iyo *et al.*, in preparation.
[3] K. Togano *et al.*, PRL **93**(2004) 247004.

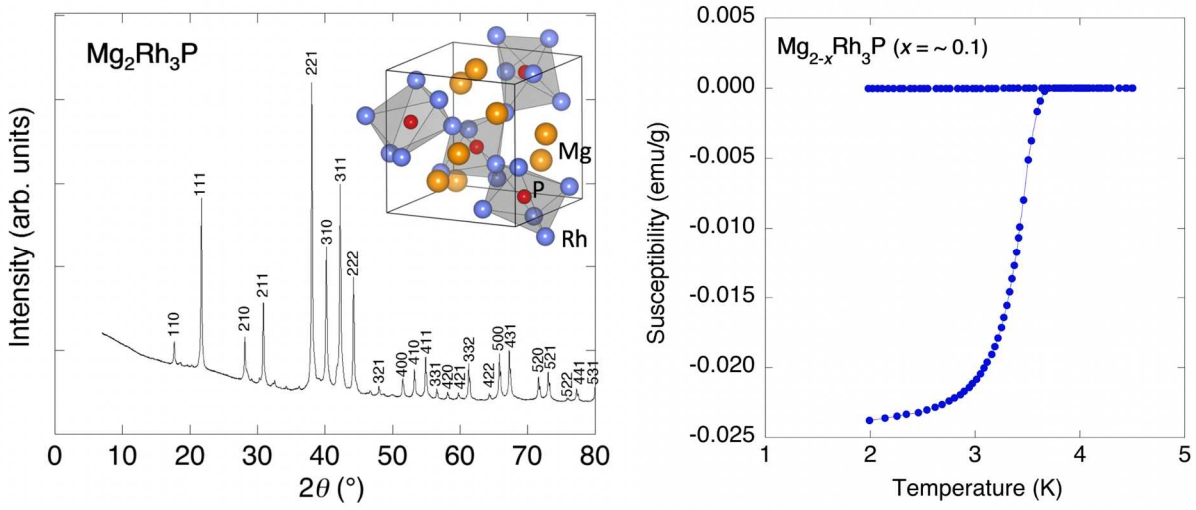

Figure 1 (a) Crystal structure and X-ray diffraction pattern, and (b) temperature dependent susceptibility for of Mg_2Rh_3P.

Keywords: New superconductor, non-centrosymmetric structure, Mo3Al2C-type structure, Mg2Rh3P

PCP5-5

Topochemical Fluorination of Layered Iridium Oxide and Its Physical Properties

*Kenta Kuramochi[1,2], Tomohito Shimano[1,2], Taichiro Nishio[1], Kazumasa Horigane[3], Hirotaka Okabe[4], Jun Akimitsu[3], Hiraku Ogino[2]

Department of Physics, Tokyo University of Science[1]
National Institute of Advanced Industrial Science and Technology[2]
Research Institute for Interdisciplinary Science, Okayama University[3]
Institute of Materials Structure Science/J-PARC Center, KEK[4]

Layered Iridate Sr_2IrO_4 has attracted much attention due to its various physical properties such as J_{eff} = 1/2 Mott insulator induced by strong spin-orbit interaction [1]. Moreover, Watanabe *et al.* theoretically suggested that the high-T_c superconducting phase emerge in highly electron-doped Sr_2IrO_4 [2]. Electron doping such as La substitution for Sr site was already attempted, [3] but emergence of superconductivity has not yet been reported. On the other hand, layered oxyfluoride $Sr_2TiO_3F_2$ was synthesized by topochemical fluorination of Sr_2TiO_4 which has a similar crystal structure [4]. This compound has TiO_2 plane with more anisotropic structure by insertion of fluorine layer. Thus, we attempted the search for analogous compounds and carrier doping by topochemical fluorination for Sr_2IrO_4.

Precursor Sr_2IrO_4 was synthesized by a conventional solid state reaction. Thereafter, it was mixed with various fluorinating argents such as ZnF_2, CuF_2 or PVDF (Sr_2IrO_4 : fluorinating agents = 1 : 1), and the mixture was heated at 250-550 °C for 12 hours in air. Phase identification was performed by powder X-ray diffraction method. Magnetic susceptibility and resistivity were measured using a SQUID magnetometer and a four-probe method.

The figure shows powder XRD pattern of the compounds and their crystal structure. New layered oxyfluoride $Sr_2IrO_3F_2$ was successfully synthesized by topochemical fluorination with ZnF_2, CuF_2 or PVDF. Consequently, *c*-axis length was largely enhanced from approximately 12 to 16 Å because fluorine layer was inserted in the rock salt layer. Interestingly, *c*-axis length of $Sr_2IrO_3F_2$ was slightly different depending on kind of fluorinating argent as well as condition of the fluorination. It indicates there are difference of fluorine content or oxygen vacancy in the compounds. The magnetization measurements showed that canted antiferromagnetism of Sr_2IrO_4 disappeared and the absolute value of magnetic susceptibility drastically decreased. Meanwhile, the electronic transport properties of $Sr_2IrO_3F_2$ exhibited semiconducter behavior like the parent compound Sr_2IrO_4.

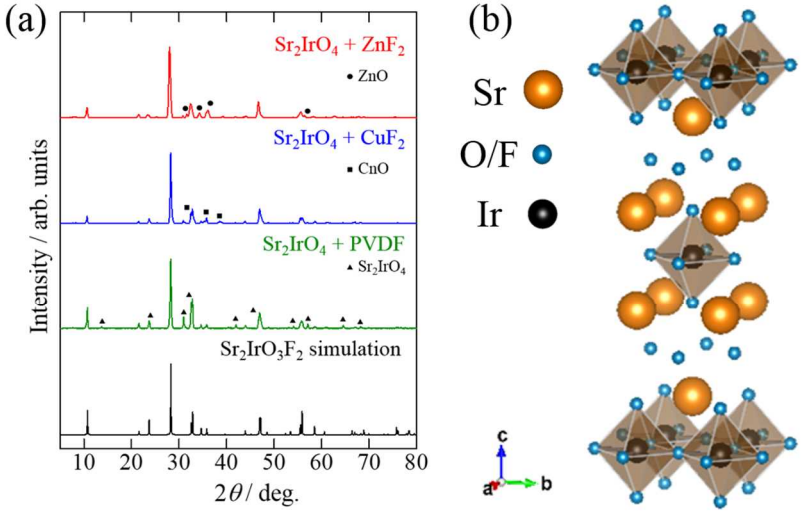

Fig. (a) Powder XRD pattern of $Sr_2IrO_3F_2$. (b) Crystal structure of $Sr_2IrO_3F_2$.

[1] B. J. Kim *et al.*, Science **323**, (2009), 1329.
[2] H.Watanabe *et al.*, *PRL.* **110**, (2013), 027002.
[3] K. Horigane, *et al.*, *PRB.* **97**, (2018), 064425.
[4] P. R. Slater *et al.*, J. Matter. Chem. **12**, (2002), 291.

Keywords: Layered perovskite, Sr2IrO4, Fluorination, Oxyfluoride

PCP5-6

STM and STS study on Se doped 1*T*-TaS_2

*Daichi Fujii[1], Yuita Fujisawa[2], Kenta Akiyama[1], Takahiro Iwasaki[1], Satoshi Demura[3], HIdeaki Sakata[1]

Department of Physics, Tokyo University of Science[1]
Okinawa Institution of Science and Technology[2]
College of Science and Technology, Nihon University[3]

The layered transition metal dichalcogenides (TMDs) show various orderings such as charge density wave (CDW) and superconductivity. 1*T*-TaS_2, one of TMDs, exhibits both commensurate CDW (CCDW) state in which 13 Ta atoms form a cluster called David-star, and Mott insulating state at the same time below 180 K [1]. It has been recently reported that substitution of Se for S melts the CCDW and Mott states and induces superconductivity [2]. Although the macroscopic electronic properties of Se doped 1*T*-TaS_2 have been measured, the microscopic effect of Se on CDW and the electronic states have not been clarified yet. In this study, we conducted STM/STS study in 1*T*-$TaS_{2-x}Se_x$ (x = 0.0. 0.3, 0.5, 1.0, 1.5) single crystal at 4.2 K.
We observed novel domain structure in the sample with x = 0.5, 1.0 and 1.5: the CCDW region is separated by domain walls, which are composed of double rows of distorted David-stars. This structure resembles metallic mosaic observed in 1*T*-TaS_2 and the domain structure observed in Fe doped 1*T*-TaS_2 [3, 4]. In addition to the metallic domain, we also found Mott insulating domain in the samples with x = 1.0 and 1.5, which show superconductivity.
In the presentation, we will discuss the origin of the domain structure and the appearance of metallic and insulating domains.

[1] J. A. Wilson *et.al,* Adv. Phys. **24**, 117 (1975)
[2] Y. Liu *et. al*, Appl. Phys. Lett. **102**, 192602 (2013)
[3] L. Ma *et. al,* Nat. Commun. **7**, 10956 (2016)
[4] Y. Fujisawa *et.al,* J. Phys. Soc. Jpn. **86**, 113703 (2017)

Keywords: TaS2, STM, CDW

PCP5-7

Microscopic Study of Domain Structure in Charge Density Wave States in 2*H*-$TaS_{2-x}Se_x$

*Shun Ohta[1], Yuita Fujisawa[2], Satoshi Demura[3], Hideaki Sakata[1]

Department of physics, Tokyo University of Science[1]
Okinawa Institution of Science and Technology[2]
College of Science and Technology, Nihon University[3]

In some transition metal dichalcogenides (TMDC), it has been reported that elemental substitution suppresses charge density wave (CDW) order and enhances superconductivity. For example, in 1*T*-TaS_2, superconductivity is enhanced by substitution of Ta for small amount of Fe about a few percent [1]. In such a sample, appearence of peculiar domain structure was reported [2]. On the other hand, in 2*H*-$TaS_{2-x}Se_x$, superconductivity is enhanced in wide range of Se substitution [3]: 2*H*-TaS_2 and 2*H*-$TaSe_2$ undergo phase transition to a commensurate CDW state at 78 K and 90 K, and has the transiton to superconductng state at 0.8 K and 0.14 K, respectively. When Se is substituted by S, CDW transition is suppressed between $0.35 < x < 1.48$, and T_C about 4 K appeares between $0.1 < x < 1.9$. To investigate this appearence of superconductivity in wide range, we examined CDW states in 2*H*-$TaS_{2-x}Se_x$ microscopically.

We performed scanning tunneling microscopy and spectroscopy (STM/STS) measurements on 2*H*-$TaS_{2-x}Se_x$ ($1.0 < x < 1.8$) at 4.2 K. We observed CDW states even in the samples whose electric resistivity anomaly due to CDW transition was completely suppressed. It was found that the domain sturucture emerges in the CDW states and the size of the domain was the smallest at $x = 1.0$.

In the presentation, we will discuss the CDW domain state and the electronic state on the 2*H*-$TaS_{2-x}Se_x$ ($1.0 < x < 1.8$) from the STM images and the tunneling spectra, and compare the results to those in 1*T*-$Fe_xTa_{1-x}S_2$.

References
[1] L. J. Li *et al.*, EPL **97** 67005 (2012)
[2] Y. Fujisawa *et al.*, J. Phys. Soc. Jpn. **86**, 113703 (2017)
[3] Lijun Li *et al.*, npj Quantum Materials **2**, 11 (2017)

Keywords: 2H-TaS2-xSex ($0 < x < 2$), CDW, STM/STS

PCP5-8

Observation of microscopic electronic states in $ZrTe_{3-x}Se_x$ by STM/STS

*Kazuki Miyata[1], Ryota Ishio[1], Satoshi Demura[2], Hideaki Sakata[1]

Department of physics, Tokyo university of science, Japan[1]
College of science and technology, Nihon university, Japan[2]

$ZrTe_3$, belonging to transition metal trichalcogenide, is a low dimensional conductor, which has the stacking of trigonal prisms along the *b* axis. This material has a charge density wave (CDW) transition at about 63 K and filamentary superconducting transition below 2 K. In addition, it has been reported that the CDW state is suppressed and bulk superconductivity emerges by partial substitution of Te with Se [1]. To investigate the effect of Se substitution microscopically, we performed STM/STS measurements in $ZrTe_{3-?}Se_?$ (?=0, 0.01, 0.04).

In STM images of a parent material $ZrTe_3$, several streaks which extends along the *a* axis were observed. The streaks are considered to involve Te defects. In samples with Se, in addition to the streaks, black spots were observed. The spots are considered to be Se atoms because the numbers of the spots in each sample nearly correspond to those of Se atoms. As reported previously [2], in parent material, the CDW whose period is 14 times as long as the lattice constant was observed. The similar CDW was also observed in $ZrTe_{2.99}Se_{0.01}$. This result is consistent with the electric resistivity measurements which show the coexistence of the CDW transition and the bulk superconducting transition in this composition. In the presentation, we will discuss about the change of electronic states in each composition.

[1] X. Zhu et al., Sci. Rep. 6. 26974 (2016)
[2] R. Ishio et al., The Annual Meeting of JPSJ 2018 (Tokyo univ of science)

Keywords: transition metal trichalcogenide, charge density wave, STM/STS

PCP6-1

Influence of Microfabrication on Superconducting Properties of Exfoliated Thin Films of Layered Superconductor $NbSe_2$: Reactive Ion Etching

*Hikari Tomori[1], Naoki Hoshi[1], Dai Inoue[1], Akinobu Kanda[1]

University of Tsukuba, Japan[1]

Recently, the method of forming atomically thin films (micromechanical cleavage) developed in the graphene research have been applied to layered superconductors, and researches on exfoliated superconductors having a thickness reaching one atomic layer have been intensively carried out. In most studies so far, a cleaved film with random shape have been used as it is, but shape processing is necessary for elucidation of detailed superconducting properties and device application. Therefore, in this study, we applied reactive ion etching (RIE), which is often used for shape processing of graphene, to superconductors and investigated the influence of RIE processing on superconducting properties of cleaved superconducting thin films.

In the experiment, thin wires of layered superconductor $NbSe_2$ (thickness: several 10 nm) were formed using electron beam lithography and RIE. For the narrowest wire (width: 0.5 μm), the broadening of the superconducting transition was observed. In the current-voltage characteristics, several voltage steps were observed at currents higher than the critical current, regardless of the width of the thin wire. For most steps, the temperature dependence of the step current is consistent with the temperature dependence of the critical current of the unprocessed $NbSe_2$ film, so it is inferred that the wire is separated into several grains. On the other hand, we observed steps with temperature dependence quite different from that of the critical current. In the presentation we will discuss its origin.

Keywords: microfabrication, layered superconductor, NbSe2, transport measurement

PCP6-2

Real Space Observation of Ag-Intercalated 2*H*-$NbSe_2$ by Scanning Tunneling Microscopy

*Kenta Mogami[1], Kosuke Takahashi[1], Shun Ohta[1], Daichi Fujii[1], Satoshi Demura[2], Hideaki Sakata[1]

Department of Physics, Tokyo Univ. of Science,Japan[1]
College of Science and Technology, Nihon Univ. ,Japan[2]

Intercalation of atoms to the interlayer of transition metal dichalcogenides (TMDC) influences the physical properties, because this enhances low dimensionality by expanding the interlayer distance. In 2*H*-$NbSe_2$, which is one of typical TMDCs, the transition to the CDW state at around 33 K is suppressed, and in the vicinity of 130 K, a new $2\sqrt{3}a_0$ superstructures appears by Ag intercalation (Ag_xNbSe_2 (x = 0.33)). These transitions were observed from electric resistance and electron diffraction measurements [1] [2]. On the other hand, little has been reported on the real space observation of the superstructure and the electronic states in the intercalated Ag_xNbSe_2 (x = 0.33), except the appearance of 1T structure at room temperature [3].

In this study, we performed real space observation of the superstructure in Ag_xNbSe_2(x = 0.33) at 4.2 K using scanning tunneling microscope (STM) in order to clarify the superstructure and the electronic states. The sample surface was prepared by cleavage at 4.2K. We found the superstructure of Se atoms whose direction is shifted by 30 ° from the crystal axis.

In the presentation, we discuss the superstructure and the electronic states of Ag_xNbSe_2 (x = 0.33) from the result of STM / STS measurements.

[1]Journal of the Less-Common Metals 118 (1986) 117-122
[2]phys. stat. sol. (a) 87,157 (1985)
[3]PHYSICAL REVIEW B 54 (1996) 11706-11709

Keywords: NbSe2, STM, CDW, Intercalation

PCP6-3

Reduction of *T*c by Ag intercalation in 2*H*-$NbSe_2$

*Kosuke Takahashi[1], Kenta Mogami[1], Syun Ohta[1], Yuto Sakai[1], Daiti Fujii[1], Satoshi Demura[2], Hideaki Sakata[1]

Department of Physics,Tokyo Univ.of Science[1]
College of science and technology,Nihon Univ.[2]

Transition metal dichalcogenides (TMDC) have been paid much attention because of their low dimensionality since 70's. Peculiar phenomena such as superconductivity or charge density wave (CDW) have been reported in many TMDCs. In recent years, research on monolayer samples in which low dimensionality has been promoted to the limit has been studied. In the monolayer sample of 2*H*-$NbSe_2$, an increase in the upper critical magnetic field not seen in bulk, fluctuation in resistance due to reduction in dimension have been reported [1]. In addition, it has been reported that the CDW transition, which was around 33 K in the bulk sample, rose to around 150 K and the superconducting transition temperature, which was around 7 K, decreased to around 3 K in the monolayer sample [2].

On the other hand, it has long been known that physical properties of a base material are changed by intercalating totally different atoms from the outside between layers of TMDCs. In the sample Ag_xNbSe_2 ($x \cong 0.33$), the transition to the supermodulation order is reported at near 130 K from the electrical resistance measurements and the electron diffraction studies [3]. It is interesting that the transition temperature to the supermodulation order is close in the monolayer sample and the intercalated sample. However, change in superconducting temperature has not been reported in intercalated sample.

In this study, we have performed electrical resistivity measurements in Ag_xNbSe_2 ($x \cong 0.33$) which is prepared electrochemically. The measurement was performed in a temperature range between 3 K and 300 K, which is wider than that in the previous study. Observed temperature dependence of the resistivity showed the transition to the supermodulation order at 150 K and superconducting transition at about 3K. This result is similar to that of the monolayer sample.

In the presentation, we discuss the relation between intercalated samples and monolayer samples from the results of temperature dependence of the electrical resistance and upper critical field.

Keywords: NbSe2, Intercalation, Resistivity measurement

PCP6-4

Substitution effect in $(La,Sr)O_{0.5}F_{0.5}Bi_{1-x}Pb_xS_2$

*Shotaro Shobu[1], Satoshi Demura[2], Hideaki Sakata[1]

Tokyo University of Science[1]
Nihon University[2]

Recently, an anomalous hump in temperature dependence of electrical resistivity have been reported in Pb doped $La(O,F)BiS_2$ single crystals with Pb concentation 6% - 9%. These specimens, which show the hump, tend to have higher superconducting transition temperature (*Tc*) than the specimens without the hump[1]. The appearance of the hump is thought to be related to the structural instability in the crystal structure in BiS_2 system though the reason has not elucidated yet. It is interesting problem whether such Pb substitution effects occur in other BiS_2-based materials.

We investigated the effect of substitution of Pb for Bi in $(La,Sr)O_{0.5}F_{0.5}BiS_2$ single crystals because the enhancement of the substitution of Pb is expected in $(La,Sr)O_{0.5}F_{0.5}BiS_2$, where La is replaced with Sr, which have larger ionic radius than La ion. We carried out structure analysis by X-ray diffraction experiments and measurements of temperature dependence of electrical resistivity to confirm the existence the anomalous behavior similar to that observed in $La(O,F)Bi_{1-x}Pb_xS_2$ -.

The observed temperature dependence of electrical resistivity in $(La,Sr)O_{0.5}F_{0.5}BiS_2$ showed enhanced hump in temperature dependence of electrical resistivity as expected. Moreover, the onset of the *Tc* was enhanced with increasing Pb concentration.

[1]S.Otsuki, *et al.* Solid State Communications 270 (2018) 17-21

Keywords: BiS2-based superconductor, Element substitution, Layered materials

PCP6-5

CDW state in misfit transition-metal dichalcogenide (MS)(TaS2) (M=Bi,Pb,Sb,Sn)

*Shun Doyama[1], Yuta Sugai[1], Shun Ohta[1], Satoshi Demura[2], Hideaki Sakata[1]

Tokyo university of science, Japan[1]
Nihon university, Japan[2]

The misfit layered compound $(MS)(TX_2)_n$(n=1,2,3) has a layered crystal structure in which a MS layer (M = Bi, Pb, Sb, Sn or lanthanoid) forming a square lattice is inserted between transition metal dichalcogenide TX_2(T=Ta,Nb,Ti,V,Cr X=S,Se) which has a triangular lattice. Because staking of the triangular and the square lattice breaks spatial inversion symmetry, the spin orbit interaction affects the electronic states. Furthermore, because of the low dimensionality of the crystal structure in the misfit layered compound, the appearance of charge density wave (CDW) and superconductivity has been reported in these materials from electrical resistivity measurements. In M = Bi, both CDW and superconductivity was observed, whereas in M = Sb and Pb, only superconductivity was observed [1-4]. The origin of CDW or difference in superconducting transition temperature, however, have not been fully understood. In this study, we investigated the misfit layered compound with M = Sn, whose CDW or superconducting transition has not been studied, to compare with other misfit layered compounds.
Single crystal of $(SnS)(TaS_2)$ and $(PbS)(TaS_2)$ were synthesized by vapor transport method. The structural analysis by X-ray diffraction and electric resistivity measurements 1.4K to room temperature were performed. We found both CDW suppression and superconducting transition. In the presentation, we discuss the difference of CDW and superconducting transition temperature in misfit layered compounds.

Keywords: TaS2, CDW, misfit, transition metal dicalcogenide

PCP6-6

High pressure synthesis and substitution effect on InTe superconductor

*Masayoshi Katsuno[1], Rajveer Jha[1], Kazuhisa Hoshi[1], Yosuke Goto[1], Yoshikazu Mizuguchi[1]

Department of Physics, Tokyo Metropolitan University, Tokyo, Japan[1]

SnTe with a rock-salt structure is a topological crystalline insulator. In-doped $Sn_{1-x}In_xTe$ maintains the rock-salt structure up to a high indium content of $x \sim 0.4$ under ambient pressure [1]. The $Sn_{1-x}In_xTe$ system has been reported as a topological superconductor candidate. InTe (x = 1) can be regarded as heavily hole-doped SnTe from band-structure point of view. High pressure synthesized InTe has a rock-salt structure and shows superconductivity, while InTe obtained by conventional solid-state-reaction has a TlSe-type structure and does not show superconductivity [2]. In this study, polycrystalline samples of $InTe_{1-x}Se_x$ were prepared by a high pressure synthesis method (3 GPa, 500 ℃, 0.5 h). For the crystal structure analysis, we performed powder x-ray diffraction (PXRD). To investigate the superconducting properties, the temperature dependence of magnetization was measured under a magnetic field of 10 Oe using a SQUID magnetometer. We measure the temperature dependence of resistivity for $InTe_{0.85}Se_{0.15}$ under magnetic field from 0-0.5 T by a four-terminal method. The specific heat measurements were performed by a relaxation metohd on Physical Property Measurement System (PPMS).
The PXRD (Fig. 1(a)) shows that $InTe_{1-x}Se_x$ has a rock-salt structure for x = 0–0.2. The surface of the sample has blue metallic luster. The temperature dependence of magnetization shows that superconductivity is observed for those samples. The transition temperature increases by Se substitution (Fig. 1(b)). Resistivity under magnetic field reveals that H_{c2} of $InTe_{0.85}Se_{0.15}$ is about 0.6 T. From specific heat data, $D C/gT_c$
was estimated as 1.43, which is consistent with conventional superconductivity. In the presentation, we will show several substitution effects on InTe.

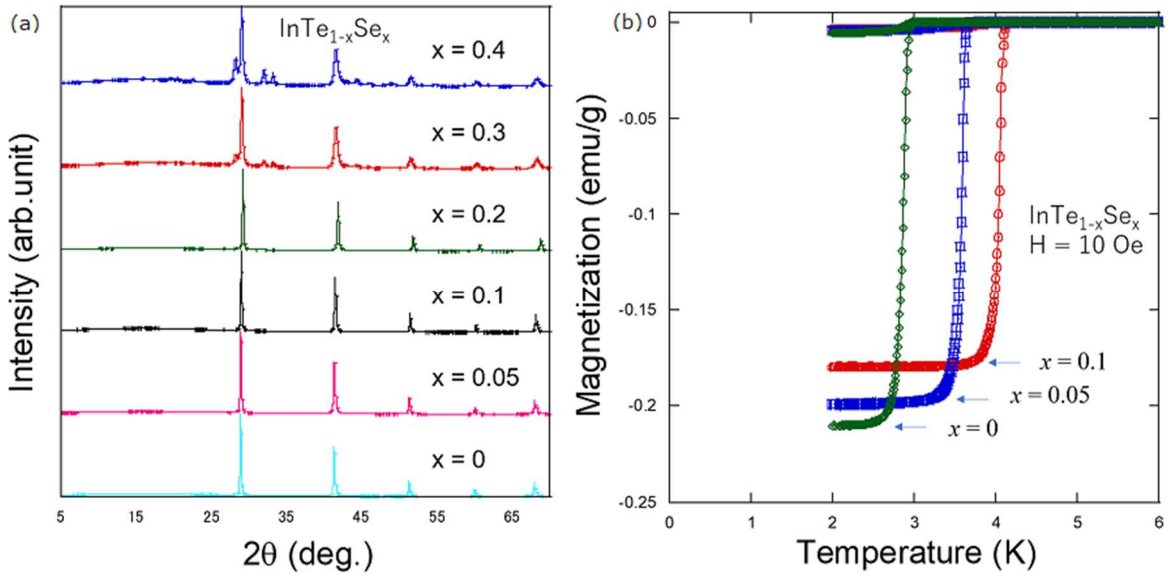

Fig. 1(a). PXRD patterns for x = 0–0.4.(b)Temperature dependences of magnetization for x = 0–0.1.

References

[1] N Haldolaarachchige, *Phys. Rev. B* **93**, 024520 (2016).
[2] M Kriener *Phys. Rev. M* **2**, 044802 (2018).

Keywords: Topological Superconductor, High Pressure Synthesis, Heat Capacity

PCP6-7

Synthesis, Crystal Structure, and Physical Properties of New Layered Oxychalcogenide Superconductor $La_2O_2Bi_3AgS_6$

*Yudai Hijikata[1], Osuke Miura[1], Yoshikazu Mizuguchi[2]

Dept. of Electrical and Electronic Engineering, Tokyo Metropolitan University, Hachioji, Tokyo 192-0397, Japan[1]
Dept. of Physics, Tokyo Metropolitan University, Hachioji, Tokyo 192-0397, Japan[2]

We report the superconductivity in layered oxychalcogenide $La_2O_2Bi_3AgS_6$ compound. The $La_2O_2Bi_3AgS_6$ compound has a tetragonal structure with the space group P4/nmm. The crystal structure of $La_2O_2Bi_3AgS_6$ can be regarded as alternate stacks of $LaOBiS_2$-type layer and rock-salt-type (Bi,Ag)S layer. The insertion of a rock-salt-type chalcogenide into the van der Waals gap of BiS_2-based layered compounds, such as $LaOBiS_2$, will be a useful strategy for designing new layered functional materials in the layered chalcogenide family. The electrical resistivity and Seebeck coefficient suggested that the electronic states of $La_2O_2Bi_3AgS_6$ are more metallic than those of $LaOBiS_2$ and $LaOBiPbS_3$. We measured low-temperature electrical resistivity and observed superconductivity at 0.5 K. The observation of superconductivity in the $La_2O_2Bi_3AgS_6$ should provide us with the successful strategy for developing new superconducting phases by the insertion of a rock-salt-type chalcogenide layer into the van der Waals gap of BiS_2-based layered compound like $LaOBiS_2$. We evaluated the critical current density of these layered oxychalcogenide.

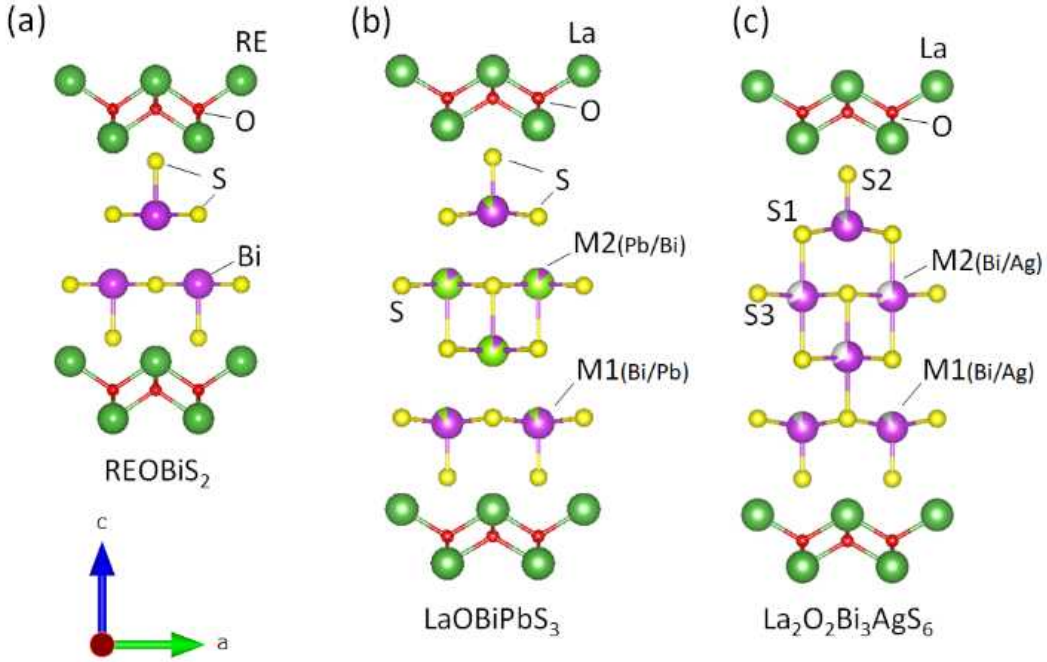

Keywords: Layered Superconductivity, BiS2

PCP6-8

Measurement of Seebeck coefficient in BiS_2 Based Superconductors

*Ryunosuke Shirota[1], Takahiro Kaneko[1], Shotaro Kawano[1], Yuto Sakai[1], Naoki Ishida[1], Shotaro Shobu[1], Hideaki Sakata[1]

Tokyo univ. of Science, Japan[1]

Low-dimensional materials can have potential high thermoelectric power and have been studied extensively for some applications such as power generator etc. Since BiS_2 based superconductors are layered materials, it is expected to show high thermoelectric power. The Seebeck coefficient of the polycrystalline LaO1-xFxBiS2 at high temperature has been reported [1].

On the other hand, the Seebeck coefficient is useful for detecting the change in the electronic states or information of carriers because it contains information of the electronic states near the Fermi level and, in some cases, can show more remarkable anomaly than the electric resistance when the sample undergoes phase transitions or structural changes. In BiS_2 based superconductors, anomaly in temperature dependence of the electrical resistivity or appearance of supermodulation have been observed at low temperature. Thus, the measurements of the Seebeck coefficient possibly give the information about the structural change in BiS_2 based superconductors.

In this study, we observed the temperature dependence of the Seebeck coefficient of Pb doped $LaO_{1-x}F_xBiS_2$, in which the anomaly of the temperature dependence of the electronic resistivity has been reported [2]. To do this measurement, we prepared the apparatus by which the Seebeck coefficient of small single crystals can be measured down to 5 K. In the presentation, we present the effects of Pb doping in $LaO_{1-x}F_xBiS_2$ on the temperature dependence of the Seebeck coefficient.

References
[1] A. Omachi *et al.*, J. Appl. Phys. **115**, 083909 (2014)
[2] S. Otsuki*, et al.,* Solid State Communications **270** (2018) 17-21

Keywords: Thermoelectric power, BiS2 superconductor

PCP7-1

Exploration of Topological Superconductors in Layered Compounds with a Bi Square-net

Masayuki Murase[1], *Takao Sasagawa[1]

Laboratory for Materials and Structures, Tokyo Institute of Technology[1]

Recently, topological materials such as 3D Dirac semimetals (3DDSMs) and topological superconductors (TSCs) have attracted considerable interest in condensed matter physics. Particularly, TSCs have been studied actively because it is theoretically predicted that TSCs will host Majorana fermions, which are anti-particles themselves and are expected to be utilized for fault-tolerant topological quantum computation. It is important to find a superconductor possessing a stoichiometric composition, a cleavage property, and topological surface electronic states.
In this study, in order to explore such TSC candidates, $SrPd_2Bi_2$, $SrAg_2Bi_2$, and $SrAgBi_2$ were studied. The crystal structures of $SrPd_2Bi_2$/$SrAg_2Bi_2$ and $SrAgBi_2$ resemble the 122 and 112-type iron arsenide superconductors while the As zigzag-chains are replaced by Bi square-nets.
Among these compounds, we succeeded in growing sizable single crystals of $SrAgBi_2$ by a self-flux method. Obtained crystals had a platelet shape and the cleavage property. XRD patterns from the cleaved surfaces of $SrAgBi_2$ consisted only of the (0 0 *l*) peaks, indicating that this crystal was cleaved along the *ab*-plane. The resistivity along the *ab*-plane showed metallic behavior in the temperature range from 300 K to 1.8 K, whereas superconducting transition was not observed down to 1.8 K. From the first principles calculations, the large influence of spin orbit coupling was found in $SrAgBi_2$. Investigations of possible superconductivity below 1.8 K and topological nature of electronic states have been in progress.

Keywords: Topological Superconductors, Crystal Growth

PCP7-2

Crystal Growth and Superconducting Properties of Misfit-Layer Bi-Compounds having Strong Spin Orbit Coupling

*Shun Takeda[1], Takao Sasagawa[1]

Laboratory for Materials and Structures, Tokyo Institute of Technology[1]

Recently, cation-intercalated Bi_2Se_3 has been extensively studied as promising candidates for a topological superconductor. In the case of $Nb_xBi_2Se_3$ (T_c^{max}～3.6 K) [1], besides the tendency of inhomogeneous spatial distribution of the intercalant, it was suggested that $(BiSe)_{1+\delta}(NbSe_2)$ was contained as an impurity phase. It is noted that $(BiSe)_{1+\delta}(NbSe_2)$ is reported to be a superconductor with a similar T_c (～2.5 K) [2]. $(BiSe)_{1+\delta}(NbSe_2)$ has a layered structure in which distorted rock salt structure BiSe layers and prismatic $NbSe_2$ layers are alternately stacked with their lattice constants incommensurate with each other. In addition to this misfit structure, the former layers introduce strong spin orbit coupling due to the heavy Bi element, while the latter layers break the in-plane space inversion symmetry by the triangular prismatic lattice. Therefore, $(BiSe)_{1+\delta}(NbSe_2)$ will be a great candidate material for both a topological and/or a parity-mixing superconductor. In this study, we have grown single crystals of $(BiSe)_{1+\delta}(NbSe_2)$ and evaluated their superconducting properties.

Single crystals of $(BiSe)_{1+\delta}(NbSe_2)$ were grown by the chemical vapor transport method. Crystals having a cleavage property were successfully obtained. From transport measurements, superconductivity was observed. It was found that T_c was sensitively depended on the details of the growth conditions, and the maximum of T_c was about 3.6 K. This value is very close to that reported for $Nb_xBi_2Se_3$. Therefore, the superconductivity of $Nb_xBi_2Se_3$ should be carefully evaluated with taking into consideration of this $(BiSe)_{1+\delta}(NbSe_2)$ misfit phase.

[1] Y. Qiu *et al.*, arXiv:1512.03519 (2016).
[2] Y. Gotoh *et al.,* Chem. Lett. 18, 1559 (1989).

Keywords: Misfit Layer Compounds, Topological Superconductor, Parity-Mixing Superconductor, Crystal Growth

PCP7-3

Crystal Growth and Superconducting Properties of Quasi-1D Bismuth Compounds

*Keitaro Matsukawa[1], Takao Sasagawa[1]

Tokyo Institute of Technology, Japan[1]

In a compound composed of heavy elements, band inversion due to strong spin-orbit coupling is expected to occur, which will induce a topological electronic phase. In the case of a superconducting material, a topological superconducting phase having a unique gapless superconducting state on the surface or edge/vortex core will emerge while a superconducting gap exists in the bulk. In this work, we have studied $NiBi_3$ (T_c = 4.06 K [1]) based superconducting compounds, which are expected to have strong spin-orbit coupling due to bismuth. $NiBi_3$ has a crystal structure composed of one-dimensional Ni-zigzag chains surrounded by Bi, which are bonded in two perpendicular directions by van der Waals force. Furthermore, by scanning tunneling spectroscopy (STS) measurements in $NiBi_3$ films, the observation of zero bias conductance peaks in the vortex cores suggesting the topological superconductivity was recently reported [2]. Therefore, we have considered $NiBi_3$ is a very interesting system for the exploration of topological superconducting states.

From our first principles calculations, it was suggested that hole-carrier doping could increase T_c. Therefore, we have tried to substitute Pb for Bi or Rh for Ni to dope hole carriers. We succeeded in growing single crystals of $NiBi_{3-x}Pb_x$ with x up to 0.3 and $Ni_{1-x}Rh_xBi_3$ with x up to 1.0 ($RhBi_3$) by using the self-flux method. The detailed superconducting properties of $NiBi_{2.7}Pb_{0.3}$ and $Ni_{0.9}Rh_{0.1}Bi_3$, with the maximum T_c (4.16 K and 4.40 K) in each elemental substitution, were evaluated as well as those of $NiBi_3$ and $RhBi_3$ (T_c = 3.30 K). Furthermore, the first principles calculations revealed that $NiBi_3$ and $RhBi_3$ could host topological surface electronic states by their topological crystalline semimetal natures. This discovery supports the appearance of the topological superconductivity as suggested by the results of STS measurements in $NiBi_3$.

[1] Y. Fujimori *et al.*, *J. Phys. Soc. Jpn.* **69**, 3017 (2000).
[2] W. Wang *et al.*, *Phys. Rev. B* **97**, 134524 (2018).

Keywords: NiBi3, Superconducting Properties, Single Crystal, Electronic Structures

PCP7-4

Interplay of Stress and Nematic Superconducting Order: The Case of $Cu_xBi_2Se_3$

*Pye Ton How[1], Sung-Kit Yip[1,2]

Insitute of Physics, Academia Sinica[1]
Institute Of Atomic And Molecular Sciences, Academia Sinica[2]

$Cu_xBi_2Se_3$ is a candidate for topological superconductor, and has been the subject of intensed experimental and theoretical studies since the discovery of its superconductivity. It has been suggested in the literature that its superconducting state has a nematic order, which spontaneously breaks the rotational symmetry of the underlying trigonal crystal. On the other hand, experimental efforts thus far are mainly focused on situations with an applied magnetic field, which explicitly breaks the rotational symmetry, and is solely responsible for the observed two-fold anisotropy.

Assuming the superconducting state does exhibit a nematic order, we theoretically consider the interplay between the nematic order parameter, the trigonal crystal anisotropy, and an applied stress (or strain) in the basal plane of the crystal, by constructing the Ginzburg-Landau free energy of this superconductor. We map out all possible phase diagrams, show that the superconducting transition must split into two under applied stress. The critical temperatures and specific heat jumps of both transitions exhibit non-trivial dependence on the orientation of the applied stress. We further predict that there may be an additional first order phase transition at a lower temperature. Experimental observation of thses features can serve as a conclusive test for nematic superconducting state in trigonal crystal.

Keywords: CuxBi2Se3, Nematic Superconductor, Ginzburg-Landau Theory, Topological Superconductor

PCP7-6

New Oxide Diluted Magnetic Semiconductor System $La_{1-x}Ca_xCu_{0.9}Mn_{0.1}SO$ with Independent Spin and Charge Doping

*Li Zhang[1], Haoze Chen[1], Linxian Li[1], Yuke Li[2]

China Jiliang University[1]
Hangzhou Normal University[2]

We report the synthesis of a new bulk oxide diluted magnetic semiconductor (DMS) system $La_{1-x}Ca_xCu_{0.9}Mn_{0.1}SO$ (x = 0, 0.025, 0.05, 0.075, 0.1 and 0.125) which is identical to that of the“1111”iron-based superconductors[1,2]. The joint hole doping via (La,Ca) substitution & spin doping via (Cu,Mn) substitution results in ferromagnetic order with Curie temperature up to 130 K and demonstrates that the ferromagnetic interactions between the localized spins are mediated by the carriers[2]. To understand the electronic structure of the host semiconductor $La_{1-x}Ca_xCu_{0.9}Mn_{0.1}SO$, we also calculated the bandgap of (La,Ca)(Cu,Mn)SO by first-principles calculations.The system provides a rare example of oxide DMS system with p-type conduction, which is important for formation of high temperature spintronic devices.

PCP7-7

Influence of Microfabrication on Superconducting Characteristics of Exfoliated Thin Films of Layered Superconductor $NbSe_2$: Focused Ion Beam

Hikari Tomori[1], Naoki Hoshi[1], Dai Inoue[1], *Akinobu Kanda[1]

University of Tsukuba, Japan[1]

In recent years, exfoliation techniques developed for the research of graphene (monolayer of graphite) have been applied to layered superconductors to form clean superconductors with atomic thickness, and novel properties such as strong suppression of the critical temperature with decreasing thickness have been revealed. In most researches conducted so far, cleaved films with random shape were used without further shape processing. However, for the detailed study of the superconducting properties as well as application to superconducting devices, shape processing is indispensable. Here, we investigate the influence of the focused ion beam (FIB) processing, which is commonly used for shape processing of the high-temperature superconductors, on properties of layered superconductors. Here we note that the FIB damage in the high-temperature superconductor is on the 10-nm scale.[1]

In the experiment, thin wires of layered superconductor $NbSe_2$ were formed using FIB. The width and thickness of the wire are 2 μm and several 10 nm, respectively. We observed that the critical temperature, below which the supercurrent flows, was strongly suppressed. Furthermore, in the current-voltage characteristics, we observed several voltage steps. Since the temperature dependence of the step current was consistent with the temperature dependence of the critical current of the unprocessed $NbSe_2$ film, it is inferred that the wire was separated into several grains. Interestingly, the critical temperature deduced from the temperature dependence of the step current exhibited several values, indicating that the layer was also separated in the thickness direction. These results show that the FIB processing affects the thin layered superconductors on the micro-meter scale.

[1] Y. Kakizaki *et al.*, Jpn J. Appl. Phys. 56, 043101 (2017).

Keywords: layered superconductor, microfabrication, NbSe2, transport measurement

PCP7-8

Transmission EBSD (t-EBSD) as tool to investigate nanostructures in superconductors

*Anjela Koblischka-Veneva[1,2], Michael R Koblischka[1,2], Jörg Schmauch[1,2], Masato Murakami[1]

Superconducting Materials Laboratory, Department of Materials Science and Engineering, Shibaura Institute of Technology, 3-7-5 Toyosu, Koto-ku, Tokyo 135-8548, Japan[1]
Experimental Physics, Saarland University, P.O. Box 151150, 66041 Saarbrücken, Germany[2]

The transmission electron backscatter diffraction (t-EBSD) technique has proven to be an indispensable tool for the analysis of microstructures of superconducting samples, both high-Tc samples (YBCO, Bi-2212) as well as MgB_2 or FeSe. In both types of samples, the knowledge of the grain boundary properties (misorientation, length, width) are essential for the further optimization of sample performance. Any addition of secondary phase(s) to improve the flux pinning is required to be of nanometer dimensions, so the higher achievable resolution and the better imaging properties is important to obtain reasonably high image quality to enable automated mapping of orientations. The orientation maps reveal not only the location and the shape of the inclusions within the superconducting matrix or e.g., at the grain boundaries, but also their influence on the surrounding superconducting matrix which also plays an important role in flux pinning. In the case of sintered MgB_2 bulk samples, the demand for higher critical current densities leads to MgB_2 grains in the 100-nm range, which is already difficult to be studied by means of conventional EBSD [1]. Furthermore, t-EBSD is useful for the analysis of specific microstructures of unconventional superconductors like superconducting foams [2] or superconducting nanowire networks [3].
In this contribution, we review the present state-of-the-art, and give several examples of applications of the t-EBSD technique on different superconducting materials.

[1] A. Koblischka-Veneva *et al.*, Supercond. Sci. Technol. 29 (2016) 044007
[2] M. R. Koblischka *et al.*, J. Adv. Ceram. 3 (2014) 317
[3] A. Koblischka-Veneva *et al.*, J. Phys. Conf. Ser. 1054 (2018) 012005

Keywords: high-Tc superconductors, nanostructures, Electron backscatter diffraction, transmission mode

PCP8-1

Porous high-T_c superconductors: Advantages and applications

*Michael R Koblischka[1], Anjela Koblischka-Veneva[1], S. Pavan Kumar Naik[1], Denis Gokhfeld[2], Masato Murakami[1]

Superconducting Materials Laboratory, Department of Materials Science and Engineering, Shibaura Institute of Technology, 3-7-5 Toyosu, Koto-ku, Tokyo 135-8548, Japan[1]
Kirensky Institute of Physics, Siberian Branch of the Russian Academy of Sciences, Akademgorodok 50/38, Krasnoyarsk, 660036 Russia[2]

Porous high-T_c superconductors are promising materials representing an alternative preparation route to enable the fabrication of large-scale, light-weight superconducting samples. There are several advantages of such samples including the much easier (and faster) oxygenation process, a simpler scalability to produce large samples, and of course, the reduced weight. Two different types of such samples were prepared in the literature: (i) Superconducting foams, prepared using polyurethane foams converted to green phase foams followed by an infiltration growth (IG) process. The original samples of this type were prepared at RWTH Aachen, Germany, many years ago [1]. (ii) Superconducting nanowire networks prepared by spinning from sol-gel precursors [2,3]. Such fabric-like nanowire networks are extremely light-weight, but show very interesting properties.

In this contribution, we discuss the properties of such samples concerning both the physical parameters and the respective microstructures and give an overview about possible applications.

[1] E. S. Reddy and G. Schmitz, Supercond. Sci. Technol. 15 (2002) L21
[2] M. R. Koblischka *et al.*, IEEE Trans. Appl. Supercond. 26 (2016) 1800605
[3] M. Rotta *et al.*, Ceram. Int. 42 (2016) 16230

Keywords: high-Tc superconductors, porous materials, foams, nanowire network fabrics

PCP8-2

New Cuprate Superconductor, (Nb,Pb)$Sr_2EuCu_2O_z$ (z~8)

*Yoshihiro Yamada[1], Toshihiko Maeda[1,2]

Kochi University of Technology[1]
Center for Nanotechnology[2]

Nb-based "1-2-1-2"-type cuprates, $NbBa_2LaCu_2O_z$ and $NbBa_2PrCu_2O_z$ (z~8) which are structurally related to $YBa_2Cu_3O_{7-\delta}$ (YBCO) have been synthesized for the first time in 1991 by Ichinose *et al.* [1] and Kim *et al.* [2] have recently reported that Sn doping into their related compounds, $NbSr_2EuCu_2O_z$, makes it superconducting by generating carriers due to Sn^{4+}substitution for Nb^{5+}. It has been shown that Nd and Sm also give the Nb-"1-2-1-2" when used instead of Eu. This Nb-"1-2-1-2" has not been made superconducting by Ca-substitution so far. Ichinose *et al.* [1] have also shown by X-ray Rietveld analysis that Nb occupies a 6 oxygen-coordinated crystallographic site corresponding to Cu(1) in YBCO forming a so-called Cu-O one-dimensional chain. In this study, substitution effects of some metallic elements for Nb site in $NbSr_2RECu_2O_z$ (RE: Nd, Sm, Eu or Gd) are investigated and it is found that Pb substitution for Nb makes $NbSr_2EuCu_2O_z$ superconducting.

Samples are prepared by a solid-state reaction method mainly using Nb_2O_5, PbO, $SrCO_3$, RE_2O_3 and CuO. Nominal compositions of $(Nb_{1-x}Pb_x)Sr_2EuCu_2O_z$ ($0 \leq x \leq 0.4$) are used. Characterization of the samples is carried out by means of powder X-ray diffractometry (XRD) for phase identification and four-probe method in order to measure the temperature dependence of electrical resistivity. XRD profile for the sample of x=0.2, $(Nb_{0.8}Pb_{0.2})Sr_2EuCu_2O_z$, shows that it is a nearly single Nb-"1-2-1-2" phase having a tetragonal unit cell with a=3.877 Å and c=11.656 Å. This sample exhibits superconductivity with a superconducting transition temperature (T_c) of 43 K (onset). Dependence on x of phase formation and T_c will be discussed.

[1] A. Ichinose *et al.*, J. Ceram Soc. Jpn. **97**, 1065-1070 (1989). (*in Japanese)*
[2] K. Kim *et al.*, Physica **C492**, 165-167 (2013).

Keywords: New cuprate superconductor, (Nb,Pb)Sr2RECu2Oz, Nb-"1-2-1-2"

PCP8-3

Effect of co-substitution of Ca for Y and Sr sites in (Pb,Cu)$Sr_2YCu_2O_z$ (z~7)

Keisuke Ozaki[1], Toshihiko Maeda[1,2]

Kochi University of Technology[1]
Center for Nanotechnology[2]

(Pb,Cu)Sr_2(Y,Ca)Cu_2O_z ((Pb,Cu)-"1-2-1-2"; z~7) has been synthesized for the first time by Subramanian *et al.* [1] and Ono *et al.* [2] have observed superconductivity for samples of $(Pb_{0.65}Cu_{0.35})Sr_2(Y_{0.7}Ca_{0.3})Cu_2O_z$ quenched from 860˚C after sintering. Chemical composition of the (Pb,Cu)-"1-2-1-2" has been shown to be described by the formula $(Pb_{(1+x)/2}Cu_{(1-x)/2})Sr_2(Y_{1-x}Ca_x)Cu_2O_z$ [3]. Ca substitution for Y and the quenching procedure are believed to play a crucial role for the occurrence of superconductivity. Additionally, Ca substitution for Sr site in parallel with that for Y site is found to improve superconductivity [4]. Therefore, superconductivity of this (Pb,Cu)-"1-2-1-2" seems fairly complex and its mechanism of carrier-doping for its superconductivity is still the most important problem to be solved. In this study, effect of co-substitution of Ca for Y and Sr sites on phase formation and superconductivity is investigated.

Samples are prepared by a solid-state reaction of PbO, $SrCO_3$, Y_2O_3, $CaCO_3$ and CuO. Powder X-ray diffractometry (XRD) and four-probe method are respectively used for phase identification and measurement of temperature dependence of resistivity. Improvement of superconductivity by Ca substitution for Sr is observed. Relationship between complex site distribution of Ca in Sr and Y sites will be discussed.

[1] M. A. Subramanian *et al.*, Physica **C159**, 124 (1989). [2] A. Ono and Y. Uchida, Jpn. J. Appl. Phys. **29**, L586 (1990). [3] T. Maeda *et al.*, Phys. Rev. **B43**, 7866 (1991). [4] T. Maeda *et al.*, Physica **C185-189**, 687 (1991).

Keywords: (Pb,Cu)-"1-2-1-2", co-substitution of Ca

PCP8-4

Enhancement of local magnetic moment on Cu ion by excess oxygens in T'-cuplates

*Kunito Yamazaki[1], Hiroki Tsuchiura[1], Pavel Novák[2]

Department of Applied physics, Tohoku University, Japan[1]
Institute of Physics, The Czech Academy of Sciences, Czech Republic[2]

In the typical phase diagram of cuprates, there exists antiferromagnetism(AF) around half-filling, and d-wave superconductivity(dSC) emerges with chemical carrier doping. However, a series of experimental studies for the electron-doped cuprates with T'-structure(T'-cuplates) have suggested that the phase boundary between AF and dSC is strongly influenced by the annealing condisions. Moreover, they have claimed that dSC appears in thin-film samples of chemically undoped T'-cuprates [1]. The main effect of annealing is expected to remove excess oxygen, which can be inevetably introduced in the as-grown samples [2]. Thus we can speculate that the excess oxygen atoms can be nucleation centes for the AF found in the usual T'-cuplates.

In this contribution, we study the local electronic state around an excess oxygen atom located between the CuO_2-planes in T'-cuprates using the LDA+U method. We find that the Cu ion just below the excess oxygen atom approaches a $3d^8$ configuration due to the strong hybridization between the $3dz^2$ and the oxygen 2p-orbitals, resulting in the enhancement of the local magnetic moment on the Cu ion. We will discuss how this enhancement can be detected in the hyperfine field distributions.

[1] A. Tsukada *et al.*, Solid State Commun. **133**, 427 (2005).
[2] A. J. Schultz *et al.,* Phys. Rev. B **53**, 5157 (1996).

Keywords: Electron-doped cuprates, T'-structure, annealing effect, Local density approximation + U

PCP8-5

Study of Critical Temperature for Alkali Metal Adsorbed Copper Oxide High-T_c Superconductors

*Chikako Sakai[1], Tsunehiro Takeuchi[2], Sakura N. Takeda[3], Hiroshi Daimon[3]

National Institute for Materials Science, Japan[1]
Toyota Technological Institute, Japan[2]
Graduate School of Science and Technology, Nara Institute of Science and Technology, Japan[3]

From the 1980s, the electrical conductivity measurements of copper oxide high-T_c superconductor (HTSC), which alkali metal was doped during making samples, have been done for studying the effect of element dopant. Kawai *et al.* reported the change of superconducting properties with the addition of Pb, Bi, Ba, Sr, Ca, Cu, and alkali metals to Bi-Sr-Ca-Cu-O superconductor (BSCCO). Li has the smallest ionic radius. Their results showed that the Li-added BSCCO has the highest critical temperature (T_c) [1]. Dou *et al.* reported that the increase of T_c was observed by doping Li, Na, and K to BSCCO [2].

However, study of T_c for alkali metal adsorbed copper oxide HTSC has not been done until now. To study the effect of alkali metal adsorption to copper oxide HTSC, we deposited cesium (Cs) on clean surface of the specimen and measured its conductivity in ultrahigh vacuum (UHV). Cs was selected since electrons are most easily removed from atoms among alkali metals.

In the case of optimally doped $Bi_2Sr_2CaCu_2O_{8+\delta}$ (OP Bi2212) copper oxide HTSC single crystal, the decrease of $T_{c\ zero}$ (the phase with 95 K) was observed by Cs adsorption (Fig.) [3]. In the case of over-doped $Bi_{1.9}Sr_{0.2}CaCuO_{8+\delta}$ as grown copper oxide HTSC single crystal, the increase of $T_{c\ midpoint}$ (the phase with 83 K) was observed by Cs adsorption. It suggests that the change of the hole concentration of CuO_2 plane was occurred by adsorbing alkali metal. This is a new method to change T_c easily after crystal growth of copper oxide HTSC. We will also introduce the equipment, which was made to enable this research.

[1] T. Kawai *et al.*, Physica C **161** (1989) 561.
[2] S. X. Dou *et al.*, Physica C **172** (1990) 295.
[3] C. Sakai *et al.*, Rev. Sci. Instrum. **84** (2013) 075103.

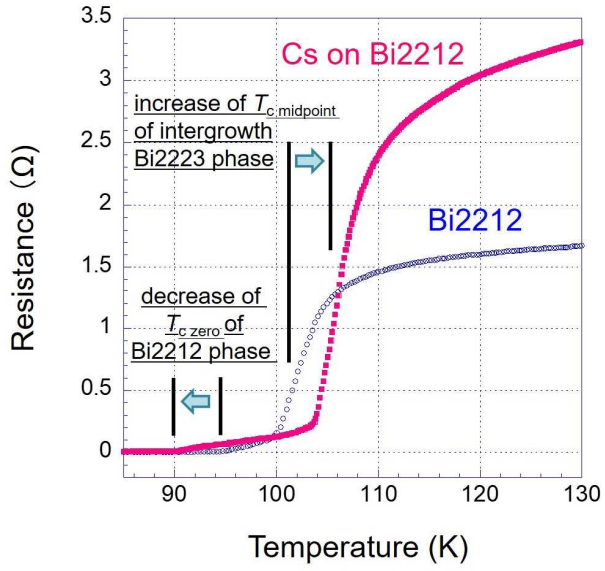

Fig. Electrical conductivity measurement results of the OP Bi2212 specimen before and after Cs adsorption

Keywords: copper oxide HTSC, alkali metal adsorption, critical temperature measurement

PCP8-6

Difference of Local structure between $YBa_2Cu_3O_z$ and $PrBa_2Cu_3O_z$ Compounds

*J. Yu[1,2], C.Y. Zhang[2], C.Q. Guo[2], L. Li[2], H. Zhang[2]

Yellow River Conservancy Technical Institute, Kaifeng, Henan, 475004, China[1]
Materials Physics Laboratory, State Key Laboratory for Mesoscopic Physics, Department of Physics, Peking University, Beijing 100871, China[2]

$PrBa_2Cu_3O_z$ (PrBaCuO) and $YBa_2Cu_3O_z$ (YBaCuO) share same crystalline structure, but YBaCuO is superconducting when PrBaCuO is not. By single and double substitutions of cations in both compounds, it makes the local structures of them change a little. The x-ray diffraction and Rietveld refinement were used to detect the subtle changes of the local structures. It was found that the behaviors of the Cu-O plane in the PrBaCuO and YBaCuO systems were different. In the YBaCuO system, the Cu-O plane was relatively stable, which was not in the PrBaCuO. Raman spectroscopy was also used to determine the changes of these local structures. The results showed that, both the Raman shift of the out-of-plan *c*-axis O(2)-O(3) buckling mode around 335 cm^{-1} and the in-plane Cu(2)-O(2) bond-stretching mode around 534 cm^{-1} were independent of the doping level in the YBaCuO system. Meanwhile, in the PrBaCuO systems, these two modes were not detected yet. Such results give the possible reason for the difference between superconducting YBaCuO system and non-superconducting PrBaCuO system. That is, the YBaCuO system has smooth and stable Cu-O plane when the PrBaCuO system hasn't. This reason instead of the hybridization of Pr 4f and O 2p orbitals in PrBaCuO system maybe makes it non-superconducting.

Keywords: Crystalline structure, Raman spectroscopy, Superconductivity

PCP8-7

Uniform hole doping in $HgBa_2Ca_2Cu_3O_{8+\delta}$ studied by ^{63}Cu NMR

*Yutaka Itoh[1], Akihiro Ogawa[2], Seiji Adachi[3]

Dep. of Physics, Graduate School of Science, Kyoto Sangyo University, Kamigamo-Motoyama, Kika-ku, Kyoto 603-8555, Japan[1]
Chugoku Electric Power Company Inc. Energia Research Institute, 3-9-1 Kagamiyama, Higashi Hiroshima, Hiroshima 739-0046, Japan[2]
Superconducting Sensing Technology Research Association, 2-11-19 Minowa, Kohoku, Yokohama, Kanagawa 223-0051, Japan[3]

We studied the site-selective magnetic properties of three CuO_2 layer superconductors $HgBa_2Ca_2Cu_3O_{8+\delta}$ with rich ^{63}Cu isotope, an as-synthesized underdoped sample (T_c = 125 K) and the O_2-annealed optimally doped sample (T_c= 134 K) by the ^{63}Cu NMR spin-echo technique. The temperature dependences of the ^{63}Cu nuclear spin-lattice relaxation rate $^{63}(1/T_1)$ and the spin Knight shift of the inner plane Cu(1) site were found to be nearly the same as those of the outer plane Cu(2) site in the normal states. The spin gap temperature $T_s$defined as the maximum temperature of $^{63}(1/T_1T)$ was 190 K for the underdoped T_c= 125 sample and 143 K for the optimally doped T_c= 134 K sample. The NMR results indicate the uniform hole distribution in the three layers, which is consistent with a coalescence of the three-derived Fermi surfaces predicted by the band theory [1].

[1] D. J. Singh, and W. Pickett: Phys. Rev. Lett. **73**, 476 (1994).

Keywords: Hg1223, NMR

PCP8-8

Kinetics of $YbBa_2Cu_3O_Y$ thick film formation on MgO substrates

*Atsuhiko Hattori[1], Muralidhar Miryala[1], Masato Murakmai[1]

Shibaura Institute of Technology[1]

The production of best thick $YbBa_2Cu_3O_y$ films on MgO substrates are crucial for the utilization of this technology in silver sheeted wire as similar to Bi-2223. In this presentation, in order to optimize $YbBa_2Cu_3O_y$ films on MgO substrates, a mixture of alpha-terpineol and 2-ethyl acetate was utilized as a solvent to which 100 nm sized stoichiometric powder mixture of Yb_2BaO_4, $BaCuO_2$ and CuO was added and grinded for several hours to form a highly dense paste. Thick film precursors were prepared by spreading the paste over MgO substrates with a screen printing technique and various sintered temperatures by adopting two-step process. The maximum temperature (T_m) was kept constant at 975 ^oC for 10 min. and varied growth temperature (T_g) between 800 ^oC, 820 ^oC, 825 ^oC, 840 ^oC, 860 ^oC, 880 ^oC, and 895 ^oC for 120 min. in air and cooled to room temperature for 100 ^oC/h. The films were characterized by XRD and SEM analyses. All the samples were annualized, characterized, optimized for a good quality thick film $YbBa_2Cu_3O_y$ on MgO substrate utilizing double step heating.

Keywords: thick YbBa2Cu3Oy films , Yb2BaO4, XRD, SEM

PCP8-9

Fabrication of Mesa-like Device on a Bi2212 Cross-Whisker Junction

*Yoshito Saito[1,2], Ryo Matsumoto[1,2], Shintaro Adachi[1], Masanori Nagao[3], Hiroyuki Takeya[1], Yoshihiko Takano[1,2]

National Institute for Materials Science, Tsukuba 305-0047, Japan[1]
University of Tsukuba, Tsukuba 305-8577, Japan[2]
University of Yamanashi, Kofu 400-8511, Japan[3]

Intrinsic Josephson Junction (IJJ) realized in layered high temperature superconducting materials have been attracting interest because of its unique physics and application. For application, an IJJ mesa structure shaped on $Bi_2Sr_2CaCu_2O_{8+\delta}$ (Bi2212) single crystal is developed for terahertz emission. Conventional mesa structure [1] is fabricated with photolithography and Ar ion milling or FIB micro-fabrication technique. Also, Au deposition is required to make electrodes on it. Another way to fabricate IJJ mesa structure is to take advantage of a cross-whisker junction [2]. In a cross-whisker junction, two Bi2212 whiskers are electrically connected by annealing process and contains IJJs in the cross-sectional area without any complex micro-fabrication technique. In this study, an array of IJJs was fabricated from a cross-whisker junction without lithography and Au deposition process. Fig.1(a) shows the I-V characteristic and an image of a cross-whisker junction. Additionally, FIB was employed to adjust the depth of the mesa-like structure. Fig.1(b) shows the I-V characteristic and an image of the fabricated IJJ mesa-like structure. The structure has a width of 12μm, a length of 26μm, and a depth of 0.6μm. The multi-branched structure of IJJs with voltage gaps of several tenth of mV was observed.

[1] L. Ozyuzer *et. al.*, Science **38**, 1291 (2007)
[2] Y. Takano *et.al.*, Supercond. Sci. Technol. **14**, 765 (2001)

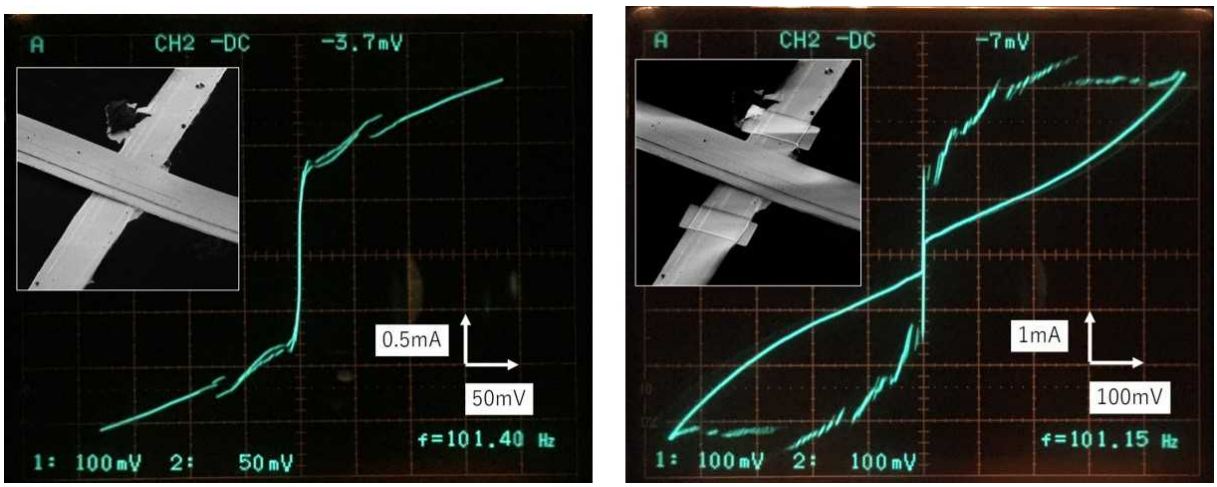

Fig.1. (a) Current-voltage characteristic of the cross-whisker junction at 10K. The inset is the SIM micrograph of the cross-whisker junction. (b) Current-voltage characteristic and the SIM micrograph of FIB fabricated mesa like structure from (a).

Keywords: intrinsic Josephson junction , Bi2212, micro fabrication

PCP8-10

Microscopic Theory of Exotic Phases in Superconducting Cuprates

*Kazuhisa Nishi[1]

University of Hyogo[1]

There has been much interest in various exotic phases of superconducting cuprates such as the pseudogap, the charge density wave (CDW), electron-nematic order and strange metal in normal state [1]. However, in spite of much intensive study about these exotic phases, its microscopic mechanism still remains an unsolved problem. Here a microscopic theory is considered using the theory emphasizing that the electronic state of superconductors can be described by the composed fermions [2,3]. This is constructed with the Hamiltonian which is so modified by the unitary transformation using these fermion operators as to apply the mean field approximation. It is indicated that the interesting properties of these exotic phases in cuprates can be explained by the proposed microscopic theory.

[1] B. Keimer *et al.* Nature **518** (2015) 179.
[2] K. Nishi, J. Phys. Conf. Ser. **871** (2017) 012033.
[3] K. Nishi, J. Phys. Conf. Ser. **1054** (2018) 012013.

Keywords: High-temperature Superconductor, Cuprate, Exotic Phase

PCP8-11

Effects of vicinal substrates on the orientation of $Bi_2Sr_2CaCu_2O_{8+x}$ thin films when the metal-organic decomposition method is used

*Yasuyuki Yamada[1], Tomoichiro Okamoto[2]

Department of Innovative Electrical and Electronic Engineering, National Institute of Technology, Oyama College, Japan[1]
Electrical, Electronics and Information Engineering, Nagaoka University of Technology, Japan[2]

We are attempting to prepare planar type intrinsic Josephson oscillator devices that are not required etching processes. These new type devices can be prepared by a combination of orientation control technique of $Bi_2Sr_2CaCu_2O_{8+x}$ (Bi2212) thin film by metal-organic decomposition method and application of raw material solution by printing method. In order to prepare planar type devices, it is necessary to form a current path parallel to the substrate, so that the *c*-axis of Bi2212 is required to be parallel to the substrate.

Bi2212 is an orthorhombic crystal having a lattice constant of a = 5.414 Å, b = 5.418 Å, c = 30.6 ~ 30.9 Å [1,2]. $NdGaO_3$ (NGO) is also orthorhombic with lattice constants a = 5.427 Å, b = 5.497 Å, c = 7.707 Å [3]. The length of the *a*-axis of Bi2212 is approximately equal to the length of the *a*-axis of NGO, and that of *c*-axis of Bi2212 is approximately equal to four times that of *c*-axis of NGO. Since these values are very close, it is expected that lattice matching occurs well and Bi2212 will be epitaxially grown. Actually, we succeeded in growing (010) oriented Bi2212 crystal grains. However, (11*n*) oriented crystal grains are also formed, which is a problem to be solved.

Bi2212 thin films were prepared by the MOD method using a stoichiometric metal-organic solution. Substrates used were flat and vicinal NGO (100) substrates with the size of 10 × 10 × 0.5 mm and the miscut angle $\varphi = 5°$ toward the direction [001]. Figure 1 shows a comparison of the observed surface morphologies by SEM with flat and vicinal NGO (100) substrates. From the viewpoint of lattice matching, in fig.1 (a), elongated crystal grains in the lateral direction in the part surrounded by the white broken line is considered to be the (010) oriented grain. The white solid arrow indicates the *c*-axis direction of the (010) oriented grain. In fig. 1 (b), dashed surrounding line and arrow are omitted. It can be seen that more elongated crystal grains are formed in fig. 1 (b). Therefore, it is concluded that using vicinal substrates is effective.

[1] Sunshine S A et al., 1988 Phys. Rev. B 38 893
[2] Horiuchi S et al., 1988 Jpn. J. Appl. Phys. 27 L1172
[3] Vasylechko L et al., 2000 J. Alloys Compd. 297 46

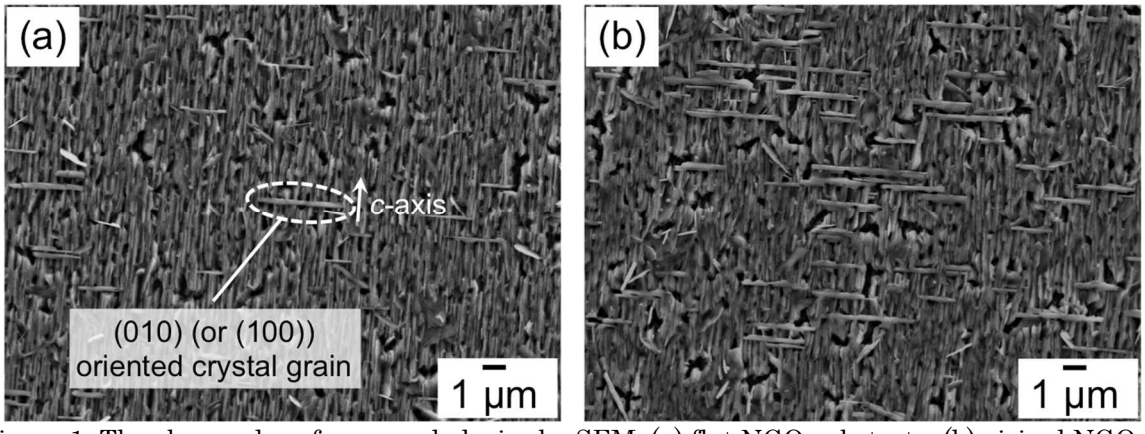

Figure 1. The observed surface morphologies by SEM. (a) flat NGO substrate. (b) vicinal NGO substrate.

Acknowledgments: This work was supported by JSPS KAKENHI Grant Number JP17K06377.

Keywords: BSCCO, metal-organic decomposition method, orientation control

PCP9-1

Variational Approach to Impurity Problem in Hubbard Model---Effects of Short-Range Antiferromagnetic Order and One-Body Screening Projector

*Hisatoshi Yokoyama[1], Ryo Sato[1], Kenji Kobayashi[2]

Department of Physics, Tohoku University, Japan[1]
Department of Natural Science, Chiba Institute of Technology, Japan[2]

The results of recent numerical studies [1] on the two-dimensional Hubbard (t-t'-U) model that antiferromagnetic (AF) (or phase-separated) states, instead of superconducting states, prevail up to δ~0.2 of doping rate for any t'/t obviously contradict the behavior of cuprate superconductors.To reconcile this contradiction, we have studied the effects of point-type impurity potential inherent in cuprates on paramagnetic (PM) and the AF states using a variational Monte Carlo (VMC) method. In preceding publications [2,3], we found that impurity potential V of $-U \lesssim V < V_{\mathrm{M}}$ with $V_{\mathrm{M}} \sim 2t$ ($U=12t$), namely in moderately attractive and weakly repulsive cases, is almost screened out for strong correlation ($U \gtrsim 8t$). As a result, the properties of the PM and AF states for the uniform case ($V=0$) are preserved in this range of V. And that metal-to-insulator and insulator-to-metal transitions are induced at $V=V_{\mathrm{M}}$ with impurity density of $\delta_{\mathrm{imp}} \geq \delta$ and at $V=V'_{\mathrm{M}}$ [$\sim -U$ (AF) or $-U/2$ (PM)] at half filling, respectively. These were confirmed as filling-control-type Mott transitions. On the other hand, convergence of optimization within the variational wave functions used becomes bad or sometimes intractable for $V \gtrsim V_{\mathrm{M}}$, especially, in PM cases. Thus, we have room for improvement for repulsive potential.
In this study, we reconsider the same problem with $V>0$ using a VMC method with a wave function constructed from different angles: (1) An AF order is introduced by a projector of a short-range correlation $P_S=\beta^{\hat{\sigma}}$ with β being a parameter and $\hat{\sigma}=\Sigma_{\langle i,j\rangle} S_i^z S_j^z$, instead of long-range Hartree-Fock-type correlations used in the previous studies. (2) We introduce an onsite screening effect on V by a single-particle projection factor $P_\theta=\theta^{\hat{\kappa}}$ [4] with θ being a parameter and $\hat{\kappa}=\Sigma_{\ell,\sigma} n_{\ell\sigma}(\ell=1,\cdots,N_{\mathrm{imp}})$, instead of integrating the screening effect into the Hartree-Fock Slater determinant. Details will be discussed in the presentation.

[1] R. Sato, H. Yokoyama, J. Phys. Soc. Jpn. **85**, 124707 (2016), and references therein.
[2] H. Yokoyama, R. Sato, K. Kobayashi, J. Phys. Conf. Ser. **871**, 012032 (2017).
[3] H. Yokoyama, R. Sato, K. Kobayashi, J. Phys. Conf. Ser. **1054**, 012014 (2018).
[4] T.M. Rice and W.F. Brinkman, Phys. Rev. B **5**, 4350 (1972).

Keywords: cuprate, impurity potential, Mott transition, screening factor

PCP9-2

Relationship between superconductivity and anisotropy in two-dimensional Hubbard model

*Kenji Kobayashi[1], Hisatoshi Yokoyama[2]

Chiba Institute of Technology, Japan[1]
Tohoku University, Japan[2]

Recently, symmetry-breaking phenomena are successively found in cuprate superconductors; electronic nematic order breaking the rotational symmetry [1] and charge density wave breaking the translational symmetry [2] were experimentally discovered along with superconductivity (SC). These symmetry breakings attract much interests because they may provide important insights into the relationship between SC and an enigmatic pseudogap state. Pomeranchuk instability, a spontaneous breaking of fourfold rotational symmetry of the Fermi surface without lattice distortion, is a noteworthy candidate for the nematicity observed in cuprate superconductors [3].

In this presentation, we will check whether the x-y anisotropy spontaneously appears in the two-dimensional strongly correlated Hubbard model using a variational Monte Carlo (VMC) method, and consider the relationship between the anisotropy and superconducting state when the model parameters and doping rate are varied. In order to ensure the accuracy of x-y isotropy/anisotropy in calculation, we use a slightly tilted square lattice and apply periodic boundary conditions in both x and y directions. In the trial wave function for VMC calculations, we introduce the following features:

(1) We adopt a mixed state of antiferromagnetic (AF) and SC orders, by which we can treat a continuous description of their interplay from mutual exclusivity to coexistence.

(2) The band renormalization effect owing to electron correlation is independently introduced into AF and SC orders by adjusting the parameters of hopping integrals, some of which have anisotropy of x and y directions.

(3) As multi-body correlation factors, a doublon-holon binding factor important for Mott physics and an on-site Gutzwiller factor, are used to capture the essence of strong correlation.

By applying the VMC method with this wave function to the Hubbard (t-t'-U) model, we will elucidate the relationship between SC and anisotropy in electronic states in the strongly correlated regime.

[1] Y. Sato, *et al.*, Nat. Phys. **13**, 1074 (2017).
[2] S. Kawasaki, *et al.*, Nat. Commun. **8**, 1267 (2017).
[3] B. Edegger, V. N. Muthukumar, and C. Gros, Phys. Rev. B **74**, 165109 (2006); H. Yamase and W. Metzner, Phys. Rev. B **73**, 214517 (2006).

Keywords: Cuprate superconductor, Hubbard model, Nematicity, Pomeranchuk instability

PCP9-3

The coexisting state of the staggered flux and d-wave superconducting order in a t-J type model

*Shuhei Fukuda[1], Kunito Yamazaki[1], Hiroki Tsuchiura[1], Masao Ogata[2]

Department of Applied Physics, Tohoku University, Japan[1]
Department of Physics, University of Tokyo, Japan[2]

A series of experimental studies have revealed that the pseudogap (PG) phase found in underdoped cuprate superconductors is accompanied by a phase transition with broken-symmetries. It has also been suggested that the pseudogap phase and d-wave superconductivity (dSC) can coexist roughly in the first half of the superconducting dome. One of the experimental evidences of the coexisting pseudogap phase with dSC is a gap-structure in the ARPES data opening with broken particle-hole symmetry found in Bi-2201 [1].

Quite recently, we have shown that the observed gap-structure can be understood if we assume that the staggered flux (SF) state exists in the PG phase and also the first half of the dome. However, theoretically, it has been pointed out not only that the SF state does not have a lower energy than dSC, but that the SF and dSC state do not coexist [2].

In this contribution, we reexamine the stability the of the SF phase based on the t-J model with a nearest-neighbor Coulomb repulsion term, within the Gutzwiller approximation and mean-field theory. We find that the SF can coexist with dSC around the first half of the dSC dome in the calculated phase diagram, and that the SF phase appears above the dSC dome. We also find the so-called two-gap structure in the quasiparticle spectra of the coexisting state, which is consistent with those observed by ARPES experiments.

[1] M. Hashimoto, et al., Nature Phys. **10**, 483-495 (2014).
[2] H. Yokoyama, S. Tamura, and M. Ogata, J. Phys. Soc. Jpn. **85**, 124707 (2016).

Keywords: Cuprate, Pseudogap, Staggered flux, Coexisting state

PCP9-4

Antiferromagnetism, superconconductivity, renormalization and phase diagram in materials with strong correlation

*Takashi Yanagisawa[1]

National Institute of Advanced Industrial Science and Technology[1]

It is important to clarify the mechanism of high-temperature superconductivity. We investigate electronic properties of correlated electron systems by using the optimized variational Monte Carlo method. This method is suitable in the study of a strongly correlated electron system [1,2]. Our wave function gives the best estimate of the ground-state energy of the two-dimensional Hubbard model and also the three-band model with d and p orbitals. We argue that high-temperature superconductivity occurs in the strongly correlated region (Fig.1). It is important to control antiferromagnetic correlation in materials with strong correlation to realize high-temperature superconductivity. This is achieved by optimizing band and interaction parameters in candidate materials with strong correlation.

[1] T. Yanagisawa, S. Koike, K. Yamaji: J. Phys. Soc. Jpn. 67, 3867 (1998).
[2] T. Yanagisawa: J. Phys. Soc. Jpn. 85, 114707 (2016).

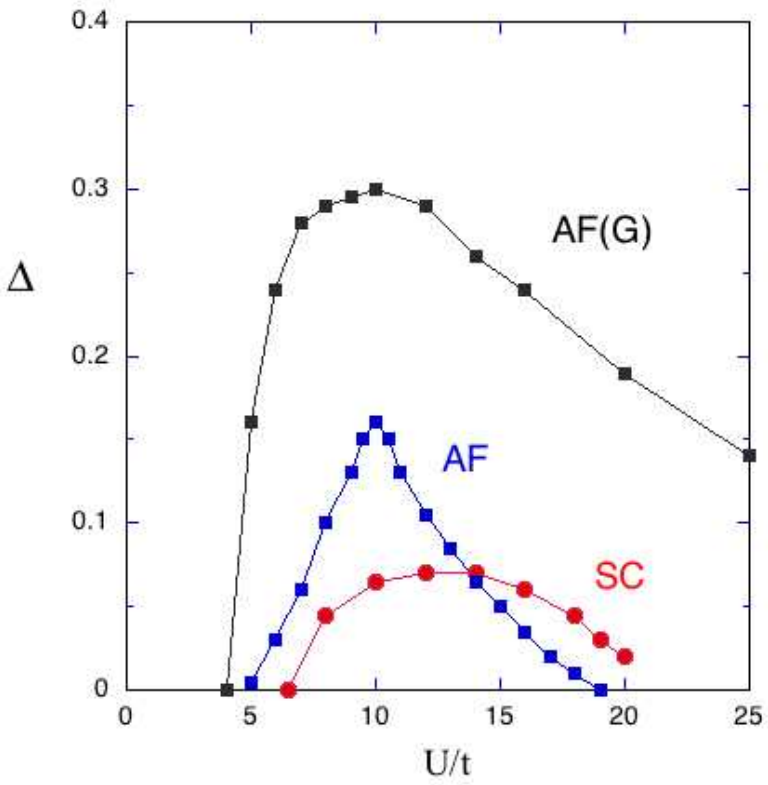

Keywords: high-temperature superconductivity, mechanism of superconductivity, phase diagram, many-body effect

PCP9-5

Electronic Structure of Novel Non-centrosymmetric Superconductor Mg_2Rh_3P

*Izumi Hase[1], Takashi Yanagisawa[1], Akira Iyo[1], Hiroshi Eisaki[1], Kenji Kawashima[2]

National Institute of Advanced Industrial Science and Technology (AIST)[1]
IMRA Material R&D Co. Ltd.[2]

Superconducting materials without inversion symmetry attract much attention due to the possibility of exotic parity mixing of the order parameter by the spin-orbit interaction (SOI). Among them, $Li_2(Pd_{1-x}Pt_x)_3B$ series have been vigorously studied since we can control the effective strength of SOI [1]. Moreover, this system is also favorable for constructing effective model because its point-group is cubic [2]. Recently we have discovered another non-centrosymmetric superconducting compound Mg_2Rh_3P which has the same crystal structure as $Li_2(Pd_{1-x}Pt_x)_3B$ [3]. In this paper we investigated the electronic structure of Mg_2Rh_3P and hypothetic Mg_2Ir_3P from first principles. The density of states at the Fermi level (=$D(E_F)$) of Mg_2Rh_3P is very small (8.3 Ry^{-1} per Mg_2Rh_3P), and the Fermi level (E_F) is located at almost a dip of DOS. This is consistent with the experimental finding that the superconductivity only appears when Mg is deficient, i.e. the composition of the superconducting phase is ~$Mg_{1.9}Rh_3P$. On the other hand, hypothetical compound Mg_2Ir_3P has rather large $D(E_F)$, 14Ry^{-1} per Mg_2Ir_3P. As for Mg_2Ir_3P, E_F is also located at almost the dip of DOS. This difference mainly comes from the more expanded Ir-5d orbital than Rh-4d orbital.

[1] K. Togano *et al.* Phys. Rev. Lett. **93** (2004) 247004, P. Padica *et al.* J. Phys. Soc. Jpn. **74** (2005) 1014.
[2] K. V. Samokhin and V. P. Mineev, Phys. Rev. B **77** (2008) 104520.
[3] A. Iyo *et al.* in preparation.

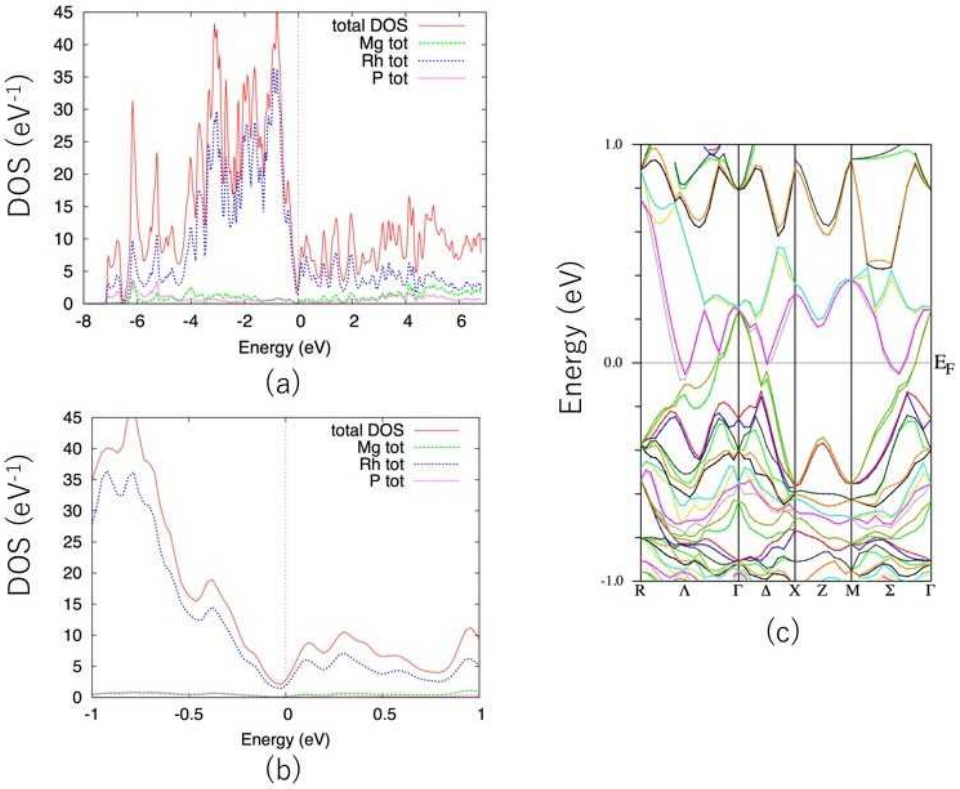

Fig. (a) Overview and (b) Close-up view near E_F of DOS of Mg_2Rh_3P. (c) Energy dispersion of Mg_2Rh_3P.

Keywords: Mg2Rh3P, Non-centrosymmetric Superconductor, first-principles calculation, spin-orbit interaction

PCP9-6

Effect of impurity potential on superconductivity in strongly correlated Hubbard model

*Ryo Sato[1], Hisatoshi Yokoyama[1]

Tohoku University Japan[1]

In contrast to previous studies, in which d-wave superconductivity resulted, recent more accurate numerical studies on the t-J, Hubbard, and d-p models showed that antiferromagnetic (AF) order, instead of superconducting (SC) order, extensively prevails in the underdoped regime [1], which is inconsistent with the behavior of cuprates. One possible reason for this discrepancy is that the inhomogeneity inherent in cuprates is disregarded in most theoretical models. It is important to clarify how this inhomogeneity affects the physics realized in the homogeneous models. The inhomogeneity in cuprates originates in the potential of dopant atoms, excess or loss of oxygen atoms, and deformation of lattice sites, and so on. We started a study of a simple case, namely, point-type impurity potential V (repulsive or attractive) for paramagnetic (or normal) and AF states in the two-dimensional Hubbard (t-t'-U) model, using a variational Monte Carlo (VMC) method [2]. It is found for strong correlations (U>W=8t) that V is strongly (sometimes almost completely) screened, and impurity-induced (filling-control-type) Mott transitions arise in peculiar conditions: The state becomes Mott insulating at a partially filling, or metallic at half filling. This research showed that AF orders remain robust.

In this study, we extend this framework of VMC to a SC state. Actually, we use a Jastrow-type wave function $\Psi=P\Phi$ (P: projectors, Φ: a one-body Slater determinant). In the previous studies [2], random impurity effects are included in Φ. However, we would like to consider in a certain way: Similarly to [2], we solve a Bogolioubov-de Gennes equation that includes the information of random impurity potential, and construct a one-body part [3]. Many-body effects, introduced through P, are distinguished between impurity and host sites.Details and results will be discussed in the presentation.

[1] R. Sato, H. Yokoyama: J. Phys. Soc. Jpn. 85, 074701 (2016) and references therein; and submitted to J. Phys. Soc. Jpn. [2] H. Yokoyama, R. Sato, K. Kobayashi, J. Phys. Conf. Ser. 871, 012032 (2017); ibid. 1054, 012014 (2018). [3] For example, S.-D. Liang, T. K. Lee: Phys. Rev. B 65, 214529. [4] T. M. Rice and W. F. Brinkman, Phys. Rev. B 5, 4350 (1972).

Keywords: Hubbard model, impurity, strong interaction, variational Monte Carlo

PCP9-7

Nonlinear dynamics of Josephson junction networks driven by external currents with spatiotemporal modulation

*Takaaki Kawaguchi[1]

Toho University, Japan[1]

Nonlinear dynamics of phases and vortices in Josephson junction networks (JJN) in an external magnetic field is studied using a computer simulation based on the resistively shunted junction model. We consider JJN which consists of a two- or one-dimensional array of superconducting grains where each pair of the nearest-neighbor sites is connected by a Josephson junction. The array has some type of structural disorder. We focus on the spatiotemporal dynamics of JJN with disorder in the presence of both dc and spatiotemporally modulated currents. The dynamics of JJN shows complicated behaviors, and the dynamical properties depend on some controllable parameters. There exist some synchronization phenomena and related dynamical correlation under certain conditions. Due to the effect of randomness in the system, there also appear inhomogeneous behaviors in dynamical states, such as plastic vortex flow. We clarify the details of the spatiotemporal dynamics of JJN in comparison with the dynamics of another related system. The physical mechanism that governs the synchronization dynamics and dynamical correlation effects of JJN in the presence of disorder are also clarified.

WBP1-1

Improvement of anisotropy of superconducting properties in Y-rich $YBa_2Cu_3O_y$ film in magnetic field

*Motoki Shiomi[1], Yusuke Ichino[1], Yuji Tsuchiya[1], Ataru Ichinose[2], Yutaka Yoshida[1]

Nagoya Univ.[1], CRIEPI[2]

The introduction of artificial pinning centers (APCs) effectively enhances the flux pinning properties in $REBa_2Cu_3O_y$ (REBCO: RE = rare earth) films. Especially, Y_2O_3 and Y_2BaCuO_y (Y211) are reported as one of the APC materials which forms nano-particles within REBCO films, and they are expected to improve the anisotropy of the critical current density in a magnetic field [1, 2]. It has also been reported that superconducting properties change by increasing RE composition [3].

Our goal is to fabricate a REBCO film that there are no anisotropy of J_c angular dependence at sub-cooling temperature of liquid nitrogen (65 K). We fabricated $Y_{1+x}Ba_2Cu_3O_y$ (Y_{1+x}BCO) films by pulsed laser deposition (PLD) method, and investigated the dependence of critical current density (J_c) in magnetic field on x, substrate temperatures (T_ss) and repetition frequency of the pulsed laser (f_Ls). Fig. 1 (a) shows angular dependence of critical current density ($J_c - B - \theta$) of Y_{1+x}BCO films at 65 K and 3 T those films were fabricated at T_s = 840ºC and f_L = 20 Hz. It shows as x increases, J_c around θ = 0º enhanced up to x = 0.2, and the behavior of J_c - B - θ also changed greatly due to the difference in x, so we found the optimum x for improving the characteristics in the magnetic field was 0.2. When x is 0.4 or more, it is considered that the size of APC is so large as to inhibit the superconducting current due to excessive addition of Y. Fig. 1 (b) shows f_L dependence of J_c - B - θ with x = 0.2, and isotropy of J_c was improved by decreasing f_L. From the viewpoint of the minimum J_c value around θ = 90°, it was found the f_L = 5 Hz film shows the highest value, while in the other applied angle range, J_c of the f_L = 10 Hz film was the highest. It indicates that the number density and size of APCs change depending on the deposition rate. The dependency of the substrate temperature will also be explained on site.

This work was partly supported by a Grant-in-Aid for Scientific Research (15K14301、15K14302、16K20898), Japan Science and Technology Agency (JST): Advanced Low Carbon Technology Research and Development Program (ALCA).

[1] P. Mele *et al.*: Supercond. Sci. Technol. **21**, 125017 (2008).
[2] T. Haugan *et al.*: Nature **430**, 867 (2004).
[3] Wang H *et al.*: *J. Appl. Phys.* **100** 053904 (2006).

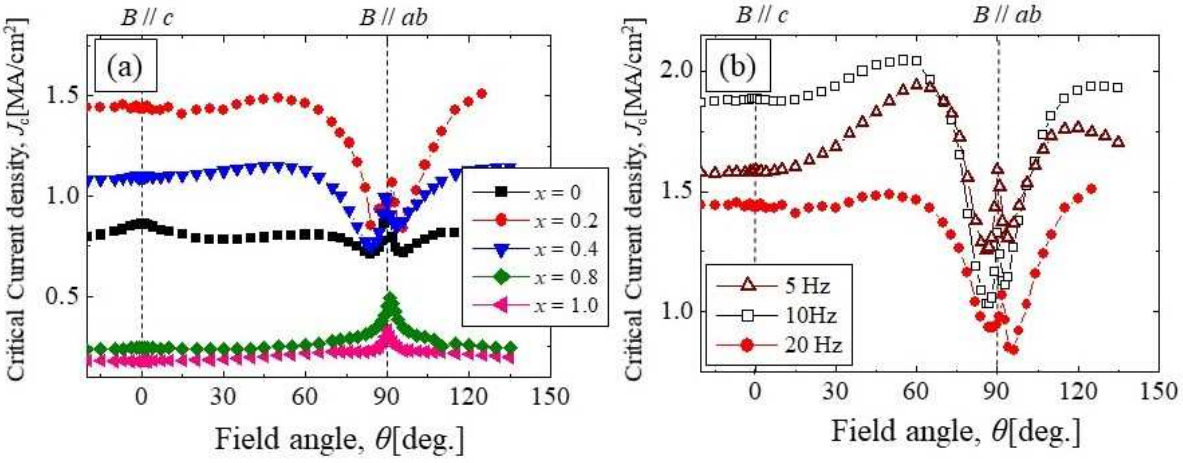

Fig.1 Magnetic field angular dependence of J_c at 65 K under 3 T (a) fabricated at f_L = 20 Hz with x = 0 - 1.0 and (b) at f_L = 5 - 20 Hz with x = 0.2.

Keywords: anisotropy, nano-particles

WBP1-2

Deposition of Ag thin film by reel-to-reel pulsed laser deposition system

*Jin Matsuzaka[1], Yuji Tsuchiya[1], Yusuke Ichino[1], Yutaka Yoshida[1]

Nagoya University[1]

Ag are deposited on REBCO tapes as a stabilizing layer. The metal stabilizing layer protects the superconducting layer from moisture and corrosion. Furthermore, the layer also bypasses current and diffuses heat when dissipation exists in the superconducting layer. In most cases, the Ag layer is fabricated by a sputtering method. The sputtering method has an advantage of a large deposition area, and on the other hand, it has a disadvantage of a low deposition yield. Due to the wasted material, the material cost increases when an expensive material such as Ag is used. In the case of the pulsed laser deposition (PLD) method, a small deposition range and high deposition yield. Therefore, in this study, we fabricated Ag thin films on metal tapes by a reel-to-reel PLD system to improve the deposition yield compared with the sputtering method.

Ag was deposited on Hastelloy tapes in a vacuum of 10^{-3} Pa using a PLD method with a KrF excimer laser (wavelength: 248 nm). The deposition parameters were as follows: the laser energy was 90 mJ, the repetition frequency was 100 Hz, the distance between target and substrates was 40-80 mm, and the laser spot size was 1.8-2.2 mm^2. Figures 1(a) and 1(b) shows the dependency of the deposition rate in the PLD method on (a) the distance between the target and the substrates and (b) the laser spot size. The deposition rate increased at the closer target-substrate distance or the larger laser spot size. Figures 1(c) and 1(d) are SEM images of an Ag thin film fabricated by the PLD method and the sputtering method. In the PLD film, many droplets with sizes of 1-5 μm were observed. The particle size was small as 100 nm or less. The sputtering film also has about the same particle size. The average surface roughness Ra was 2.44 nm in the PLD film, and was 1.89 nm in the sputtering film. Since the droplets are large, Ra of the PLD film is larger than that of the sputtering film.

In this presentation we will report about the Ag stabilizing layer fabricated by moving system and the Ag deposition yield of the PLD and sputtering methods.

This work was partly supported by JST-ALCA.

[1]A. C. Carter *et al:* J. Mater. Res. **13**(1998) 6

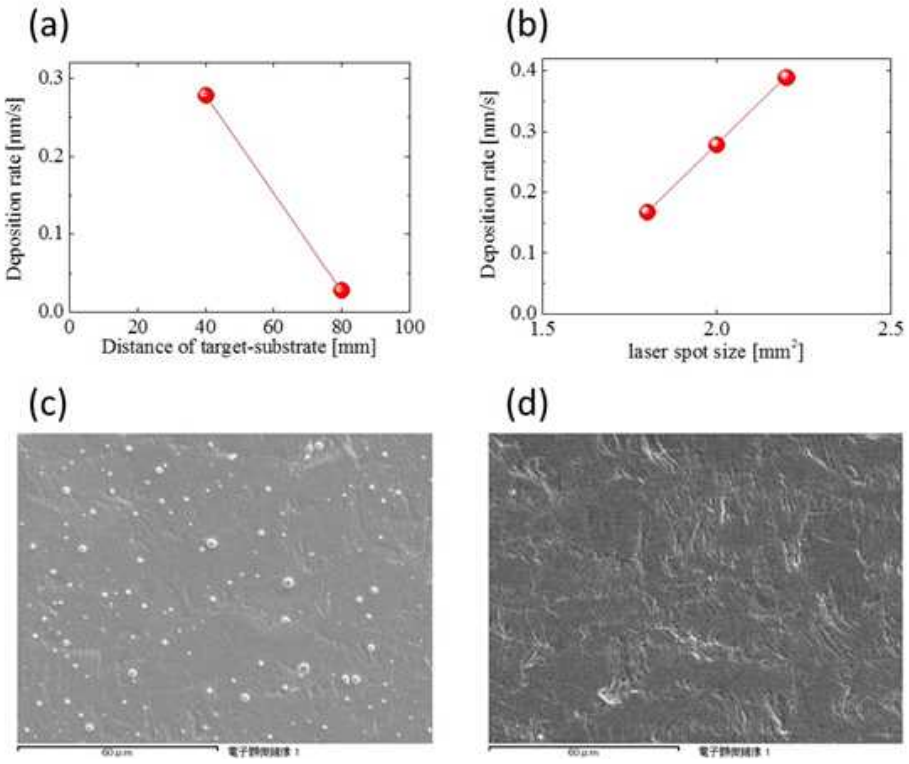

Fig.1 (a) Distance between target and substrate and (b) laser spot size dependence of deposition rate, SEM image of Ag films deposited by (c) PLD and (d) sputtering method.

Keywords: Stabilizing layer, Ag thin film

WBP1-3

Effects of $Sm_{1+x}Ba_{2-x}Cu_3O_y$ films with non-stoichiometric composition fabricated by combinatorial pulsed laser deposition method on the superconducting properties

*Gohki MURASE[1], Yusuke ICHINO[1], Yuji TSUCHIYA[1], Yutaka YOSHIDA[1]

Dept of Electrical Engineering,Nagoya Univ.[1]

$REBa_2Cu_3O_y$ films have high critical current density (J_c), so that they are expected to be applied for various applications. Our group reported that $Sm_{1+x}Ba_{2-x}Cu_3O_y$ (Sm-rich) thin films to be changed the composition had higher J_c in magnetic fields and irreversible fields than stoichiometric $SmBa_2Cu_3O_y$ (SmBCO) thin films [1, 2]. We reported that the Sm-rich films had many dislocations and Low-T_c phases due to Sm/Ba substitution and they acted as artificial pinning centers (APCs). On the other hand, Ichinose *et al.* suggested that Sm-rich films which contained APCs such as $BaSnO_3$ (BSO) had lower superconducting properties in magnetic fields than those of a stoichiometric SmBCO film with BSO [3]. They inferred that superconducting phases need more Ba atom than BSO and then lack of Ba atoms for formation of BSO nanorods.

It has not been detailed discussions about properties of Sm-rich films contained Low-T_c phases and $BaMO_3$ (M = metal) with changing x. In this study, to clarify the features of APC doped Sm-rich films, we fabricated $Sm_{1+x}Ba_{2-x}Cu_3O_y$ films using combinatorial pulsed laser deposition (C-PLD) method with x = 0.00 ~ 0.20 on a metallic substrate. C-PLD method enables to prepare a film with continuously changing composition across a single substrate [4]. We prepared films which were changed the substrate temperatures (T_s) from 800°C to 880°C. The Sm-rich films were annealed at 350°C in oxygen flow. We investigated effects of x and T_s on superconducting properties.

Fig. 1(a) shows critical temperature (T_c) and c-axis length depending on x in the T_s of 840°C. This graph indicates that T_c decreases and c-axis length also decreases as x increases. Even in the same sample, there is T_c distribution from 89.8 K to 92.7 K. We found the similar feature in films deposited at 800°C and 880°C. Fig. 1(b) shows J_c in magnetic fields. J_c values decrease as x increases. We will discuss superconducting properties of APC doped Sm-rich films compared with non-APC doped Sm-rich films.

This work was partly supported by JSPS (16K20898, 16H04512), JST-ALCA. The metal substrates were provided from AIST.

[1] Y. Yoshida, *et al.*: Jpn. J. Appl. Phys. **44** (2005) L546-L548; [2] M. Miura, *et al.*: Jpn. J. Appl. Phys. **45** (2006) L701-L70; [3] A. Ichinose, *et al.*; J. Japan Inst. Met. Mater. **80** (2016) 420-427
[4] H. Koinuma, *et al.*: Nature Mater. **3** (2004) 429-438

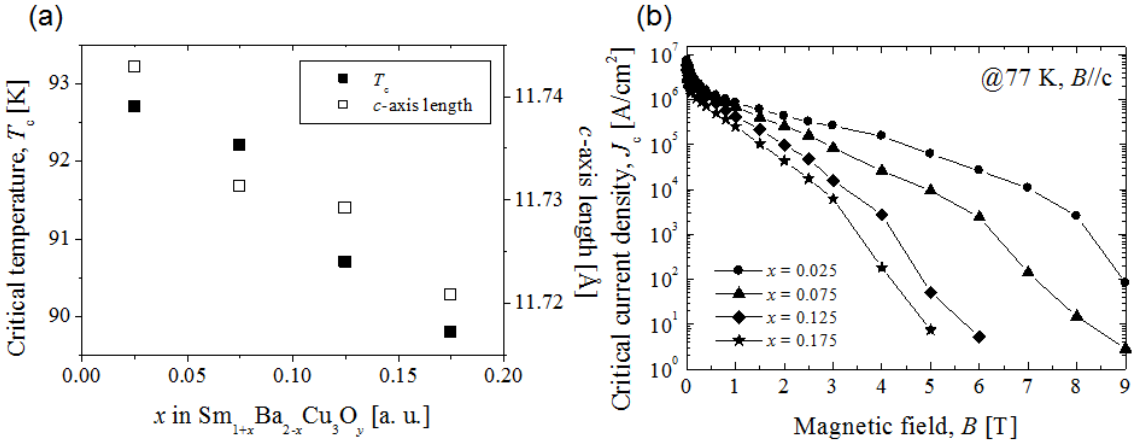

Fig. 1 (a)Criitical temperature(T_c) and c-axis length depending on x, and (b)critical current density(J_c) in magnetic fields. The film was deposited at 840°C

Keywords: Sm1+xBa2-xCu3Oy , thin films, Combinatorial Pulsed Laser Deposition, non-stoichiometric composition

WBP1-4

Evaluation of superconducting properties for $YBa_2Cu_3O_y$ coated conductors fabricated by self-heating technique in Pulsed Laser Deposition method

*Sato Wataru[1], Yuji Tsuchiya[1], Yusuke Ichino[1], Yutaka Yoshida[1]

Department of Electrical Engineering, Nagoya University, Japan[1]

$REBa_2Cu_3O_y$ (REBCO) coated conductors (CCs) is expected for high critical currents (I_c). In order to improve the I_c, it is essential to increase the film thickness while maintaining the high critical current density (J_c). However, it has been reported that *a*-axis oriented grains as the film thickness increases are generated and J_c decreases[1]. The occurrence of *a*-axis grains is due to decrease of surface substrate temperature (T_s) during deposition. Thus, many research groups have studied the method of heating substrate. For example, one of the methods is self-heating (S-H) technique. This technique is a method to heat the substrate by the Joule effect after applying a heating current through the Hastelloy metal substrates. The system provides rapid thermal response compared with the conventional heating system that heats the substrate with a heater[2]. Therefore, it is possible to suppress *a*-axis grains during deposition by S-H technique. In this study, we fabricated $YBa_2Cu_3O_y$ (YBCO) CCs on IBAD-MgO substrates which were heated by S-H technique in pulsed laser deposition (PLD) method. T_s was measured by pyrometer before deposition. We fabricated a thick film of which thickness was about 3 μm was prepared under the conditions of T_{s0} = 850°C, oxygen partial pressure P_{O2} = 400 mTorr, and laser energy density D = 1.25 J/cm^2. In addition, T_s was changed, following Eq. 1, during the film deposition.

$$T_s(t) = T_{s\infty} - (T_{s\infty} - T_{s0}) \exp(-t/\tau) \quad (1)$$

In Eq. 1, the $T_s(t)$ pattern depending on deposition time (t) can be changed by the time constant τ s. We studied the orientation and supeconducting properties of the thick film by changing τ.
Fig. 1 shows XRD intensity ratio of *a*-axis peak of YBCO (200) to *c*-axis peak of YBCO (005). It was confirmed that *a*-axis grains was suppressed by decreasing τ. J_c was 0.32 MA/cm^2 (77 K, 0 T) when T_s was fixed T_{s0}. On the other hand, J_c reached 1.65 MA/cm^2 (77 K, 0 T) at τ = 1500 and $T_{s\infty}$ = 1045°C. We will discuss *a*-axis grains ratio and J_c at various film thicknesses and τ.
This work was partly supported by JSPS (16K20898 and 16H04512), JST-ALCA project. The metal substrates were provided from AIST.

[1] L. Zeng et al., J. Appl. Phys. 112 (2012) 053953
[2] G. Majkic et al., IEEE Trans. Appl. Supercond. 25 (2015) 3

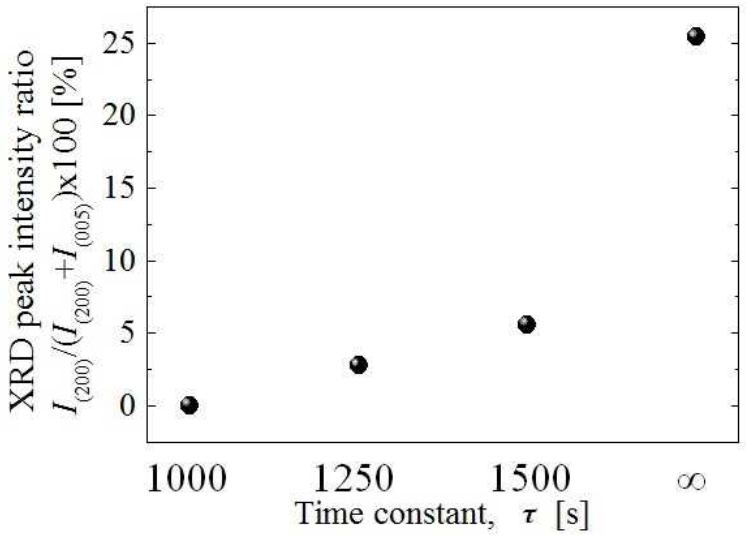

Fig. 1 XRD peak intensity ratio of YBCO films with the thickness of 3 mm depending on time constant.

Keywords: YBCO, PLD method, self-heating technique

WBP1-5

Liquid phase stabilization and superconducting properties by adding Ag to $SmBa_2Cu_3O_y$ coated conductors fabricated by Vapor-Liquid-Solid growth technique

*Kento Yasuda[1], Tomohiro Ito[1], Yuji Tsuchiya[1], Yusuke Ichino[1], Ataru Ichinose[2], Yutaka Yoshida[1]

Department of Electrical Engineering, Nagoya University, Japan[1]
Central Research Institute of Electric Power Industry, Japan[2]

In fabricating $REBa_2Cu_3O_y$ (REBCO) superconducting coated conductors, in order to reduce the production cost of superconducting coated conductors, it is necessary to increase the deposition rate. However, when using the conventional method, the crystallinities of the REBCO layer are deteriorated by increasing the deposition rate. From our early studies, by using the VLS (Vapor Liquid Solid) growth technique, we found that the VLS technique is possible to fabricate favorable crystallinities and high deposition rate. Oxygen partial pressure was increased as increasing deposition rate. However, since the melting point of the liquid phase increased with increasing the oxygen partial pressure, the liquid phase partially solidified. Therefore, we attempted to add Ag for the purpose of lowering the melting point of the $Ba_3Cu_7O_{10}$ (nominal composition of the liquid phase) [*]. In this study, we focused on the stability of the liquid phase adding Ag and aimed to improve superconducting properties of superconducting coated conductors fabricated by Vapor-Liquid-Solid growth technique.The VLS growth technique consists of the following three steps by Pulsed Laser Deposition (PLD) method. The first step is to fabricate a solid Sm123 layer. The second step is to form a liquid layer on the solid layer. As described above, this liquid phase target contains Ag. The last step is to supply Sm123 through the vapor phases on the liquid and solid layer.

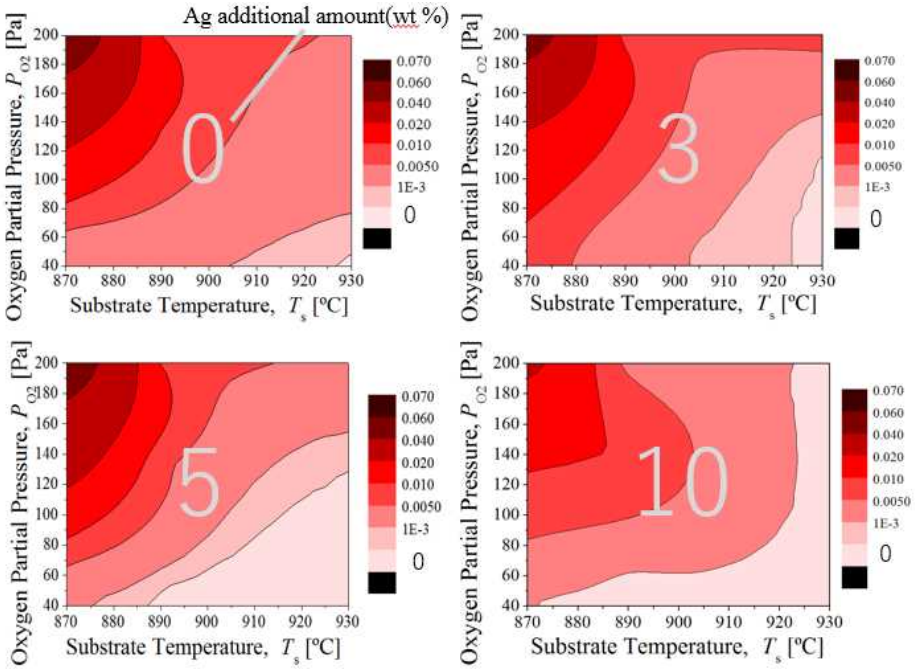

Fig. 1 shows contour plots of XRD peak intensity ratio of $BaCuO_2$ to CeO_2 depending on substrate temperature and oxygen partial pressure and Ag additional amount. The shading of color represents the XRD peak intensity ratio. It can be seen that regions, where the peak intensity is low in the lower right part of the figures, become wider with increasing Ag. Therefore the liquid phase is more likely to be generated. From this result, it is considered that addition of Ag lowers the melting point, so that the liquid phase generation region expands. Consequently, By adding Ag to the liquid phase of the VLS growth technique, it is possible to fabricate the film with favorable crystallinity at higher speed.

This work was partly supported by JSPS (16H04512,16K20898), JST-ALCA, and NU-AIST alliance project. The metal substrates were provided from AIST.[*] T. Ito *et al.*: The 96th CSJ Spring Meeting 2018

Keywords: superconducting coated conductors, Vapor-Liquid-Solid growth technique

WBP1-6

Crystallinities and superconducting properties of $SmBa_2Cu_3O_y$ coated conductors using Vapor-Liquid-Solid growth techniques.

*Tomohiro Ito[1], Yuji Tsuchiya[1], Yusuke Ichino[1], Yutaka Yoshida[1]

Nagoya univ.[1]

In order to apply $REBa_2Cu_3O_y$ (RE123) superconducting coated conductors (CCs), it is indispensable to reduce the fabrication cost. That is why the CCs are required to increase deposition rate and crystallinities. In order to reduce fabrication, we used Vapor-Liquid-Solid (VLS) growth technique, combing pulsed laser deposition (PLD) methods and liquid phase epitaxy (LPE) methods [1]. In this study, we aimed to improve both deposition rate and crystallinities using VLS growth techniques, especially changing O_2 partial pressure to increase deposition rate and conducted thickening CCs to improve superconducting properties such as critical current density (J_c).

The VLS growth technique consists of the following three steps by PLD method. The first step is to fabricate a solid Sm123 layer. The second step is to form a liquid layer on the solid layer. The last step is to supply Sm123 through the vapor phases on the liquid and solid films.

We achieved increasing a deposition rate from 7.02 nm/sec to 27.5 nm/sec by changing O_2 partial pressure. A deposition rate and a film thickness and a J_c reached 27.5 nm/sec and 1.7 mm and 1.67 MA/cm^2, respectively [2].Furthermore, we fabricated thick films to improve superconducting properties. We supplied liquid phase and Sm123 using surface modified target of Sm123 by Ba-Cu-O to prevent evaporation of liquid phase. Using this modified target, we achieved fabricating thickened CCs of 4.0 mm. Fig. 1 shows a cross-sectional TEM image of a Sm123 film with the thickness of 4 mm using VLS growth techniques. From this image, there are little defects in VLS-Sm123 films. Fig. 2 shows crystallinities of Sm123 films prepared by PLD method and VLS growth techniques. There are no *a*-axis oriented grains in the films prepared by VLS growth technique. Moreover, it was confirmed that the FWHM of the Sm123 006 reflection decreases with increasing the film thickness. It is clear that we could fabricate CCs having high crystallinities when thickened using VLS growth techniques. We will discuss the superconducting properties of APC-doped VLS-Sm123.

This work was partly supported by JSPS (16H04512, 16K20898), JST-ALCA.

[1] A. Kursumovic *et al.*: Supercond. Sci Technol. **17** (2004)

[2]T. Ito *et al.*: The 96th CSJ Spring Meeting 2018

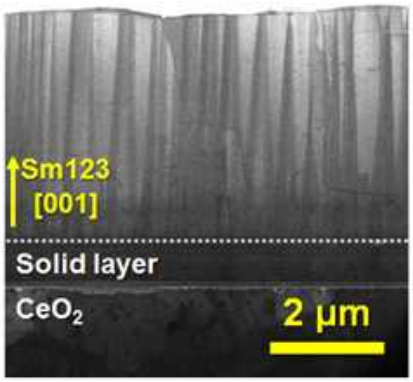

Fig. 1 Cross-sectional TEM image of a Sm123 film prepared by VLS growth technique with the thickness of 4 μm.

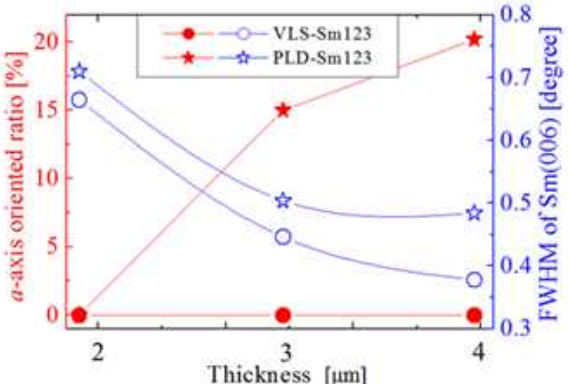

Fig. 2 film thickness dependence of crystallinities such as (left vertical axis) ratio of a-axis oriented grains and (right vertical axis) FWHM of Sm123 006 reflection.

Keywords: Vapor-Liquid-Solid growth technique, thick films, superconducting coated conductor

WBP2-1

The Influence of $BaHfO_3$ nanorods on J_c in the longitudinal magnetic field for PLD $EuBa_2Cu_3O_y$ coated conductors

*Jun Nishimura[1], Kenji Miyata[1], Kota Hirai[1], Masashi Miura[1], Akira Ibi[2], Teruo Izumi[2], Masaru Kiuchi[3], Teruo Matsushita[3]

Seikei University Japan[1]
AIST Japan[2]
Kyushu Institute of Technology Japan[3]

T. Matsushita *et al.* proposed that a superconducting DC cable employing a longitudinal magnetic field (i.e., a Lorentz force-free cable) can achieve higher current-carrying capacity compared with a conventional superconducting cable [1]. $REBa_2Cu_3O_y$ *(REBCO, RE = rare earth element)* coated conductors (CCs) produced by Pulse Laser Deposition (PLD) are promising candidates for power applications, such as superconducting DC cables, because of their high reproducibility and high superconducting performance. However, for a practical force-free cable using the PLD-REBCO CCs, it is necessary to further enhance the critical current density (J_c) in longitudinal magnetic field. Recently, artificial defects in PLD-REBCO films have been found to be effective for enhancement of J_c in longitudinal magnetic field [2].

In this work, we prepared different mol% of $BaHfO_3$ nanorod (BHO NR) doped PLD-$EuBa_2Cu_3O_y$ (+3.5 BHO and +5.0 BHO) CCs to investigate the influence of the BHO density of the NR on the longitudinal magnetic field. The critical temperature of the +3.5 BHO and +5.0 BHO CCs are almost the same as that of standard EuBCO CC. The +3.5 BHO CC shows a J_c of 4.3 MA/cm^2 at 77 K and 0.5 T longitudinal magnetic field, which is higher than that of +5.0 BHO and standard EuBCO CCs under the same conditions. We will discuss the influence of BHO NR on J_c in longitudinal magnetic field for PLD-EuBCO CCs based on microstructures and in-field J_c measurements.

Acknowledgements: This work was supported by a research grant from the Japan Power Academy. A part of this work is supported by JSPS KAKENHI (17H03239 and 17K18888).

Reference:
[1] T. Matsushita *et al.*, *AIP Conf. Proc* **1574** (2014) 225.
[2] K. Sugihara *et al.*, *Supercond. Sci. Technol.* **28** (2015) 104004.

Keywords: Critical Current, Longitudinal Magnetic Field, PLD, Coated Conductor

WBP2-2

Influence of $BaHfO_3$ nanorods on in-field J_c in $EuBa_2Cu_3O_y$ coated conductors produced by PLD

*Shuji Anno[1], Kenji Miyata[1], Masashi Miura[1], Akira Ibi[2], Teruo Izumi[2]

Seikei University, Japan[1]
AIST, Japan[2]

Pulsed Laser Deposition (PLD) is one of the most attractive processes to produce long length $REBa_2Cu_3O_y$ (REBCO, RE=rare earth) coated conductors (CCs) because of the high superconducting performance and reproducibility. However, for magnet applications, even higher in-field critical current density (J_c) is required. The addition of artificial pinning centers, such as BMO (M=Zr, Sn, Hf) nanorods [1] and nanoparticles [2], into REBCO CCs is an effective way to achieve higher in-field performance. It has been reported that PLD- EuBCO CCs with $BaHfO_3$ nanorods (BHO NRs) show higher in-field J_c compared with that of CCs with BZO NRs[3]. For further enhancement of the in-field J_c for PLD-REBCO CCs, understanding the effect of size, density, distribution and shape of the BHO NRs on in-field performances is very important.

In this work, we prepared PLD-EuBCO CCs with and without BHO NRs in order to investigate the effect of BHO NRs on in-field performance. The PLD-EuBCO+BHO NRs CC show slightly lower T_c and self-field J_c ($J_c^{s.f.}$) compared to that of samples without BHO NRs because oxygen deficient regions surrounding the NRs due to *c*-axis expansion by coherent interface [1] slightly degrade these properties. On the other hand, the in-field J_c for PLD-EuBCO+BHO NRs CC is higher at 77 K, in all fields compared to that of PLD-EuBCO CC. Moreover, The minimum J_c as a function of angle at 77 K, 3 T in +BHO CC is 0.42 MA/cm^2, which is 1.8 times higher than samples without BHO NRs. We will discuss the influence of BHO NRs on the in-field J_c and flux pinning properties in PLD-EuBCO CCs at various magnetic field angles and amplitudes.

Acknowledgements: This work is supported by the New Energy and Industrial Technology Development Organization (NEDO) and the Fujikura Foundation. A part of this work was supported by JSPS KAKENHI (17H03239 and 17K18888).

Refarence
[1] B. Maiorov *et al., Nature Materials* **8**, (2009) 398.
[2] M. Miura *et al., NPG Asia Materials* **9 (2017) e447.**
[3] H. Tobita, *et al.* : *Supercond. Sci.Technol*, **25** (2012) 062002.

Keywords: Coated Conductor, REBCO, PLD, Critical Current

WBP2-3

Improved pinning in Zn doped $YBa_2Cu_3O_{6+\delta}$ films

*Kai Ackermann[1], Jens Hänisch[1], Bernhard Holzapfel[1]

Karlsruhe Institute Of Technology, Germany[1]

Among the high temperature superconductors, the *RE*BCO compounds are widely known for their high current carrying capacity at liquid nitrogen temperature. For that reason, most of the ongoing investigations focus on improving the pinning properties at 77 K by adding nanocolumnar or nanoparticulate defects, like $BaHfO_3$ or $BaZrO_3$. Beside these characteristics, *RE*BCO materials offer the capability for high magnetic field applications like NMR or MRI due to their high irreversibility field at low temperatures. Because of the small coherence length in this temperature regime, small-scale pinning centres like atomic defects are required to further improve the application-relevant properties, such as critical current density j_c, pinning force density F_p and anisotropy. Hence, we investigated the influence of Zn doping on such properties in the temperature range between 5 K and 50 K.
$YBa_2(Cu_{1-x}Zn_x)_3O_{6+\delta}$ film samples were prepared on $SrTiO_3$ and $(LaAlO_3)_{0.3}(Sr_2TaAlO_6)_{0.7}$ single crystalline substrates by pulsed laser deposition using a Nd:YAG laser (λ = 355 nm). The resistively and inductively measured transport properties of films with doping levels between x = 0.1% and x = 0.8% are presented in relation to the microstructure, which was determined by atomic force microscopy, scanning electron microscopy and x-ray diffractometry.

Keywords: REBCO, YBCO, PLD, Pinning

WBP2-4

In-Plane Anisotropy of Critical Current Density in $BaTbO_3$-doped $SmBa_2Cu_3O_y$ Films

*Hiroki Kato[1], Yuji Tsuchiya[1], Yusuke Ichino[1], Ataru Ichinose[2], Yutaka Yoshida[1]

Nagoya University, Japan[1], Central Research Institute of Electric Power Industry, Japan[2]

The artificial pinning centers (APCs) improve the superconducting properties in REBCO films in the fields. $BaTbO_3$ (BTbO) is one of the APC materials for the REBCO films[1]. There are few reports about the superconducting properties and the shape of APCs in the REBCO films with a large amount of BTbO. From our previous research, BTbO formed thick and rectangular nano-rods by using the TEM. The rectangular nano-rods probably produced an in-plane anisotropy for the flux pinning. In this study, we fabricated SmBCO films with high BTbO contents and investigated their transport properties.

BTbO-doped SmBCO films were fabricated on IBAD-MgO buffered metallic substrates by using the PLD method. The films had contents of BTbO up to 20.0vol.%. Field dependence of the critical current density J_c of films was measured at temperatures of 77 and 83 K and at fields of 0-9 T. TEM images showed that the shape of the BTbO-APC was rectangular. To clarify the in-plane anisotropy, J_c was measured at 77 and 83 K, 0-9 T and ϕ = 0° and 45°, where ϕ was defined as an in-plane angle from the *a* or *b*-axes of SmBCO. To fix the current direction, micro bridges were fabricated with different ϕ (= 0° and 45°) by using a laser etching as shown in Fig.1(a).

Figs.1(b) and (c) showed magnetic field dependence of J_c and normalized anisotropy of J_c in 0 and 12.0vol.% BTbO-doped SmBCO films at 77 and 83 K, *B*//*c*, respectively. The anisotropy showed a ratio of J_c between 0° and 45° and was normalized at 0 T. As a result, the anisotropy exceeded over 3 at fields more than 3 T and 7 T for 83 K and 77 K, respectively. On the other hand, J_c was isotropic in the pure film. The anisotropy of J_c in the BTbO-doped films was possibly explained by the anisotropy of flux pinning or irreversibility fields. We will compare the above results with the in-plane anisotropy in SmBCO films with various kinds of $BaMO_3$ materials.

[1] T. Yoshimura *et al.*: Physica C **471** (2011) 947-950.

This work was partly supported by KAKENHI (15H04252 and 16H04512). A part of this work includes the results supported by JST-ALCA. The IBAD-MgO metal substrates were provided from Dr. T Izumi, Dr. A Ibi, and Dr. T Machi of AIST.

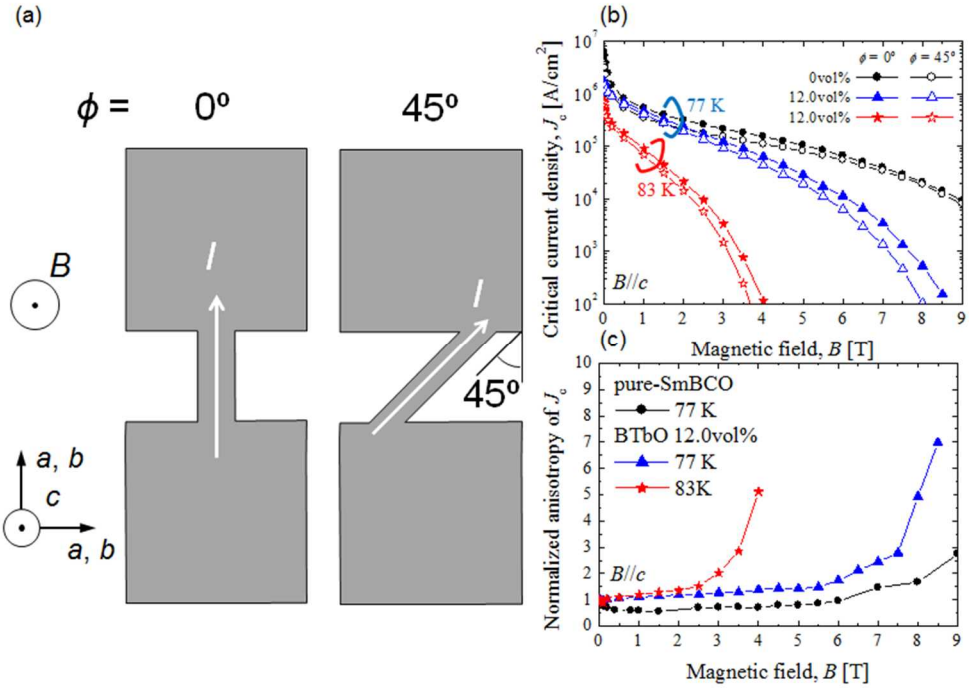

Fig. 1 (a) Schematic drawings of micro bridges in SmBCO films with ϕ = 0° and 45°. Magnetic field dependence of (b) J_c and (c) normalized anisotropy of J_c in BTbO-doped SmBCO films at 77 and 83 K, *B*//*c*, ϕ = 0° and 45°.

Keywords: High Temperature Superconductivity, Artificial pinning centers, BaMO3, Anisotropy of Jc

WBP2-5

Improvement of in-field performance for REBCO with heavily doped BMO coated conductors by PLD method

*Akira Ibi[1], Takato Machi[1], Koichi Nakaoka[1], Michio Sato[1], Teruo Izumi[1], Jun Nishimura[2], Masashi Miura[2], Daisaku Yokoe[3], Tomohiro Kato[3], Takeharu Kato[3], Tsukasa Hirayama[3]

National Institute of Advanced Industrial Science and Technology (AIST)[1]
Seikei University[2]
Nanostructures Research Lab. , Japan Fine Ceramics Center (JFCC)[3]

We have been investigated the long $REBa_2Cu_3O_X$ (REBCO, RE: rare earth element) with or without $BaMO_3$ (BMO, M: metal) coated conductors by the combination of the ion-beam assisted deposition (IBAD) and the pulsed laser deposition (PLD) method. We have found that $EuBa_2Cu_3O_X$ (EuBCO) with $BaHfO_3$ (BHO, 3.5 mol%) coated conductors show high critical current ($I_{c\ (min.)}$) of 144 A/cm-w at 77 K in 3T and 411 A/cm-w at 65 K in 3 T. However, in order to realize REBCO with BMO coated conductors for industrial and commercial applications, the much higher in-field performance is required.

It is known that critical temperature (T_c) of REBCO layers decreases with increasing amount of artificial pinning centers (APCs). It is thought that because of the strain of the REBCO by doping of APCs. Therefore, it is difficult to improve the critical current density (J_c) in magnetic field of REBCO with BMO coated conductors only by increasing doping amount of APCs. To solve this problem, we tried to optimize deposition conditions, especially deposition temperature, and O_2 annealing processes. We fabricated the EuBCO with BHO (3.5 - 10 mol%) coated conductors by the multi-plume and multi-turn PLD method with several different deposition temperature conditions. In addition, we tried to O_2 annealing process at relatively low temperature (200 - 300 ℃) still for long time. As a result of high temperature deposition and low temperature annealing, the T_c of EuBCO with BHO (10 mol%) coated conductors were 88.9 K at setting deposition temperature of 1095 ℃ and 93.9 K at setting deposition temperature of 1135 ℃, respectively, and $J_{c\ min.}$ of EuBCO with BHO (5 mol%) coated conductors was 0.57 MA/cm^2 at 77 K and 3 T (setting deposition temperature of 1150 ℃ and annealing temperature of 250 ℃). The details of the influence by the deposition conditions, annealing processes and in-field performance of EuBCO with hevily doped BHO coated conductors by PLD method will be discussed.

This work was supported by the New Energy and Industrial Technology Development Organization (NEDO), Advanced Medical Services from the Japan Agency for Medical Research and development (AMED), and Ministry of Economy, Trade and Industry (METI).

Keywords: REBCO with BMO coated conductors, heavy dope, deposition condition, annealing processes

WBP2-6

Development of high uniformity multi-filamentary structure long REBCO with BMO coated conductors by plane-plume PLD method

*Akira Ibi[1], Takato Machi[1], Koichi Nakaoka[1], Michio Sato[1], Teruo Izumi[1], Kohei Higashikawa[2], Takanobu Kiss[2]

National Institute of Advanced Industrial Science and Technology (AIST)[1]
Dept. of Electrical Engineering, Kyushu University[2]

Long $REBa_2Cu_3O_X$ (REBCO, RE: rare earth element) with $BaMO_3$ (BMO, M: metal) coated conductors have been expected for the industrial and commercial applications. It is known that critical current (I_c) of REBCO coated conductors (with or without artificial pinning centers) in magnetic field at high temperature is superior to the other superconducting wires. Especially, we have found that $EuBa_2Cu_3O_X$ (EuBCO) with $BaHfO_3$ (BHO) coated conductors show higher critical current densities (J_c) and I_c at high temperatures in self and magnetic fields than those of $YBa_2Cu_3O_X$ and $GdBa_2Cu_3O_X$ with BHO coated conductors. However, in order to realize EuBCO with BHO coated conductors for applications such as an armature coil, the much higher uniformity of not only longitudinal and but transversal I_c distributions of long coated conductors with high in-field performance for filamentary structure is required. The plane-plume PLD (pulsed laser deposition) method is performed by shortening the target-substrate distance and increasing the number of multi-plume with scam of X-Y axes directions to increase the deposition rate and obtain the uniformity I_c distributions. We fabricated the EuBCO with BHO coated conductors (of 0.6 m in length and 10 mm in width) by the combination of the ion-beam assisted deposition (IBAD) and the plane-plume PLD method and then we processed the multi-filamentary structure EuBCO with BHO coated conductors (of 8 filaments of 440 mm, 0.6 m in length and 5 mm in width) by using the excimer laser scribing to reduce the AC loss and shielding current. I_c distribution in a width direction of this EuBCO with BHO coated conductor was improved as an uniformity of filament-I_c of 4.3 %. Recently, we tried the fabrication of multi-filamentary structure long EuBCO with BHO coated conductors fabricated by the combination of plane-plume PLD and excimer laser scribing method. The details of uniformity of I_c distributions of multi-filamentary structure long EuBCO with BHO coated conductors will be discussed.

This work was supported by the New Energy and Industrial Technology Development Organization (NEDO), Advanced Medical Services from the Japan Agency for Medical Research and development (AMED), and Ministry of Economy, Trade and Industry (METI).

Keywords: plane-plume PLD, long REBCO with BMO coated condutors, uniformity of Ic distributions, laser scribing method

WBP3-1

The Effect of the Ba/Y ratio on in-field J_c in TFA-MOD $(Y_{0.77},Gd_{0.23})Ba_2Cu_3O_y$+$BaHfO_3$ CCs

*Kazuki Shimizu[1], Junya Kawanami[1], Masashi Miura[1], Koichi Nakaoka[2], Izumi Teruo[2]

Seikei University[1]
AIST[2]

Trifluoroacetate metal organic deposition (TFA-MOD) produced $REBa_2Cu_3O_y$ (REBCO) coated conductors (CCs) are an important research subject because of the potential for low-cost and excellent superconducting properties. A high critical current density (J_c) in magnetic field for REBCO CCs is critical for magnet applications. In a previous study, we succeeded in enhancing the in-field J_c by introducing $BaHfO_3$ (BHO) nanoparticles in TFA-MOD $(Y_{0.77},Gd_{0.23})Ba_2Cu_3O_y$ CCs ((Y,Gd)BCO+BHO) [1]. However, the influence of the Ba/Y ratio for TFA-MOD starting solution on in-field J_c for our (Y,Gd)BCO+BHO wires is not clear.

In this work, we fabricated TFA-MOD (Y,Gd)BCO+BHO CCs with various Ba/Y ratios in the starting solutions (Ba/Y = 1.5, 1.8 and 2.0) to study improving the in-field J_c. The (Y,Gd)BCO+BHO CC with Ba/Y=2.0 shows the highest self-field J_c = 5.9 MA/cm^2 at 77 K in this experiment, which is 1.1 times higher than that of the CCs with Ba/Y=1.5. Moreover, (Y,Gd)BCO+BHO CC with Ba/Y=2.0 shows a high and nearly isotropic angular dependence of J_c at 77 K and 3 T compared to other CCs. The mechanism of the improvement of the in-field performance by the controlling Ba/Y ratios in the starting solutions will be discussed based on microstructural studies.

Keywords: Critical Current, Flux Pinning, MOD, Coated Conductor

WBP3-2

The effect of $BaZrO_3$ nanoparticles on critical current density in TFA-MOD $(Y_{0.77}Gd_{0.23})Ba_2Cu_3O_y$ films on CeO_2 buffered R-Al_2O_3 substrates

*Yoshinori Kamada[1], Ryota Oku[1], Keita Sakuma[1], Masashi Miura[1]

Seikei University[1]

$REBa_2Cu_3O_y$ (REBCO) coated conductors (CCs) produced by the TFA-MOD process are promising candidates for magnet applications, because of the low cost and high superconducting performance. The R-Al_2O_3 substrate is a good candidate for high sensitivity NMR pick up coils because of the low dielectric constant. For NMR pick up coils, a (Y,Gd)BCO film with high in-field critical current density (J_c) is required because the surface resistance (R_s) is strongly correlated with J_c ($R_s \propto 1/J_c$)[1]. Although the TFA-MOD (Y,Gd)BCO films on CeO_2 buffered R-Al_2O_3 substrates indicate high self-field J_c ($J_c^{s.f.}$) at 77 K, the in-field J_c of TFA-MOD (Y,Gd)BCO films rapidly decreases with increasing magnetic fields [2]. For further improvement of the in-field J_c, introducing $BaZrO_3$(BZO) nanoparticles (NPs) as flux pinning centers is of key importance. So far, we have succeeded in obtaining high in-field J_c by introducing BZO NPs into TFA-MOD (Y,Gd)BCO ((Y,Gd)BCO+BZO) films on CeO_2 buffered metallic substrates [3,4]. However, the influence of the BZO NPs on the in-field superconducting properties for (Y,Gd)BCO films on CeO_2 buffered R-Al_2O_3 substrates has not been clear.

In this work, in order to investigate the effect of BZO NPs on the superconducting properties in a magnetic field, we fabricated the (Y,Gd)BCO and (Y,Gd)BCO+BZO films on CeO_2 buffered R-Al_2O_3 substrates using the TFA-MOD process. The (Y,Gd)BCO+BZO films show higher in-field J_c compared with that of standard (Y,Gd)BCO films. Moreover, the minimum J_c at 77 K and 3 T for (Y,Gd)BCO+BZO films is 4.2 times higher than that of the (Y,Gd)BCO films. These results suggest that the BZO NPs play an important role in the improvement of in-field properties for TFA-MOD (Y,Gd)BCO films on CeO_2 buffered R-Al_2O_3 substrates.

Acknowledgements
MM is supported by JSPS KAKENHI (17H03239 and 17K18888).

Reference
[1] A. Saito *et al.*, *IEEE Trans. Appl. Supercond.*, **15** (2005) 3696-3699.
[2] K. Sakuma *et al.*, *Jpn. J. Appl. Phys.* **57** (2018) 033102.
[3] M. Miura *et al.*, *Scientific Reports* **6** (2016) 20436.
[4] M. Miura *et al.*, *NPG Asia Materials* **9** (2017) e447.

Keywords: MOD, nanoparticle, flux pinning, critical current

WBP3-3

The influence of an intermediate heat treatment temperature on the in-field J_c of $BaHfO_3$ doped TFA-MOD $(Y_{0.77},Gd_{0.23})Ba_2Cu_3O_y$ wires

*Junya Kawanami[1], Kazuki Shimizu[1], Masashi Miura[1], Ryuji Yoshida[2], Takeharu Kato[2], Koichi Nakaoka[3], Teruo Izumi[3]

Seikei University, Japan[1]
Nanostructures Research Laboratory, Japan[2]
AIST, Japan[3]

The Trifluoroacetate-Metal Organic Deposition (TFA-MOD) process is one of the most attractive ones for magnet application because of the low-cost and the high critical current density (J_c) obtained. However, magnet applications require higher in-field J_c performance. So far, we have succeeded in obtaining high in-field J_c by addition of $BaHfO_3$ (BHO) nanoparticles (NPs) into TFA-MOD $(Y_{0.77},Gd_{0.23})Ba_2Cu_3O_y$ ((Y,Gd)BCO+BHO) wires [1]. For further enhancement of J_c, controlling the size and density of the BHO NPs is one of the key factors. Recently AIST successfully controlled the size of $BaZrO_3$ NPs by introducing an intermediate heat treatment (IHT) before the conversion process [2]. However, the effect of the IHT temperature (T_{IHT}) on the in-field J_c for our (Y,Gd)BCO+BHO wires is not clear.

In this work, in order to investigate the influence of the IHT temperature (T_{IHT}) on the in-field superconducting properties, we fabricated (Y,Gd)BCO+BHO wires using various T_{IHT}. These wires have almost the same critical temperature. The (Y,Gd)BCO+BHO wire with T_{IHT}=570°C shows a higher in-field J_c and less angular dependent J_c compared to the other wires. The minimum J_c ($J_{c,min}$) for wire with T_{IHT}=570°C at 77 K, 3 T is 0.63 MA/cm^2 which is 1.1 times higher than that of wire with T_{IHT}=550°C. From microstructural measurements, the BHO NPs in the (Y,Gd)BCO+BHO wire with T_{IHT}=570 °C are smaller in size and higher in density compared to a wire with T_{IHT}=550 °C. Our results demonstrate that controlling of the IHT temperature is an important way for controlling the size and density of BHO NPs and improving the in-field J_c of TFA-MOD wires.

Acknowledgements: This work is supported by JSPS KAKENHI (17H03239 and 17K18888). A part of this work was supported by Kato Foundation for Promotion of Science (KJ-2744).

[1] M. Miura *et al., NPG Asia Materials* **9 (2017) e447.**
[2] K. Nakaoka *et al., IEEE Trans.Appl. Supercond.* **26** (2016) 800304.

Keywords: Critical Current, Flux Pinning, MOD, nanoparticles

WBP3-4

Influence of the twin boundaries on the in-field J_c in $BaZrO_3$ doped TFA-MOD $(Y_{0.77}Gd_{0.23})Ba_2Cu_3O_y$ CCs

*Kenji Miyata[1], Ryota Oku[1], Masashi Miura[1], Masaru Kiuchi[2], Teruo Matsushita[2]

Seikei University Tokyo, Japan[1]
Kyushu Institute of Technology, Japan[2]

$REBa_2Cu_3O_y$(RE=Rare Earth: REBCO) coated conductors (CCs) produced by TFA-MOD are expected to be valuable for magnet applications because of the low production cost and high critical current density (J_c) performance. However, further enhancement of the in-field J_c is required for practical applications. To achieve this, we introduced $BaMO_3$ (M=Zr, Hf) nanoparticles as a three-dimensional magnetic flux pinning center in TFA-MOD (Y,Gd)BCO and succeeded in obtaining high in-field J_c [1,2]. The twin boundaries (TBs) introduced naturally in the (Y,Gd)BCO CCs result in *c*-axis correlated pinning centers (2D pinning center) because they remain continuous through the film thickness [2,3]. For further enhancement of the in-field J_c, understanding the influence of the TBs on in-field J_c in TFA-MOD-(Y,Gd)BCO+BZO CCs is important.

In this work, we fabricated TFA-MOD-(Y,Gd)BCO+BZO CCs with two differently patterned transport bridges in order to investigate the influence of the orientation of the TB planes on in-field J_c. In the I-shaped bridge, the TB planes are oriented 45°to the transport current flow. In the Z-shaped bridge, the TB planes are oriented at either 0°or 90°to the current flow. Although both CCs have almost the same critical temperature and self-field J_c, at 77K, 8T the (Y,Gd)BCO+BZO CC with Z-shape shows higher J_c values than that with the I-shape. Furthermore, similar results were obtained with a (Y,Gd)BCO CC. This behavior is considered to be due to a difference in the strength of the magnetic flux pinning of the TBs for the Z-shape and I-shape. Our results indicate that the orientation of the TB planes plays an important role in the enhancement of the in-field J_c in TFA-MOD-(Y,Gd)BCO+BZO CCs.

Acknowledgements: This work is supported by JSPS KAKENHI (17H03239 and 17K18888). A part of this work was supported by a research grant from the Japan Power Academy.

References
[1] M. Miura *et al., NPG Asia Materials* **9** (2017) e447.
[2] M. Miura *et al.*, *Scientific Reports* **6** (2016) 20436.
[3] V. Rouco *et al., Supercond. Sci. Technol.* **27** (2014) 125009

Keywords: Critical Current, Twin Boundaries, MOD, Coated Conductor

WBP3-5

Optimization of interim heat treatment condition on TFA-MOD process for fabrication of $Y_{0.77}Gd_{0.23}Ba_2Cu_3O_y$ coated conductors with $BaHfO_3$

*Koichi Nakaoka[1], Ryuji Yoshida[2], Michio Sato[1], Akira Ibi[1], Takato Machi[1], Takeharu Kato[2], Teruo Izumi[1]

National Institute of Advanced Industrial Science and Technology (AIST)[1]
Nanostructures Research Lab., Japan Fine Ceramics Center (JFCC)[2]

The trifluoroacetate metal-organic deposition (TFA-MOD) process has been recognized as a cost effective process to fabricate $REBa_2Cu_3O_y$ (RE: rare-earth, REBCO) coated conductors (CCs) with high performance in a self-field. However, that had been low comparing with the CCs by the vapor process in a magnetic-field. On the other hand, low cost CCs with high performance in the magnetic-field have been required for electric power applications. Recently, we have developed two new techniques which were called interim-heat-treatment (IHT) [1] and ultrathin-once-coating (UTOC) [2] in order to enhance the in-field critical current density ($J_c(B)$) of MOD-REBCO CCs with $BaMO_3$ (M: metal element) artificial pinning centers, and achieved significant improvement of the $J_c(B)$ property. The IHT process which is the new heat treatment step at temperature of around 580°C introduced between calcination and crystallization steps is a process to form an appropriate precursor film before the crystallization process of the REBCO. As a result, IHT process gives improving the uniformity of the REBCO matrix and homogeneous dispersion of the finer $BaMO_3$. The fundamental theoretical analysis of IHT was previously reported [1]. In this study, we have optimized the IHT conditions, particularly process time, for further improvement of $J_c(B)$ property of $Y_{0.77}Gd_{0.23}Ba_2Cu_3O_y$ with $BaHfO_3$ (YGdBCO/BHO) CCs. Although, the $J_c(B)$ value at 77 K and 3 T ($B//c$) for YGdBCO/BHO CC without IHT was 0.21 MA/cm^2, the YGdBCO/BHO CC with IHT at 580°C for 90 min exhibited the increase of the $J_c(B)$ value to 0.31 MA/cm^2 at 77 K and 3 T ($B//c$). By the longer IHT process time of 120 min, YGdBCO/BHO CCs with *a*-axis orientation were obtained, and the degradation of $J_c(B)$ properties were observed. XRD measurements of quenched films after IHT at 580°C for >120 min confirmed the coarsening of CuO before the crystallization process. This might be due to the cause of formation of a-axis orientation.

This work was supported by the New Energy and Industrial Technology Development Organization (NEDO), Advanced Medical Services from the Japan Agency for Medical Research and development (AMED), and Ministry of Economy, Trade and Industry (METI).

[1] K. Nakaoka *et al.*, *IEEE Tran on Appl. Supercond.* **26** (2016) 8000304
[2] K. Nakaoka *et al.*, *Supercond. Sci. Technol.* **30** (2017) 055008

WBP3-6

Superconducting properties of $(Y_{1-x}Eu_x)Ba_2Cu_3O_y$ coated conductors by TFA-MOD process

*Michio Sato[1], Koichi Nakaoka[1], Akira Ibi[1], Takato Machi[1], Teruo Izumi[1]

National Institute of Advanced Industrial Science and Technology[1]

$REBa_2Cu_3O_y$ (REBCO, RE: rare-earth element) coated conductors (CCs) derived from trifluoroacetate-metal organic deposition (TFA-MOD) are expected to be applied to various electric power applications, such as superconducting cables, motors and generators, because of the low-cost and high critical current densities (J_c) under high magnetic field even at liquid-nitrogen temperature. However, the improvement of the in-field J_c in TFA-MOD REBCO CCs has been required for these applications. So far, we have reported that $Y_{0.77}Gd_{0.23}Ba_2Cu_3O_y$ ((Y,Gd)BCO) CCs showed higher performance on not only critical temperature (T_c) but also in-field J_c than those of $YBa_2Cu_3O_y$ (YBCO) CCs. It means that partial substitution of RE site is effective way to improve the in-field J_c in TFA-MOD REBCO CCs. For further enhancement of in-field J_c, we have chosen Eu as a partial substitution element in TFA-MOD REBCO CCs, because $EuBa_2Cu_3O_y$ bulk materials have higher T_c than that of YBCO and $GdBa_2Cu_3O_y$.

In this work, we fabricated TFA-MOD $Y_{1-x}Eu_xBa_2Cu_3O_y$ ($0 \leq x \leq 1$) CCs with various heating temperature and partial oxygen pressure in conversion steps in order to investigate the influence of Y/Eu partial substitution and the heat-treatment on superconducting properties. At least, it was confirmed that the $Y_{0.77}Eu_{0.23}Ba_2Cu_3O_y$ CC shows higher T_c (T_c ~91.5 K) than that of (Y,Gd)BCO CC. Additionally, the irreversibility field in $Y_{0.77}Eu_{0.23}Ba_2Cu_3O_y$ CC were higher than (Y,Gd)BCO CC.

In this presentation, we will discuss the details of superconducting properties in $Y_{1-x}Eu_xBa_2Cu_3O_y$ CCs fabricated with different conditions.

Acknowledgements: This work was supported by the New Energy and Industrial Technology Development Organization (NEDO).

Keywords: Y1-xEuxBa2Cu3Oy, TFA-MOD, Coated conductor

WBP3-7

Film thickness dependence of critical current density in (Y,Gd)BaCuO+$BaZrO_3$ nanoparticle CCs

*Go Tsuchiya[1], Kota Hirai[1], Masashi Miura[1], Masaru Kiuchi[2], Teruo Matsushita[2]

Seikei University[1]
Kyusyu Institute of Technology[2]

TFA-MOD is a good process for low-cost and high critical current density $REBa_2Cu_3O_y$ (REBCO) coated conductors (CCs). However, practical applications require further enhancement of the in-field critical current (I_c). For high in-field I_c, the suppression of the formation of large second phase precipitates (i.e., high matrix crystallinity) and uniform dispersion of pinning centers (i.e., enhancement of flux pinning) are even important in thick films. So far, we have succeeded in obtaining high in-field critical current density (J_c) even for 2 μm thickness by controlling the crystal growth rate and introducing $BaZrO_3$ nanoparticles (BZO NPs) into the TFA-MOD (Y,Gd)BCO CCs [1,2]. However, understanding of the influence of thickness on crystallinity and J_c in CCs grown by the TFA-MOD process remains an open issue.

In order to investigate the film thickness dependence of self-field ($J_c^{s.f.}$), we prepared $(Y_{0.77},Gd_{0.23})Ba_2Cu_3O_y$ (YGdBCO) and 3 wt.% $BaZrO_3$ doped YGdBCO (YGBCO+3BZO) CCs with various thickness. For YGBCO, $J_c^{s.f.}$ decreases rapidly with increasing thickness, especially for $t >$ 400 nm, and the $J_c^{s.f.}$ value at t = 1 μm is 2 MA/cm^2 at 77 K. On the other hand, YGBCO+3BZO shows a high $J_c^{s.f.}$ over 4 MA/cm^2 at 77K for large thickness. We find several common features observed in PLD and MOD REBCO CCs [2, 3]. For thinner films with and without BZO NPs, a rapid decay of $J_c^{s.f.}$. ($J_c^{s.f.} \propto 1/t^{0.5}$) is observed. For over 300 nm for both samples, the J_c value is nearly constant. Such a thickness dependence for $J_c^{s.f.}$ may results from the transition from the two-dimensional pinning of rigid vortex lines in thinner films (at L_c (critical thickness) > t) to three-dimensional pinning of deformable vortices even for completely uniform pinning nanostructures. We will discuss the influence of natural defects and BZO NPs on the thickness dependence of $J_c^{s.f.}$ in MOD-REBCO CCs based on a theoretical model.

Keywords: Critical Current, MOD, Thickness Dependence, BZO

WBP3-8

The longitudinal magnetic field dependence of critical current density in multilayered TFA-MOD $REBa_2Cu_3O_y$ Coated Conductors

*Keiichi Sato[1], Jun Nishimura[1], Kota Hirai[1], Keita Sakuma[1], Masashi Miura[1], Masaru Kiuchi[2], Teruo Matsushita[2]

Seikei University, Japan[1]
Kyushu Institute of Technology, Japan[2]

The critical current density (J_c) for superconductor coated conductors (CCs) in the longitudinal magnetic field is higher than that in the transverse magnetic field, because the longitudinal magnetic field is a Lorentz force-free state [1]. T. Matsushita suggested that a superconducting $REBa_2Cu_3O_y$ (REBCO) DC cable using the longitudinal magnetic field effect and it can realize high current-carrying capacity compared to a conventional superconducting cables [2]. The TFA-MOD process derived REBCO CC is one of the attractive candidates for a LFF DC cable because they are low-cost and high superconducting performance [3,4]. However, for practical LFF DC cable, further enhancement of J_c in the longitudinal magnetic field is required. Recently, Nagoya University Group reported that **multilayered SmBCO films** derived from pulsed laser deposition **show higher J_c in the longitudinal magnetic field than that of standard SmBCO film [4]. However, t**he influence of the multilayered structure on J_c in the longitudinal magnetic field for T**FA-MOD REBCO** CC has not yet been clarified.
In this work, in order to investigate the effect of multilayered structure *on* the longitudinal magnetic fields of J_c property, we fabricated the ((Y,Gd)BCO/(Y,Gd)BCO+$BaHfO_3$) multilayered CC on metallic substrates derived from TFA-MOD. The critical temperature of multilayered (Y,Gd)BCO CC is the same as that of standard (Y,Gd)BCO CC. The J_c in the longitudinal magnetic field at 77 K for multilayered (Y,Gd)BCO CC is 5.81 MA/cm^2 at 0.5 T, which is 1.92 times higher than that of standard (Y,Gd)BCO CC. Our present results indicate that the introduction of $BaHfO_3$ nanoparticles and multilayered structure for TFA-MOD (Y,Gd)BCO CC play an important role in the enhancement of the J_c also in the longitudinal magnetic field.

Acknowledgements: This work was supported by a research grant from the Japan Power Academy. A part of this work is supported by JSPS KAKENHI (17H03239 and 17K18888).

[1] G. W. Cullen and R. L. Novak, *Appl. Phys. Lett.* **4**(1964) 147-149.
[2] T. Matsushita *et al., AIP Conf. Proc.* **1574** (2014) 225.
[3] M. Miura *et al., NPG Asia Materials* **9 (2017) e447.**
[4] K. Sugihara *et al., Supercond. Sci. Techonl.* **28** (2015) 104004.

Keywords: Critical Current, Longitudinal Magnetic Field, MOD, DC Cable

WBP3-9

Comparison of different CSD-grown *RE*BCO (*RE* = Yb, Er, Ho, Y, Dy, Gd, Sm, Nd) compounds with respect to applicability as Coated Conductors

*Manuela Erbe[1], Pablo Cayado[1], Wolfram Freitag[1], Jens Haenisch[1], Bernhard Holzapfel[1]

Karlsruhe Institute Of Technology, Germany[1]

The introduction of *RE*$Ba_2Cu_3O_{7-x}$-based (*RE*BCO, *RE* = rare-earth elements) Coated Conductors (CC) into commercial applications requires reliable, cost-effective growth processes and in many cases a good performance in applied magnetic fields. Chemical solution deposition methods, such as the TFA-MOD process using metal-organic trifluoroacetates or low-fluorine routes, are absolutely capable of meeting those requirements. The simplicity of the fabrication process renders them cheap and versatile. Composition and stoichiometry of the precursor solutions can be readily modified, and artificial pinning centres are conveniently introduced via the solutions. This allows for an easy adaption of the CC performance to the demands of the according applications.
So far, YBCO has been the compound with the highest popularity since it has been one of the first known systems with T_c values above 90 K and, therefore, has gone through thorough investigations. Yttrium is also comparably well available and amongst the rare-earth elements the least expensive. However, other *RE* elements promise further performance enhancements in consequence of higher T_c values, but also process simplification and an increase of the reproducibility due to broader processing windows.
Here, we show results of our investigations on different single-*RE*-$Ba_2Cu_3O_{7-x}$ compounds, both to establish clarity about their according T_c values when grown by the same MOD process, since literature values are rather contradictory, and to develop a deeper understanding of their processing windows in formation temperature and optimal process gas composition (p(O2), p(H2O)). We focussed on Yb, Er, Ho, Dy, Gd, Sm and Nd as substituents for Y and investigated their growth behaviour and resulting physical (T_c, $J_c(B)$, $J_c(\Theta)$) and structural properties (XRD, SEM) when grown as pristine films on single-crystalline $LaAlO_3$ and $SrTiO_3$ substrates and compare them to similar films with 12 mol% BHO.

Keywords: REBCO, TFA-MOD

WBP3-10

Dominate Effect of Fluorine on Decomposition Phase Evolution towards High Performnce GdBCO Films

*Lihua Jin[1], Yang Bai[1], Chengshan Li[1], Jianqing Feng[1], Pingxiang Zhang[1]

Northwest Institute for Nonferrous Metal Research[1]

An intensive analytic study on the decomposition evolution of $GdBa_2Cu_3O_y$ (GdBCO) precursor solutions with different fluorine contents was presented. The fluorine contents of GdBCO precursor solutions were adjusted as 0%, 3.8%, 11.5%, 19.2%, respectively. Thermal gravimetric-differential thermal analysis (TG-DSC), Fourier transform infrared spectroscopy (FTIR) and X-ray diffraction (XRD) were performed to determine composition and the chemical reaction of all series of low fluorine precursors. It was worthy noted that fluorine had a great influence on the phase transformation during the pyrolysis process. With increasing fluorine content in solution, the decomposition reaction region became narrow. Fluorine could catalyze the reaction and make pyrolysis abruptly at the case of high fluorine content. The kinetics evolution of intermediate phases was investigated, including BaF_2, $Ba_{1-x}Gd_xF_{2+x}$ (BGF), $BaCO_3$, Gd_2O_3, CuO and Cu_2O etc. It was concluded that fluorine could tune non-equilibrium phase transformations. The results would be helpful for the optimization of thermal decomposition process and the intermediate phase composition, which might influence the reaction path towards high performance and epitaxial GdBCO films.

Keywords: Chemical solution deposition, Phase evolution, GdBCO, Fluorine

WBP3-11

Enhancement of critical current densities for Hf and La doped Gd123 films fabricated by fluorine-free MOD method

Joichiro Fukui[1], Takumi Takahashi[1], Osuke Miura[1], Ryusuke Kita[2]

Dept. of Electrical Engineering and Computer Science, Tokyo Metropolitan University, Japan[1]
Electrical and Electronic Engineering, Shizuoka University, Japan[2]

We have fabricated Hf and La doped FF-MOD $GdBa_2Cu_3O_y$ (Gd123) thin films on $LaAlO_3$ substrates and investigated their flux pinning properties. Temperature dependence of J_c in magnetic fields parallel to the c-axis orientation up to 7 T was estimated from the width of the magnetization curves using the modified critical state model. Critical temperature for Gd123 thin films indicated around 92 K, and T_c varied little by Hf doping. Hf 10 mol% doped film achieved high critical current densities of 2.72 MA cm^{-2} at 77.3 K under 0 T, and 0.27 MA cm^{-2} at 77.3 K under 1 T. With increasing Hf doping amount, F_p gradually increased, and the peak of F_p shifted to the high magnetic field side. The elementary pinning force and the effective pinning center density also increased. We believe that $BaHfO_3$ are introduced into FF-MOD Gd123 thin films by Hf doping. Furthermore, Gd123 thin films with La addition showed the enhancement of J_c at self-magnetic fields and the decrease in number of density of holes on the film surface. We studied critical current densities for Hf and La co-doped Gd123 films fabricated by fluorine-free MOD method.

Keywords: fluorine-free metal organic deposition, GdBa2Cu3Oy, Hf and La doping.

WBP3-12

Effect of Zirconium Doping Using a New Metal-organic Material on the Fabrication of Fluorine-free MOD-GdBCO Films

*Koyuki Kosugi[1], Ryusuke Kita[1], Joichiro Fukui[2], Osuke Miura[2]

Shizuoka University[1]
Tokyo Metropolitan University[2]

REBCO films with high Jc-B performances are essential to develop REBCO coated conductors of a low cost and excellent mass productivity for the application of the REBCO superconducting films to high current-carrying superconducting wires and strong magnets. We have been studied the fabrication of REBCO films by a fluorine-free metal organic deposition (FF-MOD) method to accomplish the purpose. In our previous works, we studied the effect of Zr doping using 2-ethylhexanates on the fabrication of FF-MOD-GdBCO films, and found the improvement on the Jc-B performance. However, Zr doping over 1mol% caused the degradation of the crystallization and surface morphology of the GdBCO films.
In the present study, we have studied the Zr doping effects on the growth and superconductivity properties of FF-MOD GdBCO films by using a new fluorine-free metal-organic Zr material. Zr-doped GdBCO films with 7 mol% content showed the enhancement of the c-axis orientation compared to the pure GdBCO film. The decrease of the average size and density of the hole were observed for the 7-mol%-Zr doped film surface. The Jc-B performance of the Zr-doped GdBCO films will be discussed on the paper.

Keywords: REBCO thin film, Metal-organic deposition, Fluorine-free, Doping

WBP3-13

Investigation of temperature and oxygen partial pressure diagram for $LaBa_2Cu_3O_y$ film

*Tomohiro Miyajima[1], Ryo Teranishi[1], Yukio Sato[1], Kenji Kaneko[1]

Kyushu University, Japan[1]

$LaBa_2Cu_3O_y$ (LaBCO) film is expected to show high critical temperature among $REBa_2Cu_3O_y$ supercodunducting films [1], however, it is reported that fabrication of LaBCO film is difficult due to the substitution of La^{3+} ion for Ba^{2+} ion [2]. Fabrication temperature and oxygen partial pressure (PO_2) should be controlled to suppress the substitution of La^{3+} ion for Ba^{2+} ion based on a temperature and PO_2 diagram. Nevertheless, that for LaBCO film has not been reported so far. In this work, the temperature and PO_2 diagram for LaBCO film was investigated by volume fraction of LaBCO film (VF_{LaBCO}) fabricated at various temperatures and PO_2.

Fluorine-free starting solutions containing organic salts of La, Ba, and Cu were spin-coated onto substrates of $CeO_2/LaMnO_3/MgO/Gd_2Zr_2O_7$/Hastelloy. The samples were calcined at 773 K in pure oxygen gas flow to prepare precursor films. The precursor films were crystallized at 1023, 1123, and 1223 K for 4 h with PO_2 of 0.1, 1, 10, 100, and 1000 Pa. These samples were examined by an X-ray diffractometer (XRD), and their VF_{LaBCO} were estimated by the integrated intensity ratio of LaBCO peak against all peaks including LaBCO peak.

Fig. 1 shows a temperature and PO_2 diagram for LaBCO film which summarizes VF_{LaBCO}, where double circle, single circle, triangle, dot, and square mean VF_{LaBCO} of larger than 90%, between 80 and 90%, between 20 and 80%, smaller than 20%, and 0%, respectively. It was confirmed by XRD that all LaBCO crystals were oriented to *c*-axis with misorientation of 2.7~4.3 degrees. Within the region which LaBCO was present, VF_{LaBCO} was larger at low temperature and low PO_2, which indicates that the La^{3+}/Ba^{2+} substitution was suppressed at low temperature due to poor atom diffusion, and also suppressed at low PO_2 [3].

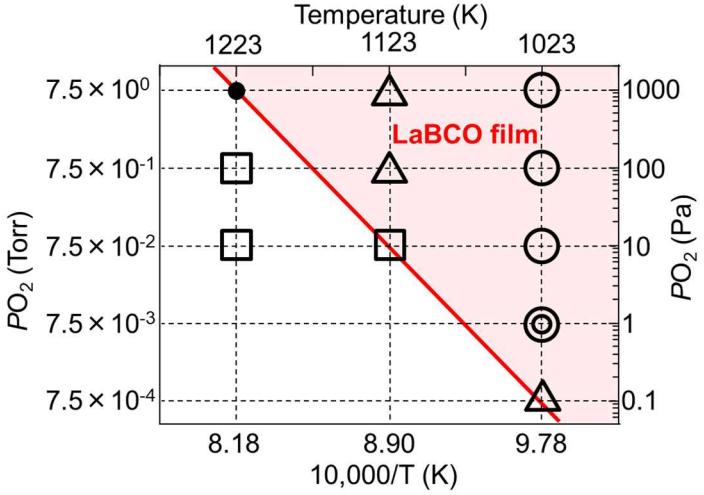

Fig. 1. Temperature and PO_2 diagram for LaBCO film.

[1] Tao, F. et al. *Mater. Lett.* **1999**, *40*, 222.
[2] Ichino, Y. et al. *Phys. C. Supercond.* **2008**, *468*, 1623.
[3] Yao, X. et al. *Phys. C Supercond.* **2004**, *412*, 90.

Keywords: LaBCO, MOD, Coated conductor

WBP4-1

Electron Backscatter Diffraction Study of $EuBa_2Cu_3O_y$ Coated Conductors Fabricated by Pulsed Laser Deposition

Daisaku Yokoe[1], Ryuji Yoshida[1], *Takeharu Kato[1], Akira Ibi[2], Teruo Izumi[2], Tsukasa Hirayama[1]

Nanostructures Research Laboratory, Japan Fine Ceramics Center[1]
Department of Energy and Environment, National Institute of Advanced Industrial Science and Technology[2]

$EuBa_2Cu_3O_y$ (EuBCO) coated conductors with $BaHfO_3$ (BHO) nanorods have high in-field properties [1,2]. Therefore, they are candidate materials for superconducting devices, such as magnetic resonance imaging (MRI) and heavy ion medical accelerators etc. In this study, an electron backscatter diffraction (EBSD) method was used to analyze grain alignments and distributions of secondary phases in the EuBCO layer. The EuBCO layers with BHO nanorods are fabricated on a Hastelloy™ tape with textured $CeO_2/LaMnO_3/MgO/Y_2O_3$/Gd-Zr-O buffer layers by pulsed laser deposition [1]. Cross-sections of the EuBCO layers were prepared by Ar ion milling in a Hitachi IM-4000 system at an accelerating voltage of 6-1 keV. The specimens were examined in a JSM-7800F PRIME scanning electron microscope with a Digiview V EBSD system produced by TSL Solutions. Clear EBSD patterns of EuBCO grains were not taken from the cross-section layer milled by an Ar beam at an accelerating voltage of 6 kV because of a damaged layer formed on the cross-section caused by the Ar beam. Therefore, a low energy Ar beam at that of 1 kV was applied to the cross-section to remove the damaged layer. Clear EBSD patterns corresponding to not only EuBCO grains but CuO grains in the EuBCO layers were taken from the cross-section after applying the Ar beam at 1 kV. The EuBCO layers were mainly composed of *c*-axis oriented EuBCO grains (matrix). Outer-growth EuBCO grains which had different orientations relative to the matrix grains were formed on CuO grains in the layer. There seemed to be no orientation relationship between the matrix/the outer-growth EuBCO grains and the CuO grains. We would like to perform three-dimensional orientation analysis of coated conductors using a focused ion beam-SEM system and these preparation techniques in the future.
A part of this research was supported by Advanced Medical Services from the Japan Agency for Medical Research and development (AMED), New Energy and Industrial Technology Development Organization (NEDO) and Ministry of Economy, Trade and Industry (METI).

[1] A. Ibi et al., *Physics Procedia*, **81**, 97-100 (2016).
[2] D. Yokoe et al., *AMTC Letters*, **5**, 194-195 (2016).

Keywords: EBSD, SEM, PLD, EuBCO

WBP4-2

Fatigue Behaviors of Differently Stabilized REBCO Coated Conductor Tapes at 77 K

Mark Angelo Diaz[1], Zherwinjay Bautista[1], *Hyung-Seop Shin[1]

Department of Mechanical Design Engineering, Andong National University, Andong, 36729, Korea[1]

In the HTS superconducting magnet application fields like motors, generators and SMES, 2G coated conductor (CC) tapes will be subjected to alternating stress or strain during manufacturing and operation. The repeated load affects the mechanical integrity and eventually the electrical transport property of CC tapes. Therefore, in such applications, mechanical and electromechanical properties of CC tapes should be evaluated. In this study, firstly, a high-cycle fatigue test procedure for 2G CC wires at cryogenic temperature has established. Using the procedure, it is tried to evaluate the electromechanical properties of CC tapes. The fatigue behaviors of differently stabilized REBCO CC tapes under high-cycle fatigue load have been evaluated. A relation between applied maximum stress and fatigue life (S–N) was obtained at 77 K. Considering the practical operating environment, the effect of the stress ratio R, on the degradation behavior of I_c and n-value during fatigue load was also examined. The correlation between the mechanically determined fatigue strength and electromechanical fatigue strength under specified test conditions was examined.

This work was supported by a grant from National Research Foundation of Korea (NRF-2017-001109), funded by the Ministry of Science and ICT (MSIT), Republic of Korea. This research was partially supported by the Korea Electric Power Corporation. (Grant number: R18XA03).

Keywords: REBCO coated conductor, Fatigue strength, Stress ratio, Electromechanical fatigue limit, Mechanical fatigue limit

WBP4-3

Dependence of AC Loss in Stacked $REBa_2Cu_3O_y$ Superconducting Tapes on the Interval among Tapes under Perpendicular Magnetic Field

*Hiromasa Sasa[1], Goki Kawasaki[1], Shun Miura[1], Masataka Iwakuma[1], Teruo Izumi[2], Takato Machi[2], Akira Ibi[2]

Institute of Superconductors Science and Systems, Kyushu University, Japan[1]
National Institute of Advanced Industrial Science and Technology, Japan[2]

For AC applications of $REBa_2Cu_3O_y$ (REBCO, RE = rare earth, Y, Eu, Gd) superconducting tapes, the quantitative prediction of the AC loss in REBCO superconducting tapes is one of the most serious issues. It is important for the design of the cooling system. Especially, in a conduction-cooling system, it may cause a severe temperature rise of superconducting windings and result in thermal runaway. Therefore, it is necessary to understand the AC loss property of a REBCO superconducting tape in detail and to reduce that.

In this study, the AC loss properties of the EuBCO + $BaHfO_3$ tapes, which were stacked into a multi-layer in perpendicular to the tape face were investigated. The tapes were fabricated by the IBAD-PLD method. The width of the tape is 5 mm and the thickness of the superconducting layer is 0.7 μm. The external magnetic field was applied to the tape face in perpendicular.

In the case that superconducting strips are stacked, whole of them can be considered as a slab when the ratio of the distance between the neighboring strips, D, to their width, w, (D/w) is smaller than 0.1 [1]. Recently, we found out that, under this assumption, for the amplitude of the applied field, B_m, below the penetration field, B_p, the AC loss of n-layer stacked non-scribed REBCO superconducting tapes decreases to $1/n$ of that of 1-layer tape. However, in practical applications, the REBCO tapes are preferred to be scribed for reducing the AC loss in B_m above B_p. Then, the D/w of each filament of the scribed tape exceeds 0.1. Therefore, the dependence of the AC loss on D/w which is larger than 0.1 should be investigated.

Fig. (a) shows B_m dependence on the AC losses of the 1-layer tape, 3-layer tapes with D/w = 0.058 (< 0.1) and the 3-layer tapes with D/w = 0.392 (> 0.1) at 50 K. For B_m above B_p, they agree with each other regardless of the conditions. Fig. (b) shows the AC losses normalized by the approximation curve of AC loss for the 1-layer tape in B_m below B_p shown in fig. (a) as dashed line. The AC loss of the 3-layer tapes with D/w = 0.058 decreases to 1/3 of that of the 1-layer tape. Moreover, the AC loss of 3-layer tapes increases with increasing D/w. The purpose of this study is to clear such dependence of the AC loss of stacked REBCO superconducting tapes in B_m below B_p on D/w. For that purpose, we have conducted further experiments for various D/w and the results will be reported on ISS 2018.

[1] Mawatari Y 1996 *Phys. Rev. B* **54** 13215

Keywords: AC loss, REBCO

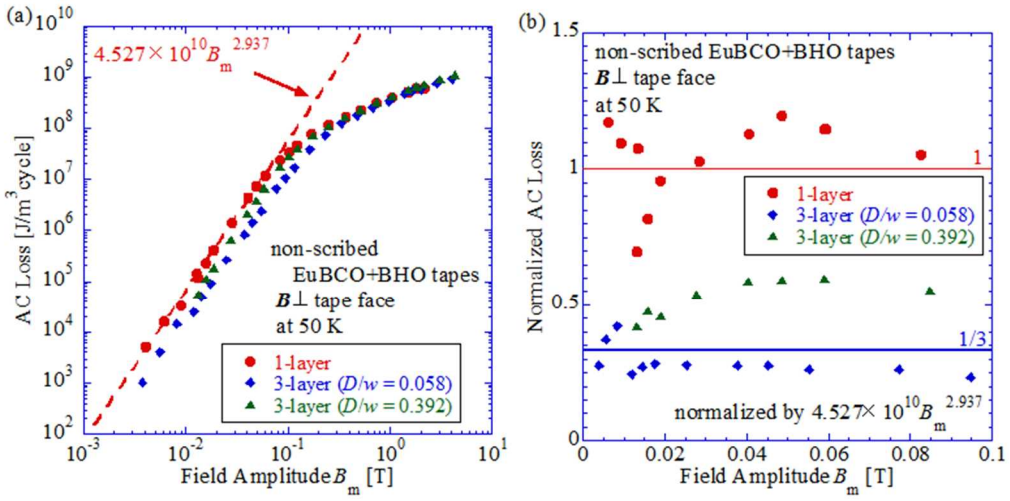

Fig. (a) the B_m dependences of AC losses of 1-layer tape, 3-layer tapes with D/w < 0.1 and with D/w > 0.1 and (b) the ratios of the AC losses to those of 1-layer tape for $B_m < B_p$.

WBP4-4

Electormagnetic coupling of multifilamentary helically-wound superconducting tapes in a rapidly swept magnetic field

*Yoichi Higashi[1], Yasunori Mawatari[1]

National Institute of Advanced Industrial Science and Technology (AIST)[1]

High temperature superconducting $YBa_2Cu_3O_{7-\delta}$ coated conductor on round core (CORC) wire has been developed for the last decade [1,2]. The CORC wire is a promising candidate of a superconducting wire for an application to high field magnets. This is because a coated conductor can be wound on a thin former with the diameter of a few mm and with a short pitch of a few tens of mm, reducing the average perpendicular component of a magnetic field penetrating the tape. Owing to a short pitch of the CORC wire, electromagnetic coupling is suppressed even if the tape is striated and further reduction of losses of the CORC wire is expected.

The present study reports electromagnetic coupling of multi-filamentary helically-wound superconducting tapes with a pitch of a few tens of mm subjected to a rapidly swept magnetic field with varying the former radius. We suppose, for instance, rapid demagnetization of a MRI magnet in the case of emergency stop. On the basis of the thin sheet approximation, the Faraday's law in the steady state is reduced to the two dimensional equation on the tape surface. Our recent analysis successfully demonstrates electromagnetic properties of a twisted tape [3] and a helically-wound tape on a hollow cylinder [4]. By solving numerically the obtained two dimensional equation, we evaluated magnetization loss on multifilamentally helically-wound tapes. For large sweep rates, electromagnetic coupling occurs even in the case of a short pitch. However, we show that electromagnetic coupling can be suppressed with decreasing the former radius.

This work is based on the results obtained from a project commissioned by the New Energy and Industrial Technology Development Organization (NEDO).

[1] D. C. van der Laan, Supercond. Sci. Technol. **22**, 065013 (2009).
[2] Jeremy D. Weiss et al., Supercond. Sci. Technol. **30**, 014002 (2017).
[3] Y. Higashi, H. Zhang and Y. Mawatari, unpublished.
[4] Y. Higashi and Y. Mawatari, presentation in 6th International Workshop on Numerical Modelling of High Temperature Superconductors (2018).

Keywords: electormagnetic coupling, multifilamentary helically-wound tapes, rapidly swept magnetic field

WBP4-5

Fabrication of a Compact High-field Magnet by Coated Conductor Stacks

*Tomohiro Hashimoto[1], Sunseng Pyon[1], Yasuhiro Iijima[2], Shiori Sugiura[3], Sinya Uji[3], Taichi Terashima[3], Tsuyoshi Tamegai[1]

Department of Applied Physics, The University of Tokyo, Japan[1]
Fujikura Ltd., Japan[2]
Reserch Center for Functional Materials Quantum Transport Properties Group, National Institute for Materials Science, Japan[3]

Coated conductors (CCs) of 123-type superconductors with a large critical current density (J_c) have been successfully developed for applications of power transmission and generation of high magnetic fields. Such CCs can find applications in other purposes. One of them is an alternative method to generate a high magnetic field like bulk materials of high temperature superconductors. When one attempts to magnetize an ordinary bulk materials, one faces problems of mechanical strength and thermomagnetic instability. In order to solve such problems of the bulk magnet, stacking short segments of CCs has been proposed, and a modest field has been successfully trapped [1]. In the latest report, a record-high magnetic field of 17.7 T has been successfully trapped at the center of a stack consisting of 416 CCs, one with square and another circular CCs (total height: 37.75 mm) [2].

In the present study, we aimed at fabricating a compact magnet by modeling the bulk magnet using CCs with better J_c-H characteristics. For that purpose, we used EuBCO CCs with artificially introduced $BaHfO_3$ nanorods. Two stacks of each 50 pieces of EuBCO CCs were placed next to each other and miniature Hall probes for measuring the trapped field were placed at the center of the stacks. They were cooled down to 4.2 K in a magnetic field of 14.5 T, and the field was reduced to zero at a rate of 1 T/min. In this condition, we have succeeded in trapping 12.6 T at the center of the stacks. Although this trapped magnetic field is lower than the report of ref. [2], we have succeeded in reducing the height down to about one sixth of ref. [2] (total height: 6.5 mm), and volume down to about one thirty-seventh. We have also succeeded in increasing the ramp rate from 15.5 mT/min to 1 T/min. It took only 15 minutes to trap 12.6 T in the present study, while it took 20 hours to trap 17.7 T in the latest report.

We also report the evaluation of the local magnetic characterizations of the EuBCO CCs used for trapping magnetic fields, and discuss the effect of temperature rise in the course of magnetization.

[1] A. Patel, K. Filar, V. I. Nizhankovskii, S. C. Hopkins, and B. A. Glowacki, Appl. Phys. Lett. **102**, 102601 (2013).
[2] A. Patel, A. Baskys, T. Mitchell-Williams, A. McCaul, W. Coniglio, J. Hänisch, M. Lao, B. A. Glowacki, Supercond. Sci. Technol. **31**, 102789 (2018).

Keywords: Coated Conductor, Bulk Magnet

WBP4-6

A study on the effect of slitting and packaging processes on the critical current of HTS tapes

Zhuyong Li[1], *Yuqian Li[1], Wenyi Li[2], Zhijian Jin[1], Zhiyong Hong[1], Longbiao Wang[1]

Shanghai Jiao Tong University[1]
Inner Mongolia University of Technology[2]

The study reports the effect of slitting and packaging processes on the critical current of high-temperature superconducting (HTS) tapes. The Critical current is one of the important criteria for HTS tapes. In this study, the loss of the critical current after cutting the 4mm wide HTS tapes into the 1mm wide HTS tapes is investigated. The cutting sections of these tapes are studied through the microscope in order to find the relationships between the cutting sections and the reducing of the critical current. Changes in the cutting sections of different HTS tapes during the slitting process are also compared. Moreover, the effect of packaging processes on the critical current is tested by packaging the 1mm HTS tapes into packaged tapes. All tests are performed in liquid nitrogen at 77K. The results of this paper could provide possible references for the future slitting and packaging processes on the HTS tapes.

Keywords: HTS tapes, slitting and packaging processes, critical current

WBP4-7

Influence of the contacting terminal on transport current distributions along the ReBCO tape

*Shinnosuke Matsunaga[1], Tetsuhiro Obana[1,2], Yoshiro Terazaki[2], Nagato Yanagi[1,2]

SOKENDAI (The Graduate University for Advanced Studies)[1]
National Institute for Fusion Science[2]

The Fusion Engineering Research Project at the National Institute for Fusion Science has proposed the use of high-temperature superconductor (HTS) as one of the conductor options for winding the helical coils of the LHD-type helical fusion reactor FFHR [1]. A STARS (stacked tape assembled in rigid structure) HTS conductor has been investigated as an approach to develop a practical HTS helical coil; ReBCO tapes are simply stacked into a copper stabilizer and a stainless steel reinforcing jacket [2]. It has widely been recognized that non-uniform electric current distributions occur in a superconductor without having twisting nor transposition. This argument points to a need for quantitatively evaluating the non-uniformity of the transport current, which depends on the reactor's operations. Prior to study on the current distributions among multiple tapes, we investigated the current distribution along a single tape.
To evaluate the transport current distributions in the single tape, an experimental apparatus, which measures magnetic fields generated by transport current, has been developed. Hall sensors, set on the upper side of a tape sample in a row, observing parallel fields to the width direction, composed one array. The current distributions can be estimated by observing fields at the sensors. The employed sample was the GdBCO tape made by Fujikura Ltd. (FYSC-SC10, 10 mm width, critical current ~650 A at 77 K, self-field). To examine the influence of terminal, three contacting conditions between the terminal and the sample were prepared, namely, (a) normal condition, (b) half cut contacting area, and (c) partially insulated area by tapes, and, as shown in Fig.1. As a result, no significant variations of the current distributions were observed. The field distribution at either array approximately corresponded with the calculated result of uniform current. This indicated that the electric contacting condition at a terminal hardly affect the transport current distributions along a ReBCO tape. In other words, it was suspected that the cross-sectional transport current distribution in a superconductor depends upon cross-sectional geometrics and external magnetic fields.

[1] A. Sagara et al., Nuclear Fusion, Vol. 57, 086046, 2017
[2] N. Yanagi et al., 26th IAEA Fusion Energy Conference, FIP/P7-11, 2016

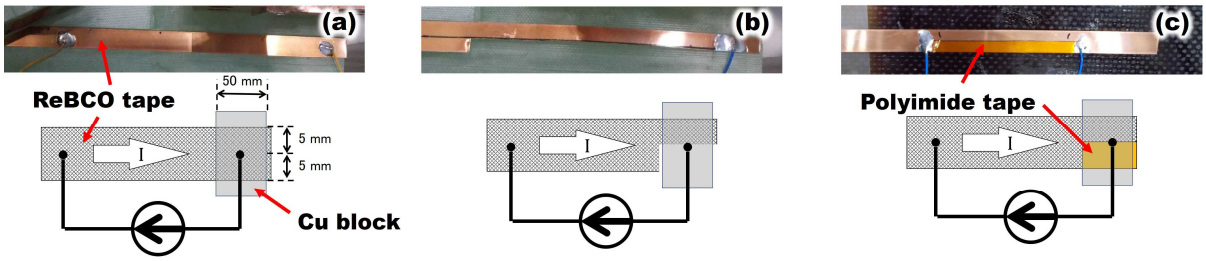

Keywords: Current distribution, ReBCO tape

WBP5-1

Study of joint mechanism for superconducting joint of $GdBa_2Cu_3O_y$ coated conductors

*Tomohiro Miyajima[1], Ryo Teranishi[1], Yukio Sato[1], Kenji Kaneko[1], Miyuki Nakamura[2], Valery Petrykin[2], Sergey Lee[2], Satoshi Awaji[3], Tatsunori Okada[3], Akiyoshi Matsumoto[4]

Kyushu University, Japan[1]
SuperOx, Japan[2]
Tohoku University, Japan[3]
National Institute for Materials Science, Japan[4]

Recently, several superconducting joints have been reported to fabricate long $REBa_2Cu_3O_y$ coated conductors (CCs) for electrical power application [1-3]. Fabrication temperature and oxygen partial pressure (PO_2) should be controlled to suppress the formation of secondary phase based on temperature and PO_2 diagram. Nevertheless, that for jointed sample has not been reported so far. In this work, the temperature and PO_2 diagram for jointed sample was investigated from the volume fraction of $GdBa_2Cu_3O_y$ (VF_{GdBCO}) fabricated at various temperatures and PO_2.

Joints were attempted by additional layers consisting of GdBCO grains with 0.5~1.0 μm deposited onto GdBCO CCs by a pulsed laser deposition method at 573 K. Two GdBCO CCs with the additional layers were placed with face to face, then the overlapped area was pressed in a pressure of 10 MPa. The sample was heated at 993, 1093, and 1193 K in PO_2 of 50, 500, and 5000 Pa under constant mechanical pressure. Jointed samples were peeled off, and their overlapped area and non-overlapped area were examined by X-ray diffractometer, then their VF_{GdBCO} were estimated by integrated intensity ratio of GdBCO peak against all peaks including GdBCO peak.

Fig. 1 shows a temperature and PO_2 diagram for jointed sample which summarizes VF_{GdBCO}, where circle, triangle, and square mean VF_{GdBCO} of larger than 95%, between 50 and 70%, and 0%, respectively. Red symbols and blue ones mean overlapped area and non-overlapped area, respectively. In the case of constant PO_2 of 5000 Pa, VF_{GdBCO} decreased from more than 95% to 0% below 1193 K at the both of overlapped area and non-overlapped area. On the other hand, in the case of constant temperature of 1093 K, VF_{GdBCO} decreased from more than 95% to less than 70% below 500 Pa at only overlapped area. These results indicates that VF_{GdBCO} is more sensitive to PO_2 rather than temperature probably because oxygen path was blocked at the overlapped area.

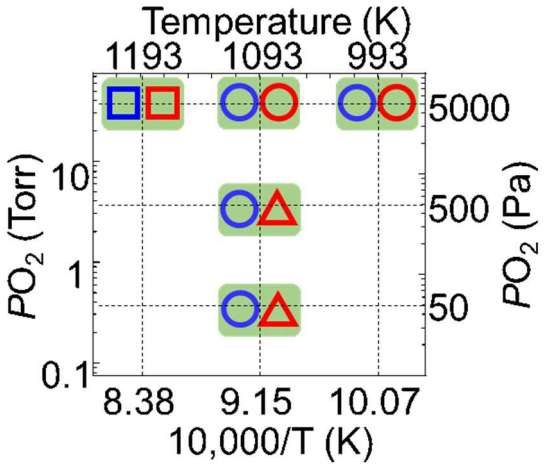

Fig. 1 Temperature and PO_2 diagram for jointed sample.

[1] Park, Y. J. et al. *Supercond. Sci. Technol.* **2014**, *27*, 085008.
[2] Jin, X. et al. *Supercond. Sci. Technol.* **2015**, *28*, 075010.
[3] Ohki, K. et al. *Supercond. Sci. Technol.* **2017**, *30*, 115017.

Keywords: Superconducting joint, REBCO, Coated conductor

WBP5-2

Influence of oxygen diffusion path on superconducting joint property of $GdBa_2Cu_3O_{7-\delta}$ coated conductor with additional deposited layer

*Shotaro Yasuyama[1], Tomohiro Miyajima[1], Ryo Teranishi[1], Yukio Sato[1], Kenji Kaneko[1], Valery Petrykin[2], Sergey Lee[2], Satoshi Awaji[3], Tatsunori Okada[3], Akiyoshi Matsumoto[4]

Kyushu Univercity[1]
SuperOx Japan[2]
Tohoku Univercity[3]
National Institute for Materials Science[4]

Lengthening of $REBa_2Cu_3O_{7-\delta}$ coated conductors (REBCO CCs) by superconducting joint has been longed for electric power application, due to its high critical temperature (T_c) and critical current (I_c) and low toxicity[(1)(2)]. Superconducting joint was applied on the GdBCO CCs with additional deposited layer and T_c of it was measured as 81.9 K lower than that of GdBCO bulk as 95 K[(3)(4)]. This low T_c was caused by the deficiency of oxygen in GdBCO lattice, so that the doping of sufficient amount of oxygen were required.

In this research, paths of introduce oxygen gas was fabricated on the surface of GdBCO CCs, to promote oxygen diffusion in the jointed sample, so that to improve the T_c value.

Jointed samples were fabricated by Metal Organic Deposition (MOD) method starting solution for GdBCO film was spin-coated onto GdBCO CC and then the samples were calcined at 823 K to fabricate precursor films. Two pieces of them were held together in a face to face manner and heated at 1073 K under the pressure of 20 MPa to crystallize and then the jointed samples were oxygenated at 773 K for 200 hours. In this study, 7 paths in the longitudinal direction was introduced with its width and interval about 35μm and 730 μm, respectively.

Fig.1 shows dependence of electric resistance on temperature for jointed sample with path and without path. T_c of the samples with and without path are 87.5 K and 81.9 K, respectively, which suggested that T_c of sample with path was enhanced about 5.6 K. In addition, ΔT of the samples with and without path are 1.3 K and 4.5 K respectively and this result prove ΔT of sample with path was suppressed about 3.2 K.

The paths prepared artificially into the joint of which suggests interface played a role of path of oxygen gas, which resulted oxygen doping efficiency and homogeneously.

Keywords: Superconducting joint, Additional deposited layer, Oxygen diffusion path, GdBCO coated conductor

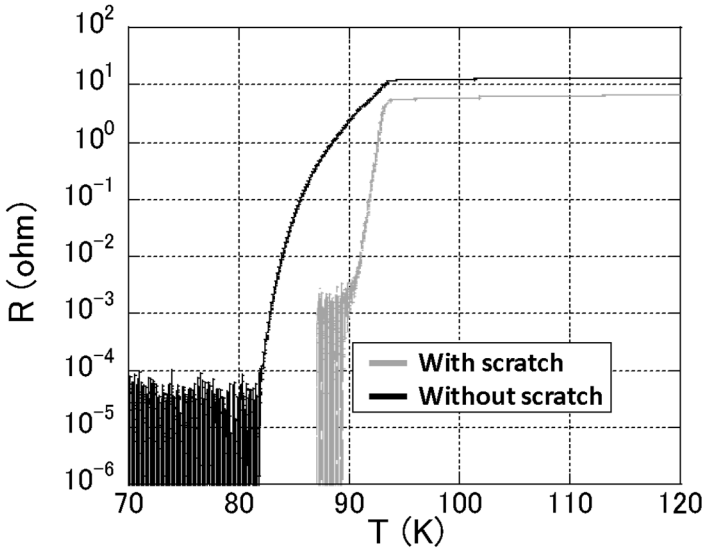

Fig.1 Dependence of electric resistance on temperature

WBP5-3

Superconducting-Joint for REBCO coated conductors by low-temperature reaction using KOH

*Shuhei Funaki[1], Yugo Miyachi[1,2], Yasuji Yamada[1]

Shimane Univ. , Japan[1], JSPS Research Fellow, Japan[2]

Many groups have endeavored to joint REBCO-CCs maintaining superconductivity, and several novel techniques for jointing were proposed. However, these techniques need long-time annealing to compensate oxygen deficiency of RE123 phase due to high process temperature above melting point. We have suggested the "KOH flux method", which is production method of REBCO film by using low-temperature liquid phase epitaxy. The KOH flux method can grow biaxially crystal-aligned RE123 and RE124 films on single crystalline substrates below 600ºC. RE124 has a rigorous stability in oxygen stoichiometry as opposed to RE123 phase. Moreover, stable temperature of RE124 phase is far lower than that of RE123 in the ambient atmosphere. Recently, synthesis of twin-free and orthorhombic Eu123 single crystal was reported by Marquez [1]. This result indicates that the Eu123 synthesized at 450ºC by using NaOH–KOH eutectic flux is grown with sufficient amounts of oxygen in Cu–O chain. In this presentation, in order to establish superconducting-joint method that requires feasible process at On-site, we endeavored to develop a superconducting-joint between two REBCO-CCs by low-temperature reaction using KOH.

Jointed samples were prepared in three steps. The first step is that RE–Ba–Cu–O raw materials were placed between RE123 films of CCs. In the second step, REBCO-CCs were pressed by two plates of metal. Finally, REBCO-CCs were heat treated at 525ºC in KOH vapor. All steps were performed at ambient pressure.

We measured *R*–*T* curves for three regions of jointed REBCO-CCs as shown figure. The REBCO-CC that is protruded jointed region showed fine conductivity and comparable T_c with bare REBCO-CC. The jointed REBCO-CCs were bonded finely, and showed T_c^{onset} ~ 76 K, T_c^{zero} ~ 60 K inclusive of jointed region. The jointed region that is peeled REBCO-CC after heat treatment showed T_c^{onset} ~ 80 K, T_c^{zero} ~ 70 K and contained RE123, RE247 phases from XRD observation.

This work was supported by JST-Mirai Program Grant Number JPMJMI17A2, Japan.

[1] L. N. Marquez et al, Chem. Mater. **5** (1993) 761

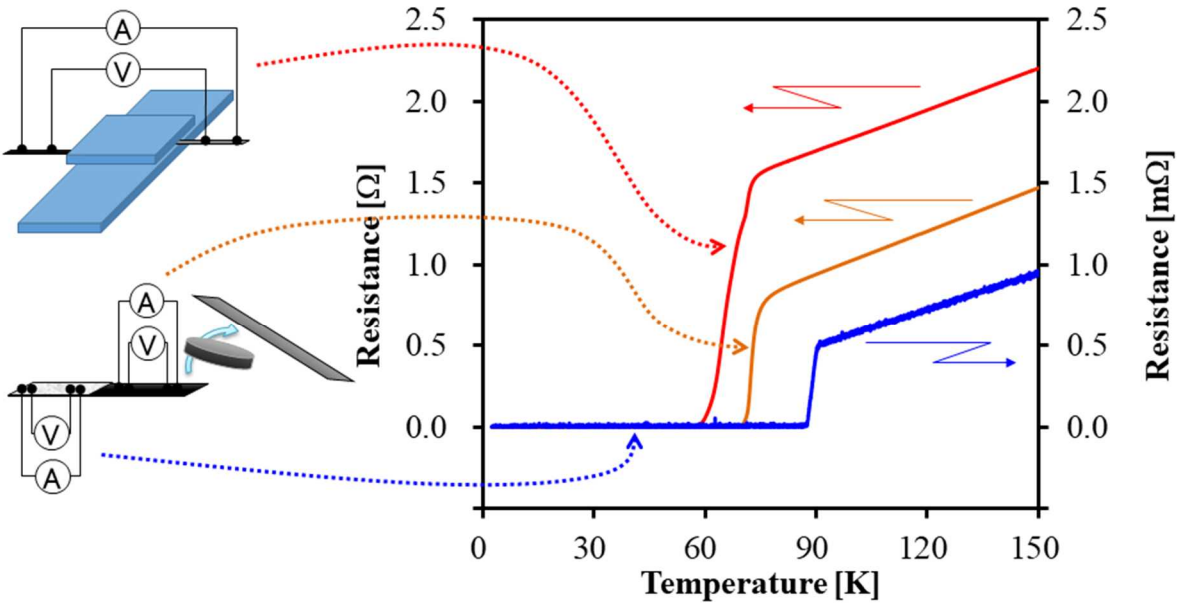

Fig. *R*–*T* curves of heat treated REBCO-CCs

Keywords: Joint, Superconducting-joint, low-temperature, KOH

WBP5-4

Superconducting Joints between Bi2223 and NbTi Wires by in-situ Sheath-Dissolution Technique

Masachika Shibuya[1], Ryo Matsumoto[1,2], Gen Nishijima[1], Hiroyuki Takeya[1], Hitoshi Kitaguchi[1], Yoshihiko Takano[1,2]

National Institute for Materials Science[1]
University of Tsukuba[2]

A development for nuclear magnetic resonance (NMR) spectrometer operated at 1.3GHz, corresponding to a magnetic field of 30.5 T, with persistent current operation is expected. As one kind of realization of the persistent current operation, the superconducting joint technique between $Bi_2Sr_2Ca_2Cu_3O_{10}$ (Bi2223) and NbTi superconducting wires is necessary. Recently we first report such a superconducting joint by an in-situ sheath-dissolution technique with Pb-Sn-Bi superconducting solders [1]. In this study, an optimal composition of Pb-Sn-Bi solders was surveyed to obtain a higher critical current property. Figure (a) shows an optical image of the solder joint between NbTi and DI-BISCCO type HT-NX. Figure (b) and (c) show SEM image of the cross-section around NbTi and Bi2223 in our superconducting joint, respectively. According to the SEM images, the sheath materials around the wires were diluted into the solder. Critical currents above 200A at 4.2K under self-field were obtained in the joints using Pb-Sn-Bi superconducting solders with the composition of $Pb_{0.3\text{-}0.7}Sn_{0.1\text{-}0.3}Bi_{0.1\text{-}0.5}$. In the symposium we will report the transport properties under magnetic field.

[1] R. Matsumoto et al., *Appl. Phys. Express* **10**, 093102 (2017).

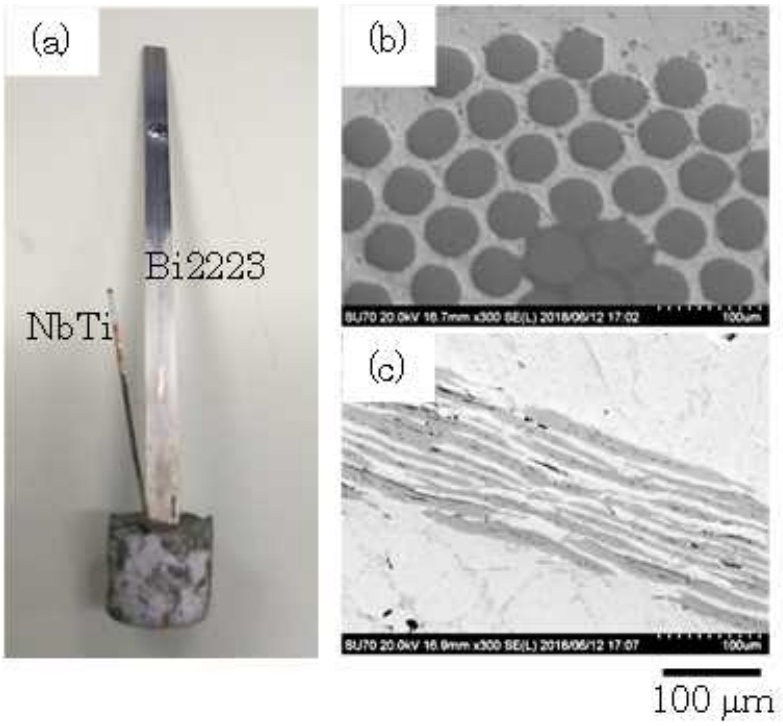

Fig. (a) Optical image of the solder joint between NbTi and DI-BISCCO type HT-NX. , (b) cross-sectional SEM image around NbTi and (c) Bi2223 in Pb-Sn-Bi superconducting solders.

Keywords: Superconducting joint, Bi2223, NbTi, NMR

WBP6-1

Study of the Superconducting Layer Microstructure and (Nb,ti,Ta)$_3$Sn *Bronze Strands Properties*

Ildar M. Abdyukhanov[1], Victor I. Pantsyrny[1], Alexander G. Silaev[1], Anastasiia S. Tsapleva[1], *Maxim V. Alekseev[1], Elena A. Dergunova[1], Konstantin A. Mareev[1], Valery A. Drobyshev[1], Marina V. Kravtsova[1], Nadezhda V. Konovalova[1], Mansur N. Nasibulin[1], Pavel A. Lykianov[1]

SC A.A. Bochvar High-Technology Research Institute of Inorganic Materials, Russia[1]

The optimization of the high field magnets systems for high energy physics or cutting-edge analytical NMR systems *requires the development of the superconducting strands with high current carrying capacity in magnetic fields up to 16 T at 4.2 K. One of the frequently used superconductors for operating in magnetic fields above 12 T are bronze route Nb$_3$Sn strands. For the increase of their critical current in high magnetic fields doping by Ti and Ta is applied. In bronze processed strands the doping element could be incorporated both into the matrix material and into the filaments material.*
Investigation results of the Nb$_3$Sn strands with Nb-7wt.%Ta and Nb-3.5wt.%Ta filaments in Cu-15.5%Sn-0.2%Ti-0.2%Zr and Cu-15.5%Sn-0.25%Ti bronze matrix are presented in this study. Diameter of the investigated strands has been varied in the range from 0.8 to 1.5 mm. For the superconducting phase formation different heat treatment regimes have been applied. The final step of reaction heat treatment temperature has been varied from *650 up to 720 °C. After heat treatment of the samples Nb$_3$Sn layer microstructure and electrophysical characteristics have been investigated. It was shown when the* temperature of the reaction heat treatment final step increases from *650 up to 720 °C*, strands critical temperature drops down from 17.5 to 16.5 K.

Keywords: Nb3Sn, doping, heat treatment, critical temperature

WBP6-2

CFETR CSMC Nb_3Sn Coil deformation analyze in Heat Treatment Process and the coil fixture design

Song Jian[1], Wu Yu[1], Qin Jingang[1], Yu Min[1], Li Tong[1], Wang Weijun[1]

Institute of Plasma physics, Chinese Academy of Sciences, China[1]

The CSMC are major components of CFETR to generate the magnetic field for **Simulating the Central Solenoid coil manufacturing process.** In the heat treatment process, the coil will have some deformation that was made of the residual stress relaxing. The coil deformation may cause the coil unable to assemble. Therefore, it need to design the coil fixture to prevent the coil deformation. It need to analyze the force on the coil and check the strength of the coil fixture in the heat treatment process. In the trials, the radius increase of the coil must be less than 4.3mm after the heat treatment process and the stress on coil fixture is less than 150MPa.

Keywords: CFETR CSMC Nb3Sn heat treatment, Coil deformation, Fixture, Residual stress

WBP6-3

Preparation of MgB_2 superconductor by the rapid heating and quenching method

Xiaofeng Zou[1], Wenjie Zhang[1], Yong Zhao[2,3], Yong Zhang[1,2]

Key Laboratory of Advanced Technologies of Materials (Ministry of Education of china), and Superconductivity and New Energy R&D Center, Southwest Jiaotong University, Chengdu 610031, China[1]
Key Laboratory of Magnetic Levitation Technologies and Maglev Trains (Ministry of Education of China), and School of Electric Engineering, Southwest Jiaotong University, Chengdu 610031, China[2]
College of Physics and Energy, Fujian Normal University, Fuzhou 350117, China[3]

MgB_2 is a simple binary semi metallic compound.It is reported that the superconducting transition temperature Tc of MgB_2 can reach 39 K.The MgB_2 superconductor has a dual-energy band structure, and the preparation method can also be various, such as in-situ reaction, hot isostatic pressing, mechanical alloying method, etc.In order to reduce the long-term annealing process and prevent excessive grain growth,we tried to prepare MgB_2 superconducting wire by RHQ method. In this paper,we successfully prepared MgB_2 superconducting wire with self-made RHQ equipment, and the effect of various Joule heating currents by RHQ method on the properties of MgB_2 superconducting wire were investigated.

Keywords: MgB2 superconductor, rapid heating and quenching, Joule heating currents, superconducting properties

WBP6-4

Fabrication and properties of 19 cores MgB_2/NbCu/Monel wires with carbon coated boron as precursor powder

*Qingyang Wang[1], Kerong Zhang[2], Fang Yang[1], Xiaomei Xiong[1], Dan Xi[3], Xifeng Pan[3], Guo Yan[3], Chengshan Li[1], Pingxiang Zhang[1,3]

Northwest Institute for non-ferrous Metal Research, Xi'an, China[1]
Xizang Minzu University, School of information technology. Xianyang, China[2]
Western Superconducting Technologies Co. Ltd., Xi'an, China[3]

For improving the mechanical properties and avoiding the filament fractures or wire breaks in multi filament MgB_2 wire, A Monel alloys with higher strenth was introduced to the MgB_2 wires fabrication process as the outer sheath. MgB_2 wire with the conducting structure of 19 filaments was fabricated by *in-situ* powder in tube method (*in-situ* PIT). Multi-filament compound billet is processed from Φ25 mm to Φ1.0 mm in diameter with drawing, rolling and annelling process. Superconducting filament is uniformly distributed and the thickness of Nb diffusion barrier is also smooth without breaking points through the microstructure analysis of the wires at each fabrication stages. The mean diameter in MgB_2 supercongducting cores is aroung 100 μm in final wires with the diameter of Φ1.0 mm. The tensile strength and yield strength of the wire heat-treated at 670℃/2h is around 396 MPa and 200 MPa respectively. The critical current density (Jc) is arrived 1.23×10^5 A·cm^{-2} at 4.2 K、4 T.

Keywords: MgB2 wire, multi filament, mechanical properties, supercongducting

WBP6-5

Development of a Monitor for Parallel-type Superconducting Level Sensor

*Naoki Tanaka[1], Kazuhiro Kajikawa[1], Hidetoshi Oguro[2], Makoto Sugino[3], Tsutomu Nakanishi[3], Itsuo Aoki[3]

Graduate School of Information Science and Electrical Engineering, Kyushu University[1]
School of Engineering, Tokai University[2]
Jecc Torisha Co., Ltd.[3]

Hydrogen that produces only water after its combustion is expected as a clean energy, and liquefied hydrogen might be used for mass storage and transport in near future. At that time, it is necessary to understand the accurate amount of liquid hydrogen in the container. A parallel-type superconducting (SC) level sensor composed of MgB_2- wire A and non-SC wire B has been proposed [1], and its usefulness to observe a level of liquid hydrogen has been confirmed so far [2]. We are also developing a monitor to control the parallel SC level sensor and indicate the liquid level in the container as shown in the figure. We install a power supply, central processing unit (CPU), analog-to-digital (AD)/digital-to-analog (DA) converter, touch panel, voltage dividers and isolators inside a monitor unit. The output voltages, V_A and V_B, from the SC level sensor with a constant current produced by the power supply are taken into the CPU via the voltage dividers, isolators and AD converter. The liquid level is evaluated according to the pre-written program code. The obtained result is displayed on the touch panel and outputted as an analog voltage via the isolator and DA converter.

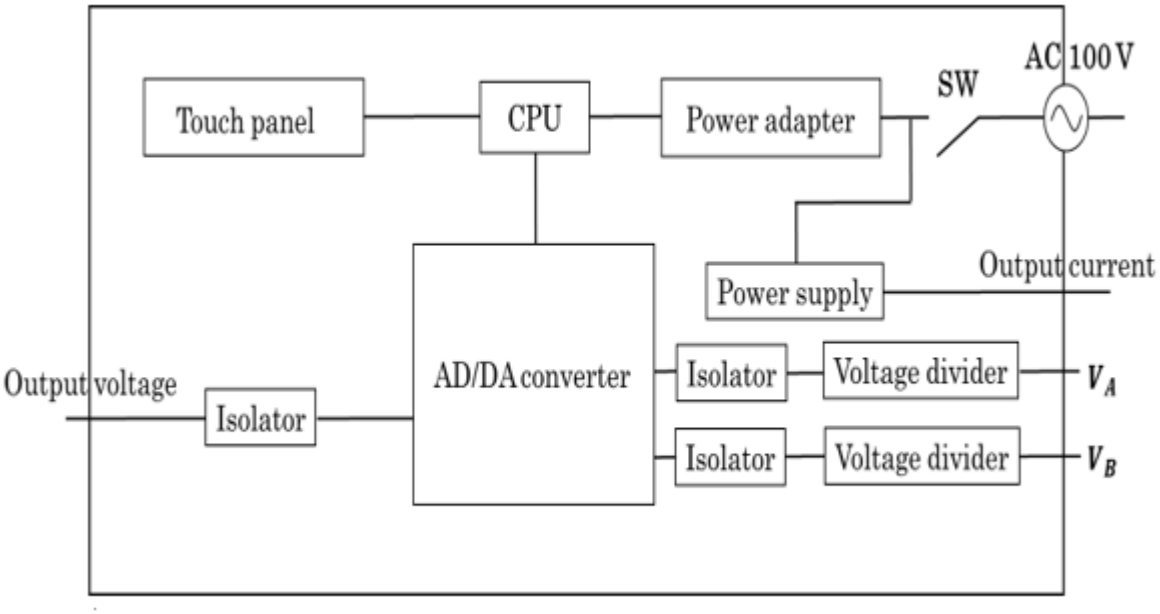

Fig. Circuit diagram of monitor

Keywords: Monitor, Liquid hydrogen, Superconducting level sensor, MgB2 wire

WBP6-6

Critical Current Properties of Superconducting Joint between $Ba_{1-x}K_xFe_2As_2$ Tapes

*Shota Imai[1,2], Shigeyuki Ishida[2], Yoshinori Tsuchiya[2], Akira Iyo[2], Hiroshi Eisaki[2], Kunio Matsuzaki[2], Taichiro Nishio[1], Yoshiyuki Yoshida[2]

Department of Physics, Tokyo University of Science[1]
National Institute of Advanced Industrial Science and Technology (AIST)[2]

Iron-based superconductors, which possess high critical temperatures T_c up to 56 K and upper critical fields over 100 T, are promising for high magnetic field applications [1]. Especially for $(Ba,K)Fe_2As_2$, the critical current density (J_c) exceeds 1.5×10^5 A/cm^2 at 4.2 K and 10 T [2]. However, in order to construct its superconducting magnets and to use that in the persistent mode of operation, a superconducting joining technique is of critical importance. Recently, Zhu *et al.* reported the first superconducting joints between $(Sr,K)Fe_2As_2$- tapes fabricated using a hot press technique, demonstrating a relatively high critical current ratio (CCR) of 35.3 % (at 4.2 K in 10 T). Meanwhile, they found cracks and a potassium loss in the joint area, which generally degrade the performance of the joints [3]. It is necessary to reduce the number of the micro cracks and to prevent the potassium content from losing.
In this study, we fabricated superconducting joints between $(Ba,K)Fe_2As_2$- tapes by using a simple cold uniaxial press technique and evaluated their performance. Figure 1(a) shows critical currents (I_c) of the joint at 4 K under magnetic fields parallel to the tape surface before and after making the joint. High CCR values over 60 % in a self-field and 20% in 3.5 T at 4 K is achieved. Figure 1(b) shows a SEM image of the cross section of the joint. Macro cracks were not observed around the jointed part, which can be associated with the higher CCR of the present joint. The details will be given in the presentation.

[1] Ma. Y. W *et al.*, Supercond. Sci. Technol., **25**, 113001 (2012).
[2] Huang. H *et al.*, Supercond. Sci. Technol., **31**, 015017 (2018).
[3] Zhu. Y *et al.*, Supercond. Sci. Technol., **31**, 06LT02 (2018).

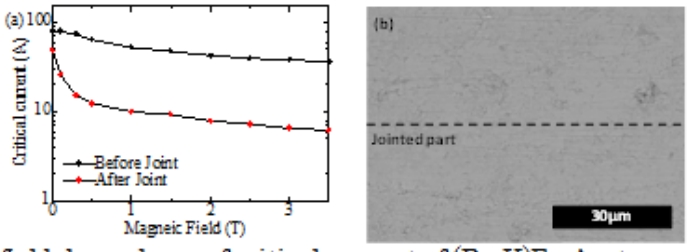

Fig. 1: (a) Magnetic field dependence of critical current of $(Ba,K)Fe_2As_2$ tape and joint at 4 K with field parallel to the tape surface. (b) SEM image of the cross section of $(Ba,K)Fe_2As_2$ joint.

Keywords: Iron-based superconductors, Superconducting joint, Critical Current Ratio, Critical current

WBP6-7

Fabrication of (Ba,Na)Fe_2As_2 round wires using HIP process

*Daisuke Miyawaki[1], Sunseng Pyon[1], Tsuyoshi Tamegai[1], Satoshi Awaji[2], Katsutoshi Takano[3], Hideki Kajitani[3], Norikiyo Koizumi[3]

The University of Tokyo[1]
Institute for Materials Research, Tohoku University[2]
National Institute for Quantum and Radiological Science and Technology[3]

Iron-based superconductors are high-temperature superconductors that have high critical temperature, high critical magnetic field, small anisotropy, and large critical current density under high magnetic fields. They are expected to be put into practical applications such as wires for high-field magnets. Among them, the most promising candidates are the group of materials called 122 type. In particular, superconducting tapes and wires using K-doped 122 type ((Ba,K)Fe_2As_2 and (Sr,K)Fe_2As_2) have been extensively studied. In addition, we have reported fabrication and characterization of (Sr,Na)Fe_2As_2 tapes [1]. However, studies on (Ba,Na)Fe_2As_2 tapes and wires have not been undertaken.

In this study, we fabricated round wires of $Ba_{0.6}Na_{0.4}Fe_2As_2$ using powder-in-tube technique and hot isostatic press (HIP) treatment. Figure 1 compares transport J_c at 4.2 K of two $Ba_{0.6}Na_{0.4}Fe_2As_2$ round wires with Ag/Cu double sheath which were processed at 700 ℃ for 4 hours at 1,750 atm. Transport J_c of wire #1 is 76 kA/cm^2 and 24 kA/cm^2 at self-field and 100 kOe, respectively, while J_c of wire #2 is slightly larger at low fields. Even at a high magnetic field of 100 kOe, J_c of wire #1 is reduced to only one third of the self-field value. It demonstrates very promising characteristics of $Ba_{0.6}Na_{0.4}Fe_2As_2$ round wires. Detailed characterizations of wires using X-ray diffraction and magneto-optical imaging will also be presented.

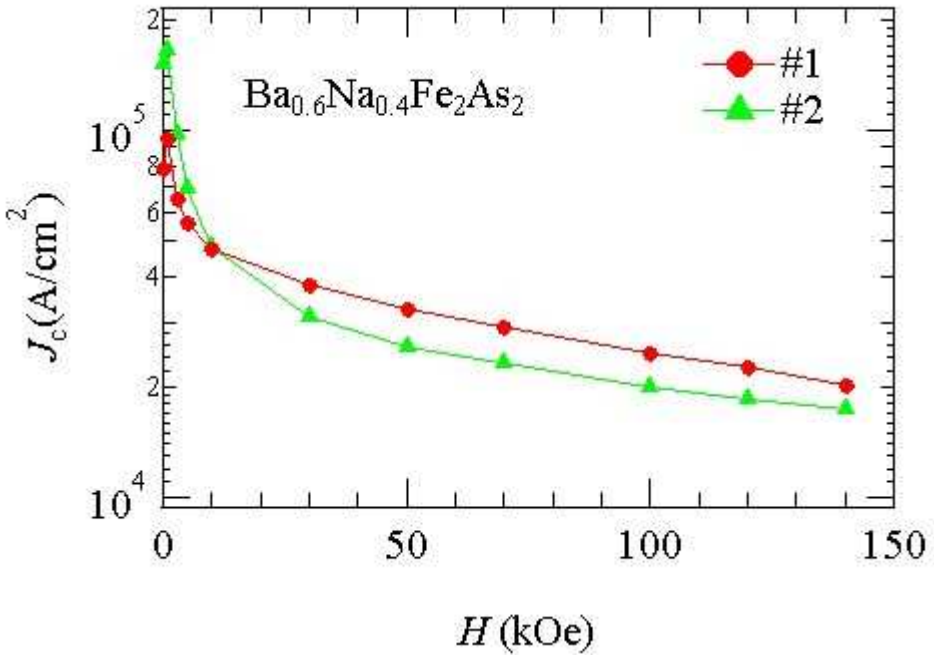

Fig.1 Magnetic field dependence of transport J_c of two $Ba_{0.6}Na_{0.4}Fe_2As_2$ HIP round wires processed at 700 ℃ and 1,750 atm for 4 hours.

[1] Suwa *et al.*, Appl. Phys. Express 11, 063101 (2018).

Keywords: Iron-based superconductor, Critical current density, HIP round wire

WBP7-1

Effects of Nd_2O_3 and TiO_2 addition on the superconducting and microstructure properties of YBCO bulk superconductors fabricated by modified infiltration and growth technique

*Fahad A Alzaid[1], Devendra K Namburi[2], Talal Aljuohani[1], Yunhua Shi[2], Anthony R Dennis[2], Maha M Khayyat[1], Abduljalil S Aljadani[1], Bandar M Alotaibi[1], David A Cardwell[2], John H Durrell[2]

Center of Excellence for Advanced Materials and Manufacturing, King Abdulaziz City for Science and Technology, Riyadh, Saudi Arabia[1]
Department of Engineering, University of Cambridge, Cambridge, UK[2]

Large single grain bulk Y-Ba-Cu-O (YBCO) superconductors are one of the most studied high temperature superconductors because of their potential of carrying high critical current density (J_c) and achieving large trapped magnetic fields. There is a wide variety of potential applications for this material, such as in magnetic levitation systems, energy storage and motors. However, it is of a great importance to improve their superconducting properties for practical use. One of the possible methods to improve J_c is by the addition of foreign dopants since their addition can introduce defects that act as pinning centers [1].

The two most widely used fabrication processes for obtaining large, single grain YBCO bulk are the top seeded melt growth (TSMG) and the top seeded infiltration and growth (TSIG). Both processes have their challenges such as porosity and micro-cracks using TSMG, and reliability and inclusions optimisation using TSIG. This study uses a modified TSIG technique that has recently been proposed to address some of these growth challenges [2].

The effects of Nd_2O_3 and TiO_2 doping on critical current density (J_c), critical temperature (T_c), trapped magnetic field and microstructure of single grain bulk YBCO superconductors fabricated by buffer-aided top seeded infiltration and growth (TSIG) process have been investigated. Three series of samples were fabricated with varying concentrations of Nd_2O_3, TiO_2 and mixtures of both. Heat treatments were tuned such that all these samples could grow into single grains. Trapped field was measured in each of these samples and compared. To obtain J_c, the parent samples were sectioned into smaller specimens as shown in the inset in figure 1. A superconducting quantum interference device (SQUID) was used to measure the M-H loops at 77 K, 65 K and 50 K with an applied field up to 6 T parallel to c-axis. Figure 1 shows that the highest J_c recorded at 77 K to be 62 kA/cm^2 for 1.0 wt% Nd_2O_3, while the overall highest J_c recorded was 240 kA/cm^2 at 50 K for 0.25 wt% Nd_2O_3. While we noticed an improvement in J_c with the addition of dopants, their unfavorable effect on T_c was negligible since all the samples had a T_c of ~ 91K.

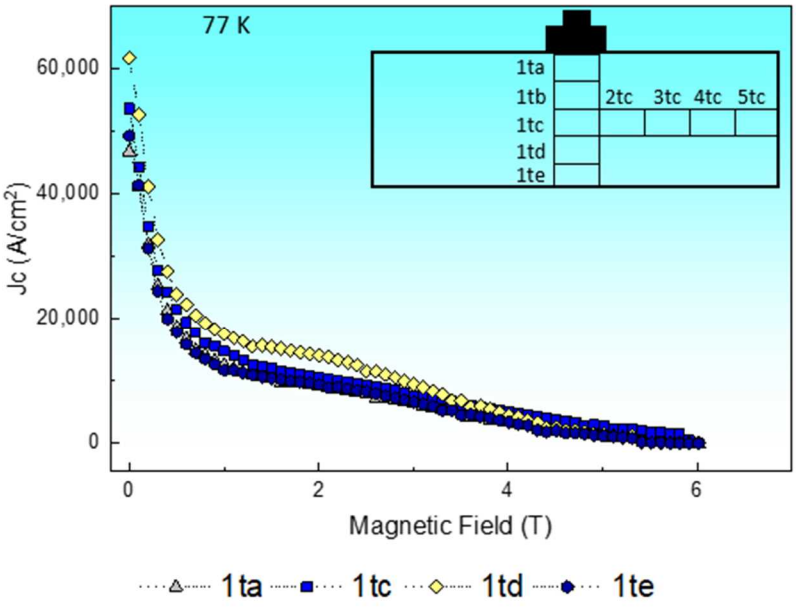

Figure 1: $J_c - B$ curves for specimens extracted from a sample with 1.0 wt% Nd_2O_3. The inset illustrates the sectioning procedure from the parent sample.

References: [1] M. Murakami, Melt Processed High Temperature Superconductors. Singapore: World Scientific, 1991.
[2] Namburi, D.K. Supercond. Sci. Technol. **29**, 095010

Keywords: Infiltration and Growth, YBCO bulk, Superconductor, Flux pinning

WBP7-2

Fracture strength properties of (Gd,Y)BaCuO large single-grain bulk at liquid nitrogen temperature

*Akira Murakami[1], Akifumi Iwamoto[2]

National Institute of Technology, Ichinoseki College Japan[1]
National Institute for Fusion Science Japan[2]

In order to investigate the low temperature fracture strength properties of a (Gd,Y)BaCuO large single-grain bulk with 100 mm in diameter, bending tests were carried out at liquid nitrogen temperature 77 K for the specimens cut from a bulk sample. The large single-grain bulk was fabricated by RE compositional gradient technique to overcome the problem of undesirable nucleation apart from the seed crystal. A precursor which consists of some regions with difference Gd and Y contents was used for the fabrication. The Y content increases with increase of the distance from the center of the precursor to decrease the peritectic decomposition temperature. Both the specimens which contained an interface between two regions with different Gd and Y contents and specimens which did not contain it were cut from the bulk sample. Bending tests for plain specimens without V-notch and those for V-notched specimens were carried out to evaluate the fracture strength and fracture toughness, respectively. The fracture strength values of the specimens with the interface were comparable to those of the specimens without the interface, which is similar to the fracture strength evaluated at room temperature in the previous study. The fracture strength at 77 K was superior to that at room temperature. Relationship between the fracture strength and fracture toughness is discussed.

Keywords: Bulk material, Single-grain, Fracture strength, Fracture toughness

WBP7-4

Optimization of Liquid Phase Mass for the Production of Single Grain IG Processed Bulk $YBa_2Cu_3O_y$ by $YbBa_2Cu_3O_y$+Liquid Phase as a Liquid Source

*Sushma Miryala[1,2], Masato Murakami[1]

Shibaura Institute of Technology, Japan[1]
Seisen, Japan[2]

The utilization of top-seeded and melt growth technique together with infiltration growth (IG) process along with an optimal amount of liquid ($Ba_3Cu_5O_8$) is efficient for peritectic growth since it is a primary requirement to produce the single grain bulk $YBa_2Cu_3O_{7-\delta}$ (Y-123). In this presentation, IG process $YBa_2Cu_3O_{7-\delta}$ superconductors with different liquid phase (LP) sources were investigated by means of varying liquid phases Yb-123+liquid (1:1, 1:1.2, and 1:1.3) as a liquid source. To compare its growth rate, all samples were produced at a similar cooling rate in 50 hours. The grown samples indicate that growth tripled in liquid phase ratio 1:1.3 as compared to 1:1. Magnetization measurements by SQUID magnetometer exhibits a superconducting transition with $T_{c,onset}$ at 92.1 K and critical current density at 77 K was around 40 kA/cm^2 (H//*c*-axis) in self-field. Scanning electron microscopy (SEM) results show an uniform Y-211 secondary phase particles dispersion in Y-123 matrix. Eventually, single grain large Y-123 material was produced utilizing a liquid phase ratio 1:1.3 and this is confirmed by the single grain nature by trapped field measurements (see Fig.1, right). Our experimental results clearly indicate that an optimal amount of liquid phase is crucial to grow a large grain Y-123 material, which is very crucial for wide-ranging industrial applications.

Figure 1. As grown bulk Y-123 superconductors produced by Top Seeded Infiltration Growth Process utilizing a mixture of Yb-123+liquid phase as a liquid source in 50 hours. Yb-123+liquid (1:1) left; Yb 123+liquid (1:1.2) middle left; Yb-123+liquid (1:1.3) middle right; Yb-123+liquid (1:1.3) right (> 50h)

Keywords: Y-123, IG Process, Critical Current Density, SEM

WBP7-5

Optimization of the *Infiltration-Growth Process* for Fabrication of Large Bulk (YEr)$Ba_2Cu_3O_y$ Superconductors

*Kento Takemura[1], Tethuo Oka[1], Muralidhar Miryala[1], Masato Murakami[1]

Shibaura Institute of Technology[1]

The infiltration growth (IG) process combined with melt growth technique allows for a uniform and controllable Y2BaCuO5 (Y211) secondary phase particles
formation in the YBa2Cu3O*y* (Y123) matrix. The flux pinning performance of the Y123 material dramatically improved after optimizing the processing conditions during the IG process. To further improve the flux pinning performance of the Y-123 material, YEr-211(90:10) preform was used and the optimum growth temperature was found utilizing the isothermal growth at the temperatures 995 oC; 990 oC; 988 oC; 985 oC; 983 oC; and 980 oC. While at 995 oC only a limited area of the growth was observed, the growth dramatically increased at 988 oC. Magnetization measurements indicated a sharp superconducting transition with *Tc* (onset) around 91.5 K. The highest critical current density (*Jc*) at 77 K and 0 T was 57 kAcm-2, in the sample produced by the isothermal growth at 990 oC. Eventually, using the optimum growth profile constructed based on isothermal growth conditions, a large grain bulk YEr-123 material was prepared, the single-grain nature of which was confirmed by trapped field measurement.

Keywords: YBCO, IG process, seed crystal, Er

WBP7-6

Improvement of trapped field of REBCO bulk activated by pulsed field magnetization with a large soft-iron yoke

*Kazuya Yokoyama[1], Tetsuo Oka[2]

Ashikaga University[1]
Shibaura Institute of Technology[2]

We study a strong magnetic field generation using an REBCO bulk activated by pulsed field magnetization (PFM) toward practical applications. In PFM, there are some advantages of compact magnet system and activating a bulk with conventional equipment, a condenser bank and a copper coil, in a short time. In our study, we developed several magnet systems using single-stage GM-type, two-stage GM-type and Stirling-type refrigerators. When a GdBCO bulk with 60 mm in diameter and 20 mm thick was magnetized in a bulk magnet system using a 13 K two-stage GM-type refrigerator with cooling capacity of 12 W at 20 K, the maximum trapped field of 3.59 T was achieved. In the PFM system, a bulk was sandwiched between two soft-iron yokes to extend the time when the magnetic field was showered on the sample. We have used a small yoke 37 mm in diameter because the size of bulk was small at the beginning. However, the bulk 60 mm in diameter is used now, and then, the yoke is expanded to 64 mm in diameter. When the same magnetizing experiment is carried out using the large yoke, a trapped field reaches 3.85 T at the center of bulk surface and the total magnetic flux is improved by 13% compared with the small yoke system.

Keywords: REBCO bulk, pulsed field magnetization, soft-iron yoke, trapped field

WBP7-7

Numerical analysis of magnetic trapped fields for bulk superconductor with weak or insulated junctions between multiple-seed-growth domains

*Mitsuru Sawamura[1], Mitsuru Izumi[2]

Steel Research Laboratories, Nippon Steel & Sumitomo Metal Corporation[1]
Tokyo University of Marine Science and Technology (TUMSAT)[2]

To open up the application fields of high-Tc melt processed Y-Ba-Cu-O(RE-Ba-Cu-O) bulk superconductors[1], it is important to increase the flexibility of size and shape. To fabricate a large-sized bulk superconductor, multiple seeding techniques are effective in reducing the fabrication (crystal growth) time. However, conventional multiple seeded bulk superconductors have some peaks for the trapped magnetic fields because the critical current density over multiple-seed-growth domains is restricted considerably owing to the insulation phases (Cu-O, RE_2BaCuO etc.) between multiple seed domains. The MUlti-Seeded seamLEss (MUSLE) technique achieves a single peak of a trapped field despite the multiple seeding technique[2]. This technique has two crystal growth steps by composition with different peritectic temperatures and removal of the first growth step part including the insulation phases.

In this study, assuming bulk superconductors with various weak or insulated junctions between 4 seed-growth domains, their trapped fields were analyzed numerically by using the finite element method for the circuit[3] extended to superconductors. The figure shows the configuration and example simulation result with a weak junction condition. For each condition, the peak value and distribution of the trap field are discussed.

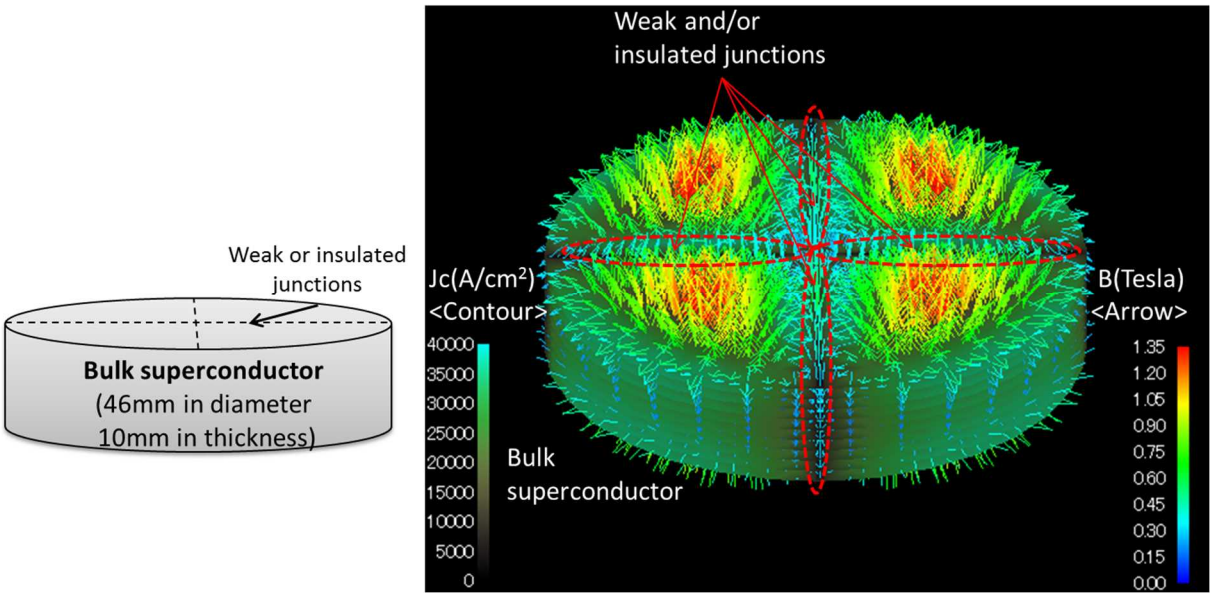

Fig. Configuration and example simulation result

[1] Morita, M., Takebayashi, S., Tanaka, M., Kimura, K., Miyamoto, K. and Sawano, K. Adv. in superconductivity III (Springer, 1991) 733.
[2] Sawamura M., Morita M. and Hirano H., Physica C 378-381 (2002) 617.
[3] Kameari, A. Journal of Computational Physics 42 (1981) 124-40.

Keywords: high Tc superconductor, trapped magnetic field

WBP7-8

Numerical analysis of magnetic levitation forces for bulk superconductors with weak or insulated junctions between multiple-seed-growth domains

*Mitsuru Sawamura[1], Mitsuru Izumi[2]

Steel Research Laboratories, Nippon Steel & Sumitomo Metal Corporation[1]
Tokyo University of Marine Science and Technology (TUMSAT)[2]

To open up the application fields of high-Tc melt processed Y-Ba-Cu-O(RE-Ba-Cu-O) bulk superconductors[1], it is important to increase the flexibility of sizes and shapes. To fabricate a large-sized bulk superconductor, the multiple seeding technique is effective in reducing the fabrication (crystal growth) time. However, conventional multiple seeded bulk superconductors have peaks for the trapped magnetic fields because the critical current density over the multiple-seed-growth domains is restricted considerably owing to the insulation phases (Cu-O, RE_2BaCuO etc.) between multiple seed domains. The MUlti-Seeded seamLEss (MUSLE) technique has been reported to achieve a single peak of a trapped field despite the multiple seeding technique[2].This technique features two crystal growth steps by composition with different peritectic temperatures and removal of the first growth step part including the insulation phases.

In this study, assuming bulk superconductors with various weak or insulated junctions between 4 seed-growth domains, their magnetic levitation forces against a permanent magnet with each gap under the zero field cooling (ZFC) was analyzed numerically by using the finite element method for the circuit [3] extended to superconductors. The figure shows the configuration and example simulation result with a weak junction condition. For each condition, the maximum levitation forces and the contributions at each depth of the bulk from the surface in the case of ZFC are discussed.

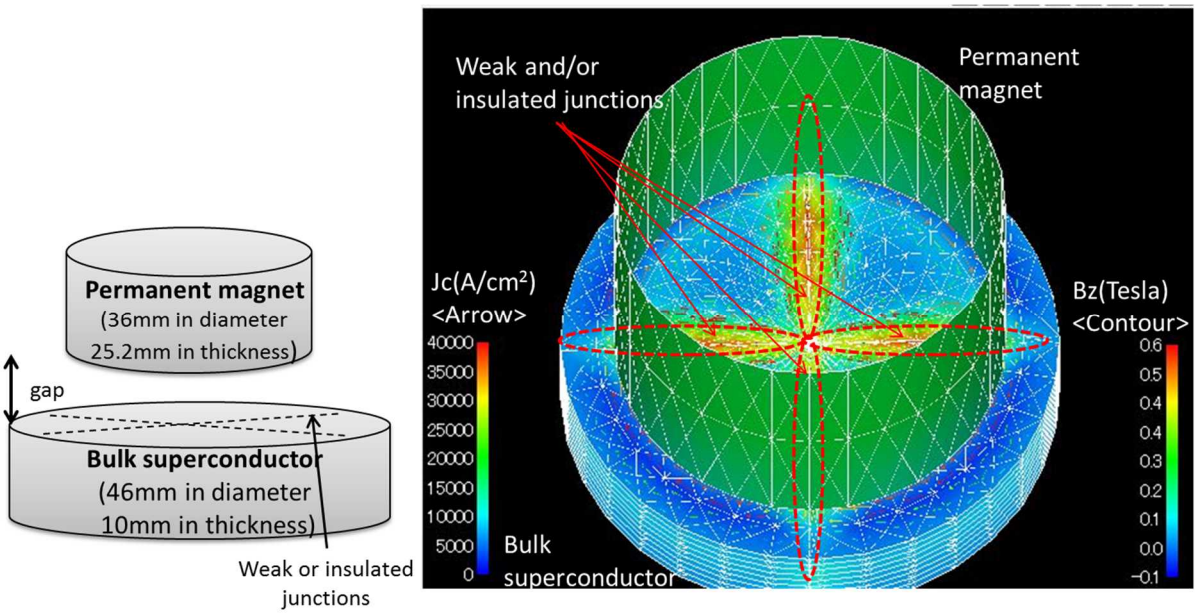

Fig. Configuration and example simulation result

[1] Morita, M., Takebayashi, S., Tanaka, M., Kimura, K., Miyamoto, K. and Sawano, K. Adv. in superconductivity III (Springer, 1991) 733.
[2] Sawamura, M., Morita M., and Hirano H., Physica C 378-381 (2002) 617.
[3] Kameari, A. Journal of Computational Physics 42 (1981) 124-40.

Keywords: high Tc superconductor, levitation force

WBP8-1

Refining effects of B powder on MgB_2 formation and vortex pinning properties in infiltration-reaction processed MgB_2 bulks

*Yuhei TAKAHASHI[1], Tomoyuki NAITO[1], Hiroyuki FUJISHIRO[1]

Faculty of Science and Engineering, Iwate University[1]

The densification of MgB_2 bulks is essential to produce practical MgB_2 bulk magnet. An infiltration and reaction process realizes the dense MgB_2 bulk without the external physical pressure. The trapped field of MgB_2 bulk prepared by infiltration and reaction process was 2.4 T at 15.9 K, which was as high as that of MgB_2 bulk prepared by in-situ hot isostatic pressing method [1]. However, there was quite a large amount of unreacted micrometric B particles due to the incomplete diffusion of Mg into B [2]. Therefore, it is expected that the trapped field of infiltration and reaction processed MgB_2 bulk can be improved by the decrease of unreacted B. In this paper, to obtain the higher trapped field, we studied a refining effects of B powder on the formation of MgB_2 and the vortex pinning properties.

Crystalline B powder was refined by ball-milling at various rotation speed of 0-600 rpm for 1 h. The B pellet and Mg pellet were placed in a stainless steel container and heat-treated at 700-900℃ for 1-24 h. From the scanning electron microscope observation, the largest particle sizes of B were about 50 mm and about 10 mm for as-purchased and ball-milled at 600 rpm, respectively. This indicated the increase of grain boundaries which acted as the pinning centers. Moreover, the volume fraction of MgB_2 using ball-milled powder is larger than that of MgB_2 using as-purchased powder. Therefore, the trapped field of the MgB_2 using ball-milled powder was higher than that of MgB_2 using as-purchased powder, except for the MgB_2 using ball-milled powder at 200 rpm (Fig. 1). In the presentation, we discuss the refining effects of B on the MgB_2 formation and the vortex pinning properties.

[1] T. NAITO et al., Supercond. Sci. Technol. 29 (2016) 115003

[2] A. OGINO et al., IEEE Trans. Appl. Supercond. 27 (2016) 6800905

Keywords: bulk magnet, infiltration and reaction process, MgB2, vortex pinning property

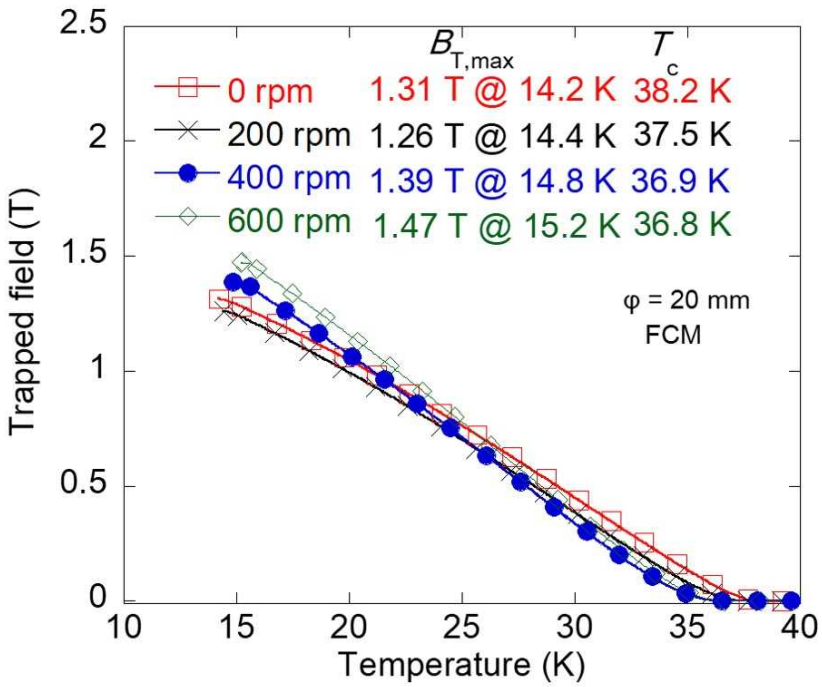

Fig. 1 Temperature dependence of the trapped field of MgB_2 bulks which were made from ball-milled powder at 0-600 rpm and heat-treated at 900°C for 24 h.

WBP8-2

Synthesis and trapped field properties of dense MgB_2 bulks by Magnesium Vapor Transportation (MVT) method

*Yu Sanogawa[1], Akiyasu Yamamoto[1,2]

Department of Applied Physics, Tokyo University of Agriculture and Technology, Tokyo, Japan[1]
Materials Research Center for Element Strategy, Tokyo Inst. of Technology, Kanagawa, Japan[2]

MgB_2 (Magnesium diboride) [1] has the highest critical temperature (T_c = 39 K) among metallic superconductors. Bulk MgB_2 trapped field magnet [2] is interesting for high field applications. On the other hand, in the case of *in situ* method (Mg + 2B → MgB_2), a commonly used synthesis technique of MgB_2, many voids are generated during reaction, resulting in low packing factor (~50%). The low packing factor and wetting phases at grain boundaries are considered to limit the effective transport current path, critical current density (J_c) and trapped magnetic field. Novel processes [3-6] were developed by various groups to achieve dense MgB_2 bulks. In the present study, we have developed a new fabrication method, Mg vapor transportation (MVT) method [7], to obtain large MgB_2 bulks with high density and high purity. The conceptual diagram of the MVT method is shown in **Fig. 1**. A disk-shaped boron pellet as a precursor of the disc-shaped MgB_2 bulk and the Mg vapor source were separately placed, and pure Mg vapor evaporated from the Mg source was transported to the boron pellet through the holed division walls, then diffused into and reacted with boron. By the MVT method, we succeeded in fabricating large MgB_2 bulks up to 30 mm in diameter with high density and low MgO content compared to the bulks fabricated by *in situ* method. The bulks fabricated by the MVT method showed high J_c which is twice as high as that of *in situ* method (**Fig. 2**). A bulk (20 mm in diameter, 2 mm in thickness) fabricated by the MVT method trapped 1.7 Tesla at 10 K at the center of the bulk surface. The detailed trapped field properties of MgB_2 bulks with different sample size will be reported.

[1] J. Nagamatsu *et al.*, *Nature.* **410**, 63 (2001).
[2] A. Yamamoto *et al.*, *Appl. Phys. Lett.* **105**, 032601 (2014).
[3] J. H. Durrell *et al.*, *Supercond. Sci. Technol.* **25** 112002 (2012).
[4] G. Giunchi *et al.*, *Supercond. Sci. Technol.* **16,** 285–291 (2003).
[5] S. Ueda *et al., Appl. Phys. Lett.* **86**, 222502 (2005).
[6] A. G. Bhagurkar *et al.*, *Supercond Sci. Technol.* **28,** 035008 (2015).
[7] Y. Sanogawa *et al.*, IUMRS-ICAM 2017, P.57 (2017).

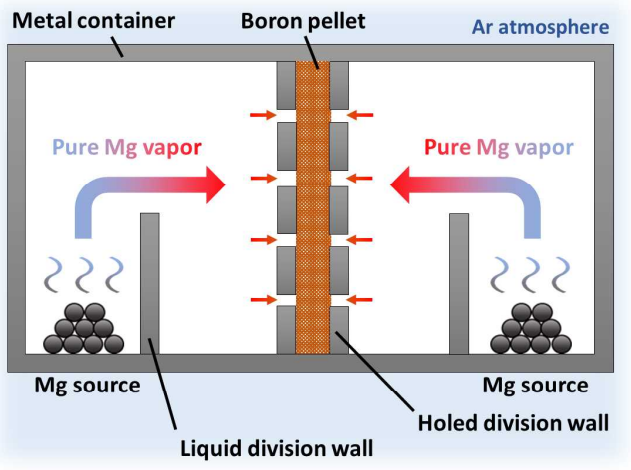

Fig. 1 Conceptual diagram of MVT method.

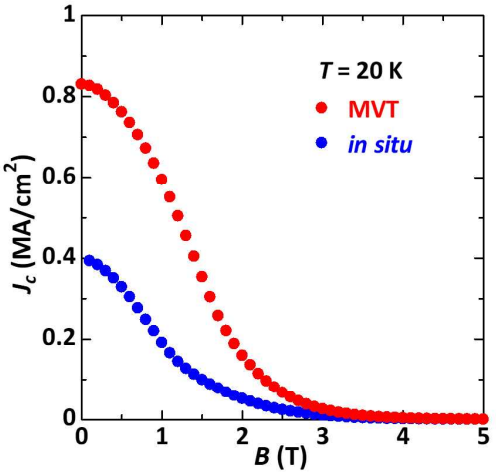

Fig.2 External magnetic field (B) dependence of critical current density (J_c) at 20 K for the MVT and *in situ* MgB_2 bulks.

Keywords: MgB2, Bulk magnets

WBP8-3

Trapped Field Properties of Pulsed Field Magnetization (PFM) of MgB_2 Bulk Fabricated by Spark Plasma Sintering (SPS) Method

*Hayami Oki[1], Akira Takeda[1], Tetsuo Oka[2], Satoshi Fukui[1], Jun Ogawa[1], Kazuya Yokoyama[3], Jaques Noudem[4], Kengo Yamanaka[2], Masato Murakami[2]

Niigata University (Japan)[1]
Shibaura Institute Of Technology (Japan)[2]
Ashikaga University (Japan)[3]
Caen University (France)[4]

Until now, some research institutes have magnetized MgB2 by Field Cooled Magnetization (FCM) which is said to be the most efficient, but FCM requires a large device and power consumption is large and the time required for magnetization is long. Therefore, this time we used Pulsed Field Magnetization (PFM) to experiment that can magnetize in a short time and compact. In this research, trapped field characteristics were evaluated by pulse magnetization of MgB_2 prepared by SPS method.

Samples used for PFM are shown in Table.1. The sample of this time was prepared by the SPS method by changing the sintering temperature, pressure and time. The sample was set on the cold stage and a hall sensor was attached to the surface center of the sample. After that, the inside of the chamber was evacuated and the sample was cooled by setting the freezer to 15 K. The pulsed magnetic field was obtained by discharging a pulse current from a capacitor charged in a conductor coil cooled to 77 K with liquid nitrogen.

FIG. 1 shows trapped fields of each bulk. In this experiment, the highest trapped field was B_T = 0.75 T of F526. Even when the applied magnetic field was increased, the trapped magnetic field did not rise significantly. Therefore, the field capture ratio decreased as the applied field was increased.

Table.1 Spec of Bulk

Sample Name	Diameter[cm]	Height[cm]	Density[g/cm^3]	Pressure[MPa]	Temperature[°C]	Time[min]
E116	1.995	1.29	2.05	90	1200	
F528	1.990	0.96	2.62	50	1150	15
I258	1.960	1.27	1.45	75	950	15
I689	1.960	1.378	1.47	100	900	20
I690	1.983	0.926	2.62	100	1100	20

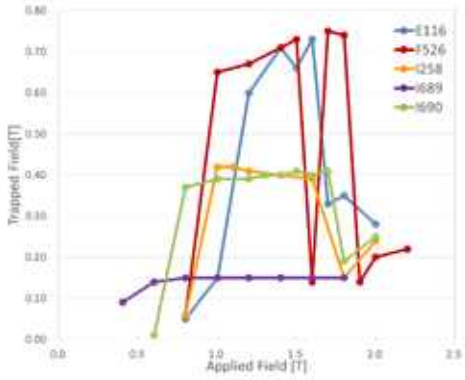

Figure.1 Trapped Field

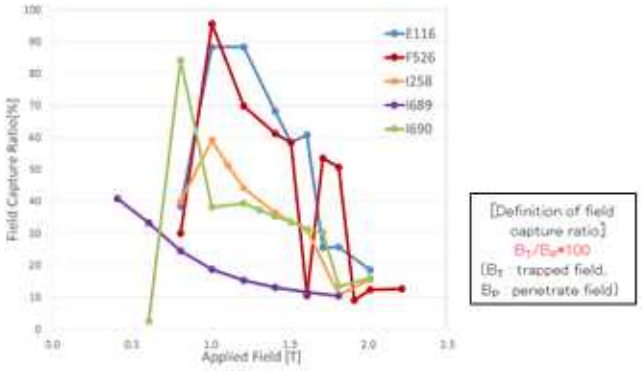

Figure.2 Field Capture Ratio

WBP8-4

Flux Pinning and Superconducting Properties of Bulk MgB_2 Using a Small Dy_2O_3 Additions

*Kotaro Kitamoto[1], Muralidhar Miryala[1], Masato Murakami[1]

Shibaura Institute of Technology[1]

The objective of this investigation is to optimize the Dy_2O_3 addition in bulk MgB_2 for a high flux pinning. High-purity commercial powders of Mg metal (99.8% purity) and nanometer-sized amorphous boron powders (98.5% purity) were mixed in the nominal composition of MgB_2 with a varying content of Dy_2O_3 (0, 0.2, 0.4, 0.6, 0.8, 1 and 2wt%) and synthesized using the solid state reaction at 800 °C for 3 h in pure argon atmosphere. All samples are characterized by x-ray diffraction, scanning electron microscopy (SEM), and superconducting performance; T_c and J_c at 20 K were recorded by SQUID magnetometer. XRD results indicated that all samples show the main phase is MgB_2 along with a small quantity of MgO. Except pure MgB_2, all samples presented a minor amount of DyB_4. The superconducting transition temperature (T_c) did not change much, but the critical current density (J_c) dramatically improved. The MgB_2 sample with 1wt% of Dy_2O_3, processed at 800 °C for 3 h, showed critical current density of 400 kA cm^{-2} and 250 kA cm^{-2} at 20 K in self field and 1 T, respectively. The improved critical current performance was explained based on the microstructural changes in the final product.

Keywords: MgB2, Dy2O3, critical current density, flux pinning

WBP8-5

FLUX PINNING AND SUPERCONDUCTING PROPERTIES OF Mg-RICH MgB_2

*Sai Srikanth Arvapalli[1], muralidhar miryala[1], masato murakami[1]

Shibaura Institute of Technology[1]

In this work, we discuss the advantageous effects of adding Mg precursor required for obtaining high critical current density (J_c) of bulk MgB_2 superconductor synthesized via solid state sintering. To obtain the best critical current density values we used carbon encapsulated boron (1.5% carbon) and added 4 wt% Ag. Slightly excess Mg precursor has been introduced to balance magnesium losses while formation of pinning phases involving Mg, vapor losses and impurities such as Ag-Mg phases and MgO respectively. Excess Mg was added in regular intervals such as 5 wt%, 7.5 wt%, 10 wt%, 12.5 wt% and 15 wt% over standard for production of bulk MgB_2 material. X-ray diffraction analysis showed the formation of AgMg and $AgMg_3$ phases and very minute amount of MgO. SQUID measurements indicated that highest J_c of 520 kA/cm^2 in self-field (10 K); 280 kA/cm^2 at 1 T (10 K), 350 kA/cm^2 in self-field (20 K) in sample with 7.5 wt% excess Mg addition. Our results clearly demonstrate that excess Mg is crucial to obtain highest critical current density of bulk MgB_2 material with the usage of carbon encapsulated boron.

Keywords: Mg-rich MgB2, carbon encapsulated boron, critical current density, flux pinning

WBP8-6

Processing and Characterization of Charcoal Added Bulk MgB_2

*Longji Dadiel[1], Muralidhar Miryala[1], Masato Murakami[1], S Pavan Kumar Naik[1]

Shibaura Institute of Technology, Japan[1]

In this study, we focus on methods to further improve the flux pinning and critical current density *(J_c)* of disk-shaped MgB_2 bulk superconductors by a comparative study between locally obtained charcoal and anthracite at optimized processing conditions. The doping of charcoal/anthracite was varied at 0.0, 0.1, 0.2, and 0.3 wt%. Bulk MgB_2 samples were produced by the in-situ solid-state reaction in Ar gas and ambient pressures using high purity commercial powders of Mg metal and amorphous B powders mixed in a fixed ratio of Mg:B = 1:2. The crystal structure and microstructural characterization have been investigated by X-ray diffractometer (XRD) and scanning electron microscopy (SEM). The effects of the dopants on superconducting properties especially critical temperature *(T_c)* and critical current density (*J_c)* have been measured by employing superconducting quantum interference device (SQUID). The flux pinning behavior has been investigated by scaling of the flux pinning force density volume. All result analyzed and explained the critical current performance on the bases of the charcoal in the final product.

Keywords: MgB2, charcoal, scanning electron microscopy, critical current density

EDP1-1

Multipoint measurements of a Pipe Using HTS-SQUID and Magnetostriction-Based Ultrasonic Guided Wave

*Yuki Azuma[1], Yuki Yokouchi[1], Shogo Kubota[1], Tomohiro Terawaka[1], Yoshimi Hatsukade[1], Seiji Adachi[2], Keiichi Tanabe[2]

Kindai University, Japan[1]
Superconducting Sensing Technology Research Association, Japan[2]

This paper describes study on remote inspection technology for pipes by using magnetostriction-based ultrasonic guided wave and high temperature superconductor (HTS) superconducting quantum interference device (SQUID) gradiometer. Two magnetized nickel plates were glued on an aluminum pipe sample. They were used as magnetostriction-based guided wave transceivers, and a coil was wound around one nickel plate as a transmitter, while the other was used as a receiver. T (0, 1) mode guided wave was generated by supplying a burst sine wave current of one cycle at several tens kHz to the coil. Multipoint measurements of the T (0, 1) mode guided waves around the pipe's circumference were carried out by setting the HTS-SQUID gradiometer above the receiver with lift-off of about 7 mm and rotating the pipe for 360 degree. Three circumferential defects were made sequentially on the aluminum pipe sample at different distances from the receiver. The multipoint measurements were performed with four patterns; the first one was with no defect, and the second to the fourth were with 1 defect, 2, and 3 defects, respectively. Magnetic signals due to the guided waves reflected at the defects were measured by the HTS-SQUID gradiometer. Contour maps of the measured signals around the pipe with and without the defects were created to estimate propagation paths of the guided waves by comparing these measurement results and those obtained with a simulation software.

Keywords: HTS-SQUID, ultrasonic guided wave, multipoint measurement, magnetostriction

EDP1-2

Design and Performance of Digital SQUID Magnetometer using sub-flux quantum feedback

*Kosuke Okabe[1], Ryo Matsunawa[1], Kohki Itagaki[1], Itsuta Oshima[1], Masato Naruse[1], Tohru Taino[1], Hiroaki Myoren[1]

Graduate School of Science and Engineering, Saitama University[1]

Digital SQUIDs with the single flux quantum (SFQ) feedback have attracted much attention because of the feasibility of realizing a wide dynamic range and high slew rate. In order to realize higher resolution, we have studied a digital SQUID with sub-flux quantum feedback. Combining the sub-flux quantum feedback to a feedback loop and the direct SFQ feedback to a main loop triggered by carry SFQ pulses from an up/down counter. After optimization of the circuit, we confirmed the maximum magnetic field amplitude exceed 1 μT, the magnetic field noise is lower than 100 pT/√Hz with a signal band frequency of 1.22 MHz. In this study, we report a design of the digital SQUID with sub-flux quantum feedback and evaluate the performance of a magnetometer using the digital SQUID. Finally we discuss the method of multi-flux quantum generation and compact design of the SFQ up/down counter for high-speed operation of the digital SQUID magnetometer.

Acknowledgement
This study has been partially supported by the VLSI Design and Education Center (VDEC) at the University of Tokyo, in collaboration with Cadence Design Systems, Inc. Circuits were fabricated in the clean room for analog-digital superconductivity (CRAVITY) of the National Institute of Advanced Industrial Science and Technology (AIST) with the standard process 2 (STP2). The AIST-STP2 process is based on the Nb circuit fabrication process developed by the International Superconductivity Technology Center (ISTEC).

Keywords: digital SQUID, sub-flux-quantum feedback, multi-flux quantum generation

EDP1-3

Line width dependence of NbN-based microwave kinetic inductance detectors

*Shun Negishi[1], Seiichiro Ariyoshi[1], Satoru Hashimoto[1], Hikaru Mikami[1], Kensuke Nakajima[2], Hirotaka Terai[3], Saburo Tanaka[1]

Toyohashi University of Technology[1]
Yamagata University[2]
National Institute of Information and Communications Technology[3]

The microwave kinetic inductance detector (MKID) detects terahertz waves by the change of kinetic inductance of superconducting film due to the absorption of a terahertz photon. The MKIDs consist of multiple resonators coupled with a microwave feed line, where the resonance frequency shift of each resonator is detected by the frequency-multiplexed readout scheme. All of the components in MKID are made of a single-layer film, which enables relatively easy fabrication of a large-scale array [1]. We propose an MKID array using niobium nitride (NbN) focusing on the shape of the resonator, where we aim to reveal the high-sensitive MKIDs' design using an electromagnetic field analysis.

In order to control resonance characteristics precisely, the line width dependence of a rewound spiral resonator was analyzed via a simulator, *Sonnet Lite*. Fig.1 (a) shows a resonator designed from the analysis model [2]. The total length of spiral was 12.5 mm corresponding to the half wavelength of resonance frequency for 5 GHz on sapphire substrates. The analysis was conducted under conditions of: frequency range of 1 ~ 10 GHz, relative permittivity of the substrate 9.8, substrate thickness 0.5 mm, thin film (150 nm) AC resistance 3.92×10^{-26} $\Omega Hz^{-2}/sq$[3], and sheet inductance 16.8 pH/sq. Resonance characteristics were analyzed on 3 resonator models; fixed line space (a) 10 µm with line width (w) varying to 10, 20 and 40 µm. The resonance frequencies (f_c) obtained 2.25, 2.75, and 3.25 GHz respectively, proving that the inductance decreases as the resonator thickness increases. The scattering-matrix elements (S_{21}) and the loaded quality factor (Q_L) were analyzed for each w (Fig.1(b)) and suggesting that the narrower w results in the shallower resonance dip and lead to the higher Q_L.

To verify the simulation results experimentally, NbN-based MKIDs with w of 10 and 40 µm were fabricated on a sapphire substrates then cooled down to 0.5 K. Evaluating the microwave characteristics with a vector network analyzer, f_c measured for the MKID with w of 40 µm was increased 1.1 GHz compared with that for 10 µm being consistent with simulation results. The detailed results will be given in this presentation.

[1] P. K. Day, et al. Nature **425** 817 (2003)
[2] S. Ariyoshi, et al. Appl. Phys. Express **6** 064103 (2013)
[3] K. Hayashi, et al. Physics Procedia **45** 213 (2013)

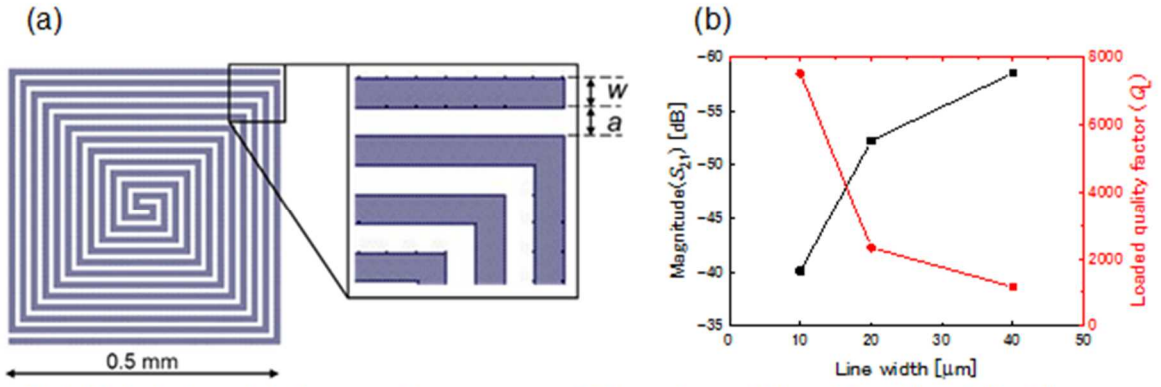

Fig1. (a) Analysis model of a rewound type resonator, (b) Dependence of S_{21} and Q_L on line width of the resonators

EDP1-4

Plug-in Wire for 200-pixel Superconducting Tunnel Junction X-ray Detector Array on Helium Three Cryostat

*Shigetomo Shiki[1], Go Fujii[1], Masahiro Ukibe[1]

National Institute of Advanced Industrial Science and Technology[1]

Superconducting tunnel junction (STJ) X-ray detector is promising for materials analysis because of its high energy resolution and high counting rate capability. However, in order to realize a practical analytical instrument based on STJ X-ray detectors, it is necessary to settle two technical difficulties as follows. One is realizing throughput as equal to that of a silicon drift detector by making a large pixel array. The other is developing a scalable wiring system between STJ array detectors at cold stage of a helium three cryostat and readout electronics in room temperature. The large format STJ array has been already developed [1]. However, realizing the scalable wiring system is difficult because in the conventional wiring system, all wires in a cryostat are usually soldered by hand. Therefore, we have developed a wire plug-in system, in which all electrical wires are attached to connectors at the both ends and the electrical connections between the STJ array to the room temperature electronics are established via the connectors.

Two hundred pair wires are installed from helium three stage to feedthrough on vacuum chamber at room temperature in a helium three cryostat. The wires are consisted of two parts as follow. One is copper based miniature coaxial cable harnesses, which is placed between room temperature to the 2.5 K stage. The other is NbTi wiring loom which is set between the 2.5 K stage to the helium three stage. After the installation of the wires, base temperature of the helium three stage is 307 mK, and the holding time is more than 80 hours. We succeeded to realize plug-in wire system for a large scale STJ X-ray detector array.

[1]“Development of superconducting tunnel junction array detectors with three-dimensional structure to exceed 1000-pixel array”, G. Fujii, M. Ukibe, S. Shiki, and M. Ohkubo, J. Low Temp. Phys., 184, 194-199, 2016.

Keywords: supeconducting tunnel junction, cryogenics, readout electronics, x-ray detector

EDP1-5

Ginzburg-Landau Theory for the Operation Principle of Superconducting Delay-Line Induction Detectors

*Tomio Koyama[1], Takekazu Ishida[1,2]

Division of Quantum and Radiation Engineering, Osaka Prefecture University[1]
Nano Square Research Institute, Osaka Prefecture University[2]

The operation principle of a superconducting delay-line inductance detector, *Current-Biased Kinetic Inductance Detector* (CB-KID), is revisited on the basis of the TDGL theory. In our previous paper [1], using the London theory for the current biased- superconducting nanowire, we derived an equation which can describe the propagation of voltage signals generated by a variation of the kinetic inductance which is caused by local heating in this detector. In the present paper instead the London theory we use the TDGL theory. The effect of heat diffusion is also incorporated by means of the heat diffusion equation. We derive a new dynamical equation for the superconducting phase difference between the superconducting nanowire and the basal superconducting layer, which is similar to the equation given in our previous paper. A systematic way to solve the equation is also presented. Our theory provides a more realistic description of the generation and propagation of voltage signals in CB-KID.

REFERENCES
[1] T. Koyama and T. Ishida, J. Phys. Conf. Ser. **1054,** 012055 (2018).

Keywords: kinetic inductance detector, superconducting nanowire, superconducting theory

EDP1-6

Temperature dependent characteristics of neutron signals from a current-biased Nb nanowire detector with ^{10}B converter

*The Dang Vu[1], Yuki Iizawa[2], Kazuma Nishimura[2], Hiroaki Shishido[2,3], Kenji M Kojima[4], Kenichi Oikawa[1], Masahide Harada[1], Shigeyuki Miyajima[2,5], Mutsuo Hidaka[6], Takayuki Oku[1], Kazuhiko Soyama[1], Kazuya Aizawa[1], Tomio Koyama[7], and Takekazu Ishida[3,7]

Materials and Life Science Division, J-PARC Center, Japan Atomic Energy Agency, Tokai, Ibaraki 319-1195, Japan[1]
Department of Physics and Electronics, Osaka Prefecture University, Sakai, Osaka 599-8531, Japan[2]
NanoSquare Research Institute, Osaka Prefecture University, Sakai, Osaka 599-8531, Japan[3]
Muon Science Laboratory and Condensed Matter Research Center, Institute of Materials Structure Science, KEK, Tsukuba, Ibaraki 305-0801, Japan[4]
Advanced ICT Research Institute, NICT, Kobe, Hyogo 651-2492, Japan[5]
National Institute of Advanced Industrial Science and Technology (AIST), Tsukuba, Ibaraki 305-8568, Japan[6]
Division of Quantum and Radiation Engineering, Osaka Prefecture University, Sakai, Osaka 599-8570, Japan[7]

A neutron beam is very useful to observe the inside of materials containing light atoms such as hydrogen, lithium, and boron, and has been utilized in the wide range of research fields (material science, physics, chemistry, biology, and agriculture) for potential applications including non-destructive transmission imaging, tomography, dark-field image and visualization of magnetic distribution. This method has been applied to various objects such as intermetallic compound, fuel cells, lithium ion batteries, cultural heritages, and others.

We previously proposed a superconducting detector named as a current-biased kinetic inductance detector (CB-KID) for detecting neutrons. In our preceding studies [1,2], we succeeded in designing to fabricate CB-KID, which consists of two perpendicular Nb-based superconducting meanderlines and an enriched ^{10}B neutron conversion layer. We obtained a clear neutron image of a ^{10}B dot array containing in the stainless-steel mesh [3]. In addition, the characteristics of a superconducting neutron detector have been studied systematically while a temperature of the detector is mostly kept at 4K [4,5]. However, it is still important to search for the best conditions to operate the CB-KID. In the present study, we investigated the dependence of neutron signals on the temperature of CB-KID. We found that the signal amplitude increases remarkably as a function of increasing temperature above 4K toward a critical temperature of Nb nanowire. According to this finding, we consider that there is an optimum temperature to enhance the detector performance of neutrons using CB-KID. We need to study further about the origin of the operation principle of CB-KID [6] to understand the temperature dependence of the signal.

This work was partially supported by a Grant-in-Aid from the Japan Society for the Promotion of Science (JSPS) (No. 16H02450).

References

[1] T. Ishida *et al.*, J. Low Temp. Phys. **176**, 216 (2014).
[2] S. Miyajima *et al.*, Nucl. Inst. Meth. Phys. Res. A **842**, 71 (2017).
[3] H. Shishido *et al.,* Phys. Rev. Applied, in press (2018).
[4] Y. Miki *et al.,* J. Phys.: Conf. Ser. in press (2018).
[5] Y. Iizawa *et al.*, J. Phys.: Conf. Ser. in press (2018).
[6] T. Koyama and T. Ishida, J. Phys.:Conf. Ser. in press (2018).

Keywords: Superconducting detector, Neutron detector, CB-KID, Pulsed neutron

EDP1-7

Si waveguide-integrated SSPD with AWG cold filter

*Hiromichi Niii[1], Kento Sakai[1], Tatsurou Hiraki[2,3], Tai Tsuchizawa[2,3], Koji Yamada[2,3], Shinji Matsuo[2,3], Daisuke Sakai[1], Hiroyuki Shibata[1]

Electrical and Electronic Engineering, Kitami Institute of Technology, Kitami, Hokkaido.[1]
NTT Device Technology Labs, NTT Corporation, Atsugi, Kanagawa.[2]
NTT Nanophotonics Center, NTT Corporation, Atsugi, Kanagawa.[3]

The silicon waveguide-integrated Superconducting Nanostrip Photon Detector (SSPD, SNSPD) is a new device developed by combining a superconducting single photon detector and a silicon waveguide. It will become a key component in the quantum photonic circuits. In this study, we evaluate the characteristics of Si waveguide-integrated SSPD by coupling with cooled arrayed waveguide grating (AWG) made of silica. Since the AWG is cooled at low temperature, it acts as the cold optical band-pass filter, which suppresses the dark count rate due to the blackbody radiation at room temperature passing through the optical fiber. Compared to the waveguide-integrated SSPD without AWG, the system dark count rate is suppressed by about two orders of magnitude. We find that the noise equivalent power (NEP) is improved from 3.8×10^{-18} to 1.2×10^{-18}.

Keywords: SSPD, SNSPD, AWG

EDP1-8

Reduction of Environmental Magnetic Field Noise for a Small Magnetic Contaminant Detection

*Takao Nishikawa[1], Ken Sakuta[1]

The University of Shiga Prefecture, Japan[1]

Recently, researches have been conducted to detect magnetic contaminants that have slipped into industrial products or the like by using a highly sensitive magnetic sensor such as SQUID magnetometer. In the case of high-sensitivity detection, it is necessary to reduce environmental magnetic noise in advance. Therefore, a magnetic shield box made of a ferromagnetic material such as permalloy is used. However, generally, the shield box has a lower cutoff rate as the noise becomes lower. In the case of metallic contaminant detection, since it measures slow and unsteady magnetic field change, it overlaps low frequency environmental magnetic noise and simple filter processing is difficult. Therefore, the application of active magnetic shield to magnetic contaminants detection was investigated. As Figure 1 indicates, this system operates according to the following principle. [1] The output voltage of the fluxgate magnetometer, which detects environmental magnetic noise is amplified by a preamplifier. [2] The amplified signal has restricted the band to slow and commercial power supply noise by a filter. [3] The restricted signal is feedbacked to the fluxgate magnetometer by compensation coil, and actively cancels environmental magnetic noise around SQUID magnetometer by generating the compensation signal.

In addition, when magnetic field gradients between the noise detection magnetometer and the signal detection magnetometer exist, since the negative feedback is applied to the noise detection magnetometer, amount of the noise reduction in the signal detection magnetometer is reduced. Therefore, we studied a method of the correction process. The noise signal in the output signal of SQUID magnetometer is extracted using a phase detection with the output signal of the fluxgate magnetometer, thereby the compensation signal is corrected.

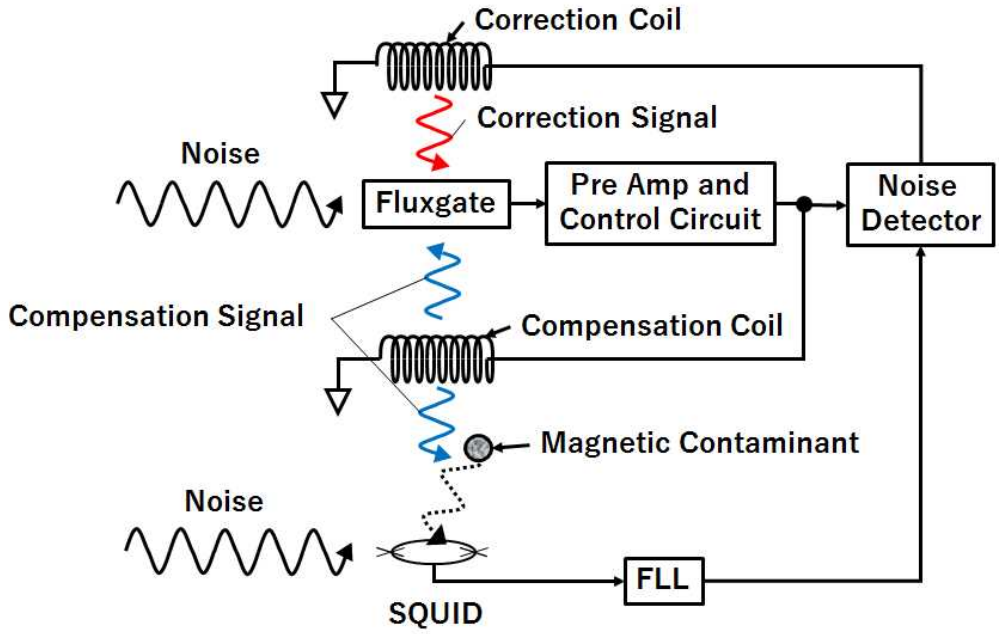

Figure1. A schematic diagram of the Active Magnetic Shielding System

Keywords: SQUID, Magnetic Contaminant Detection, Active Magnetic Shielding, Phase Detection

EDP1-9

Simple photon incidence method from the front side for Superconducting Single-Photon Detector (SSPD) using alignment mark

*Kento Sakai[1], Hiromichi Niii[1], Daisuke Sakai[1], Hiroyuki Shibata[1]

Kitami Institute of Technology, Kitami, Hokkaido, Japan.[1]

SSPD is one of the detectors with sensitivity of single photon from ultraviolet to mid-infrared region(0.3-5 mm). Because of excellent performance of high-sensitivity and high-speed response, it is expected to be applied to the future communication. Here we developed a simple photon incidence method from the front side using alignment mark.
Normally, the system detection efficiency is obtained from the product of absorption efficiency, optical coupling efficiency, and intrinsic detection efficiency. To improve the coupling efficiency, it is necessary to focus the optical spot on the nanowire. There have been two major methods for the photon incidence. One is a method of injecting photons from the back side of the substrate with a reflection mirror on the nanowire. The size of the mirror needs to be small as that of the nanowire for the alignment. Another is fabricating deep groove for sleeve so that the ferrule of the optical fiber can be directly fixed to the device without alignment. In both methods, the manufacturing procedures of the device are quite complicated. We developed a new method to solve the problem. Alignment marks are fabricated around the nanowire using Au. Since the size of the marks are mm, it is possible to observe the mark from an oblique angle for the alignment. We confirm that the detection efficiency using our simple method is almost same as that of other methods.

Keywords: Superconducting Single-Photon Detector , alignment mark, coupling efficiency, Au

EDP1-10

Photon-Number Resolving Detector using Series Array of NbN Nanowire Shunted with Ti Resistors

*Satoshi Denda[1], Masato Naruse[1], Tohru Taino[1], Hiroaki Myoren[1]

Graduate School of Science and Engineering, Saitama University, Japan[1]

We are investigating on photon-number resolving detector using series array of NbN nanowire single photon detector shunted with Ti resistor. Epitaxially grown 4-nm thick NbN thin films were grown on MgO(100) substrates at room temperature using a dc magnetron sputtering system. 120-nm wide NbN nanowires were patterned with an electron-beam lithography system and Ti resistors patterned with a lift-off method using electron-beam resist. 120-nm wide NbN nanowires showed superconducting transition temperature of 12 K and Ti shunt resistor showed resistance around 50 ohm. We fabricated a three series of NbN nanowires shunted with Ti resistors and the fabricated detector showed three discrete current pulses under 850-nm pulsed laser illumination at 4.2 K. We will present experimental results for high speed response using parallel nanowire to reducing inductance of nanowires.

Keywords: Photon-number-resolving detector, SNSPD, NbN nanowire, Ti resitor

EDP1-11

Development of High Throughput X-ray detectors using Superconducting Tunnel Junctions with a large area size

*Yuichi Fujisawa[1], Go Fujii[2], Masahiro Ukibe[2], Shigetomo Shiki[2], Masato Naruse[1], Hiroaki Myoren[1,2], Tohru Taino[1]

Saitama University[1]
AIST[2]

Materials analysis using X-rays, particularly fluorescence analysis is utilized in various research fields. In conventional X-rays analytical instruments, semiconductor detectors are used to detect X-rays. However, by using the conventional ones, it is difficult to perform the analysis of light trace elements in advanced functional materials, which are important for realizing the low-carbon society, because semiconductor X-ray detectors can't distinguish clearly the characteristic X-ray peaks of light elements due to the limitation of its energy resolution. On the other hand, a superconducting tunnel junction (STJ) X-ray detector can exhibit theoretically several tens of times higher energy resolution than that of semiconductor detectors. Therefore, to realize advance X-ray analytical instruments with a quite high energy resolution, we have developed an STJ array detector. Our fabricated STJ arrays consisting of 100 pixels have already been applied for an X-ray absorption fine structure measurement of nitrogen dopants in n-SiCs [1]. However, the analysis throughput of our STJ array detectors is currently less than one-tenth of semiconductor detectors one. To overcome the above drawback, there are two methods as follows. One is to increase the pixel number in the array. In fact, we had already developed a 400-pixel STJ array detector [2]. The other is to enlarge the pixel size. The energy resolution of the total detection system using STJs, ΔE_{total}, is assumed to be $\Delta E_{total}^2 = \Delta E_{int}^2 + \Delta E_{ele}^2$. Here, ΔE_{int} is the intrinsic detector energy resolution of the STJ and ΔE_{ele} is the electronic noise. Generally, the larger the area size of STJ become, the bigger the ΔE_{ele} become due to an enlargement of the capacitance of the STJs, which leads to the degradation of the ΔE_{total}. But if ΔE_{ele} is sufficiently smaller than ΔE_{int}, degradation of ΔE_{total} can be fairly small [3]. In this study, we fabricated two types of Nb / Al STJs with different areas (100 × 100, 160 × 160 μm) in CRAVITY [4] to evaluate the dependence of the ΔE_{total} on the STJ area size and determine the effective limit of the size of a single STJ.

[1] S. Shiki, et al., J. Low Temp. Phys., 167 (2012)
[2] G. Fujii, et al., J Low Temp. Phys., 176 (2014)
[3] M Ukibe, et al., Nucl. Instr. and Meth. A 401 (1997) 299
[4] http://unit.aist.go.jp/neri/cravity/en/index.html

Keywords: superconducting tunnel junctions, X-ray detector

EDP1-12

Hybrid of Single and Double-Component Superconductors

*Y Tanaka[1], H Yamamori[1], T Yanagisawa[1], T Nishio[2], S Ooi[3], M Tachiki[3], S Arisawa[3]

National Institute of Advanced Industrial Science and Technology (AIST), Japan[1]
Department of Physics, Tokyo University of Science, Japan[2]
National Institute for Materials Science, Japan[3]

Two-component superconductivity can emerge in an ultra-thin superconducting bilayer [1–4]. A fractional vortex is experimentally realized in this two-component superconductor [5]. Furthermore, we can realize one-component and two-component hybrid systems using an ultra-thin superconducting bi-layer [6]. The artificial realization of this hybrid system has not been realized in other multi-component superconductors such as a spin-triplet superconductor [7]. Figure 1 shows a sample hybrid system. A slit is present in the top layer, but not in the bottom layer (Fig. 1 (a)) [6]. There is no quantization condition around the center of the circle in the top layer, because the quantum phase (q_1 for the top layer, q_2 for the bottom layer) is not required to continue across the slit. Owing to this discontinuity, the bilayer disk can accept the uniform magnetic field with an interlayer phase difference texture (q_2-q_1) [8–11] as shown in Fig. 1 (b) [6]. We recall that the boundary condition is still retained in the bottom layer. The phase rotation accompanying the magnetic field is compensated by the phase shift accompanying the phase texture in the bottom layer. In contrast to a sole single layer, the bottom layer can no longer expel the magnetic field completely. We are now developing a new device to confirm this phenomenon (Fig. 1 (c)).

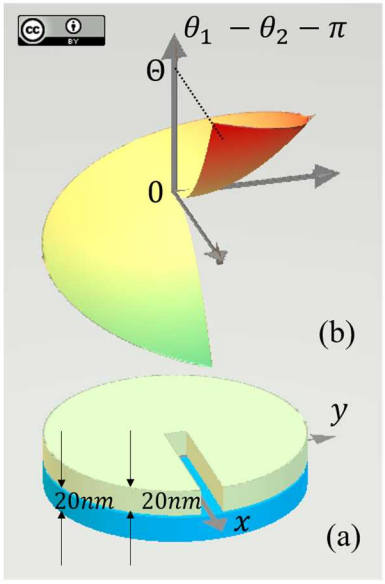

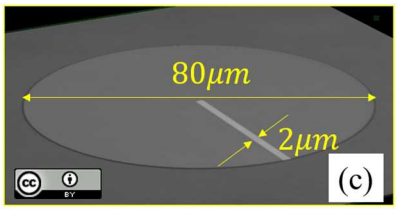

Figure 1. Phase texture and device structure of an abnormal Meissner chip. (a) Schematic of the abnormal Meissner chip consisting of two ultra-thin superconducting layers. (b) Phase texture accepting the uniform magnetic field. (c) Image of abnormal Meissner chip captured using a laser microscope.

References 1) H. Bluhm, et al. Phys. Rev. Lett. **97** (2006) 237002. 2) Y. Tanaka, Supercond. Sci. Technol. **28** (2015) 034002. 3) Y. Tanaka, et al. Physica C **538** (2017) 6. 4) Y. Tanaka, et al. Physica C **538** (2017) 12. 5) Y. Tanaka, et al. Physica C **548** (2018) 44. 6) Y. Tanaka, et al. Physica C **551** (2018) 41. 7) M. Sigrist and K. Ueda, Rev. Mod. Phys. **63** (1991) 239. 8) Y. Tanaka, Phys. Rev. Lett. **88** (2002) 017002. 9) A. Gurevich and V. M. Vinokur, Phys. Rev. Lett. **90** (2003) 047004. 10) S.–Z. Lin, J. Phys. Condens. Matter **26** (2014) 493202. 11) Y. Tanaka, et. al. Physica C **516** (2015) 10.

Acknowledgement This work was partially supported by JSPS KAKENHI Grant Number JP 16K06275 and the TIA collaborative research program “Kakehashi”; Project Name: “Controlled fractional quantization”. The device was fabricated in the clean room for analog-digital superconductivity (CRAVITY), National Institute of Advanced Industrial Science and Technology, Tsukuba, Japan.

Keywords: Abnormal Meissner effect, Nb bilayer, Multi-component superconductivity, Inter-component phase difference soliton

EDP1-13

Design and fabrication of Josephson voltage standard circuit for ac-voltage standard

*Hirotake Yamamori[1], Michitaka Maruyama[1], Yasutaka Amagai[1], Takeshi Shimazaki[1]

National Institute of Advanced Industrial Science and Technology[1]

Josephson junction array is used for primary dc 10 V voltage standard. On the other hand, a quantum ac voltage standard is still being developed. For voltage standard circuits, tens of thousands Josephson junctions connected in series consist of a co-planar waveguide, and microwaves are applied to them to generate the Shapiro step [1-2]. We have designed Josephson voltage standard circuit including 1,048,576 Josephson junctions to generate the output voltage of about 30V. The number of Josephson junction is twice larger than that for our conventional one. A small Josephson junction whose size is 1.8 x 4.0 mm^2 and a wide range power divider are introduced to the circuit. We also introduce a high impedance Josephson junction array $Z = 100\ \Omega$, that is twice larger than conventional one. The large number of the junction N significantly decreases the operating current margin due to dissipation for applied microwaves in the junction, because microwave power P at N-th junction is given by , where R_N is the junction resistance. Higher Z will reduce the power dissipation and contribute to improve the operating current margin for the voltage standard circuit.

[1] S.P.Benz et al., IEEE Trans. on Appl. Supercond., Vol.25, p. 1300108 (2015).
[2] M.Maruyama et al., J. of Phys. Conf. Series, Vol.234, p.042020 (2010).

The devices were fabricated in the clean room for analog-digital superconductivity (CRAVITY) in National Institute of Advanced Industrial Science and Technology (AIST). This work was partly supported by JSPS KAKENHI Grant No. 17K06481.

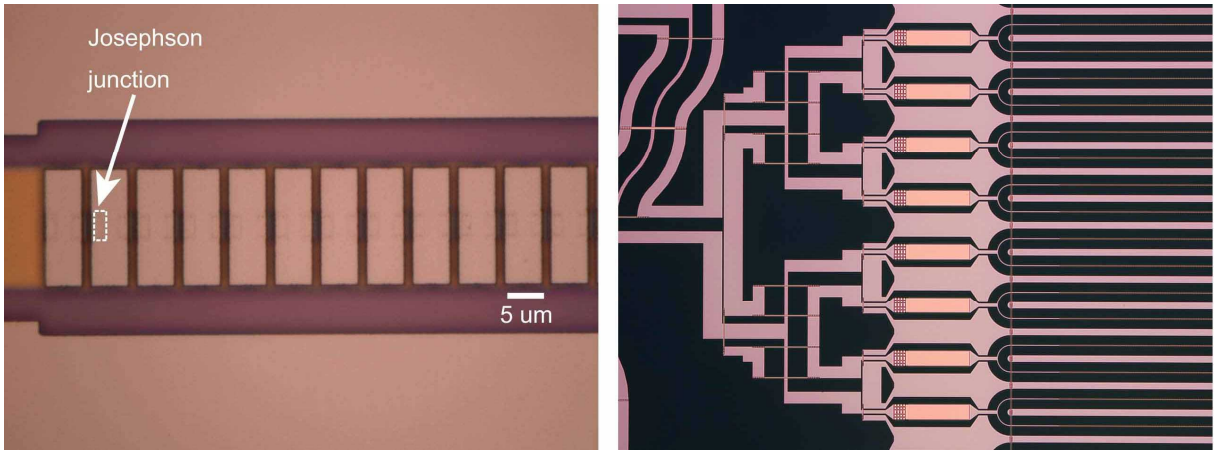

Fig. (a) Fabricated Josephson junction array, the junction size is 4 x 1.8 mm, and (b) serial-parallel power divider.

Keywords: Voltage standard, NbN, CPW, Shapiro step

EDP1-14

Unconventional Josephson effect in two dimensional electron gas-based superconductor-semiconductor Josephson junctions in quantum integrated circuits

*Kaveh Delfanazari[1,2], Pengcheng Ma[2], Ian Farrer[2,3], David Ritchie[2], Hannah J. Joyce[1], Michael J. Kelly[1,2], Charles G. Smith[2]

Engineering Department, University of Cambridge, Cambridge, UK[1]
Department of Physics, Cavendish Laboratory, University of Cambridge, Cambridge, UK[2]
Department of Electronic and Electrical Engineering, University of Sheffield, Sheffield, UK[3]

Further to the development of scalable hybrid quantum circuits introduced by us [1-5], here we report on the discovery of an unconventional Josephson effect in hybrid $In_{0.75}Ga_{0.25}As$ two-dimensional electron gas-Nb junctions that are designed and fabricated for scalable hybrid quantum circuit integration.

We find that the differential conductance as a function of source-drain voltage shows two symmetric in-gap resonances, which are strongly temperature and magnetic field dependent. The resonances amplitudes enhance with increasing in-plane magnetic fields up to a critical field where they gradually suppress and disappear. The observed supercurrent also gradually increases with applied magnetic field up to the same critical field.
We believe that these two striking observed behaviours in our devices- that cannot be explained by the conventional Josephson effect phenomenon- may be related to the context of topological superconductivity in hybrid 2D systems [6]. Detailed experimental results will be discussed.

Reference:
[1] K. Delfanazari, et al, *Adv. Mater.* 29, 1701836 (2017).
[2] K. Delfanazari, et al, *J. Magn. Magn. Mater.* 459, 282-284 (2018).
[3] K. Delfanazari, et al, *IEEE Trans. Appl. Supercond.* 28, 1100304 (2018).
[4] K. Delfanazari, *et al.*, Aharonov-Bohm type magnetoconductance oscillations in planar and ballistic Josephson junctions, *under review* (2018).
[5] K. Delfanazari, *et al.*, Two-dimensional electron gas-based quantum integrated circuits, *under review* (2018).
[6] K. Delfanazari, *et al.*, Unconventional Josephson Effect in hybrid two-dimensional electron gas-superconductor junctions for quantum circuit integration, *to be submitted* (2018).

Keywords: Quantum integrated circuitry, Josephson junctions, hybrid superconductor-semiconductor , Scalable quantum circuit

EDP1-15

Enhancement of critical current density in $YBa_2Cu_3O_7$ superconducting thin films by changing magnetic environment

*Alaa H. Hammood[1], Antony Jones[1,2], Mustafa M. AL-Qurainy[1], Sergey A. Fedoseev[1], Alexey V. Pan[1]

Institute for Superconducting and Electronic Materials, University of Wollongong, Northfields Avenue, Wollongong, NSW 2522, Australia[1]
CSIRO, Manufacturing, Bradfield Road, West Lindfield, 2070 NSW, Australia[2]

The hybrid systems consisting of superconducting $YBa_2Cu_3O_7$ thin films surrounded by ferromagnetic iron have been investigated. The magnetization measurement has been carried out and critical current densities of the thin films have been extracted. These characteristics have also been compared to the transport current values. The measurements show that the maximum critical current density (so called overcritical current densities) can exceed the critical current densities obtained in the same thin films without the iron environment. The results show that the critical current density is strongly dependent on the location of the iron environment, dimensions of the iron magnets and distance between the magnets and the thin films. The current density enhancement is attributed to the magnetic interaction between the soft ferromagnetic iron environment and superconducting thin films. This interaction is likely to result in a redistribution of supercurrents in within the films, removing excessive stray fields near the edges of thin films thereby making the supercurrent distribution more homogeneous. This prevents entry of magnetic flux in the form of vortices, hence the critical current densities determined by vortex pinning becomes less relevant. We show that the critical current density can be effectively manipulated by choosing the iron environment.

Keywords: overcritical, ferromagnetic, magnetization, superconducting

EDP1-16

Artificial ferromagnetic dot arrays for the critical current enhancement in superconducting $YBa_2Cu_3O_{7-\delta}$ thin films

*Mustafa M. AL-Qurainy[1], Antony Jones[1,2], S. Rubanov[3], Sergey A. Fedoseev[1], Alaa H. Hammood[1], Alexy V. Pan[1]

Institute for Superconducting and Electronic Materials, Northfields Avenue, University of Wollongong, New South Wales 2522, Australia[1]
CSIRO, Manufacturing, Bradfield Road, West Lindfield, 2070 NSW, Australia[2]
Electron Microscope Unit, Bio21 Institute, University of Melbourne, VIC 3010, Australia[3]

Enhancing critical current density in high temperature superconductors is a significant goal and remains a major challenge for different technological applications. One alternative approach to conventional vortex pinning is to pin (localise) the magnetic flux rather than the vortex core. This possibility has not been studied to a large extent. Introducing a lattice of periodic magnetic dots has been shown to be useful for understanding interactions between superconducting vortices and these ferromagnetic arrays, as well as the resultant effects of vortex magnetic pinning dynamics and enhancement of the critical current density (J_c). The high quality superconducting $YBa_2Cu_3O_7$ (YBCO) thin films have been grown by pulsed laser deposition (PLD). Buffered arrays of ferromagnetic dots with different configurations have also been produced by PLD on top of YBCO films. The dimensions of the individual ferromagnetic dots are comparable to the magnetic field penetration depth. Magnetization measurements have been carried out in the YBCO thin films right after deposition and then also after producing the ferromagnetic patterns. The results show that some patterns produce a striking J_c enhancement of up to 24.5% over the high magnetic field range while it achieved 22% in low magnetic field in temperature 10 and 60K respectively. The enhancement is likely due to the flux localisation (pinning) effects, rather than magnetic shielding. The J_c changes seem to depend on rather minor variations in initial pinning and corresponding J_c level of the films.

Keywords: critical current density, pinning centres, vortex

EDP1-17

Estimation of Electricity Storage Capacity of Compact SMESs Composed of Stacks of Si-wafers Loaded with Superconducting Thin Film Coils in Spiral Trenches formed by MEMS Process

Yushi Ichiki[1], Akihisa Ichiki[2], Tatsumi Hioki[1], Minoru Sasaki[3], Joo-Hyong Noh[4], Osamu Takai[4], Hideo Honma[4], *Tomoyoshi Motohiro[1,2]

Graduate School of Engineering, Nagoya University[1]
Institutes of Innovation for Future Society, Nagoya University[2]
Graduate School of Engineering, Toyota Technological Institute[3]
Materials and Surface Engineering Research Institute, Kanto-Gakuin University[4]

We have been developing a superconducting thin film coil in a spiral trench on a Si wafer for compact SMESs [1]. Having completed in fabrication of a NbN superconducting thin film coil on 76.2 mm-diameter Si wafer [2], we have replaced NbN with $YBa_2Cu_3O_{7-\delta}$[3]. The high critical current density of $YBa_2Cu_3O_{7-\delta}$ is possible to impose high electromagnetic hoop forces on the coil to crash Si wafer. To avoid the crash, the design of the spiral coil and the superconducting current must be optimized. For this purpose, estimation of magnetic field generated by the superconducting current in the spiral coil was performed based on Biot-Savart low. The spiral coil was approximated to be multiple loops with the same current in a wafer and 600 wafers were supposed to be stacked. The sum of the magnetic fields generated by each loop of 600 wafers was obtained at the innermost loop to obtain the maximum hoop stress throughout the 600 wafers. Figures 1 (a) (b) show typical two designs of the cross section of spiral trench and (d) (e) were the corresponding calculated results. One typical design gave 399 Wh/L and 187 Wh/kg which came close to the values of Li ion batteries.

[1] Sugimoto N et al., 2017, Supercond. Sci. Technol. 30, 015014
[2] Suzuki N et al., 2017, IOP Conf. Series: Journal of Physics: Conf. Series 897, 012019
[3] Ichiki Y et al., 2018, IOP Conf. Series: Journal of Physics: Conf. Series 1054, 012065

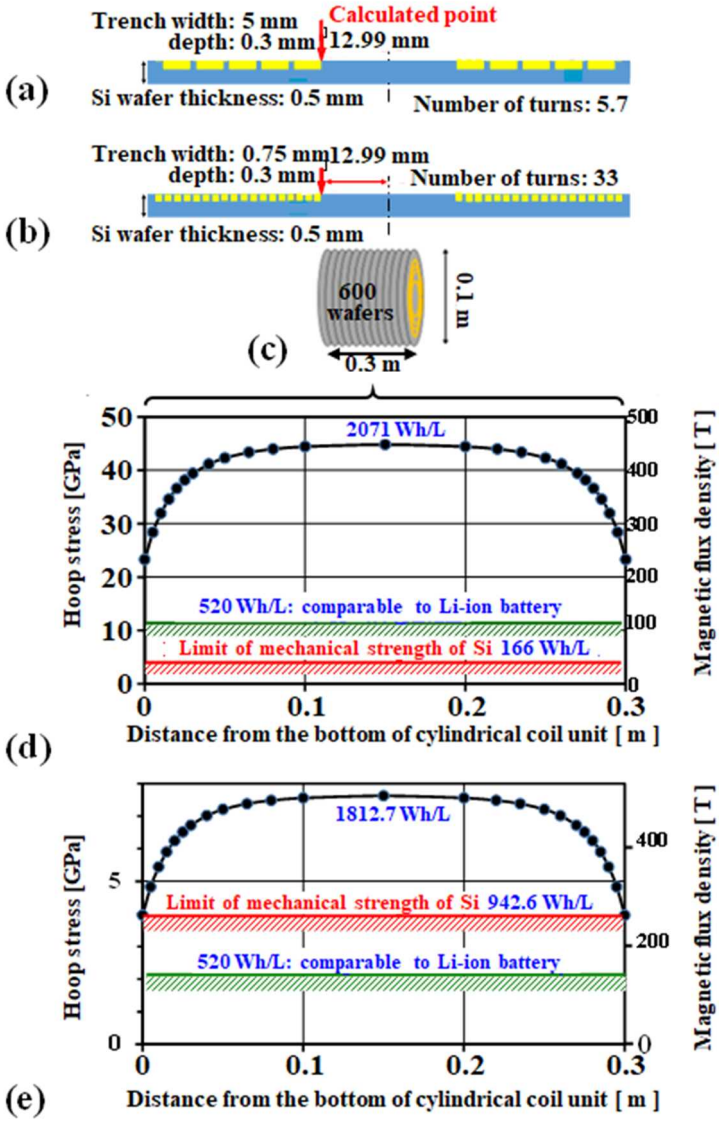

Fig.1 Calculated hoop stress at the innermost loop as a function of the position in the 0.3 m stack of Si wafers

Keywords: SMES, Si-MEMS, Magnetic field, YBa2Cu3O7-δ

EDP1-18

Micro-Fabrication of NdFeAs(O,F) Thin Films towards Particle Detector Applications

*Yasunari Tsuji[1], Takuya Matsumoto[1], Takayuki Yamada[1], Takafumi Hatano[1], Yuto Nakamura[2], Kazumasa Iida[1], Hideo Kishida[2], Satoshi Kashiwaya[2], Hiroshi Ikuta[1]

Department of Materials Physics, Nagoya University, Japan[1]
Department of Applied Physics, Nagoya University, Japan[2]

Superconducting nanowires have great potential for detector applications, such as photon, neutron, and ion detectors. Detectors having single-photon sensitivity have been fabricated using conventional BCS superconductors such as Nb and NbN. Consequently, however, the operating temperature is low due to their rather low transition temperature (T_c) [1]. There are several attempts to fabricate nanowires from MgB_2 or copper-oxides to increase the operating temperature, but so far, they suffer from a notable degradation of T_c due to fabrication damage. On the other hand, little is known about the potential of iron-based superconductors as for particle detectors. In this work, we have fabricated narrow wires from NdFeAs(O,F) thin films, which has the highest T_c among the iron-based superconductors, and studied their response to light illumination.

High-quality single crystalline thin films of NdFeAs(O,F) were grown by a molecular beam epitaxy method [2]. The film was patterned into a two-island structure connected by a narrow bridge using photolithography and dry etching. For the photon detection experiment, a He-Ne laser was employed as a light source. The light was sent through an attenuator and the middle of the bridge was irradiated. The laser spot size was 2 μmφ. A DC current slightly lower than the critical current was supplied to the bridge, and the voltage between the two islands was monitored. As shown in Fig. 1, the illumination of the light was successfully detected at 5.7 K with a 7.6 μm-wide bridge. Encouraged by this result, we further downsized the device structure to enhance the sensitivity, and obtained a bridge with reduced width of 0.8 μm by employing a laser lithography technique as shown in the inset of Fig. 2. This particular film had originally a T_c of 35 K, which decreased slightly after the micro-fabrication, but was still well above 30 K as shown in Fig. 2. This result indicates that the damage problem might be not as serious as for the other high-T_c materials.

[1] C. M. Natarajan, M. G. Tanner and R. H. Hadfield, Supercond. Sci. Technol. **25**, 063001 (2012).
[2] T. Kawaguchi, H. Uemura, T. Ohno, M. Tabuchi, T. Ujihara, K. Takenaka, Y. Takeda and H. Ikuta, Appl. Phys. Lett. **97**, 042509 (2010).

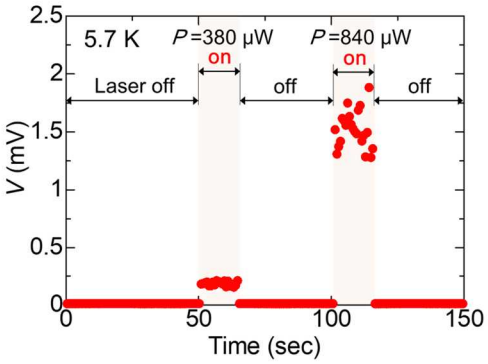

Fig. 1. Response of a 7.6 mm-wide bridge of NdFeAs(O,F) to light illumination. A voltage signal was detected during the irradiation of laser light. The incident laser power (P) is indicated in the figure.

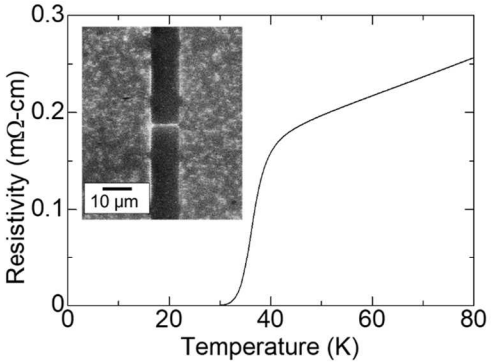

Fig. 2. Temperature dependence of the resistivity of a 0.8 mm-wide bridge of NdFeAs(O,F). The inset shows a SEM image of the test sample.

Keywords: iron-based superconductors, thin film, photon detector

EDP1-19

Measurements of phase shifts in YBCO transmission lines for evaluation of kinetic inductances

*Ryo Ishida[1], Takashi Goto[1], Hisashi Shimakage[1], Masanori Takeda[2]

Ibaraki University Japan[1]
Shizuoka University Japan[2]

A superconducting parametric amplifier has remarkable characteristics; such as wide band operation, high dynamic range, low noise performance, and so on. Recently, high performances of Nb parametric amplifier has been reported. It is known that the operating frequency of the superconducting parametric amplifier is proportional to the gap voltage of the superconductor material. By using high temperature superconductor YBCO as a superconductor material, the superconducting parametric amplifier would operate in higher frequencies because of its high gap voltage. The amplification principle of the superconducting parametric amplifier is the same as that of the optical fiber parametric amplifier, and consists of a partially degenerate four wave mixing using a third order nonlinear effect. Generally, the superconductor material has a unique inductance component called a kinetic inductance, and its nonlinearity can be utilized as the third order nonlinear components. In order to realize the superconducting parametric amplifier, it is important to evaluate the kinetic inductance in the superconducting transmission line. In this research, we report phase shifts of the transmitted electromagnetic wave in the YBCO transmission line caused by a modulation of the kinetic inductance. The applied current and the temperature dependences of the phase shifts were also investigated. The phase shifts near the critical temperature were observed, and are roughly in agreement with the numerical calculations, using the measurement results, the expected performances will be discussed

EDP2-1

Area Reduction of Adiabatic-Quantum-Flux-Parametron Register-Files by Using Asymmetric Gates

*Tomohiro Tamura[1], Naoki Takeuchi[2,3], Christopher Ayala[2], Yuki Yamanashi[1], Nobuyuki Yoshikawa[1]

Department of Electrical and Computer Engineering, Yokohama National University[1]
IAS, Yokohama National University[2]
JST-PRESTO[3]

Adiabatic quantum flux parametron (AQFP) logic, whose bit energy can be significantly reduced by adiabatic switching of Josephson junctions, has a potential to become a basic technology for future energy-efficient high-performance computing systems based on superconducting technology [1]. We have been developing extremely energy-efficient microprocessors using AQFP logic. In the previous study, we designed a 16-word by 1-bit register file using AQFP logic [2]. It was composed of three decoders based on AQFP AND gates, feedback delay latches and mergers using AQFP OR gates. The problem of this circuit is the circuit area. To reduce the circuit area of the register file, we used quantum flux parametron latch (QFPL) and asymmetric AND gates for the components of latches and decoders, respectively. The QFPL, which is composed of two write gates and a storage gate is proposed as a compact latch for AQFP logic. The storage gate of QFPL is a dc-biased quantum-flux-parametron and can hold the logic state without a feedback loop. An asymmetric AQFP gate is also employed in the present design to decrease the circuit area. The asymmetric AQFP is composed of a two-input AQFP buffer gate whose loop inductance is designed to be asymmetric to make an offset to the input signal. As a result, the output current of an asymmetric AND gate is logical “1” only when both of two input current is logical “1”. The conventional AQFP AND gate is composed of three buffer gates. Therefore the circuit area and the junction number of an asymmetric AND gate is 33% and 67% smaller, respectively, than those of the conventional AND gate. We designed 16-word by 1-bit register file using the asymmetric AND gates and QFPL. The circuit area and the junction number of the new design is 54% and 15% smaller than those of the conventional AQFP register files. The circuits were fabricated using the HSTP process in AIST. Currently, the operation of the asymmetric AND gates and QFPL were verified. We will show the latest test result of the 16-word by 1-bit register file at the conference.

[1] N. Takeuchi, et. al., IEEE Trans. Appl. Supercond., vol. 23, No. 3, 1700304, 2013.
[2] N. Tsuji, et. al., IEEE Trans. Appl. Supercond., vol. 27, No. 4, 1300904, 2017.

Keywords: AQFP, QFP, register file

EDP2-2

Design and evaluation of a one-instruction-set single-flux-quantum microprocessor for the demonstration of Josephson-CMOS hybrid system

*Yuki Hironaka[1], Yuki Yamanashi[1], Nobuyuki Yoshikawa[1]

Department of Electrical and Computer Engineering, Yokohama National University[1]

Single-flux-quantum (SFQ) circuits [1] have a great potential for VLSI applications in terms of sub-terahertz operation and low power dissipation. However, there exists an obstacle: a lack of large capacity memory. A Josephson-CMOS hybrid system [2], which is a hybridization of high-speed, low-power SFQ circuits and large-scale CMOS memories, is expected to be a good solution to realize large capacity memories for SFQ circuits. In this study, we designed a tiny one-instruction-set microprocessor using SFQ circuits for the demonstration of the real Josephson-CMOS hybrid system, where we use a low-power 64-kb Josephson-CMOS hybrid memory [3]. We adopted an extremely simplified microarchitecture that implements a single instruction SUBNEG (subtract and branch if negative) [4], which is composed of just a bit-serial subtractor and some shift registers. We implemented the SFQ microprocessor and superconducting SFQ-CMOS interface circuits on the same chip. Superconducting SFQ-CMOS interface circuits consist of a level driven DC/SFQ converter (LDDS), which detect a small current from the SFQ circuits, and a Josephson latching driver (JLD), which is a voltage amplifier driven by AC bias current. In the measurement we confirmed the correct operation of the SFQ microprocessor and interface circuits, while we observed that the AC bias current for the JLD affects the operation of SFQ digital and readout circuits, resulting in the reduction of bias margin of SFQ digital circuits.

[1] K. K. Likharev et al, “RSFQ logic/memory family: A new Josephson-junction technology for sub-terahertz-clock frequency digital systems,” IEEE Trans. Appl. Supercond., vol.1, no.1, pp.1-28, 1991.
[2] U. Ghoshal et al, “Superconductor-semiconductor memories,” IEEE Trans. Appl. Supercond., vol.3, no.1, pp.2315-2318, 1993.
[3] G. Konno et al, “Fully Functional Operation of Low-Power 64-kb Josephson-CMOS Hybrid Memories,” IEEE Trans. Appl. Supercond., vol.27, no.4, p.1300607, 2017.
[4] M. M. Shulaker et al, “Carbon nanotube computer,” Nature, vol.501, pp.526-530, 2013.

Keywords: SFQ circuits, Josephson-CMOS hybrid system

EDP2-3

Design and demonstration of an 8-bit 18-sample/cycle sine code generator using single-flux-quantum circuits

*Fei Ke[1], Yuki Yamanashi[1], Thomas Ortlepp[2], Nobuyuki Yoshikawa[1]

Department of Electrical and Computer Eng., Yokohama National University, Japan[1]
CiS Research Institute for Microsensor Konrad-Zuse-Straße 14, Erfurt 99099, German[2]

The Josephson voltage standard is the most accurate method to measure voltage by international agreement because it is an intrinsic standard in the sense that it does not depend on any physical artifact. In the Programmable Josephson Voltage Standard (PJVS) system, Josephson arrays play the role as a digital-to-analog converter programmed by binary sine codes [1]. However huge high-speed memory costs are demanded to store the discrete sine sample codes to ensure the high accuracy of the sine wave. As single-flux-quantum (SFQ) logic circuits operate at high clock frequency with low transmission latency, they are well suited for feedback structure. An SFQ-based sine code generator with a feedback structure can generate the discrete sine sample codes automatically at high speed with small hardware cost [2]. In this study, we designed an SFQ-based 8-bit 18-sample/cycle sine code generator using the AIST 10 kA/cm^2 Nb advanced process. This design can output the discrete sine samples at hundreds of MHz with the total harmonic distortion up to -59 dB. We confirmed the correct output of the first five discrete sine wave samples at low clock frequency although the fifth output was unstable. We have also tested its high-speed operation by using an on-chip high-speed test system and confirmed the correct operation up to 61GHz of most component circuits except the final adder. The comparison with a semiconductor sine code memory shows that the hardware cost of this design is less when the number of discrete sample/cycle is above 100, which can be implemented by the present SFQ integrated circuit technology.

[1] C. A. Hamilton, C. J. Burroughs, R. L. Kautz, Josephson DIA Converter with Fundament a1 Accuracv. IEEE Trans. Instrum. Meas. 44 (1995).
[2] F. Ke, Y. Yamanashi, T. Ortlepp, N. Yoshikawa, “Design and Simulation of a 7-bit 18-sample/cycle SFQ-Based Sine Wave Generator”, The 11th Superconducting SFQ VLSI Workshop (SSV 2018) / 6th CRAVITY Symposium 2018/02.

Keywords: SFQ circuits, PJVS, feedback structure, high-speed test

EDP2-4

Design and measurement of 4-unit 2-bit FPGA using single-flux-quantum circuits

*Mika Araki[1], Yuki Yamanashi[1], Nobuyuki Yoshikawa[1]

Yokohama National University, Japan[1]

Recently field programmable gate array (FPGA) based on semiconductor integrated circuits (IC) are extensively used in the implementation of information processing systems, where a designer can repeatedly define the function of digital ICs by changing the combinations and connections of logic elements. In order to cope with the recent increase in the amount of information processing, it is necessary to improve the speed and the energy efficiency of FPGAs. A new device to enhance the performance is fairly demanded to continue the progress of the information society. As a new device, a single flux quantum (SFQ) circuit [1] attracts attention due to its high-speed operation and low-power consumption.

We have been developing FPGAs based on the SFQ IC technology to realize extremely high performance and energy-efficiency in FGPAs. Our SFQ FPGA consists of logic blocks, switch boxes and connection blocks. The switch box and connection block, which are composed of NDRO (non-destructive read-out) cells, determine the connection between wires and logic blocks. In the logic bloc, the logical function defined by stored data in the look-up table (LUT) is conducted. All these functions are programmable by loading the external data to each component. In our design, loading of the program data to each circuit component is effectively performed by using d2 flip-flops (dual clocks dual outputs flip-flop), by which the circuit area is reduced compared with the previous study [2]. We designed an SFQ 4-unit 2-bit FPGA, which is composed of 6000 junctions. The collect operations of each circuit component are verified by an on-chip high-speed test, and its dc-bias margins were examined. We will show the latest test results of the SFQ 4-unit 2-bit FPGA at the conference.

Keywords: SFQ circuits, Josephson integrated circuits, FPGA

EDP2-5

Design and Operation of Distributed Double-SQUID Amplifier for RSFQ Circuits

*Komei Higuchi[1], Hiroshi Shimada[1], Yoshinao Mizugaki[1]

The University of Electro-Communications[1]

RSFQ circuitry is an attractive digital technology because it has great advantage to low power consumption and high-speed operation. Recently, various group studied on-chip RSFQ output amplifiers which are designed to connect RSFQ circuitry to room temperature electronics. One of such amplifiers is a distributed SQUID amplifier comprising SQUIDs embedded in RSFQ cascaded RS flip-flops [1]. In this paper, we propose a distributed double-SQUID amplifier, where a SQUID is replaced with a double-SQUID.

The equivalent circuit of the distributed double-SQUID amplifier is shown in Fig. (a). One stage of this circuit consists two parts. One is an SFQ storage loop with two (set and reset) terminals. The other is a double-SQUID [2] in place of a single dc-SQUID employed in the original one [1]. A double-SQUID is expected to generate the output voltage twice as large as that of a single dc-SQUID. We designed a 4-stage distributed double-SQUID amplifier. They were fabricated using the Nb 2.5kA/cm^2 process (STP2) at the National Institute of Advanced Industrial Science and Technology (AIST), Japan.

In measurements, chips were cooled in liquid helium. Fig. (b) shows the bias current versus the voltage difference between the set and reset states (I_{bias} vs. $V_{OUT,diff}$ characteristics). In measurement, the maximum $V_{OUT,diff}$ of a distributed double-SQUID amplifier was 2.93mV, which was comparable with the corresponding numerical value of 3.54mV.

[1] Q. P. Herr, *Supercond. Sci. Tech.*, **23**, (2010) 022004.
[2] T. Morooka, *Jpn. J. Appl. Phys.*, **36** (1997) L1587.

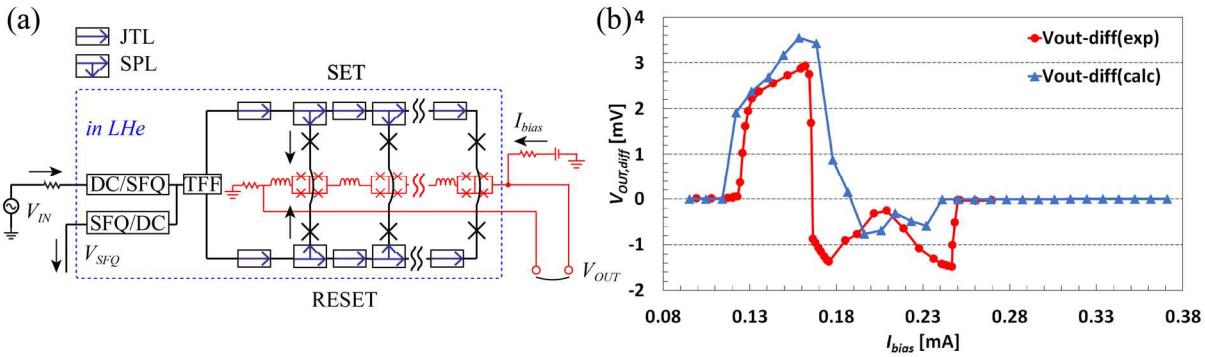

Fig. (a): Equivalent circuit of a distributed double-SQUID amplifier. (b): Experimental (circles) and numerical (triangles) I_{bias} vs. $V_{OUT,diff}$ characteristics of 4-stage distributed double-SQUID amplifier.

Keywords: distributed double-SQUID amplifier, RSFQ output amplifier, Nb integrated circuit

EDP2-6

Demonstration of 5.6 ps Latency of Adiabatic Quantum Flux Parametron using Delayed Clocking Scheme

*Mai Nozoe[1], Naoki Takeuchi[2,3], Yuki Yamanashi[1,2], Nobuyuki Yoshikawa[1,2]

Department of Electrical and Computer Engineering, Yokohama National University, Japan[1]
Institute of Advanced Sciences, Yokohama National University, Japan[2]
PRESTO, Japan Science and Technology Agency, Japan[3]

Adiabatic quantum flux parametron (AQFP) logic is an ultra-low-power superconductor device, whose bit energy can be reduced to 1 zJ (10^{-21}J) level even in 5-GHz operation. We have been developing an extremely energy-efficient microprocessor using the AQFP logic. One drawback in the AQFP circuit is relatively large latency. If we assume a 5-GHz clock frequency with four-phase clocking, the latency per logic gate is 50 ps, which is somewhat larger than that of SFQ circuits. In this study, we propose the delayed clocking scheme to reduce the latency of the AQFP logic, where multiple stages of AQFP gates are successively exited by delayed excitation lines. First, we simulated the parameter margins of an AQFP buffer chain using the delayed clocking scheme at 5 GHz. When the delay of the excitation clock between each AQFP stage was 5-60 ps, the wide parameter margins were obtained; especially the widest margin was achieved at 10 ps, which corresponds to a one-fifth reduction of the latency at 5 GHz. We have implemented a buffer chain, an AND gate and an XOR gate based on the delayed clocking scheme using the AIST HSTP process and demonstrated their correct operation. The delay in the excitation line between each stage is 5.6 ps in the demonstration. At 200 kHz, 5 MHz and 10 MHz, we confirmed the correct operations with wide excitation current margins ranging -40 - 40%. It indicates that the latency of the AQFP logic per gates can be reduced to about 5 ps, which corresponds to the SFQ circuits operating at 200 GHz.

Keywords: Josephson integrated circuit, Adiabatic circuit, QFP, Delayed clocking

EDP2-7

Design of High Timing resolution SFQ Time-to-Digital Converter for Time-Resolving Photon Detection System using SNSPDs

*Ryotaro Kamiya[1], Kota Aita[1], Masato Naruse[1], Tohru Taino[1], HIroaki Myoren[1], Jian Chen[2], Peiheng Wu[2]

Graduate School of Science and Engineering, Saitama University, Japan[1]
Research Institute of Superconductor Electronics, Nanjing University, China[2]

Superconducting nanowire single photon detectors (SNSPDs) , those have a low dark count rate characteristics, fast and low jittering response, and high quantum efficiency, are expected to be used in the time-resolving photon detection system. A readout circuit using superconducting single-flux-quantum (SFQ) logic circuits has been developed to realize fast and low-jittering readout for an array of SNSPDs. To enhance timing resolution, we are investigating a high-timing resolution time-to-digital conveter using SFQ logic circuit based on the CONNECT cell library. Using a series array of a time-resolving SFQ gates, we could obtain a timing resolution of 1/8 clock period, less than 20 ps. We will present details of design of the time-to-digital conveter, measurement results of fabricated circuits at the CRAVITY, the AIST.

Acknowledgement

This study has been partially supported by the VLSI Design and Education Center (VDEC) at the University of Tokyo, in collaboration with Cadence Design Systems, Inc. Circuits were fabricated in the clean room for analog-digital superconductivity (CRAVITY) of the National Institute of Advanced Industrial Science and Technology (AIST) with the standard process 2 (STP2). The AIST-STP2 process is based on the Nb circuit fabrication process developed by the International Superconductivity Technology Center (ISTEC).

Keywords: SNSPD, SFQ readout circuit, time-to-digital converter

EDP2-8

Tunable Microwave Single Photon Source Based on Transmon Qubit with High Emission Efficiency

*Yu Zhou[1,2], Zhihui Peng[2], Yuta Horiuchi[1], Jaw-Shen Tsai[1,2]

Department of Physics, Tokyo University of Science, 1-3 Kagurazaka, Shinjuku-ku, Tokyo 162-8601, Japan[1]
Center for Emergent Matter Science, RIKEN, 2-1 Hirosawa, Wako, Saitama 351-0198, Japan[2]

Single photon sources of high efficiency are of great interest because they are the key elements in many prospective quantum technologies and applications. Based on our previous work, here we demonstrate a high-quality tunable microwave single photon source based on transmon qubit with emission efficiency up to ~97.7%. To further confirm the single photon property of the source, we study the single photon interference in a Hanbury Brown-Twiss type setup and measure the correlation functions of the emission field using linear detectors with GPU-enhanced signal processing technique. The antibunching in the second-order correlation function is clearly observed. Such a high-quality single photon source may be used as a building block in the quantum communication and quantum information processing.

Keywords: Single photon source, Microwave regime, Tunable, Correlation function

EDP2-9

A transition edge sensor with broadband optical absorption for biological imaging

*T. Konno[1], S. Takasu[1], R. Kobayashi[1,2], K. Hattori[1], S. Inoue[2], D. Fukuda[1,2]

National institute of advanced industrial science and technology (AIST)[1]
Graduate school of science and technology, Nihon university[2]

Transition edge sensors (TES) exhibiting high energy resolution of a single optical photon have been designed for communication technology using quantum information to be sensitive only to photons of specific energy with a detection efficiency of almost 100 %. Now, we are aiming to achieve photon-counting microscopy for biological imaging to detect photons in the range of from optical wavelength to near-infrared wavelength with high efficiency. As detection efficiency is dependent of optical absorptance of TES, it is necessary for TES to show large absorptance for photons in the above range. We designed optical absorption cavity structures surrounding TES of Ti/Au bilayers such as shown in Fig. (a). According to the simulation using complex reflection indexes of respective materials at room temperature, an optimized cavity exhibits theoretical absorptance of over 90 % as shown in Fig. (b).

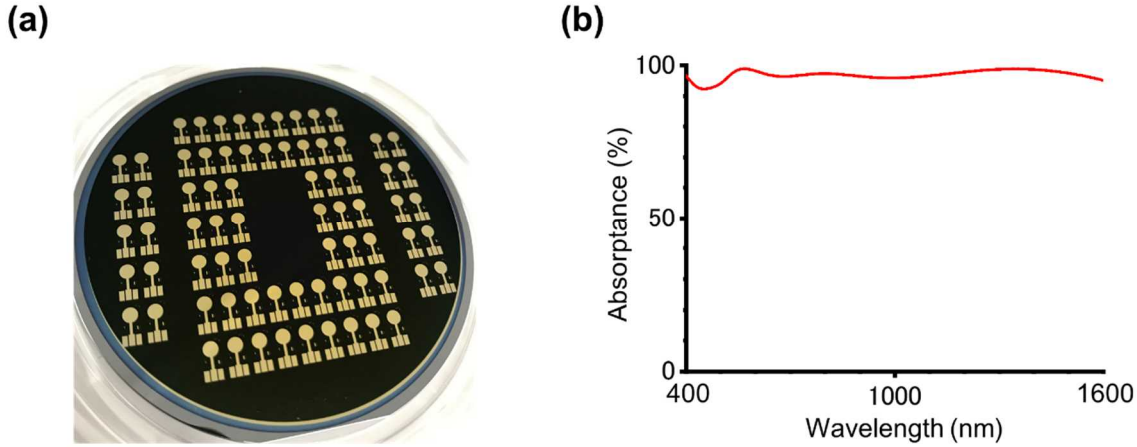

Fig. (a) TES enfolded an optical cavity with broadband absorption on a 3 inch Si substrate, (b) the theoretical values of optical absorptance of a cavity simulated using optical property value of each material at room temperature.

[Acknowledgment] This study is partially endorsed by JST, CREST, JPMJCR17N4.

EDP2-10

Development of a Superconducting Microwave Beam Splitter for Boson Sampling Experiments

*Julia Zotova[2,1], Yu Zhou[1], Rui Wang[3,1], Oleg Astafiev[2,4], Jaw-Shen Tsai[3,1]

Center for Emergent Matter Science, RIKEN, Japan[1]
Moscow Institute of Physics and Technology, Russia[2]
Tokyo University of Science, Japan[3]
Royal Holloway University of London, United Kingdom[4]

Superconducting quantum circuit is one of the most robust ways for realization of quantum systems. One of the most interesting effects can be observed due to single photons interactions[1]. To conduct these experiments different devices like single-photon source and an element for entanglement of quantum states are required. The most natural realization for such element is a beam splitter [2]. In microwave range it is convenient to use a hybrid beam splitter [1]. For single photon experiments a commercial beam splitter is not suitable because of dispassion in connectors and wires. Therefore, it is natural to use a beam splitter on-chip. In the talk the investigation of this kind of beam splitter with possible experiments will be reported.

[*1] C Lang, C Eichler, L Steffen, JM Fink, MJ Woolley, A Blais, and A Wallraff. Correlations, indistinguishability and entanglement in Hong–Ou–Mandel experiments at microwave frequencies. Nature Physics, 9(6):345, 2013.*
[2] Gregor Weihs and Zeilinger. Photon statistics at beam-splitters: an essential tool in quantum information and teleportation. Coherence and Statistics of Photons and Atoms, pages 262–288, 2001.

EDP2-11

Characterization of C-shunt flux qubit and its further applications in circuit-QED

*Gopika Lakshmi Bhai[1,2], Rui Wang[1,2], Yu Zhou[2], Hasegawa Makoto[1], Jaw-Shen Tsai[1,2]

Tokyo University of Science, Shinjuku, Japan[1]
RIKEN, Wakoshi, Japan[2]

Superconducting Josephson junction-based qubits operating in the microwave domain is one of the promising cavity QED architectures. In the past decade, impressive progress has been made to address, readout and scale superconducting qubits in the strong coupling regimes of circuit QED. However, the main limitation of this field is to improve the coherence time of the qubit preserving its large anharmonicity. The design variabilities and advanced fabrication techniques have improved the coherence time of qubits such as transmon qubits nearly to the millisecond, but the tradeoff is in the significant reduction of the anharmonicity. Recently, [1,2] put forward the idea of the capacitively shunted flux qubits achieving higher coherence time than the traditional flux qubits. Moreover, the improved design provides additional controllable qubit parameters which make this qubit more suitable for quantum optics experiments in the circuit QED scheme. Here we present the results on the experimental characterization of such a qubit and briefly discuss its applications in quantum optics experiments.

[1] Fei Yan et al., Nature Commun. 7: 12964 (2016)

[2] J. Q You et al., Phys. Rev. B 75, 140515 (2007)

Keywords: Superconducting qubit, Josephson junction, Flux qubit

APP1-1

Magnetic field measurements of the JT-60SA CS1 module

*Tetsuhiro Obana[1], Kazuya Takahata[1], Shinji Hamaguchi[1], Hirotaka Chikaraishi[1], Suguru Takada[1], Akifumi Iwamoto[1], Shinsaku Imagawa[1], Toshiyuki Mito[1], Haruyuki Murakami[2], Kyohei Natsume[2], Kaname Kizu[2]

National Institute for Fusion Science[1]
National Institutes for Quantum and Radiological Science and Technology[2]

The JT-60 tokamak is being upgraded to an advanced superconducting tokamak to be called the JT-60 Super Advanced (JT-60SA) at the National Institute for Quantum and Radiological Science and Technology in Japan. In the JT-60SA, the magnet system consists of a central solenoid (CS), 18 toroidal field coils, and six plasma equilibrium field coils. As the CS is composed of four modules, CS1, CS2, CS3, and CS4. Fig.1 shows the photograph of the CS1 module. In the superconducting coil test facility of the National Institute for Fusion Science, a cold test of the CS1 module was conducted before the CS1 module was installed in the magnet system of the JT-60SA. In this conference, the measurement of self-magnetic fields generated by the CS1 module in the cold test is presented. In addition, magnetic fields with long time constants observed in the CS1 module are discussed.

Keywords: JT-60SA, Central solenoid, Nb3Sn Cable-in-conduit conductor, Magnetic field measurement

APP1-2

Numerical simulation of the fast processes in HTS tapes under the pulsed current load

*Irina Anischenko[1], Sergey Pokrovskii[1], Igor Rudnev[1], Maxim Osipov[1], Dmitriy Abin[1]

National Research Nuclear University "MEPHI"(NRNU MEPHI), Russia[1]

This paper presents the results of a numerical modeling of high-temperature superconducting tapes REBCO under the stationary current effects and nonstationary effects of pulsed currents and magnetic fields. Simulations were perform by the Finite Elements Method (FEM), which was implemented using the Comsol Multiphysics software. The calculations are performed in 2D and 3D modes, the model takes into account the real geometric HTS tapes dimensions, as well as the features of the layered structure of each tape (real tapes architecture).

The results of multiphysical simulation of the transport and thermal characteristics of the HTS tapes are presented. Investigations for the stationary mode of the transport currents, significantly higher than the critical (up to 3 times) were performed. Model takes into account the possibility of the existing of inhomogeneous critical current domains. The calculations were carry out for the cases of cooling by the liquid nitrogen, as well as for the liquid-free cooling of the stack (cryocooler cooling mode). For all of above calculations, the cryocooling cooling of superconducting elements is carried out in the range of temperatures from 40 K to 80 K.

The high steadiness and stability of the tapes characteristics were shown for stationary current loads. In the nonstationary regime, under the current impulses are more than critical current of HTS tapes and under the magnetic fields pulses (LN2 cooling), the delay of the thermal instabilities in the tape occurrence is indicated. That can be caused by the heat-removal parameters in liquid nitrogen under the heating.

The currents and fields distributions in the system before and after the loads were shown. The dynamics of thermal processes in the HTS tape shown for the stationary and pulsed effects. The power required for the cryocooler cooling system for various loading regimes was also calculated. The influence of the thickness of the stabilizing layers on the transport and thermal characteristics of the stack is shown. Comparison with the experimental results was carry out. Creating an integrated model helps predict the behavior of the system and optimize the devices to achieve high technical performance.

The work is supported by the Russian Foundation for Basic Research under the grant 17-29-10024.

Keywords: HTS, pulsed current load, Finite Elements Method (FEM), transport current

APP1-3

Observation of a Non-Uniform Current Distribution in Stacked High Temperature Superconducting Tapes

Tim A.J. Meulenbroeks[1], Yoshiro Terazaki[2], Shinnosuke Matsunaga[3], Nagato Yanagi[2,3]

Eindhoven University of Technology[1]
National Institute for Fusion Science[2]
SOKENDAI (The Graduate University for Advanced Studies)[3]

High Temperature Superconductors (HTS) improve upon low temperature superconductors in many ways and the ability to cope with a non-uniform current distribution might be one of those improvements. To put this to the test, an experimental setup is designed to force a non-uniform current upon a stack of 5 HTS tapes, using a worst case current feeding method. The experiment can help determine the potential of this conductor design and is part of the ongoing effort to develop a non-transposed stacked HTS conductor for the helical fusion reactor FFHR. The results clearly show that the conductor sample is able to stably conduct a current equal to its critical current, although at an elevated electric field of roughly 5 mV/m. This means non-transposed stacked tape conductors remain stable, even if a worst case non-uniform current is constantly forced upon them. A hypothesis to explain this abnormally high electric field is formulated on the basis of the results, however additional research is needed to verify it. It states that the electric field is necessary for the tapes to share current and would mean that in a properly engineered application, these losses due to the electric field, would only occur during start-up. Overall it is clear that this experiment proves the excellent stability of non-transposed stacked HTS tapes and their ability to conduct a non-uniform current.

Keywords: HTS, stacked tapes conductor, non-uniform current distribution, stability

APP1-4

Analysis of current distribution in a simply-stacked HTS tapes conductor based on an electrical network model

*Shinnosuke Matsunaga[1], Tim A. J. Meulenbroeks[2], Yoshiro Terazaki[3], Yuta Onodera[3], Nagato Yanagi[1,3]

SOKENDAI (The Graduate University for Advanced Studies)[1]
Eindhoven University of Technology[2]
National Institute for Fusion Science[3]

The conceptual design studies on the helical fusion reactor FFHR series are progressing at National Institute for Fusion Science. For the magnet system of FFHR, the High-Temperature Superconductor (HTS) is the primary option to be employed. One of the candidate conductors is called the STARS (Stacked Tapes Assembled in Rigid Structure), and a prototype sample achieved 100 kA at 5.3 T magnetic field and 20 K temperature [1]. The STARS conductor has an internal structure that ReBCO tapes are simply stacked. It has widely been recognized that non-uniform current distributions occur among HTS tapes unless twisting and transposition are included, which may affect the cryogenic stability of the conductor. An unexpected current distribution also generates an error magnetic field, which may deteriorate the plasma confinement. Thus, the non-uniformity of transport current must be evaluated quantitatively. For this purpose, a scaled-down experiment of a simple stacking of HTS tapes conductor was performed using five ReBCO tapes imbedded in a copper jacket. In order to intentionally produce a non-uniform current distribution, so that this could simulate the possible situation of a long-length STARS conductor, the current was supplied from one side of the HTS tape stacking at the terminals. The magnetic field signal generated by the transport current was monitored by Hall probes to estimate the current distribution. The voltage generation in each tape was also monitored. The experimental results indicate that the current smoothly transfers from the tape that reaches the critical current to others so that the current distribution among tapes becomes more uniform. In order to analyze the current distributions measured in the experiment, the conductor sample is modeled in an electrical circuit based on the electrical network theory. For example, the system of a stack of three HTS tapes is shown in Fig. 1. The numerical calculation is done to simulate the experimental observation of the magnetic field distribution and the voltage generation. In the presentation, comparisons between the experimental results and simulation results are discussed.

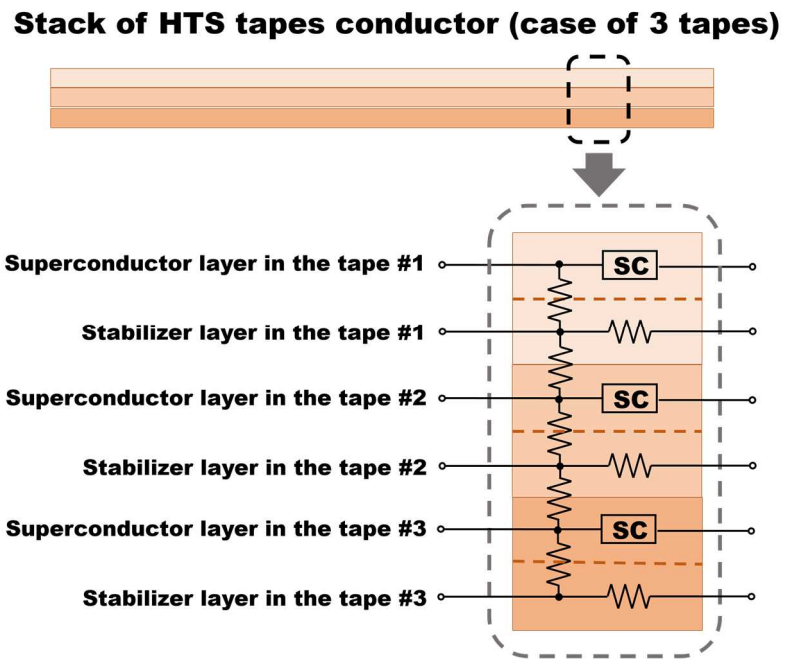

[1] N. Yanagi et al., "Magnet design with 100-kA HTS STARS conductors for the helical fusion reactor", Cryogenics, Vol. 80, 243-249, 2016

APP1-5

Transport Current Characteristics of High Temperature Superconducting Busbar

*Yoshiro TERAZAKI[1], Nagato YANAGI[1]

National Institute for Fusion Science[1]

The conceptual design activities of the LHD-type helical fusion reactor FFHR-d1 are progressing at National Institute for Fusion Science (NIFS). The helical coils of FFHR-d1 have the major radius of 15.6 m and the toroidal magnetic field of 4.7 T [1]. To produce this field, an operating current of 94 kA is required for a conductor of the helical coils at the maximum magnetic field of 11.8 T. We proposed a conductor using the high-temperature superconductor (HTS) as one of the options of the helical coil conductor. This conductor is consisted of simply-stacked REBCO HTS tapes, a copper stabilizer and a rigid stainless-steel structure. For the development of such a HTS conductor suitable for the FFHR-d1, we fabricated and tested 100 kA-class prototype HTS conductors and the transport current of 100 kA was successfully measured at 20 K, 5.4 T.

Then, we planned to test 50-kA-class and HTS coil, which is 4-turns double pancake coil with 20 GdBCO tapes. For this test, a superconducting busbar is fabricated. The busbar has also the simply-stacked-tapes concept and is consist of 48 GdBCO tapes. The tapes are stacked in a copper jackets, and the jackets are covered with the stainless-steel plates. The details of the results will be reported in the presentation.

[1] A. Sagara et al., Fusion Eng. Des., **89** (2014) 2114–2120
[2] Y. Terazaki et al., IEEE Trans. Appl. Supercond., **24** (2014) 4801305.
[3] S. Ito et al., Plasma and Fusion Research, **9** (2014) 3405086.

Keywords: HTS, Superconducting Busbar, Fusion Magnet

APP1-6

Preload Structure Optimization Design and Mechanical Analysis of the CFETR Central Solenoid Model Coil

Dapeng Yin[1,2], Yu Wu[1], Aihua Xu[1,2], Houxiang Han[1,2]

Institute of Plasma Physics, Chinese Academy of Sciences, PO Box 1126, Hefei, Anhui 230031, China[1]
University of Science and Technology of China, No.96, JinZhai Road Baohe District, Hefei, Anhui 230026, China[2]

The central solenoid model coil (CSMC) for China Fusion Engineering Test Reactor is being developed in the Institute of Plasma Physics, Chinese Academy of Sciences (ASIPP). It is a hybrid superconducting magnet with Nb_3Sn and NbTi coils. The maximum magnetic field is 12 T in the bore of the Nb_3Sn coils. It has a 1.5 T/s changing rate under 47.65KA operating current. The structure of the CSMC has been designed, mainly including Nb_3Sn coils, NbTi coils, preload structure, coil buffer zone, joints, supports, feederthroughs, helium pipes and pipe supports. The preload structure is one of the most important components of the CSMC, consisting of 15 preload beams, 30 preload rods and support plates. And a 75MN preload force will be applied on the preload structure at room temperature. This paper describes the optimization design process and the mechanical analysis of the preload structure. The mechanical analysis results show that the preload structure design is reasonable and feasible.

Keywords: Central solenoid (CS) model coil, superconducting magnets, optimization design, mechanical analysis

APP1-7

Measurement of the critical current for Bi-2212 subcable by using Four Hall Sensor Arrays

W Chen[1], *X S Yang[1], C H Chen[1], Y Zhao[1]

Southwest Jiaotong University[1]

High-temperature superconducting material of Bi-2212 ($Bi_2Sr_2CaCu_2O_x$) **is considered to be used in the next generation of fusion reactors such as China Fusion Engineering Test Reactor (CFETR) due to extremely high critical current density as well as high critical field at low temperature. The critical current as well as its inhomogeneity is one of the important factors to evaluate the performance of the Bi-2212 wire, cable and conduct, and also it is important for** the design of the superconducting magnet system**. Commonly, the** critical current is detected by four-probe method (electric method). The electric method, however, has its limitations, such as without the local characteristics and the need of large current source. In this work, n**on-destructive evaluation (NDE) by using Hall sensor array, a magnetic method, will be used for testing local critical current of Bi-2212 subcable. NDE is more effective and faster method for testing local critical current of** high temperature superconductor **compared with conventional electrical method.**

APP2-1

Experimental and Analytical Study on Load Characteristics of a 50 kW Class High Temperature Superconducting Induction/Synchronous Motor

*Kentaro Kuroda[1], Taketsune Nakamura[1], Masaaki Yoshikawa[2], Yoshitaka Itoh[2], Ryohei Nishino[1], Takuro Ogasa[1], Toshihisa Terazawa[2], Terazawa Fukui[3], Mitsuho Furuse[4], Yoshimasa Ohashi[5]

Kyoto University, Japan[1]
IMRA MATERIAL R&D Co., Ltd, Japan[2]
Niigata University, Japan[3]
National Institute of Advanced Industrial Science and Technology (AIST), Japan[4]
AISIN SEIKI Co., Ltd, Japan[5]

High Temperature Superconducting (HTS) materials have been applied in motors to improve the efficiency and increase the torque density. In recent years, many research institutes and companies all over the world have been conducting research on HTS motors. However, most of studies are for synchronous motor with the HTS field windings.
In our project group, we focus on the features of induction motor and have developed HTS Induction/Synchronous motor (HTS-ISM), which replaced its winding with HTS wires. The HTS-ISM, which has been studied so far, is mainly a motor using HTS wire for cage-shaped rotor windings of an induction motor. And then, the high torque density and high efficiency can be realized, by applying a large current to the secondary side windings. However, the copper winding used for the stator has a large Joule loss when the primary current increases. Hence, the reduction of loss in the stator windings has been a problem from the viewpoint of heat generation and efficiency. Therefore, we have been trying to develop a fully HTS-ISM, which uses HTS wires for not only the rotor windings but also the stator windings. Since the superconducting motor is an alternating current (AC) machine, AC loss will be generated by applying an alternating current to a HTS stator winding. However, compared with motors with copper windings, the loss of fully HTS-ISM would be less value.
In this paper, we have succeeded in fabricating a 50 kW class fully superconducting HTS-ISM, of which so-called ring-windings are adopted for the stator windings. And then, we have succeeded in realizing variable speed load test. Such characteristics have also been reproduced by means of the analysis based on finite element method (FEM) and nonlinear electrical equivalent circuit.
This work has been supported by Japan Science and Technology Agency under the program of Advanced Low Carbon Technology Research and Development Program (JST-ALCA) in Japan.

Keywords: HTS-ISM, Fully superconducting motor, Variable speed control, Load test

APP2-2

Design of a 750 kW Class HTS Wind Generator with HTS Modules

*Oyunjargal Tuvdensuren[1], Hae-Jin Sung[1], Byeong-Soo Go[1], Minwon Park[1], In-KeunYu[1]

Changwon National University. Republic of Korea[1]

Recently, high temperature superconducting (HTS) generators are being studied with the advantages of high efficiency, and the weight, volume compared with the conventional generator. However, the HTS generators have problems, such as HTS coils typically require a power supply, a current lead and a slip ring for transferring the DC current into the HTS coils. The current lead can be a bridge between the cryogenic environment and room temperature, which causes heat transfer loss. Also, relating to high electromagnetic force because of their high current density and magnetic field. Therefore, structure design of the module coil for HTS generator has been suggested to overcome these problems.

This paper presented with a design of the 750 kW class superconducting generator with HTS modules. The 750 kW HTS generator had 84 HTS modules. One HTS module coil including HTS coils and bobbin structure, coil supports, thermal shield, cryostat, current leads were drawn by the 3D CAD program. The 750 kW generator's HTS module coil was designed based on electromagnetic, thermal and mechanical stress analyses obtained using the 3D finite element method (FEM). Critical current was estimated by the perpendicular magnetic flux density.

As a result, the perpendicular and maximum magnetic flux densities were 2.4 T and 4.4 T, respectively. The total heat load was minimized and the temperature achieved lower than 20 K at the HTS coil. The Lorentz force and torque of the HTS module coil and the maximum stress and displacement of the structure were calculated. Structural stress was less than the allowable material stress, and displacement was within the permissible range. The structural design and thermal, mechanical stress analysis results of the HTS field coil can effectively be utilized to develop a superconducting wind power generator.

Keywords: Electromagnetic analysis, Heat load, HTS, Mechanical stress, Module coil

APP2-3

Numerical Analysis of AC loss and Power Density of 10 MW Fully Superconducting Generators for Electric Aircrafts from the viewpoint of Armature Winding Configuration

*Masataka Komiya[1], Takuya Aikawa[1], Koichi Yoshida[1], Shun Miura[1], Masataka Iwakuma[1], Takashi Yoshida[1], Teruyoshi Sasayama[1], Akira Tomioka[2], Masayuki Konno[2], Teruo Izumi[3]

Research Institute of Superconductor Science and Systems, Kyushu University, Fukuoka 819-0395, Japan[1]
Fuji Electric Co. Ltd., Ichihara-city 290-8511, Japan.[2]
National Institute of Advanced Industrial Science and Technology, Tsukuba 305-8564, Japan.[3]

The development of fully-turbo electric propulsion systems for future aircrafts has been started worldwide to realize low emission, low noise and low fuel consumption. Conventional electric rotating machines which are composed of iron cores and copper wires are too heavy to apply to them. So fully-superconducting rotating machines with more compactness and lighter weight are expected to be developed. In this study, 10 MW fully superconducting generators were designed with REBCO superconducting tapes and the electromagnetic properties, total weight, efficiency and so on were evaluated by numerical simulation. Mainly the influence of the configuration of an armature winding, such as a distributed-winding and a concentrated-winding, on AC loss and output power density was investigated. For superconducting armature windings, concentrated-windings have been usually adopted due to the simplicity in winding process. However, for conventional generators, lap-windings and wave-windings are studied out for the distributed-windings and have been generally adopted. It is known that the winding density of the distributed-windings is larger than that of the concentrated-windings. Therefore, the improvement of efficiency and output power can be expected. In advance of study, the properties of REBCO superconducting tapes were investigated over a wide range of temperatures by using a saddle-shaped pick-up coil. The numerical analysis of generators was performed by using JMAG (Analysis software for electric equipment by JSOL). As a result, in the case of the concentrated-winding model at T_{op} = 20 K and B_g = 1.5 T, the output power density attained to 17.8 kW/kg with an efficiency of 92.0 %. On the other hands, in the case of the lap-winding model, the efficiency attained to 99.4 % with an output power density of 17.2 kW/kg. The results in detail will be reported on ISS 2018.

Keywords: Generators, AC Loss and Power Density, Superconducting tapes, Electric Aircrafts

APP3-1

Suspension Stability of Side-Suspended HTS Maglev System in Evacuated Tube

D J Zhou[1], F N Cai[2], L F Zhao[2], Y Zhang[2], *Y Zhao[1,2]

Fujian Normal University[1]
Southwest Jiaotong University[2]

For the high-speed HTS maglev system in evacuated pipe, the side-mounted permanent magnet double-track is used to provide suspension and guidance for the train. When the maglev is running in a round track or a curve, the centrifugal force exerts a side pressure on the track, causing displacement in the suspension direction. In this paper, the static simulation experiment is used to study the instability caused by suspension displacement during the dynamic process of maglev. The results show that under the premise of a given field cooling airgap, the suspension force decreases with the decrease of the suspended airgap and strengthens with the increase of the suspension displacement. In addition, reducing the field cooling airgap can increase the suspension force and reduce the suspension displacement. When the field cooling air gap on the spot is 10mm and the initial suspension displacement is 2mm, the suspension displacement will not exceed 2mm when the train runs to the rated airgap of 5mm, so that the train maintains high side suspension stability. The research results of this paper provide useful design reference for the application of high speed HTS maglev train in the evacuated tube.

APP3-2

Vertical vibration characteristics of HTS Maglev systems under a long term external disturbance

*Shunshun Ma[1]

Applied Superconductivity Laboratory, State Key Laboratory of Traction Power, Southwest Jiaotong University, Chengdu 610031, P. R. China[1]

The high-temperature superconducting (HTS) maglev system, owning to the capability of passive stabilization, has the potential to achieve high-speed transportation with low energy consumption. The vibration characteristics under a long-term external disturbance have a great influence of the safety and ride comfort. To study the reliability of HTS maglev systems under a long term disturbance, a bespoke experimental device composed of a vibration table and a HTS maglev system was employed to simulate the disturbance caused by the track irregularity. Two sets of experiments were carried out, one is that the position of HTS bulks were fixed, and the other is in free levitation. The levitation height under different frequencies and amplitudes conditions was measured respectively by laser displacement sensor every ten minutes. It is found that under the same operation conditions, the larger the amplitude, the more the levitation height decreases, and the levitation height decreases more at the resonant frequency. The fixed HTS bulks decreased more in the levitation height compared with the freely levitated HTS bulks at the same frequency and amplitude. These findings are potentially significant in the design and application of HTS maglev systems.

Keywords: high temperature superconductor, maglev, vibration characteristics, long term

APP3-3

Vibration suppression of high-temperature superconducting maglev system via electromagnetic eddy current damper

*Jinbo Yu[1], Haitao Li[1], Shuai Zhang[1], Ruixue Sun[1], Xiaochen Sang[1], Zigang Deng[1]

Applied Superconductivity Laboratory, State Key Laboratory of Traction Power,Southwest Jiaotong University.P.R.China[1]

The high-temperature superconducting (HTS) Maglev system is characterized with self-stable levitation, low energy consumption, pollution-free operation and it has been considered as a promising technology for implementing high-speed transport systems. The previous studies have shown that the damping of such system is relatively low, which may cause large-amplitude nonlinear vibration of the system easily. This phenomenon will affect the long-term stability and running performance of HTS maglev in rail transit application. In order to suppress the harmful vibration, we designed a damper utilizing the interaction between a coil and the maglev track. The natural frequency of the damper is adjusted to a value close to that of the moving maglev system. In this way, the damper becomes most effective because the moving vehicle body and the circuit resonate simultaneously. The performance of the damper is investigated through systematic simulations and experiments in typical working conditions. The results show that under the random external disturbance, the damper can effectively attenuate the amplitude of vibration. It can be predicted that the vehicle will run more steady along the track with this damper. This research work is important for the further practical application of the technology.

Keywords: High-temperature superconducting maglev, vibration, permanent magnet track, eddy current damper

APP3-4

Emulation and Analysis of an Axial Superconductor Magnetic Bearing

*Elkin Rodriguez[1,2], Zigang Deng[2]

Laboratory of Applied Superconductivity – LASUP / UFRJ, Rio de Janeiro, Brazil.[1]
Applied Superconductivity Laboratory, State Key Laboratory of Traction Power, Southwest Jiaotong University,, P. R. China[2]

Magnetic levitation is being used in different applications [1]-[8]. Even in applications in which energy consumption is a problem [1][2]. In this area, passive magnetic levitation gains over active magnetic levitation. Also, it does not need the loop control system for levitation. Superconducting magnetic levitation shows good technical features by its stability in all axes, in comparison with other techniques of passive magnetic levitation [3].
Nowadays, it is common to find devices or prototypes using two or more levitation techniques for good performance [4]-[8]. This is possible by the appropriate coupling between them. In order to achieve this, it is necessary to know each technique properly.
Aiming at the dynamic implementation, this paper presents the test bench to be used in emulation of the movement in superconductor magnetic levitations. This bench is used to experimental tests and can be move in X, Y and Z direction. This movement can be simultaneous or each separate axis offering greater flexibility for testing. It is possible by the proper communication between the control hardware and the control processing software. Three load cells are used to measure the forces of levitation and guidance. Finally, the experimental data will be shown to validate the good performance of the test bench.

Keywords: Dynamic test, bench test, magnetic levitation

APP3-5

Energy losses in magnetic contactless bearings on the base of high-Tc superconducting tapes

*Igor Rudnev[1], Dmitriy Abin[1], Maksim Osipov[1], Sergey Pokrovskii[1], Irina Anischenko[1], Alexsey Podlivaev[1]

National Research Nuclear University MEPHI (Moscow Engineering Physics Institute)[1]

High-temperature superconducting tapes are very promise for application in rotary magnetic bearings owing to its excellent magnetic and transport properties as well as possibility to easy create magneto-levitation systems of various geometry. One of problem arising in the rotation superconducting bearings is the presence of the energy losses resulting from the magnetization hysteresis due to inhomogeneous of magnetic field from permanent magnets. In this report we present results of experimental and theoretical studies of rotation losses in the model superconducting bearing based on commercial high temperature superconducting (HTS) tape. The bearing stator has a cylindrical shape and is made of a multilayer HTSC tape. The bearing rotor is made of permanent magnets located at the same radius relative to the axis of rotation. The rotation energy losses were estimated from the decay time of the rotor rotation speed. The experiments were carried out using various configurations of magnets. The experimental data were compared with results of numerical calculations which were carried out in the framework of the critical state model taking into account the double-exponential dependence of the critical current density on external applied field. It was found that the experimental and numerical results are in a good agreement.
The study was carried out at the expense of a grant from the Russian Science Foundation (project No. 17-19-01527).

Keywords: HTSC tapes, magnetic bearings, energy losses

APP3-6

Levitation characteristics of superconducting stators with addition of a ring-shaped magnet

*Muneo Futamura[1], Ryo Shindo[1]

Akita Prefectural University[1]

High magnetic rigidity is needed in order to make optimum use of the high performance of superconducting levitation. We proposed a hybrid stator comprising a superconductor and a ring-shaped permanent magnet, and measured the levitation characteristics of a magnet levitating above various hybrid stators. The magnetic force between the hybrid stator and a levitating magnet was measured by displacing at semistatically. By adding a ring shaped magnet, the vertical and the horizontal attractive magnetic force and stiffness were increased compared with those of a simple superconducting stator. Analysis of the calculated magnetic field for the ring magnet determined that the attractive force of the ring magnet and superconducting pinning force were effectively combined on the proposed hybrid stator. The magnetic force showed a hysteresis against the displacement of the levitating magnet. The oscillation frequency of levitating magnet above the hybrid stator is higher than that of the simple superconducting stator. With the hybrid stator, a faster decay due to the hysteresis energy loss and Small amplitude from the Enhanced magnetic stiffness were observed.
An improvement in the stability of the levitating magnet is realized by the hybrid stator using a superconductor and a ring-shaped magnet.

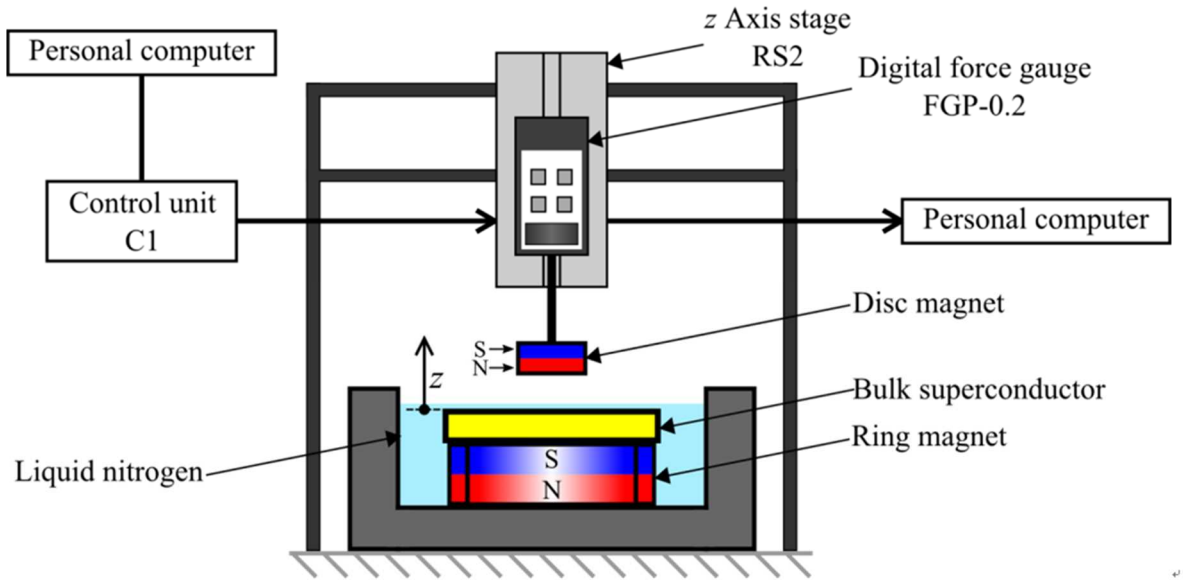

Keywords: Superconducting levitation, Ring shaped magnet, Magnetic force , Magnetic stiffness

APP3-7

Evaluation of loss characteristics of superconducting magnetic bearings for LiteBIRD satellite by three-dimensional finite element method analysis

*Yukimasa Hirota[1], Yutaka Terao[1], Hiroyuki Ohsaki[1], Tomotake Matsumura[2], Yuki Sakurai[2], Hajime Sugai[2], Nobuhiko Katayama[2]

The University of Tokyo, Japan[1]
Kavli IPMU, The University of Tokyo, Japan[2]

LiteBIRD is a strategic large scale satellite program of JAXA Institute of Space and Astronautical Sciences, aiming for launch in mid-2020s. The purpose of this satellite is to observe the polarization of the cosmic microwave background radiation (CMB) and test the presently proposed "inflation hypothesis" at the early universe.

In this satellite, a polarization modulator is mounted as one of the instruments constituting the optional system. The polarization modulator is required the continuous rotation of the half-wave plate (HWP) below the temprature of about 10 K. It is important issue to reduce heat generation due to rotation loss, because the refrigerator capacity of the satellite is limited.

We studied a rotation mechanism in a cryogenic environment by a superconducting magnetic bearing (SMB) using the pinning effect of the bulk superconductor. A levitated rotor of the SMB achieves stable rotation due to the pinning effect. Thus, we can avoid the frictional heat due to the physical contact.

The HWP is mounted inside of the rotor of the SMB. The rotor consists of a permanent magnet and an iron yoke. Due to the prospective diameter of 400 mm, the permanent magnet has to be segmented to form a ring. As a result, there is a potential gap between the magnets. This becomes a source of the magnetic inhomogeneity and leads to the magnetic friction and eventual heat dissipation.

We report the numerical estimation of the heat energy loss in the SMB from the rotation with the inhomogeneity of the rotor magnet using the three-dimensional finite element method. We first use JMAG Designer 17.0 to estimate the static magnetic field distribution crated by the rotor magnet. Then, we imported this magnetic field to the COSMOL Multiphysics 5.3a, rotate this magnetic field, and estimate the loss generated by the bulk superconductor, YBCO. We employ the n-value model for a bulk superconductor. In this talk, we introduce the overview, and the associated challenge, and we discuss the numerical evaluation of the energy loss from the SMB and validity of the results.

Keywords: LiteBIRD, Superconducting Magnetic Bearing, Finite Element Method, Bulk Superconductor

APP4-1

A feasibility study of smart high-temperature superconducting cable to improve stability of KEPCO system

*Sangsoo Seo[1], Seung Ryul Lee[1], Jeonwook Cho[1]

Korea Electrotechnology Research Institute[1]

The Korean system is a very tightly coupled island system. The installed capacity is about 100 GW and the load demand is gradually increasing. Especially in metropolitan areas where the load is concentrated, the system fault current often exceeds the breaker capacity due to the strong connection. The system operator limits the fault current by bus split operations considering the breaker capacity but this reduces system stability. Therefore, various efforts have been made using a fault current limiter to overcome these problems. A smart superconducting cable is a type of superconducting power transmission cable. It has not only standard structure of the existing superconducting power cable but also a fault current limiter. The cable has a superconducting characteristic in a normal state, while when a fault occurs, it can limit a fault current through generating impedance that adjusts electrical and thermal properties of superconducting cable and material and cross-sectional area of superconducting cable. In this paper, a technique is proposed to reduce system fault current while improving the system stability using a smart high-temperature superconducting cable. In addition, the appropriate cable capacity and locations are selected to improve the reliability of the Korean power systems using smart superconducting cables. The proposed locations and capacities will be applied to the smart superconducting cable development project that started in May last year.

Keywords: High temperature superconductor, Superconducting cable, Fault current limiting, Power system stability

APP4-3

Conceptual design and performance analysis of a multi-layer 3 phase coaxial HTS

*Seong-Yeol Kang[1], Seok-Ju Lee[1], Minwon Park[1],In-Keun Yu[1], Du-YeanWon[2], Hyung-Suk Yang[2]

Changwon National University. Republic of Korea[1]
KOREA, KEPCO Research Institute, Republic of Korea[2]

Recently, high-temperature superconducting (HTS) power cables have been developed due to their advantages over conventional cables. For high current capacity, two or more layers are required on one phase of the HTS cable. Different radii between each phases and each layers cause problems of inherent imbalance and non-uniform current distribution for 3-phase currents, which must be minimized by properly designing the pitches of the cable. On the other hand, the characteristics of HTS cable including transient, current distribution between layers, critical characteristics, dielectric loss, and induced current loss in the shield layer are normally complicated to analyze. In this paper, the authors designed a 23 kV/60 MVA multi-layer 3 phase coaxial HTS cable and its characteristics were analyzed by the PSCAD/EMTDC component and simulation method. The conceptual design of the multi-layer 3 phase coaxial HTS cable includes the radii of each layer, the number of layers in each phase, and the pitch design of each layer of the cable. Based on the impedance matching program, the current imbalance can be minimized and the current distribution in the layers of the phase can be uniformed by adjusting the pitch length and winding direction. The characteristics of HTS cables were analyzed by using proposed PSCAD/EMTDC component. In this component, the dynamic resistance of current and temperature dependent HTS cables is added to the HTS model. Transient simulation was performed for a three-phase fault of the 3 phase coaxial HTS cable using the PSCAD/EMTDC-based simulation method. One phase of the 23 kV/60 MVA HTS power cable was designed with a two-layer structure, and the pitch was designed to allow uniform current distribution. The simulated current distribution, induced current loss results from the proposed PSCAD/EMTDC components were the same as those obtained using the finite element method program and calculated results. The analysis results will be effectively utilized for the actual design of 23 kV/60 MVA multi-layer 3 phase coaxial HTS power cable.

Keywords: Multi-layer HTS co-axial cable, Transient, PSCAD/EMTDC, HTS

APP4-4

Structural Study on a Single-phase Bi2223 High Temperature Superconducting Transformer for a 1 kHz-1 kA Class Power Supply

*Takafumi Adachi[1], Nozomu Nanato[1], Takahito Yamanishi[1]

Okayama University[1]

The presenters have been developing a large AC current source with a single-phase Bi2223 superconducting transformer [1-3]. The intended use of the source is to grasp current conduction characteristics of high temperature superconductors. The presenters aim to develop the source supplying current with maximum frequency of 1 kHz and maximum amplitude of 1 kA. However, their conventional transformer had some leakage inductance resulting in high voltage drop and therefore it was unable to transport the current with high frequency and large amplitude. In the presentation, the presenters propose a configuration of the transformer with less leakage inductance than the conventional one and show its improved current transport characteristics. In addition, a protection system for normal transitions in the transformer will be presented.

[1] N Nanato, S Tanaka and S Tenkumo, Study on a Magnetic Flux Detection Coil for Detection of Normal Transitions in a Hybrid Single-phase Bi2223 Superconducting Transformer by the Active Power Method, Journal of Physics: Conference Series, Vol. 1054, 012070 (2018)
[2] N Nanato, T Ono, T Adachi and T Yamanishi, Protection System for Normal Transitions in a Single-phase Bi2223 Full Superconducting Transformer by the Active Power Method under Flowing Currents of Various Frequencies, Journal of Physics: Conference Series, Vol. 1054, 012068 (2018)
[3] N Nanato, N Kishi, Y Tanaka and M Kondo, Basic study for a large AC current supply with a single phase air-core Bi2223 high temperature superconducting transformer, Journal of Physics: Conference Series, Vol. 871, 012101 (2017)

Keywords: HTS transformer, Large AC current source, Normal transitions, Protection

APP4-5

Design of an Air-core Bi2223 High Temperature Superconducting Transformer with Pancake Structure for a Large AC Current Supply and its Protection System for Normal Transitions

*Mikishi Kondo[1], Nozomu Nanato[1], Hokuto Yamada[1]

Okayama University, Japan[1]

The presenters have developed a large AC current supply with a single-phase Bi2223 HTS transformer of which rated current is 1 kA [1, 2]. In order to minimize weight and volume of the transformer, the presenters have been studying a feasibility of an air-core HTS transformer [3]. Magnetic coupling between a primary coil and secondary one of the air-core transformer is weak and therefore more primary current is needed to output specified secondary current than that of the iron-core transformer [3]. The presenters propose the air-core transformer with pancake structure to strength the magnetic coupling and show experimental and numerical results. They also present a protection system of the air-core transformer for normal transitions, especially for self-protection based on a low exciting impedance of the air-core transformer.

[1] N Nanato, S Tanaka and S Tenkumo, Study on a Magnetic Flux Detection Coil for Detection of Normal Transitions in a Hybrid Single-phase Bi2223 Superconducting Transformer by the Active Power Method, Journal of Physics: Conference Series, Vol. 1054, 012070 (2018)
[2] N Nanato, T Ono, T Adachi and T Yamanishi, Protection System for Normal Transitions in a Single-phase Bi2223 Full Superconducting Transformer by the Active Power Method under Flowing Currents of Various Frequencies, Journal of Physics: Conference Series, Vol. 1054, 012068 (2018)
[3] N Nanato, N Kishi, Y Tanaka and M Kondo, Basic study for a large AC current supply with a single phase air-core Bi2223 high temperature superconducting transformer, Journal of Physics: Conference Series, Vol. 871, 012101 (2017)

Keywords: Current supply, Air-core HTS transformer, Magnetic coupling, Self-protection

APP4-6

Optimum Design of Cryogenic Pump for Circulation Cooling of High Temperature Superconducting Cables

*Kenta TADAKUMA[1], Kazuhiro KAJIKAWA[1], Yasuharu KAMIOKA[2], Atsushi ISHIYAMA[2], Shinsaku IMAGAWA[3], Taketsune NAKAMURA[4], Hirokazu HIRAI[5], Shinsuke OZAKI[5]

Graduate School of Information Science and Electrical Engineering, Kyushu University[1]
Waseda University[2]
National Institute for Fusion Science[3]
Kyoto University[4]
Taiyo Nippon Sanso Corporation[5]

High temperature superconducting (HTS) wires in the form of a tape can be cooled using liquid nitrogen with the boiling temperature of 77 K. A lot of research-and-development projects for power transmission cables using the HTS wires have been in progress all over the world because the HTS cables are expected to be small energy dissipation and low installation cost under the ground. A liquid nitrogen pump with high efficiency, enough discharge pressure and allowable maintenance interval would be required to realize a long-length HTS cable in near future, but such a pump has not been developed yet. Therefore, our group aims to develop a liquid nitrogen circulation pump composed of cryogenic magnetic bearings and HTS motor. The specifications of the target pump are determined as the discharge pressure of 1 MPa using a 2-stage impeller, the flow rate of 100 L/min and the rotating speed of 5000 rpm on the basis of the specific speed in turbomachinery. The pressure drops and temperature rises caused by the cooling with liquid nitrogen are also estimated for two typical examples of HTS cables. One is the three-in-one-type AC cable located inside a corrugated pipe as shown in Fig. (a) [1], and the other is the single-core-type DC cable located inside a straight pipe [2]. The theoretical expressions of pressure drop and temperature rise indicate the contributions from three components such as the friction between the liquid nitrogen and the wet surfaces, ratio of the heat inleak to the mass flow rate of liquid nitrogen and vertical change of position along the cooling pipe. Fig. (b) shows the profiles of pressure drop and temperature rise along the three-in-one HTS cable. The numerically estimated results are validated by comparing them with the test results carried out by the other groups [1,2]. Furthermore, the maximum feeding distance of HTS cable can be determined by adjusting the flow rate of pump if the maximum permissible pressure drop and temperature rise are fixed in advance.

[1] H. Yumura, et al.: IEEE Trans. Appl. Supercond. 23 (2013) 5402306
[2] H. Watanabe, et al: IEEE Trans. Appl. Supercond. 27 (2017) 5400205

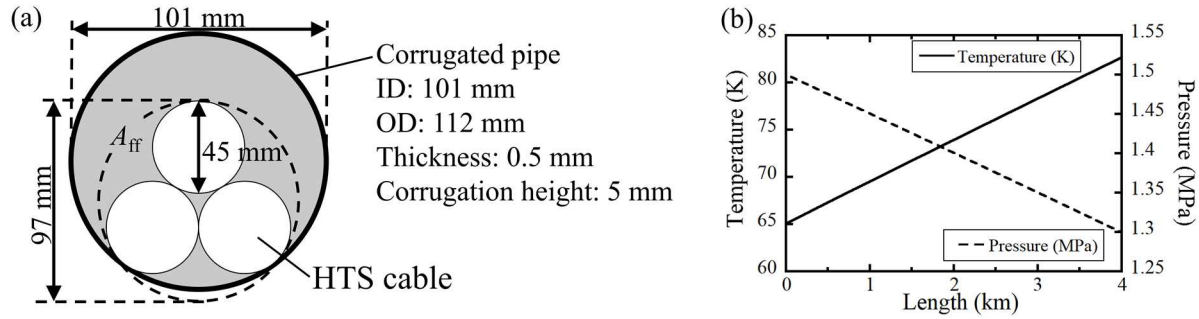

Fig. (a) Modeling of three-in-one-type HTS cable located inside corrugated pipe, (b) profiles of pressure drop and temperature rise along HTS cable.

Keywords: Cryogenic pump, High temperature superconducting cable, Liquid nitrogen, Pressure drop

APP4-7

Heat Load to the cryogenic system in the 1000 m Class Superconducting DC Power Transmission System

*Hirofumi Watanabe[1], Yury V Ivanov[1], Noriko Chikumoto[1], Satarou Yamaguchi[1], Kotaro Ishiyama[2], Zenji Oishi[2], Michihiko Watanabe[3], Takato Masuda[3]

Chubu University[1]
Chiyoda Corporation[2]
Sumitomo Electric Industries, Ltd.[3]

A 1000 m class superconducting DC power transmission system was constructed in Ishikari, Japan, which has been used to obtain data for the future longer transmission lines. Previously, we reported the heat leak of the cryogenic pipe of the system at specific outer pipe temperatures [1]. However, since the radiative and conductive heat transfers depend on the outer pipe temperature, the heat leak varies with the change of the environmental conditions, such as, temperature, weather, and sunshine. Accordingly, the heat load to the cryocooler, which reflects the history of the heat leak variation during circulation, changes every moment in the actual operation of the system. We have measured a heat load to the cryocooler and its consumption power over a month and a half in the second cooling test of the 1000 m system. The heat load to the cryocooler varied in the range around 1.8-2.5 kW by the change of the environmental conditions. Based on the results, the efficiency of the system was investigated.
This work was supported in part by the Japanese Ministry of Economy, Trade and Industry (METI) and by the New Energy and Industrial Technology Development Organization (NEDO).
[1] H. Watanabe et al. J. Phys. Conf. Ser. 1054 (2017) 012076.

Keywords: Superconducting DC power transmission, Heat load, Efficiency

APP5-1

Early Detection of Normal Transitions in a High Temperature Superconducting Transformer Wound with a Plurality of HTS Tapes Using the Active Power Method

*Hiroki Aoyama[1], Nozomu Nanato[1]

Okayama University[1]

The presenters have been developing an AC power source with a high temperature superconducting (HTS) transformer which is small in size and can supply large AC current [1-3]. The HTS transformer needs a detection system of normal transitions for high reliability. The presenters have reported the active power method as the detection system[1, 2]. However the conventional method could not detect early the normal transition in a secondary coil of the transformer which was wound with a bundle of some HTS tapes. Because resistive voltage in the normal area is too small due to current sharing among the HTS tapes. In this presentation, the presenters propose a method to detect the normal transitions in the bundle conductor by improving the active power method. The improved system uses voltage taps and current leads attached to all the HTS tapes to achieve early detection. It is shown in the presentation that the system works successfully for the early detection.

[1] N Nanato, S Tanaka and S Tenkumo, Study on a Magnetic Flux Detection Coil for Detection of Normal Transitions in a Hybrid Single-phase Bi2223 Superconducting Transformer by the Active Power Method, Journal of Physics: Conference Series, Vol. 1054, 012070 (2018)
[2] N Nanato, T Ono, T Adachi and T Yamanishi, Protection System for Normal Transitions in a Single-phase Bi2223 Full Superconducting Transformer by the Active Power Method under Flowing Currents of Various Frequencies, Journal of Physics: Conference Series, Vol. 1054, 012068 (2018)
[3] N Nanato, N Kishi, Y Tanaka and M Kondo, Basic study for a large AC current supply with a single phase air-core Bi2223 high temperature superconducting transformer, Journal of Physics: Conference Series, Vol. 871, 012101 (2017)

Keywords: Normal transition, HTS transformer, Bundle conductor, Active power method

APP5-2

Experimental investigation of the processes of degradation and transition to the normal state in CC-tapes under the action of current pulses

*Maxim Osipov[1], Sergey Pokrovskii[1], Dmitriy Abin[1], Irina Anishenko[1], Igor Rudnev[1]

National Research Nuclear University MEPhI (Moscow Engineering Physics Institute)[1]

The study of the behavior of CC tapes under the action of nonstationary current loads was conducted: a transition to the normal state was observed, as well as processes of CC-tape degradation. The obtained data make it possible to solve the problems associated with the creation of high-speed switching devices based on high-temperature superconductors, intended for functioning in superconducting energy storage devices, energy distribution and transmission systems, current limiters, and new types of transport. In addition to superconducting switches, pulsed current loads can occur in the mentioned above systems due to short-circuit conditions or other factors, and can lead to local heating of HTSC, especially if there is an inhomogenity in the critical current in the CC-tapes.
In this paper, we carried out experimental studies of the behavior of CC-tapes under nonstationary current loads with amplitudes considerably exceeding the value of the critical current. The studies were carried out on samples of CC-tapes of various manufacturers with a width of 4 and 12 mm. The tape was loaded with a current close in magnitude to the critical current. Further, a short current pulse was additively added so that the total transport current exceeded the critical current. The effect of such parameters as the magnitude of the initial transport current, the amplitude and duration of the additional current pulse on the transition of the CC-tape to the normal state and return to the initial superconducting state was investigated. For certain parameters of the current impulse, damage was observed in the superconducting layer of CC-tape. Observation of the distribution of the damaged zone, as well as an assessment of the degradation of the superconducting properties of CC-tapes, were carried out by using Hall magnetometry and magneto-optical mycroscopy. These techniques were used to evaluate the effect of the initial homogeneity of the critical current of CC-tapes on the parameters of current loads that lead to irreversible changes in the transport properties of the tapes.
Analysis of the experimental data and the conclusions of this work can be useful for practical application in the development of high-speed switching devices based on CC-tapes.
The work is supported by the Russian Foundation for Basic Research under the grant 17-29-10024.

Keywords: CC-tapes, Critical current

APP5-3

Three-Dimensional Electromagnetic and Thermal Coupled Analysis of an SFCL REBCO Coil Immersed in 65 K Liquid Nitrogen

*Kezhen Qian[1], Yutaka Terao[2], Hiroyuki Ohsaki[2]

Graduate School of Engineering, The University of Tokyo, Japan[1]
Graduate School of Frontier Sciences, The University of Tokyo, Japan[2]

A resistive type SFCL using REBCO tapes has shown high potential in limiting fault currents rapidly and improving the power system reliability. Operation at 65 K appears very promising for quicker recovery of superconductors and rapid collapse of the bubbles during the fault current limitation in comparison with 77 K. However, the superconductor is more sensitive to hot spots for low prospective current faults [1].

In this paper, we have developed a 3D electromagnetic and thermal coupled FEM analysis model to study the transient characteristics of an SFCL REBCO coil which immersed in 65 K liquid nitrogen. In computation of current distribution in the SFCL coil, a thin-plate approximation is applied to the REBCO tapes. Then, orthogonal curvilinear coordinate systems and coordinate transformation are utilized to conduct the electromagnetic analysis of REBCO coils that have 3D structures in 2D calculation space. Therefore, the computational amount can be reduced to about 1/3. The governing electromagnetic equation is given by $\nabla\times(\rho\nabla\times\boldsymbol{T})=-\mathrm{d}\boldsymbol{B}/\mathrm{dt}$ ($\boldsymbol{T}$: current vector potential; ρ: electric resistivity; $\boldsymbol{B}$: magnetic flux density), where $\boldsymbol{T}$ is defined by $\boldsymbol{J}=\nabla\times\boldsymbol{T}$ ($\boldsymbol{J}$: current density) [2]. In thermal analysis, the 3D structure of REBCO coil is modeled and the temperature rise is calculated under the condition of Joule heating, heat conduction, heat transfer, and cooling characteristics of liquid nitrogen. With this analysis model, we studied the influence of a local J_C degradation on the hot spot behavior, as well as the transient temperature rise and normal zone propagation velocity during the current limitation. Furthermore, countermeasures against the hot spot problem were also discussed.

[1] Tixador P, Vialle J and Badel A 2018 Operation of an SCFCL at 65 K *IEEE Transactions on Applied Superconductivity* **28** 1–5
[2] Ohsaki H, Sekino M and Nonaka S 2009 Characteristics of Resistive Fault Current Limiting Elements Using YBCO Superconducting Thin Film With Meander-Shaped Metal Layer *IEEE Transactions on Applied Superconductivity* **19** 1818–22

Keywords: superconducting fault current limiter, finite element method (FEM), coated conductor, electromagnetic and thermal analysis

APP6-1

Recovery of strontium, rubidium and lithium from solution utilizing a rotary type high gradient magnetic separation with rice hull magnetic activated carbon

*Keisuke Ishida[1], Tatsuya Shiina[1], Osuke Miura[1]

Dept. of Electrical and Electronic Engineering, Tokyo Metropolitan University, Japan[1]

We have newly developed a rice hull magnetic activated carbon (RH-MAC) and studied its adsorption properties for strontium, rubidium and lithium from solution and high gradient magnetic separation properties. RH-MAC was synthesized by impregnating rice hull with an iron nitrate solution and heat-treatments in nitrogen and carbon dioxide atmosphere.
In those processes, many meso-pores and nano-size magnetite were generated inside the activated carbon grains. The magnetization of RH-MAC increased with increasing concentration of iron nitrate solution. The magnetization of RH-MAC3 made from 1.6 mol/L iron nitrate solution reached 22.2 Am^2/kg at 1 T. To study adsorption properties RH-MAC of 5, 10, 20, 30 mg was put into strontium, rubidium and lithium solution of 7.8, 0.12, 0.17, 3 ppm and stirred for 1 hour. The removal ratio of strontium, rubidium and lithium achieved about 14.3, 60.5, 42.0% for RH-MAC of 30 mg. For magnetic separation the multiple magnetic line filtering system wound around the permanent magnet drum was used. RH-MAC3 having a high magnetization of 22.2 Am^2/kg was captured at 99.2% by using double filter with 0.5 T with the flow rates of 300 mL/min.

Keywords: Rice hull magnetic activated carbon, Valuable metals, Adsorption, High gradient magnetic separation

APP6-2

Levitation properties of valuable metals utilizing magneto-Archimedes effect in a high magnetic field gradient

*Daiki Yamamoto[1], Kenichi Yamagishi[1], Osuke Miura[1]

Tokyo Metropolitan University, Department of Electrical and Electronic Engineering, Japan[1]

We propose a magnetic separation using magneto-Archimedes levitation for valuable resource recovery from urban mine. Magneto-Archimedes effect is a phenomenon that materials levitate at a particular position in a paramagnetic liquid medium by applying magnetic field gradient due to the difference of magnetic susceptibility and density between the liquid medium and the materials. We have been studying the magnetic levitation properties for various metals and electronic substrate powders for the valuable resource recovery from urban mine. However, there is a limitation of the magnetic force factor BdB/dz because of a limitation of the magnitude of magnetic fields and magnetic field gradient for the realistic specifications of the current superconducting magnet. Therefore some metals that are difficult to levitate exist. In this study, we challenged the magnetic levitation of heavy precious metals by magneto-Archimedes effect under a high magnetic field gradient utilizing ferromagnetic materials arranged in magnetic fields. In order to extend the range of the high magnetic field gradient, we designed a hexagonal arrangement of ferromagnetic cylinder. As a result extending the range of the high magnetic field gradient and the high BdB/dz were achieved. We succeeded in levitating almost all valuable metals under 5T.

Keywords: magneto-Archimedes levitation, high magnetic field gradient, valuable resource recovery, urban mine

APP6-3

Enhancement of the magneto-Archimedes levitation force by optimized ferromagnetic materials arrangement in magnetic fields

*Kenichi Yamagishi[1], Daiki Yamamoto[1], Osuke Miura[1]

Dept. of Electrical and Electronic Engineering, Graduate School of Science and Engineering, Tokyo Metropolitan University, Japan[1]

We have studied the levitation properties for valuable metals utilizing magneto-Archimedes effect under a high magnetic field gradient. In order to enhance the power factor *BdB/dz* for the magnetic force in vertical direction an iron cylinder having a diameter of 5 mm and a length of 50 mm was set into the room temperature bore of a 10T superconductor solenoidal magnet. The maximum *BdB/dz* achieved the high value of -1598 T^2/m with arranging only one ferromagnetic material. This value was about 3.68 times larger than that without ferromagnetic materials. Furthermore we studied the optimization of the shape and arrangement of the ferromagnetic materials placed at the center of the superconducting magnet. As a result, the effective range of the magnetic force was extended to about 4 times as compared with the case that the arrangement of the ferromagnetic material was not optimized. This suggests that it is possible to propose a device that separates a large amount of valuable resource with wide range in lower magnetic fields.

Keywords: magneto-Archimedes levitation, ferromagnetic material, valuable resource recovery

APP6-4

Design and Trial Production of Magnetic Filter for Medical Protein Screening System using High Gradient Magnetic Separation

*Masaki Mori[1], Mikihisa Kubota[1], Takuro Abe[2], S.B Kim[1], Hiroshi Ueda[1]

Okayama University Graduate School of Natural Science and Technology[1]
Okayama University Faculty of Engeneering[2]

Biomedicine is indispensable for the treatment of diseases such as cancer, diabetes mellitus (DM) and so on. Biomedicine has been developed not only in Japan but in foreign countries. Above all, antibody drugs, which use immune system, are thought to become the mainstream of medical supplies because it can have a great influence on curing diseases and cause little side effect.
The essential technology in developing antibody drugs is massive, sequential, and fast separation and refinement of protein for medicine. Therefore, we propose the medical protein screening system using high gradient magnetic separation by a superconducting magnet. This system enables us to capture and recover the magnetic beads which have fixed a specific protein.
Capturing and recovering point is placed in high magnetic field by a superconducting magnet. And beads are captured by magnetic force around the filter for magnetic separation.
In our research in 2017, we have analyzed the motion of magnetic beads in filter for magnetic separation. This research aims to design the high capture ratio filter. Then, in this presentation, the new results of the numerical simulation and experiments are reported.

Keywords: magnet, protein, magnetic separation, medical

APP6-5

Fundamental Study on Cancer Therapy by Blocking Newborn Blood Vessels Using a Rotating Magnetic Field

*Makoto Kirimura[1], Yoko Akiyama[1]

Div. of Sustainable Energy and Environmental Eng., Graduate School of Eng., Osaka Univ., Japan[1]

A novel cancer treatment with low side effect and less invasiveness by blocking newborn blood vessels around the diseased part was proposed. In the therapy, ferromagnetic particles are accumulated in the newborn blood vessels using Rotating Magnetic Field (RMF). It results in the blockage of the blood vessels which can prevent cancer from growth and metastasis.

We considered an application of the treatment to pancreatic cancer as an example. The pancreas is located about 200 mm from the body surface, and the size is about 10 mm at the initial stage. We aimed to design RMF that can locally accumulate particles within a spherical range of 10 mm in diameter and 200 mm away from a magnetic field source.

To investigate the accumulation range of the particles by RMF, a small scale experiment was conducted. As shown in **Fig. 1**, simulated blood in which 0.1 μm of magnetite particles were dispersed in 500 ppm was flown into simulated blood vessels. After accumulating the particles by RMF, the distribution on the rotating plane of the simulated organ was examined. A simulated organ consists of a syringe (φ30 mm×64mm) filled with glass beads (0.25 mm in daimeter). The glass beads form the flow path with approximately 54 μm in diameter, simulating that of capillary and newborn blood vessels. As simulated blood, 3.8 wt. % gelatin solution simulating blood viscosity was used (4.2 mPa·s at 25 ° C). The flow velocity simulated blood flow in the capillary vessel (1.0 mm/s). A neodymium magnet (φ30 mm×15 mm, magnetic flux density: 0.50 T) was used as a magnetic field source. The radius of RMF was 25 mm, and the frequency was 2.4 Hz and 3.6 Hz.

Fig. 2 shows the state of the cross-section of the rotating plane after particle accumulation. **Fig. 2(c)** shows that the particles are not accumulated in the particular side but are distributed over the entire cross-section under the RMF. **Fig. 2(d)** shows that the accumulation range on the cross section becomes smaller as the frequency of the RMF is increased. When a low-frequency RMF is applied, a magnetic force in a particular direction is applied for a long time. On the other hand, in the high-frequency, multidirectional magnetic force is evenly applied to the particles, and the particles accumulate around the central axis of RMF.

Acknowledgment: A part of this research was supported by Magnetic Health Science Foundation.

Keywords: deep target, particle accumulation, rotational magnetic field, ferromagnetic particles

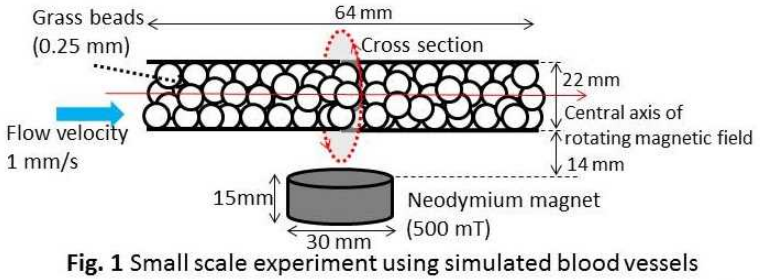

Fig. 1 Small scale experiment using simulated blood vessels

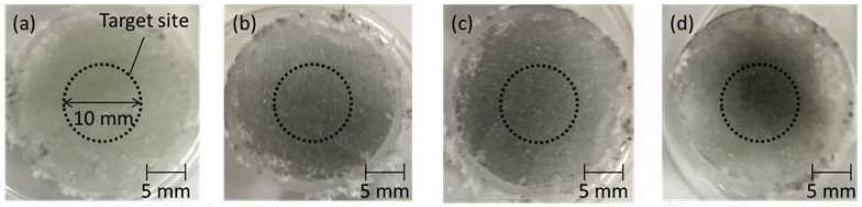

Fig. 2 Accumulation of particles on the cross section of rotating plane of magnetic field
(a)without magnetic field **(b)**static magnetic field
(magnetic field source is located under the syringe)
(c)rotating magnetic field (2.4 Hz) **(d)** rotating magnetic field (3.6 Hz)

APP7-1

Magnetic field design of a cosine-theta superconducting magnet with active shielding for a rotating gantry

*Tetsuhiro Obana[1], Toru Ogitsu[2]

National Institute for Fusion Science[1]
High Energy Accelerator Research Organization[2]

In heavy particle therapy, a rotating gantry enables charged particles to be delivered to a tumor with great accuracy. Therefore, cancer therapy that does not damage a patient can be realized by using a rotating gantry. In 2015, the world's first rotating gantry composed of superconducting magnets was developed in the National Institutes for Quantum and Radiological Science and Technology. Using superconducting magnets instead of conventional magnets, it became possible to make a smaller, lighter gantry.

The superconducting magnet for the rotating gantry is composed of a cosine-theta superconducting coil surrounded with an iron yoke which is the heaviest part of the weight of the magnet. The weight of one superconducting magnet reaches a couple of tons, and the rotating gantry is equipped with ten superconducting magnets. Precise rotation control is required under the condition that several ten tons are mounted on the frame of the rotating gantry. In this study, a superconducting magnet composed of an active shielding coil for the gantry has been proposed in order to simplify the control system and the frame structure of the rotating gantry by reducing its weight. Using an active shielding coil instead of an iron yoke to shield the leakage magnetic field, the magnet's weight can be reduced. In this paper, magnetic field design of a cosine-theta superconducting magnet with active shielding for a rotating-gantry is presented.

Keywords: Magnetic field calculation, cosine-theta superconducting magnet, active shielding, rotating gantry

APP7-2

Measurement of trapped magnetic field in REBCO single-turn loop including a joint

*Shinji MATSUMOTO[1], Gen NISHIJIMA[1], Akinobu NAKAI[2], Hisaki SAKAMOTO[2], Shinichi MUKOYAMA[2], Yasuyuki MIYOSHI[3], Kazuyoshi SAITO[3], Mamoru HAMADA[3]

National Institute for Materials Science, Japan[1]
Furukawa Electric Co., Ltd., Japan[2]
Japan Superconductor Technology, Inc., Japan[3]

Practical REBCO superconducting joint technologies for REBCO-MRI magnets are under development. Superconducting joint will be indispensable to operate REBCO-MRI magnets in persistent current mode. A joint resistance less than 10^{-12} ohm is required to achieve the magnetic field stability of 0.1 ppm/h. A REBCO single-turn loop cooled by a 40-K G-M cryocooler was prepared to estimate the joint resistance in magnetic fields. The measured decay rate of trapped magnetic field in the loop gives the REBCO joint resistance. An external magnetic field up to 1 T was applied to the joint. The external magnetic field was parallel along the laminated REBCO conductors. The decay of trapped magnetic field was measured at 47 K, and the joint resistance was estimated.

Acknowledgements

This work was conducted as a part of "Technology Development to Promote Commercialization of High-Temperature Superconductivity" sponsored by New Energy and industrial technology Development Organization (NEDO).

Keywords: MRI magnet, REBCO, single-turn loop, superconducting joint

APP7-3

Three dimensional model for numerical computations of screening currents in REBCO coils

*Philippe J. Fazilleau[1], Guillaume Dilasser[1]

CEA Saclay, France[1]

Screening currents are a major drawback in the context of REBCO magnets due to the particular shape of the conductors. In previous articles, we developed numerical tools for the computation of screening currents and their effects in the cases of systems featuring 2D symmetry, axial or longitudinal. Nevertheless, 2D models are not adequate for particular 3D shapes or alternative windings configurations, like layer wound ones.
Therefore, a three dimensional model has been implemented in the in-house CAST3M finite element code, using the current function T formulation. We developed new Cast3M operators to take into account the superconducting behavior of the material and the anisotropic dependence of the current density with the magnetic induction.
We benchmarked this 3D model with success against analytical formulas on simple scenarios and we compared the generation of screening currents within a small solenoid depending on the type of winding, made either of layers or pancakes.

Keywords: screening currents, high temperature superconductors, coils, finite elements

APP7-4

Experimental and Numerical Study on the Stability of a Pancake Coil Wound with a Rutherford-Type MgB_2 Conductor for SMES

Tsuyoshi Yagai[1], *Toru Okubo[1], Moeto Hira[1], Kaoruko Abe[1], Yusuke Kuwahara[1], Masahiro Kamibayashi[1], Mana Jinbo[1], Tomoaki Takao[1], Yasuhiro Makida[2], Takakazu Shintomi[2], Naoki Hirano[3], Toshihiro Komagome[4], Kenichi Tsukada[4], Taiki Onji[5], Yuki Arai[5], Masaru Tomita[5], Atsushi Shigemori[6], Kenichi Nakajima[6], Daisuke Miyagi[7], Makoto Tsuda[7], Takarato Hamajima[4]

Sophia University[1]
High Energy Acceleration Research Organization[2]
Chubu Electric Power[3]
MAYEKAWA MFG. Co., Ltd[4]
Railway Technical Research Institute[5]
Iwatani Corporation[6]
Tohoku University[7]

MgB_2 strands produced by in-situ powder-in-tube (PIT) method are widely available for relatively low -field applications like Magnetic Resonance Imaging (MRI). Several research groups have been developed large scale conductors with circular, and rectangular cross sections. The flat cable with rectangular cross section is called Rutherford-type cable, having wide surfaces, transposing at the thin edges. For the large-current capacity operations, the number of strands of 8 is adopted as a result of the calculation of Cu heat capacity, including 4 Cu strands and a Cu mandrel due to the low Cu ratio of Monel-sheathed MgB_2 strand body. Unlike the steady-state operation in MRI applications, such multifilamentary wires should be introduced for the conductor design so that the low-AC loss coils can be fabricated for Superconducting Magnetic Energy Storage (SMES) application. Owing to the thin Nb barrier covering MgB_2 filaments and its breakage, the Ic would be sensitive to the bending strain and strand indentation that are mainly supposed to be applied during the cabling and the coil-winding processes. To fabricate the SMES coils consisting of MgB_2 conductors with minimum performance degradation, the optimum designing and manufacturing processes are still under investigation. Fig. 1 Picture of the fabricated small test coil (Wind & React Method) and experimental setup for the stability analysis.

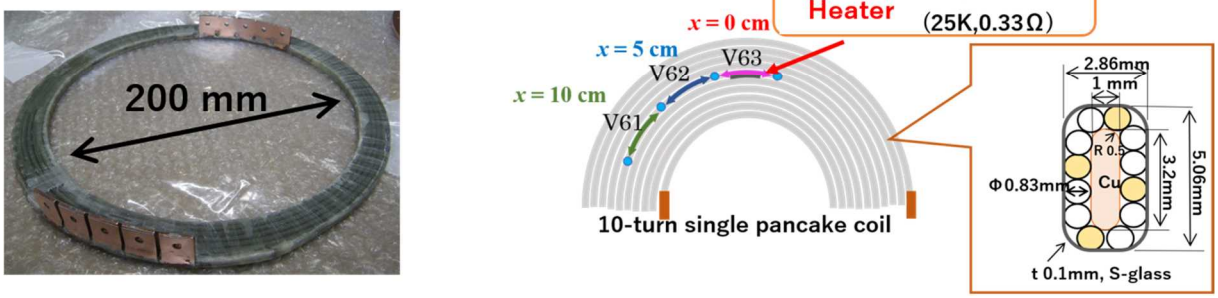

Keywords: MgB2 multifilamentary strand, Large-scale Rutherford cable, Pancake coil, Superconducting Magnetic Energy Storage

APP7-5

Characterization of conduction-cooled MgB_2 wires

Satoru Inoue[1], Xijie Luo[1], Amemiya Naoyuki[1]

Kyoto University[1]

We are characterizing MgB_2 wires using a test stand, in which a sample is conduction-cooled by using GM cryocooler. We measured the voltage (V) – current (I) characteristics of an MgB_2 wire. We focused on its current transfer length and the influence of bending.

An MgB_2 wire, fabricated by Colombus Superconductors, was conduction-cooled, and the V–I characteristics were measured. The length of the sample was 200 mm (including the 25 mm-section at each end which was soldered to the copper current terminal), and multiple voltage taps were attached on the sample. Cernox temperature sensors were attached to the sample to measure its temperature. An FPGA module was used to control the current supplied to the sample: ramping up the current at a constant rate (1.6 A/s), detecting the voltage appeared across the entire sample, and shutting down the current. Heaters, which were attached between the cryocooler and the sample, were used to control the sample temperature. The magnetic field up to 2 T was applied by a superconducting magnet. V–I characteristics were measured at (1 T, 20 K), (2 T, 15 K), and (2 T, 20 K). Using multiple voltage taps, we identified that the current transfer length was 30 mm from the current terminal. The resistance of the entire sample which we defined by dividing the linear voltage component in a V–I curve by current was around 0.03 mW. If the linear voltage component caused by this resistance was subtracted from the V–I curve at a section near the current terminal, it almost agreed with the V–I curves at other sections, in which the voltages were negligible. We will measure the V–I characteristics of the same MgB_2 wire, which is straightened after being bent with constant curvature.

LNP1-1

Analysis on DC Circuit Breaker using superconducting coil

I.S.Jeong[1], H.W.Choi[1], S.Y.Park[1], H.S.Gu[1], H.S.Choi[1]

Chosun University, Republic of Korea[1]

Development of DC interruption technology is being studied actively for enhanced DC grid reliability and stability. In this study, coil type superconductor DC circuit breaker was proposed as DC interruption. It is integration technology that combined current-limiting technique using superconductor and cut-off technique using mechanical DC circuit breaker. Superconductor was applied to the coil type. In simulation, Mayr arc model was applied to realize the arc characteristic in the mechanical DC circuit breaker. PSCAD/EMTDC had used to model and perform the simulation. To find out the protection range of coil type superconductor DCCB, the working operation have analyzed based on the rated voltage of DCCB. The results confirmed that, according to apply the limiting device, the protection range was increased in twice. Therefore, the probability of failure of interruption has lowered significantly.

[1] Frede Blaabjerg, Zhe Chen, Soeren Baekhoeh Kjaer, “Power electronics as efficient interface n dispersed power generation system”, , IEEE Transactions on Industrial Electronics, Vol.19, No.5, Sep 2004 .
[2] W R Leon Garcia, A Bertinato, P Tixador, B Raison, B Luscan, “Full-selective protection strategy for MTDC grids based on R-type superconducting FCLs and mechanical DC circuit breaker”, Renewable Power Generation(RPG) 2016, 5th IeT international Conference on, 10.1049/cp.2016.0564
[3] Byung Chul Sung, Dong Keun Park, Jung-Wook Park and Tae Kuk Ko, “Study on a series resistive superconductor to improve power system transient stability : Modeling, Simulation and experimental verification”, IEEE Transactions on Industrial Electronics, Vol.56, No.7, Jul 2009
[4] Ran Ou, Xian-Yong Xiao, Zhi-Ce Zou, Yi Zhang, and Yu-Hong Wang, “Cooperative control of superconductor and reactive power for improving the transient voltage stability of grid- connected wind farm with DFIGs”, IEEE Transactions on Applied Superconductivity, Vol. 6, No.7, Oct 2016
[5] N.S Mahajan, K.R. Patil, S.M. Shembekar, “Electric Arc model for High Voltage Circuit Breakers Based on MATLAB/SIMULINK”, Interantional Journal of Science, Spritualtiy, Business and Technology (IJSSBT), Vol. 1, No.2, FEB 2013

Acknowledgement
Following are results of a study on the “Leaders in Industry-university Cooperation +” Project, supported by the Ministry of Education and National Research Foundation of Korea

LNP1-2

Operation characteristics of superconducting coil type DC circuit breaker according to reactance value of superconducting coil using EMTDC/ PSCACD

*Hyewon CHOI[1], Huiseok Gu[1], Hyosang CHOI[1]

Department of Electrical Engineering, Chosun University, 309 Pilmun-Daero, Dong-Gu, Gwangju, Republic of Korea[1]

We analyzed the fault current limiting characteristics according to reactance of superconducting coil type DC circuit breaker. Superconducting coil type DC circuit breaker uses reactance to delay the time to reach the maximum fault current. At the same time, the quenched superconductor limits the fault current. Limited fault current is prevented by mechanical DC circuit breaker. It is necessary to select the reactance values to account for the failure of the fault limiting and the stability of the delay. The limiting current characteristics analyzed by increasing of 0.1 H in range of 0.1 H to 1 H by 0.1division. PSCAD/EMTDC program was used for the analysis. The simulation results indicated that when the input voltage was 350 kV, the superconducting coil type DC circuit breaker has no significant effects on the fault limiting limits if the system has reactance greater than 0.7 H. When analyzing the burden on the superconductor, the burden on superconducting coil type DC circuit breaker could also be reduced to less than 1 MVA.

[Acknowledgement]
Following are results of a study on the “Leaders in Industry-university Cooperation +” Project, supported by the Ministry of Education and National Research Foundation of Korea.
"This work was supported by the National Research Foundation of Korea(NRF) grant funded by the Korea government(MSIT) (No.2018R1A2B2004242)."

LNP2-1

The improvement of MgB_2 superconductivity prepared by diffusion method with ultrasonic precursor

*Hong Zhang[1], QI Wang[1], Yong Zhao[1,2], Yong Zhang[1]

Key Laboratory of Maglev Train and Maglev Technology of Ministry of Education, Superconductivity and New Energy R&D Center, Southwest Jiaotong University, Chengdu 610031, China[1]
School of Materials Science and Engineering, University of New South Wales, Sydney 2052, NSW, Australia[2]

To improve the density of MgB_2 is the key to improve the performance of the MgB_2. In this paper, the B and Graphene mixed precursor powder is ultrasonic treated to prepare MgB_2 by diffusion method. The preparation of MgB_2 by ultrasonic treatment of precursor powder can promote the uniform diffusion of Mg to B, reduce the micro-cracks, increase the density. The high-quality MgB_2 bulks are achieved with high density.

LNP2-2

Power Enhancement of the High-Tc Superconducting Terahertz Emitter with a Modified Device Structure

*H. Minami[1,2], Y. Ono[1], K. Murayama[1], Y. Tanabe[1], K. Nakamura[1], S. Kusunose[1], T. Kashiwagi[1,2], M. Tsujimoto[1,2], K. Kadowaki[1,2]

Graduate School of Pure and Applied Sciences, University of Tsukuba, 1-1-1 Ten-nodai, Tsukuba, Ibaraki 305-8571, Japan[1]
Division of Materials Science, University of Tsukuba, 1-1-1 Ten-nodai, Tsukuba, Ibaraki 305-8573, Japan[2]

The high-T_c superconductor $Bi_2Sr_2CaCu_2O_{8+\delta}$ (Bi2212) consists of a stack of equivalent atomic-scale Josephson junctions (670 layers per 1 μm thick) commonly referred to as the intrinsic Josephson junctions (IJJs) [1]. The continuous and monochromatic terahertz (THz) electromagnetic waves whose frequencies obey the ac-Josephson effect ($f = 2eV/h$) can be generated with sizable power of a few tens of μW, by passing dc current to it to induce the phase synchronization of the Josephson currents between the IJJs in the mesa-shaped device made of Bi2212 [2,3]. In the present study, we aimed to generate high power emission by modifying the device structure.

From the previous experimental results reported on the line width [4], spatial distribution [5] of the emission, *etc.*, we supposed that the relatively weak power from the IJJ emitters may be the failure of the phase synchronization of the Josephson currents to build up well in the mesa device. This may be improved by modifying the device structure in order for the Josephson current density to enhance inside the mesa. In the present case, several slots were made in the superconductor base around a rectangle-shaped mesa with the dimensions of 80 μm × 400 μm × 3.2 μm by photolithography and chemical etching techniques. The best result so far obtained is the emission power of ～80 μW at 0.4 THz, which is about 2.7 times bigger than the previous champion data in our group [3]. Figure 1 shows the example of the spectrum measured by a Fourier transformation infrared (FTIR) spectrometer with a pyroelectric detector at room temperature, together with that of mercury lamp for the comparison. The detail will be presented at the conference.

[1] R. Kleiner, et al.: Phys. Rev. Lett. 68 (1992) 2394.
[2] L. Ozyuzer, et al.: Science 318 (2007) 1291.
[3] S. Sekimoto, et al.: Appl. Phys. Lett. 103 (2013) 182601.
[4] M. Li et al., Phys. Rev. B 86 (2012) 060505.
[5] H. Minami, et al.: Appl. Phys. Lett. 95 (2009) 232511.

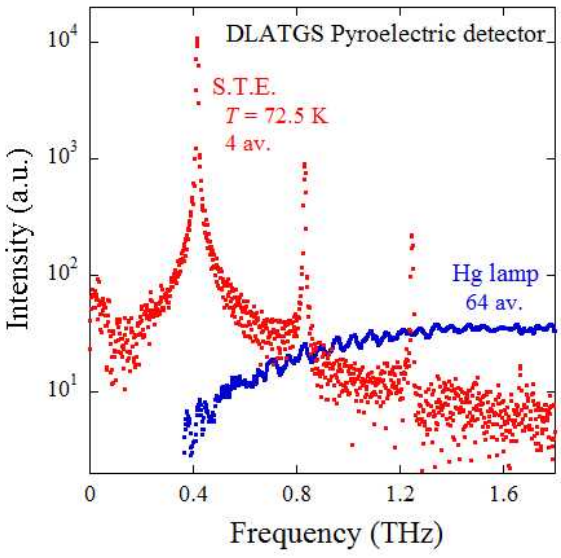

Fig. 1 The THz emission spectrum from the improved type of IJJ emitter measured by a FTIR with a pyroelectric detector (red curve). A broad and flat spectrum obtained from a mercury lamp (blue curve) is added for the comparison. Both measurements were performed with the same experimental set-up except for the data accumulation number as indicated in the graph.

Keywords: Josephson Effect, Terahertz Emission, High-Tc Superconductor

LNP2-3

Local Heating Effects on the Radiation Intensity of High-T_c Superconducting Terahertz Emitters

*K. Nakamura[1], H. Minami[1,2], R. Ota[1], K. Murayama[1], Y. Ono[1], S. Kusunose[1], T. Kashiwagi[1,2], M. Tsujimoto[1,2], K. Kadowaki[1,2]

Graduate School of Pure and Applied Sciences, University of Tsukuba, 1-1-1 Ten-nodai, Tsukuba, Ibaraki 305-8571, Japan[1]
Division of Materials Science, University of Tsukuba, 1-1-1 Ten-nodai, Tsukuba, Ibaraki 305-8573, Japan[2]

The terahertz electromagnetic waves whose frequencies obey the ac-Josephson effect ($f = 2eV/h$) can be generated with sizable power of ~30 μW by the mesa device made of high-T_c superconductor $Bi_2Sr_2CaCu_2O_{8+\delta}$ (Bi2212) single crystal comprised of multi-stacks of intrinsic Josephson junctions [1]. An idea to have stronger emission power is to increase the number of Josephson junctions. However, in practice, a thick mesa containing the large number of junctions is heated due to large amount of Joule heat, forming the inhomogeneous temperature distribution $T(r)$ in the mesa [2]. It is known that $T(r)$ affects strongly the emission line width [3]. Furthermore, the previous experiments indicated that local heating of the mesa by a focused laser beam dramatically enhances the emission intensity, even higher than that without laser heating [4]. The present study has been focused to understand the enhancement phenomenon and find a clue to make higher emission power devices.

The experiment has been performed using a mesa device with the dimensions of 80 μm × 400 μm × 2.5 μm (see Fig. 1 (a)), which is irradiated partly by a focused laser beam of λ=660 nm and P=80 mW as shown by the red spot in Fig. 1 (a). The result shows that the terahertz emission intensity reaches almost two times as large as the one with standard biases without laser irradiation as seen in Fig. 1 (b). It is interesting to note that the enhanced emission remains without losing the intensity even after switching off the laser power. This result may be interpreted by the fact that the normal current flows in the mesa in a different manner when the device is biased under laser irradiation, according to the thermoreflectance measurement [5].

[1] L. Ozyuzer et al., Science 318, 1291 (2007).
[2] H. Minami et al., Phys. Rev. B. 89, 054503 (2014).
[3] M. Li et al., Phys. Rev. B 86, 060505 (2012).
[4] C. Watanabe et al., Appl. Phys. Lett. 106, 042603 (2015).
[5] T. Kashiwagi et al., J. Appl. Phys. 122, 233902 (2017).

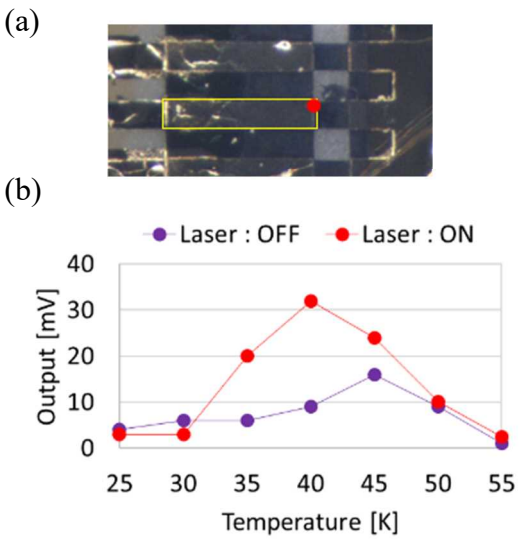

Fig. 1 (a) A photograph of the array of mesa devices. One of the mesa is highlighted by a yellow rectangle. A red dot indicates a position where a laser beam of the diameter of ~30 μm was irradiated. (b) The maximum emission intensity as a function of the bath temperature. The mesa is biased with (red dots) and without (blue dots) laser irradiation at the red dot position (a).

Keywords: Josephson Effect, Terahertz Emission, High-Tc Superconductor